University of Calabria

Methodologies for the development of molecules of pharmacological interest
XXII cycle

Ph.D. Thesis
CHIM/09

Macromolecular systems
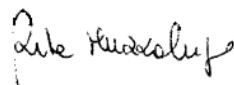# *for controlled drug delivery*

Candidata
Lorena Tavano

Ph.D. Coordinator

Ph.D. Supervisor

Prof. Bartolo Gabriele

Dr. Rita Muzzalupo

(A.A. 2006/2007-2008/2009)

Author's e-mail: uclorena@tiscali.it

Author's address:
Department of Pharmaceutical Sciences
University of Calabria
Via Pietro Bucci, Ed. Polifunzionale 155
87036 Arcavacata di Rende, Cosenza

ph.: +39 0984 493296
ph.: +39 0961 774311
cell: +39 329 6250407

Ad maiora

Abstract

In recent years, significant efforts have been devoted to the application of nanotechnology for the development of devices to be employed as drug delivery systems. The synergic combination of polymeric science, drug delivery concepts and material technology offers challenging and precious opportunities for the achievement of new useful materials. In particular surfactants, lipids and polymeric systems play an important role in modern drug delivery, where they may allow control of the drug release rate, enhance effective drug solubility, minimize its degradation, contribute to reduced its toxicity and facilitate control of its uptake. In all, they contribute significantly to therapeutic efficiency.

Acknowledgments

I am grateful to my parents Rossella and Angelo and my brother Marco for having been very understanding and for encouraging me during my PhD research.

Lucio has been so close and careful, giving me the strength to go on with my doctorate. Thank you, love!

Contents

1
Introduction

1.1Main contributions

Currently there is a growing interest in controlled drug delivery systems, which release their drugs in programmed ways. The general aim of this study is to design and to realize new devices useful for pharmaceutical applications and to evaluate the potential applications as drug delivery systems through tests *in vitro*.

1.2 Structure of the thesis

In the framework of a long–standing research activity ongoing in the Pharmaceutical Tecnology groups, at the Department of Pharmaceutical Sciences of the University of Calabria, the present work is on the development of novel macromolecular systems for controlled drugs delivery. In particular the focus of my PhD research was on the preparation of new drug carriers in the form of vesicles (II chapter), polymeric materials (III chapter) and lyotopic liquid crystals (IV chapter) aimed at the enhancement of their performance *in vitro*. In addiction a V chapter is present and it is about a scientific research project performed in collaboration with a chemical company (EUROCHEMICALS s.p.a.) on the development of niosomal preparations carrying active molecules for cosmetic applications.

The study carried out in this thesis was funded by the EUROCHEMICALS s.p.a. and it is a wider multidisciplinary research project which involved different background researchers, such as chemists, biologists and pharmaceutical technologists.

1.3 A brief overview on Drug Delivery

The method by which a drug is delivered can have a significant effect on its efficacy. Some drugs have an optimum concentration range within which maximum benefit is derived, and concentrations above or below this range can be toxic or produce no therapeutic benefit at all. On the other hand, the very slow progress in the efficacy of the treatment of severe diseases, has suggested a growing need for a multidisciplinary approach to the delivery of therapeutics to targets in tissues. From this, new ideas on controlling the pharmacokinetics, pharmacodynamics, non-specific toxicity, immunogenicity, biorecognition, and efficacy of drugs were generated.[1] These new strategies, often called drug delivery systems (DDS), are based on interdisciplinary approaches that combine polymer science, pharmaceutics, bioconjugate chemistry, and molecular biology.

To minimize drug degradation and loss, to prevent harmful side-effects and to increase drug bioavailability and the fraction of the drug accumulated in the required zone, various drug delivery and drug targeting systems are currently under development: the common feature of many current controlled release devices is that they provide a continuous release over a prolonged period of time.[2] Among drug carriers one can name micelles, vesicles (liposomes and niosomes), soluble polymers, microparticles made of insoluble or biodegradable natural and synthetic polymers, microcapsules and liquid crystals. These carriers can be made slowly degradable, stimuli-reactive (e.g., pH- or temperature-sensitive), and even targeted (Fig.1.1) (e.g., by conjugating them with specific antibodies or proteins against certain characteristic components of the area of interest).[3]
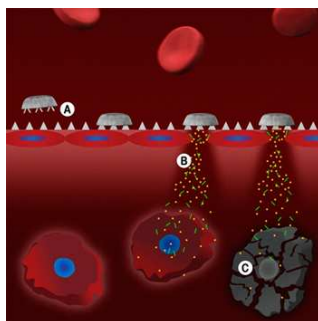
Fig.1.1 Example of targeted drug delivery

Targeting is the ability to direct the drug-loaded system to the site of interest. A strategy that could allow active targeting involves the surface functionalization of drug carriers with ligands that are selectively recognized by receptors on the surface of the cells of interest. Since ligand–receptor interactions can be highly selective, this could allow a more precise targeting of the site of interest.[4] Controlled drug release and subsequent biodegradation are important for developing successful formulations. Potential release mechanisms involve: (i) desorption of surface-bound/adsorbed drugs; (ii) diffusion through the carrier matrix; (iii) diffusion (in the case of nanocapsules) through

the carrier wall; (iv) carrier matrix erosion; and (v) a combined erosion/diffusion process. The mode of delivery can be the difference between a drug success and failure, as the choice of a drug is often influenced by the way the substance is administered. Sustained (or continuous) release of a drug involves polymers that release the drug at a controlled rate due to diffusion out of the polymer or by degradation of the polymer over time. Pulsatile release (Fig.1.2) is often the preferred method of drug delivery, as it closely mimics the way by which the body naturally produces hormones such as insulin. It is achieved by using drug-carrying polymers that respond to specific stimuli (e.g., exposure to light, changes in pH or temperature). [5]
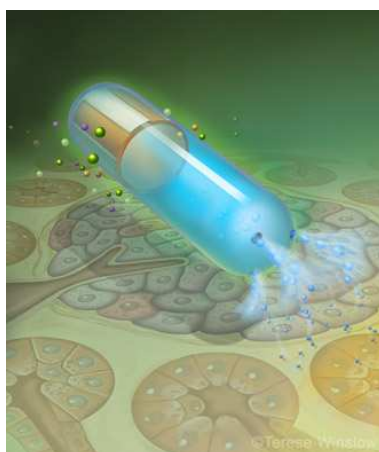
Fig.1.2 Example of pulsatile drug delivery system

1.3.1 Drug Delivery Carriers

Colloidal drug carrier systems such as micellar solutions, vesicle and liquid crystal dispersions, as well as nanoparticle dispersions consisting of small particles of 10–400 nm diameter show great promise as drug delivery systems.[6] When developing these formulations, the goal is to obtain systems with optimized drug loading and release properties, long shelf-life and low toxicity. The incorporated drug participates in the microstructure of the system, and may even influence it due to molecular interactions, especially if the drug possesses amphiphilic and/or mesogenic properties.[7]

Micelles formed by self-assembly of amphiphilic block copolymers (5-50 nm) in aqueous solutions are of great interest for drug delivery applications (Fig.1.3). The drugs can be physically entrapped in the core of micelles and transported at concentrations that can exceed their intrinsic water-solubility. Moreover, the hydrophilic blocks can form hydrogen bonds with the aqueous surroundings and form a tight shell around the micellar core. As a result, the contents of the hydrophobic core are effectively protected against hydrolysis and enzymatic degradation. In

11

addition, the shell may prevent recognition by the reticuloendothelial system and therefore preliminary elimination of the micelles from the bloodstream. A final feature that makes amphiphilic block copolymers attractive for drug delivery applications is the fact that their chemical composition, total molecular weight and block length ratios can be easily changed, which allows control of the size and morphology of the micelles.[8]
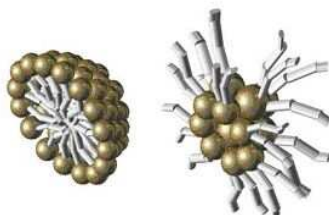
Fig.1.3 Micelles

Liposomes are a form of vesicles that consist either of many, few or just one phospholipid bilayers (Fig.1.4).[9] The polar character of the liposomal core enables polar drug molecules to be encapsulated. Amphiphilic and lipophilic molecules are solubilized within the phospholipid bilayer according to their affinity towards the phospholipids.

Reformulation of drugs in liposomes has provided an opportunity to enhance the therapeutic indices of various agents mainly through the alteration of biodistribution. They are versatile drug carriers, which can be used to control retention of entrapped drugs in the presence of biological fluids, controlled vesicle residence in the systemic circulation or other compartments in the body and enhanced vesicle uptake by target cells.[10] Liposomes composed of natural lipids are biodegradable, biologically inert, weakly immunogenic,[11] produce no antigenic or pyrogenic reactions and possess limited intrinsic toxicity.[12]
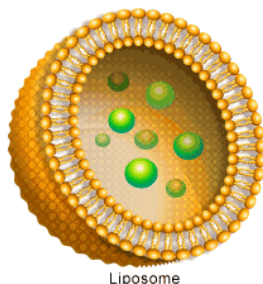
Liposome

Fig.1.4 A liposome

Encouraging results of liposomal drugs in the treatment or prevention of a wide spectrum of diseases in experimental animals and in human, indicate that more liposome-based products for clinical and veternary applications may be forthcoming.[13] These could include treatment of skin and eye diseases, antimicrobial and anticancer therapy, metal chelation, enzyme and hormone replacement therapy, vaccine and diagnostic imaging.[14]

Participation of nonionic surfactants instead of phospholipids in the bilayer formation results in niosomes.[15] Niosomes are preferred over liposomes because the former exhibit high chemical stability and economy.[16] Niosomes also exhibit special characteristics such as easy handling and storage.[17]

Liquid Crystals combine the properties of both liquid and solid states. They can be made to form different geometries, with alternative polar and non-polar layers (i.e., a lamellar phase) where aqueous drug solutions can be included.[18,19]

Nanoparticles (including nanospheres and nanocapsules of size 10-200 nm) are in the solid state and are either amorphous or crystalline (Fig.1.5).[20] They are able to adsorb and/or encapsulate a drug, thus protecting it against chemical and enzymatic degradation. Nanocapsules are vesicular systems in which the drug is confined to a cavity surrounded by a unique polymer membrane, while nanospheres are matrix systems in which the drug is physically and uniformly dispersed. Nanoparticles as drug carriers can be formed from both biodegradable polymers and non-biodegradable polymers.[21]
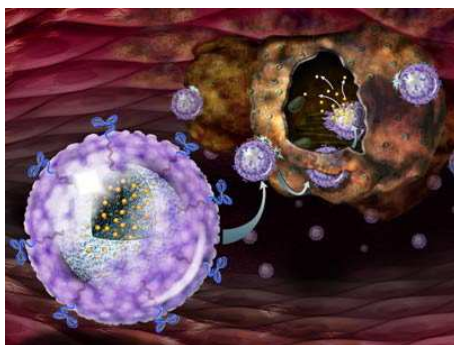
Fig.1.5 Nanoparticles

In recent years, biodegradable polymeric nanoparticles have attracted considerable attention as potential drug delivery devices in view of their applications in the controlled release of drugs, in targeting particular organs/tissues, as carriers of DNA in gene therapy and in their ability to deliver proteins, peptides and genes through the peroral route.[22]

Hydrogels are three-dimensional, hydrophilic, polymeric networks capable of imbibing large amounts of water or biological fluids.[23] The networks are composed of homopolymers or copolymers, and are insoluble due to the presence of chemical crosslinks (tie-points, junctions), or

physical crosslinks, such as entanglements or crystallites. Hydrogels exhibit a thermodynamic compatibility with water, which allows them to swell in aqueous media. They are used to regulate drug release in reservoir-based, controlled release systems or as carriers in swellable and swelling-controlled release devices.[24] On the forefront of controlled drug delivery, hydrogels as enviro-intelligent and stimuli-sensitive systems modulate release in response to pH, temperature, ionic strength, electric field, or specific analyte concentration differences.[25] In these systems, release can be designed to occur within specific areas of the body (e.g., within a certain pH of the digestive tract) or also via specific sites (adhesive or cell-receptor specific gels via tethered chains from the hydrogel surface).

References

[1] Charman W.N., Chan H.-K., Finnin B.C. and Charman S.A., Drug Dev Res, 46, (1999), 316.

[2] Kefalides PT., Ann Intern Med 128, (1998), 1053.

[3] El-Aneed A., J Contr Rel, 94, (2004), 1.

[4] Gregoriadis, G., Nature, 165, (1977), 407.

[5] Kopecek J., Eur J Pharm Sci 20, (2003), 1.

[6] Westesen K., Bunjes H., Hammer G., Siekmann B., J Pharm Sci Technol 55, (2001) 240.

[7] Muller-Goymann C.C., Eur J Pharm Biopharm, 58, (2004), 343.

[8] Bae Y., Fukushima S., Harada A. and Kataoka K., Angew Chem Int Ed, 42, (2003), 4640.

[9] Cevc G., Adv Drug Delivery Rev, 56, (2004), 675.

[10] Gregoriadis G., Florence A.T., Drugs 45, (1993), 15.

[11] Van Rooijen N., Van Nieuwmegen R., Immunol Commun 9, (1980), 243.

[12] Campbell P. I., Cytobios 37, (1983), 21.

[13] Gregoriadis G., Liposomes as Drug Carrier: Recent Trends and Progress (Ed. G. Gregoriadis), Wiley, Chichester 1988, 3.

[14] Goyal P., Goyal K., Kumar S.G.V., Singh A., Katare O.P., Mishra D.N., Acta Pharm. 55, (2005), 1.

[15] Uchegbu I.F., Vyas S.P., Int. J. Pharm., 172, (1998), 33.

[16] Hunter CA. et al., J Pharm Pharmacol, 40, (1988), 161.

[17] Biswal S., Murthy P.N., Sahu J., Sahoo P., Amir F., Int. J. Pharm. Sci. Nanotech, 1, (2008).

[18] Florence A.T., Attwood D., Physicochemical Principles of Pharmacy, second ed., Macmillan, New York, 1988.

[19] Kelker H., Hatz, R. Handbook of Liquid Crystals, Verlag Chemie, Weinheim, Germany, 1980.

[20] Westesen K., Bunjes H., Koch M.H.J., J Control Rel 48, (1997), 223.

[21] Ravi Kumar M.N., J Pharm Pharm Sci 3, (2000) 234.

[22] Brannon-Peppas L., Blanchette J.O., Adv Drug Delivery Rev, 56 (2004), 1649.

[23] Cruise G.M., Scharp D.S. and Hubbell J.A., Biomaterials, 19, (1998), 1287.

[24] Ulbrich K., Subr B., Podperova P. and Buresova, J Controll Rel 34, (1995), 155.

[25] Bae Y., Fukushima S., Harada A. and Kataoka K., Angew Chem Int Ed, 42, (2003), 4640.

2

Vesicular systems

This section reviews the scientific projects regarding the niosomal formulations produced during my research, including a first part in which I briefly introduced this class of drug carriers, the preparation method, the characterizations, the drug release and drug percutaneous permeation procedures that I used to performe these studies.

2.0 Definition

Non-ionic surfactant based vesicles (niosomes) are formed from the self-assembly of non-ionic amphiphiles in aqueous media resulting in closed bilayer structures (Fig. 1). The assembly into closed bilayers is rarely spontaneous[1] and usually involves some input of energy such as physical agitation or heat. The result is an assembly in which the hydrophobic parts of the molecule are shielded from the aqueous solvent and the hydrophilic head groups enjoy maximum contact with same. These structures are analogous to phospholipid vesicles (liposomes) and are able to encapsulate aqueous solutes and serve as drug carriers. The low cost, greater stability and resultant ease of storage of non-ionic surfactants[2] has lead to the exploitation of these compounds as alternatives to phospholipids. Niosomes were first reported in the seventies as a feature of the cosmetic industry[3] but have since been studied as drug targeting agents.
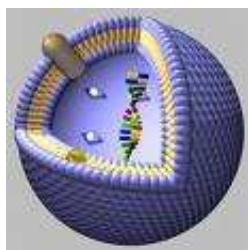
Fig.2.1 Schematic illustration of a niosome

Due to their structure, chemical composition and colloidal size, all of which can be well controlled by preparation methods, niosomes exhibit several properties which may be useful in various applications. The most important properties are colloidal size, i.e. rather uniform particle size distributions in the range from 100 nm to 10 μm, and special membrane and surface characteristics. They include bilayer phase behavior, its mechanical properties and permeability, charge density, presence of surface bound or grafted polymers, or attachment of special ligands, respectively. Additionally, due to their amphiphilic character, niosomes are a powerful solubilising system for a wide range of compounds. In addition to these physico-chemical properties, niosomes exhibit many special biological characteristics, including (specific) interactions with biological membranes and various cells.[4]

2.1 Materials and Methods

2.1.1 Preparation of niosomes

Multilamellar lipid vesicles were prepared by film rehydration method described by Bangham.[5] Briefly, the lipids were dissolved in chloroform (or appropriate organic solvent) and mixed in a

round-bottom flask. A lipid film is formed on the flask wall by removing solvent with a rotary evaporation at 25° C under reduced pressure. The resulting film was dried under vacuum for at least 4 h.
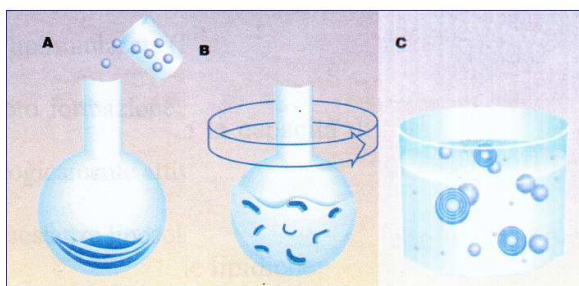
Fig.2.2 Preparation of niosomes (A= lipid dissolvation in chloroform, B= hydration, C= sonication)

The film was hydrated under mechanical stirring at 50° C for 30 minutes, with 10 mL of distilled water (empty niosomes) or with 10 mL of drug aqueous solution (loaded niosomes). In the case of polymerized vesicles, an initiator of polymerization (ammonium persulfate, AP, 1.3×10^{-5} mol) was added to the aqueous solution. After preparation, the dispersion was left to equilibrate at room ambient temperature overnight to allow complete annealing and partitioning of the drug between the lipid bilayer and the aqueous phase. Small unilamellar vesicles (SUV) were prepared starting from MLV by sonication in an ultrasonic bath for 30 minutes at 50° C.

The purification niosomes was also carried out by exhaustive dialysis for 4 h, using Visking tubing (20/30), manipulated before use in according to Fenton's method.[6]

2.1.2 Size and distribution analysis

The autocorrelation function of the scattered light was acquired by means of a commercial instrument (90 Plus Particle Size Analyzer, Brookhaven Instruments Corporation, New York, USA). Data were acquired at T = 25°C utilizing a scattering angle of 90°. The mean size and standard deviation (±S.D.) was directly obtained from the instrument fitting data by the inverse "Laplace transformation" method and by Contin.[7] Each experiment was carried out in triplicate.

2.1.3 Transmission electron microscopy (TEM)

TEM observation of niosomes dispersed in double distilled water was photographed with a ZEISS EM 900 electron microscope at an accelerating voltage of 80 kV. A drop of the dispersion was placed onto a carbon-coated copper grid, forming a thin liquid film. The films on the grid were negatively stained by adding immediately a drop of 2% (w/w) phosphotungstic acid, removing the

excess solution using a filter paper and followed by a through air-drying. Each experiment was carried out in triplicate.

2.1.4 Zeta-potential

Zeta-potential of niosomes was measured by a laser Doppler electrophoretic mobility method using the Zetasizer 2000 (Malvern Instruments Ltd., Malvern, U.K.), at 25.0± 0.1 °C). The laser was operating at 630 nm. All experiments were in triplicate. Vesicular dispersions were diluted to 1 in 100 with doubly-distilled water. The dilute niosome dispersions were located in the Zeta meter cell, equipped with gold-coated electrodes. The voltage ramps were performed according to the indications given by the purveyor (45). Tiny amounts of NaCl, usually less that 3.0 millimolar, optimized the instrumental performances. The charge on the vesicles and their average zeta potential (ZP) values, together with standard deviation (±SD) were elaborated directly from the instrument. Each mesure was carried out in triplicate.

2.1.5 Drug entrapment efficiency

Niosomes encapsulation efficiency was determined using the dialysis technique for separating the non-entrapped drug from niosomes.[7-9]

According to this method, 3 mL of drug-loaded niosomal dispersion were placed into a dialysis bag (Spectra/Por, MW cut-off 12,000, Spectrum, Canada) immersed in distilled water and magnetically stirred. Free drug was dialyzed for 30 min each time in 100 mL of distilled water and the dialysis was complete when no drug was detectable in the recipient solution. The percent of encapsulation efficiency (E%) was expressed as the percentage of the drug trapped in dialyzed niosomal formulations referred to the non dialyzed ones and it was determined by dissolving 1mL of dialyzed and 1mL of non-dialyzed in 25mL of methanol respectively, followed by the measurement of absorbance of the clear solution at the drug wavelength. Absorption spectra were recorded with a UV±VIS JASCO V-530 spectrometer using 1 cm quartz cells at appropriate wavelengths. The entrapment efficiency (E%) was calculated using the Eq. 1

$$E\% = \frac{D}{ND} \times 100 \qquad \qquad Eq.1$$

Where ND and D are the drug concentration before and after the dialysis. Each experiment was carried out in triplicate.

2.1.6 Transdermal permeation study

In vitro skin permeation studies were performed using vertical diffusion Franz cells with an effective diffusion area of 0.416 cm^2. The experiments were carried out using rabbit ear skin, obtained from a local slaughterhouse. The skin, previously frozen at -18°C, was pre-equilibrated in physiological solution at room temperature for 2 h before the experiments.

A circular piece of this skin was sandwiched securely between the receptor and donor compartments: epidermal side of the skin was exposed to ambient condition while dermal side was kept facing to receptor solution. The donor compartment was charged with an appropriate volume of niosomal dispersion, so that the drug moles were constant. The receptor compartment was filled with 5,5 mL of distilled water which was maintained at 37 ± 0.5°C and stirred by magnetic bar. Before starting the experiments the donor cell was sealed with parafilm.
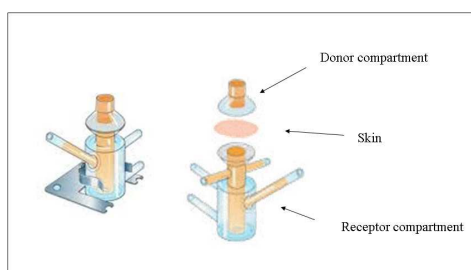
Fig.2.3 Schematic illustration of a Franz cell

At regular intervals up to 24 h the receiver compartment was removed and replaced with an equal volume of pre-thermostated (37 ± 0.5°C) fresh distilled water solution. The complete substitution of the receiver compartment was needed to ensure sink conditions and quantitative determination of the small amounts of drug permeated. The content of drug in the samples was analyzed by UV-Vis spectrometry. Each experiment was carried out in triplicate and the results were in agreement within ±4% standard error.

2.1.7 Release study

The release of a model hydrophilic drug from niosomes was examined under sink conditions. Aliquots of niosomal suspension was placed in dialysis bags (Visking dialysis tubes, 20/30), and suspended in 50 mL of distilled water at 37 °C under gentle magnetic stirring. At predetermined time intervals, 2 mL of the medium were withdrawn and the volume of receptor compartment was maintained with an equal volume of distilled water. The drug in withdrawn samples was estimated by UV-Vis spectrometry and the drug release percent was determined using the following equation:

$$Drug \quad release(\%) = \frac{M_t}{M_i} \times 100$$

Eq.2

where M_i and M_t are the initial amount of drug encapsulated in the niosomes and the amount of drug released at the time t, respectively. All the experimental procedure was repeated three times and the results were in agreement within ±4% standard error. The release of the free drug was also investigated in the same way.

2.2 Advantages of niosomes

The first report of non-ionic surfactant vesicles came from the cosmetic applications devised by L'Oreal.[10] The application of non-ionic surfactant vesicles systems in cosmetics and for therapeutic purpose may offer several advantages:

- they exhibit special characteristics such as easy handling and storage;
- they improve oral bioavailability of poorly absorbed drugs and enhance skin penetration of drugs;
- they can be made to reach the site of action by oral, parenteral as well as topical routes;
- they improve the therapeutic performance of the drug molecules by delayed clearance from the circulation, protecting the drug from biological environment and restricting effects to target cells;
- they offer the possibility to control the vesicle characteristics altering the vesicle composition;
- they can be use as a depot, releasing the drug in a controlled manner;
- in addition, there is a greater availability of surfactant classes, that show good biocompatibility, biodegradability and non-immunogenic properties.

2.3 Advances in niosomes application

Although niosomal formulations have yet to be commercially exploited, a number of studies have demonstrated the potential of niosomes for industrial productions both in pharmaceutical and cosmetic applications.

Niosomes as delivery devices have also been studied with anticancer, anti-tubercular, anti-leishmanial, anti-inflammatory, hormonal drugs and oral vaccine.[11]

2.3.1 Anti-cancer drug

Niosomes containing doxorubicin and based on C16 monoalkyl glycerol ether with or without cholesterol exhibited an increased level of drug in tumor cells, serum and lungs, but not in liver and

spleen and decreased the rate of proliferation of tumor and increased life span of tumor bearing mice. In addition the cardio toxicity effect of the loaded drug was reduced.[12]

Another study confirmed that daunorubicin hydrochloride-loaded niosomes exhibited an enhanced anti-tumor efficacy when compared to free drug. This niosomal formulation was able to destroy the Dalton's ascitic lymphoma cells in the peritoneum within the third day of treatment, while free drug took around six days and the process was incomplete. [13]

Azmin et al., quoted in their research article that niosomal formulation of methotrexate exhibits higher AUC as compared to methotrexate solution, administered either intravenously or orally. Tumoricidal activity of niosomally-formulated methotreaxate is higher as compared to plain drug solution.[14]

Niosomal formulation of bleomycin containing 47.5% cholesterol exhibits higher level drug in the lever, spleen and tumour as compared to plan drug solution in tumor bearing mice.[15]

Vincristine loaded-niosomes exhibit higher tumoricidal efficacy as compared to plain drug formulation.[16]

Also, niosomal formulation of carboplatin exhibits higher tumoricidal efficacy in S-180 lung carcinoma-bearing mice as compared to plan drug solution and also less bone marrow toxic effect.[17]

2.3.2 Anti-infective agents

Niosomal formulation of sodium stibogluconate, a choice drug for treatment of visceral leshmaniasis, exhibits higher levels of antimony as compared to free drug solution in liver[18],

thus like niosomal formulation of rifampicin exhibits better antitubercular activity as compared to plain drug.[19]

2.3.3 Anti-inflammatory agents

Niosomal formulation of diclofenac sodium with 70% cholesterol exhibits greater anti-inflammation activity as compared to free drug. Niosomal formulation of nimesulide and flurbiprofen also exhibits greater anti-inflammation activity as compared to free drug.

Incorporating them into niosomes enhances the efficacy of drug, such as diclofenac sodium, nimesulide, flurbiprofen, piroxicam. [20-22]

2.3.4 Diagnostic imaging with niosomes

Niosomal system can be used as diagnostic agents. Conjugated niosomal formulation of gadobenate dimeglcemine with [N-palmitoyl-glucosamine (NPG)], PEG 4400, and both PEG and NPG exhibit significantly improved tumor targeting of an encapsulated paramagnetic agent assessed with MR imaging .[23]

2.3.5 Ophthalmic drug delivery

Bioadhesive-coated niosomal formulation of acetazolamide prepared from Span 60, cholesterol stearylamine or dicetyl phosphate exhibits more tendency for reduction of intraocular pressure as compared to marketed formulation (Dorzolamide). The chitosan-coated niosomal formulation timolol maleate (0.25%) exhibits a relevant reduction of intraocular pressure as compared to a marketed formulation with less chance of cardiovascular side effects.[24]

A modified form of niosomes, the discomes, are also used in ophthalmic drug delivery systems.[25] Discomes are large structures (12–16 mm) derived from niosomes by the addition of non-ionic surfactant, that is Solulan C24. They have particular advantages for ocular drug delivery, since, as a result of their larger size, they can prevent their drainage into the systemic pool; also their disc shape could provide a better fit in the cul-de-sac of the eye.[26]

Discosomes have been reported successfully, as ocular vehicles for cyclopentolate. In the *in vivo* study, these carriers, independent of their pH, significantly improved the ocular bioavailability of cyclopentolate, with respect to reference buffer solution, indicating that it can be used as an efficient vehicle for ocular drug delivery.[27]

2.3.6 Transdermal drug delivery

Several mechanisms has been used to explain the ability of niosomes to modulate drug transfer through skin, e.g. (1) adsorption and fusion of niosomes on the surface of skin leading to high thermodynamic activity gradient of drug at the interface, which is the driving force for permeation of lipophilic drug, (2) reduction of the barrier properties of stratum corneum resulting from the property of vesicles as a penetration enhancer.[28] Many drugs such as estradiol[29], tretinoin[30] and dithranol[31] have been successfully encapsulated in niosomes for topical application and these systems have been reported to give a considerable drug release.[32,33] Moreover, it has been reported in several studies that compared to conventional dosage forms, vesicular formulations exhibited an enhanced cutaneous drug bioavailability.[34]

2.3.7 Niosomes in oral drug delivery

The oral delivery of drugs using niosomal formulations was first demonstrated by a study involving methotrexate loaded niosomes: an oral administration of these niosomal formulation exhibits higher concentration of drug in serum with more uptakes by the liver as compared to a free drug solution. So it concludes that gastrointestinal tract absorption of drug increases in niosomal formulation.[35]

Recently more gut labile compounds such as proteins have been administered by this route and in one of the first studies of its kind sucrose ester niosomes loaded with ovalbumin were found to cause a significant increase in the level of specific antibodies after oral administration.[36]

Some proteins and peptides such as alpha-interferon[37], cyclosporine A[38], 9-desglycinamide-8-arginine vasopressin (DGAVP)[39], GnRH-based anti-fertility immunogen[40], haemagglutinin[41], influenza viral antigens[42], insulin[43], Aciclovir[44], paclitaxel[45] have been successfully encapsulated in niosomes.
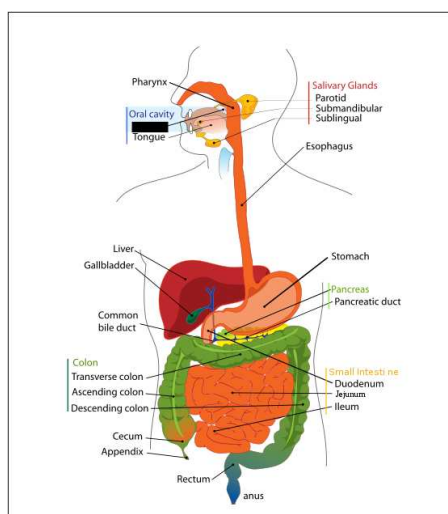
Fig.2.4 Schematic illustration of gastrointestinal tract (GIT)

2.3.8 Niosome formulation as targeted delivery system

In addition the performance of niosomal drug delivery systems might be further improved by active targeting for tumor therapy, e.g., by using a ligand coupled to the surface of niosomes, which could be actively taken up via a receptor-mediated endocytic pathway.[46,47]

References

[1] Lasic, D.D., J Coll Interf Sci, 140, (1990), 302.

[2] Florence, A.T., New Drug Delivery Systems. Chemistry and Industry, 1993.

[3] Handjani-Vila R.M., Rlbier A., Rondot B., Vanlerberghe G., Int J Cosmetic Sci 1, (1979), 303.

[4] Uchegbu I.F., Vyas S.P., Int J Pharm, 172, (1998), 33.

[5] Bangham A.D., Standish M.M. and Watkins J.C., J Mol Bio 13, (1965), 238.

[6] Fenton R.R., Easdable W.J., Meng H., Omara E.S.M., Mckeage M.J., Russel P.J.and Hambley T.W., J Med Chem, 40 (1997) 1090.

[7] a) Provencher S.W., Comput Phys Commun, 27, (1982), 213; b) S.W. Provencher, Comput Phys Commun, 27, (1982), 229.

[8] Maestrelli F., Gonzalez-Rodrıguez M.L., Rabasco A.M., Mura P., Int J Pharm, 298, (2005), 55.

[9] Trotta M., Peira E., Debernardi F., Gallarate M., Int J Pharm, 241, (2002), 319.

[10] Foco A., Gasperlin M., Kristl J., Int J Pharm, 291, (2005), 21.

[11] Buckton G., Harwood, Interfacial phenomena in Drug Delivery and Targeting Academic Publishers, Switzerland, 1995.

[12] Rogerson A. J Pharm Pharmacol, 40, (1988), 337.

[13] Balasubramanian A., Drug Dev and Ind Pharm, 28, (2002), 1181.

[14] Azmin MN., J Pharm Pharmacol, 37, (1985), 237.

[15] Naresh RAR., Ind J Pharm Sci, 58, (1996), 230.

[16] Parthasarathi G., Ind J Pharm Sci, 56, (1994), 90.

[17] Zhang JQ., Eur J Pharm Sci, 36, (2001), 303.

[18] Ballie AJ. J Pharm Pharmacol, 38, (1986), 502.

[19] Uchegbu F.I., and Vyas P.S., Int J Pharm, 172, (1998), 33.

[20] Naresh AR., Ind Drugs, 30, (1993), 275.

[21] Shahiwala A. and Misra A., J Pharm Sci 5, (2002), 220.

[22] Reddy D.N., Udupa N., Drug Dev Ind Pharm, 19, (1993), 843.

[23] Luciani A., J Radiology, 231, (2004), 135.

[24] Aggarwal D., J Pharm Pharmacol, 56, (2004), 1509.

[25] Uchegbu I.F., McCarthy D., Schatzlein A., Florence A.T., STP Pharm Sci, 6, (1996), 33.

[26] Aggarwal D., J Pharm Pharmacol, 56, (2004), 1509.

[27] Kaur I.P., Int J Pharm 269, (2004), 1.

[28] Schreier H., Bouwstra J., J Control Release 30, (1994) 1.

[29] Fang J.Y., Yu S.Y., Wu P.C., Huang Y.B., Tsai Y.H., Int J Pharm, 215, (2001), 91.

[30] Manconi M., Sinico C., Valenti D., Loy G., Fadda A.M., Int J Pharm, 234, (2002), 237.

[31] Touitou E., Junginger, H.E. Weiner N.D., Nagai T., Mezei M., J Pharm Sci, 83, (1994), 1189.

[32] Tabbakhian M., Tavakoli N., Reza Jaafari M., Daneshamouza S., Int J Pharma, 323, (2006), 1.

[33] Vyas S.P., Singh R.P., Int J Pharma, 296, (2005), 80.

[34] Manconi M., Sinico C., Valenti D., Lai F., Fadda A.M., Int J Pharm, 311, (2006), 11.

[35] Azmin MN., J Pharm Pharmacol, 37, (1985), 237.

[36] Rentel C.O., Borchard G., Naisbett B., Bouwstra J.A., Junginger H.E., Proceedings of Liposome Advances, Progress in Drug and Vaccine Delivery Systems. December 1996, London, 42.

[37] Niemac S.M., Ramachandran C., Weiner N., Pharm Res, 12, (1995), 1184.

[38] Waranuch N., Ramachandran C., Weiner N.D., J Liposome Res, 8, (1998), .225.

[39] Yoshida H., Lehr C.M., Kok W., Juninger H.E., Verhoef J.C., Bouwstra J.A., J Control Release 21, (1992), 145.

[40] Ferro V.A., Costar R., Carter K.C., Harvey M.J.A., Waterston M.M., Mullen A.B., Matschke C., Mann J.F.S., Colston A., Stimson W.H., Vaccine 22, (2004), 1024.

[41] Murdan S., Gregoriadis G., Florence A.T., Eur J Pharm Sci 8, (1999), 177.

[42] Varshosaz J., Pardakhty A., Hajhashemi V., Najafabadi A.R., Drug Deliv, 10, (2003), 251.

[43] Arunothayanun P., Turton J.A., Uchegbu I.F., Florence A.T., J Pharm Sci, 88, (1999), 34.

[44] Attia I.A., El-Gizawy S.A., Fouda MA.., Donia A.M., AAPS Pharm Sci Tech, 8, (2007).

[45] Zerrin Sezgin Bayindir, Nilufer Yuksel, J Pharm Sci, Available online

[46] Dufes C., Gaillard F., Uchegbu I.F., Schätzlein A.G., Olivier J.C., Muller J.M., Int J Pharm, 285, (2004), 77.

[47] Hong M., Zhu S., Jiang Y., Tang G., Pei Y., J. Contr Rel, 133, (2009), 96.

Research Projects

on niosomes
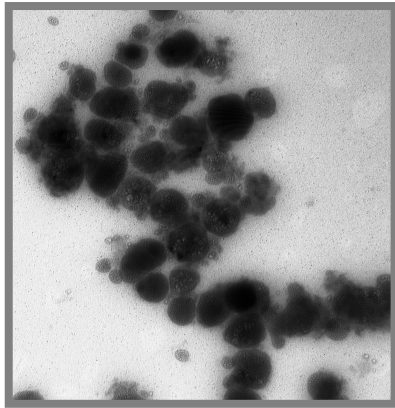
2.4.1 Characterization and permeation properties of Pluronic surfactant vesicles as carriers for transdermal delivery.

Lorena Tavano[a], Rita Muzzalupo[a], Sonia Trombino[a],

Roberta Cassano[a], Erika Cione[b] and Nevio Picci[a]

[a]*Dipartimento di Scienze Farmaceutiche Università della Calabria, Ponte P. Bucci, 87030 Rende, Italia*

[b]*Dipartimento Farmaco-Biologico, Università della Calabria, Ponte P. Bucci, 87030 Rende, Italia*

Abstract

Preparation of stable niosomes based on commercial and modified Pluronic surfactants as carriers for the delivery of Diclofenac was investigated. In particular the Pluronic surfactant was made polymerizable by including the acryloil groups. The acryloil groups were utilized for obtained also polymerized vesicles The effect on the mean vesicle diameter, drug entrapment efficiency, percutaneous permeation and release profile is monitored for a variety of vesicles with different composition. The results indicate an increase in mean vesicle diameter and entrapment efficiency with the increase of polymerizable moieties. These properties were found to be more evident when the vesicles were polymerized. Diclofenac as model drug was incorporate in the vesicles and percutaneous permeation profile was carried out by using Franz Diffusion cells at physiological condition. Moreover the *in vitro* release of incorporate drug was performed at pH 7.4 to evaluate the potential use of these new carrier in parenteral formulations. In addition cytotoxic effects was estimated. The results of this study show that niosomes based on commercial, functionalized or a mixture of both Pluronic surfactant can be used to achieve retarded or enhanced release of drug, without incurring unacceptable toxicity.

1. Introduction.

Copolymers consists of ethylene oxide (EO) and propylene oxide (PO) blocks arranged in a triblock structure, in which the hydrophobic PPO group is in the middle providing the links to the two hydrophilic PEO groups are known under a variety of trade names such as Pluronic, Synperonic, or Poloxamer. The amphiphilic nature of the Pluronics makes them extremely useful in various fields as emulsifiers and stabilizers [1] and for pharmaceutical applications [2,4].

Pluronic possesses specific pharmacological actions, in particular the dynamic PEO chains prevent particles opsonization and render them 'unrecognizable' by reticulo-endothelial system (RES), macrophages and offer an interesting alternative to reduce significant hepatic uptake [5,7].

Moreover Pluronic has been proposed as a carrier for osseous graft material either topically or systemically [8,9] and several studies reported the interaction of Pluronic with liposomes [10-12]: in particular these polymers have been used to sterically stabilize vesicles [1314], and, hence, prolonged their half-life [15].

These invaluable advantages have promoted extensive research to develop most attractive drug carriers such as polymeric micelles formed by hydrophobic–hydrophilic block copolymers, with the hydrophilic blocks comprised of PEO chains, so far, no report has been published on utilizing Pluronic surfactant to obtain niosomes.

In this light the aim of the present study was to design unilamellar niosomal formulations of Diclofenac based on Pluronic L64 to be applied topically or intravenously.

In addition, to enhance the stabilization of vesicles and to prevent degradation caused by significant dilution accompanying IV injection, polymerized niosomes have been prepared as an alternative by introducing acryloyl groups into Pluronic surfactant. The concept of polymerized vesicles as an important class of materials was introduced from early 1980s by numerous researchers, as reported in literature [16-19], with the suggestion that they exhibit greater stability than conventional vesicles but they should also retain many of their important properties e.g., the ability to promote the separation of charged photoproducts and entrap and slowly release drugs [20-22].

In this study we prepared niosomes with different ratio between L64 and L64 acrylate and both before and after the polymerization, we investigated size, morphology, drug encapsulation, *in vitro* performance of these formulations and cytotoxic effects.

2. Materials and methods

2.1 Chemicals and instruments

Pluronic L64 was kindly donated by BASF (Mount Olive, NJ, USA).

All reagents were purchased from Sigma-Aldrich (St. Louis, MO, USA). Acryloyl chloride was distilled before being used while other reagents were used with no further purifications. The solvents are of high performance liquid chromatography grade. Water from a Millipore Milli-Q® ultrapure water purification unit was used. RAT-1 immortalized fibroblasts cells were purchased from the American Type Culture Collection. Culture media were obtained from Invitrogen Life Technologies, Italy. To ensure the synthetic quality IR spectra were performed with a FT-IR JASCO 4200 spectrometer, and ^{1}H-NMR spectra were recorded with a Bruker 300 ACP NMR spectrometer. The content of drug in the release studies was analyzed by UV±VIS JASCO V-530 spectrometer using 1 cm quartz cells at 264 nm.

2.2 Preparation of L64 methacrylate monomer

The L64 acrylate monomer was synthesized according the procedure shown in the Fig.1 and reported in literature [23].

CH₃ → CH_3

$$HO\text{-}(CH_2CH_2O)_{13}\text{-}(CH_2CHO)_{30}\text{-}(CH_2CH_2O)_{13}\text{-}H$$

Et₃N, acryloyl chloride
THF dry

$$CH_2 = \overset{O}{\underset{}{C}} - O\text{-}(CH_2CH_2O)_{13}\text{-}(CH_2CHO)_{30}\text{-}(CH_2CH_2O)_{13} - C = CH_2$$
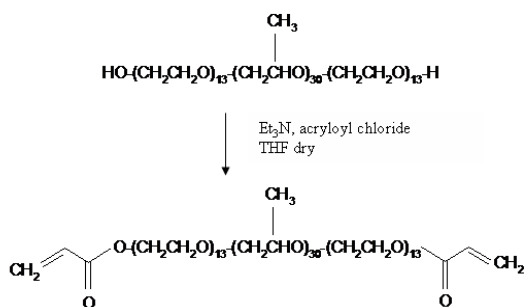
Fig.1 Schematic representation of the synthesis of L64$_{Acr}$.

Triethylamine (Et$_3$N, $1{,}44 \times 10^{-3}$ mol) was added to the stirred solution of L64 ($6{,}9 \times 10^{-4}$ mol) in 100 ml of dry THF at 25°C. After 30 min a quantity of acryloyl chloride equimolar to the amount of Et3N was added dropwise to the surfactant solution at 0°C and the reaction was left to proceed by stirring for 24 hours at 25°C. The final product was filtered remove triethylamine hydrochloride and then the functionalized surfactant was obtained by pouring the filtrate into an excess of n-hexane. Finally it was dried under reduced pressure for 24 h.

The obtained functionalized L64 monomer was a quite viscous ivory-like liquid and the yield was 90%.

IR values (on KBr) are are 3107, 1785 cm^{-1}. These peaks are significant for the formation of functionalized L64$_{Acr}$, in fact 3107 cm^{-1} is the terminal olefins stretching and 1785 cm^{-1} is the stretching C=O of new esteric bonds.

The chemical shift values of the L64$_{Acr}$ monomer protons (in ppm) performed in CDCl$_3$, at 300 MHz are reported in Fig.2.
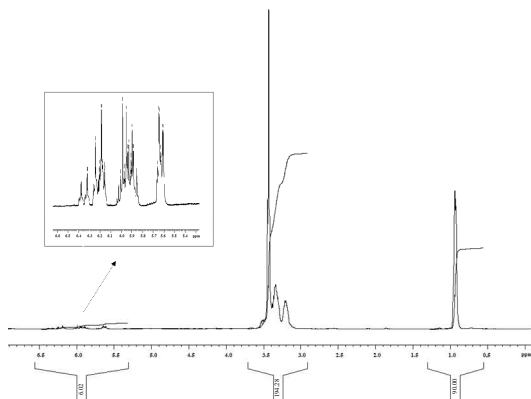
Fig.2 ^{1}H-NMR spectrum of L64$_{Acr}$.

2.3 Cell culture

RAT-1 immortalized fibroblasts (American Type Culture Collection, Rockville, MD, USA) were grown in MEM medium without antibiotics supplemented with 10% fetal calf serum and 2mM glutamine. Cells were maintained in log phase by seeding twice a week at density of $3\text{x}10^5$ cells/ml at 37°C in a humidified atmosphere at 5% CO_2 in air. Cell number has been estimated with a Burker camera. Drug free niosomes suspension were diluted in cell culture media.

2.4 In vitro evaluation of toxicity

The cytotoxic effects of the drug free niosomes on RAT-1 cells were evaluated with the trypan blue dye exclusion assay (cell mortality) and the MTT dye test (cell viability). RAT-1 were seeded at a density of 3×10^4 cells/ml in 12-well plastic culture dishes for the trypan blue dye exclusion test and at a density of 2×10^4 cells/ml in 12-well tissue culture plates for the MTT test. After 24 h of incubation, the culture medium was replaced with serum free medium and free drug niosomes were added at final scalar dilutions (0-10 μM). The toxicity experiments were carried out at 24h incubation times. Untreated RAT-1 cells were used as the control and the blank sample in various experiments, respectively. To perform the trypan blue dye exclusion assay, RAT-1 were harvested using trypsin/EDTA (1×) solution (2 ml), washed twice with phosphate buffer solution (2 ml) and transferred into plastic centrifuge tubes with 4 ml. Samples were then centrifuged with a ALC PK 120R at 1200 rpm at room temperature for 5 min. The supernatant was discarded and the pellet was suspended in 200 μl of trypan blue buffer, for 30 seconds and the amount of dead cells (blue stained cells) was observed and counted with a Burker camera using an optical microscope (Olympus CKX31). The percentage of cell mortality was calculated using the following equation:

$$Mortality(\%) = \frac{C_D}{C_T} \times 100 \qquad\qquad\qquad\qquad\qquad \text{Eq.3}$$

where C_D is the number of dead cells and C_T the total number of cells. Cell viability assay was carried out following the MTT dye test. RAT-1 cells were seeded at a density of 2×10^4 cells/ml in a 12-well culture plates for 24 h at 37°C and 5% CO_2 to allow the adhesion of culture cells. After 24 h of incubation, the culture medium was removed and substituted with serum free fresh medium, RAT-1 immortalized fibroblasts cells were then treated with drug free niosomes. At the end of the incubation time 50 μl of MTT tetrazolium salt (5 mg/ml dissolved in PBS buffer) were added to each well and at RAT-1 cells were incubated for additional 3 h, to allow the formation of violet formazan crystals. A solution of 0.04 N HCl in isopropanol (1 ml) was added to solubilize the formazan crystals in the cells. The absorbance was measured with the Ultrospec 2100 pro spectrophotometer (Amersham-Biosciences) at a test wavelength of 570 nm with a reference wavelength of 690 nm. The effect of drug treatment on the percentage of viable cells, directly proportional to the amount of formazan crystals formed, was calculated using the following equation:

$$Cell \quad viability(\%) = \frac{Abs_T}{Abs_U} \times 100 \qquad\qquad\qquad\qquad \text{Eq.4}$$

where Abs_T is the absorbance of treated cells and Abs_U is the absorbance of untreated cells. Values of cell mortality and cell viability are expressed as the mean of six different experiments ± SEM.

2.11 Statistical analyses

Statistical differences were determined by one-way analysis of variance (ANOVA). The results were expressed as mean ± SEM from three independent experiments.

3. Results and discussion

Several studies have reported that niosome were able to improve in vitro skin delivery of various drugs [24-26] and to penetrate intact skin in vivo, transferring therapeutic amounts of drugs [27] with efficiency comparable with subcutaneous administration [28].

In the present work, in order to provide new carriers suitable for above mentioned drug, we have prepared and tested niosomes made with different ratio L64-L64$_{Fun}$ to evaluate the influence of surfactant structure as well as its ability to form vesicles. The presence of surfactant containing acrylic groups prompted us to study also the niosomal systems obtained after polymerization. In this work these formulations will be reported with suffix P.

Table 1 shows all compositions of niosomes that readily formed under the conditions used in this study. All preparations were stable when kept at ambient temperature (25°C) over a period of 4 months.

Formulation Name	L64 (mg)	L64$_{Fun}$ (mg)	Ratio L64/L64$_{Fun}$
L64	290,0	0	1:0
L64-L64$_{Fun}$	145,0	150,4	1:1
L64-L64$_{Fun}$P	145,0	150,4	1:1
L64$_{Fun}$	0	300,8	0:1
L64$_{Fun}$P	0	300,8	0:1

Table 1. Composition of the vesicular systems used. The total concentration of surfactant was 1×10^{-4} M.

L64 and L64$_{Fun}$ were both able to form vesicles: different ratio L64/L64$_{Fun}$ in the vesicular suspensions leads to a variation of aggregate size, entrapment efficiency and drug release profile.

Larger vesicles were obtained with L64$_{Fun}$; when the L64$_{Fun}$ concentration was decreased from 1:0 to 0:1 (ratio L64$_{Fun}$ /L64) a systematic decrease in niosomes size was observed (Table 2). Moreover polymerized niosomes showed bigger size than respective non-polymerized.

On the basis of these results, we proposed that this fact may be due to the presence of acrylate groups in the bilayer structure made from the L64$_{Fun}$ chain surfactant that produces rigid but physically stable niosomal vesicles and could modify the microstructure of the vesicular membrane, causing a increase in the vesicle diameter. In fact, it is possible hypothesize that when the hydrophilic PEO chains present the acrylic moieties, they organized themselves withdrawing to the inside, thanks to the better affinity for the lypophilic environment and this implies an increase of niosomes diameter. A schematic model of Pluronic conformation before and after the functionalization is reported in Fig.3.
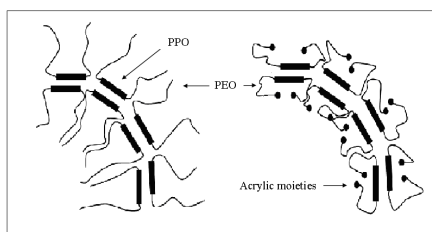
Fig.3 Model of Pluronic conformation into the bilayer before and after the functionalization.

In order to study the influence of the loaded drug on the vesicle size, drug loaded vesicles were prepared. The size of the drug-loaded niosomes detected by light scattering experiments are reported in Table 2.

Formulation Name	Empty niosomes hydrodynamic diameter (nm)	Drug	Loaded niosomes hydrodynamic diameter (nm)
L64	295±5	Diclofenac	268±5
L64-L64$_{Fun}$	349±15	Diclofenac	317±15
L64-L64$_{Fun}$P	473±20	Diclofenac	410±20
L64$_{Fun}$	440±15	Diclofenac	353±10
L64$_{Fun}$P	512±10	Diclofenac	428±10

Table 2. Hydrodynamic diameter (nm) of empty and drug-loaded vesicular systems at 25°C.
Values represent mean ± S.D. ($n = 3$).

Dynamic light scattering analyses pointed out that vesicle sizes were affected by the inclusion of the drug. In fact, empty niosomes based on L64 were smaller than the corresponding drug loaded ones.
On the other hand, L64-L64$_{Fun}$ ad L64$_{Fun}$ samples were bigger than the Diclofenac-loaded ones and it is due to the presence of acrylic moieties and the interaction between these portions and the hydrophilic drug that involves an increase of cohesion of the bilayer and a reduction in the vesicle diameter.
Polydispersity was observed to be about 0.005 for L64-based niosomes, while other formulations showed polidispersity values higher (about 0,2): these values were considered as evidence of homogeneous distribution of colloidal vesiscles.

3.1 Transmission electron microscopy (TEM)
The morphology of the monomeric and polymerized liposomes was observed using TEM and images of the different niosomal formulations are shown in Fig.4. TEM analysis shows some similarity in the vesicular nature of the preparations, in fact all vesicles were found to be spherical in shape. In particular the spherical shape of the polymerized niosomes showed that the polymerization technique has not affected the spherical morphology of the vesicles, even if the edges are irregular.
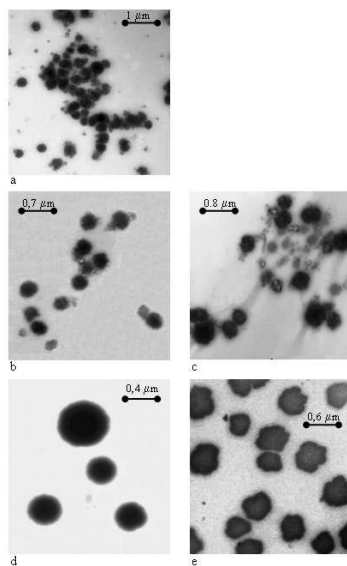
Fig.4 Photomicrographs of niosomal formulations as seen by TEM: a) L64, b) L64-L64$_{Fun}$, c) L64-L64$_{Fun}$ P, d) L64$_{Fun}$ and e) L64$_{Fun}$ P.

3.2 Drug entrapment efficiency

The ability of DDS to entrap and retain a drug is very important to evaluate the potential therapeutic use of certain carrier, particularly if the carrier has to be used for topical application. Diclofenac incorporation efficiencies of all niosomal formulations are reported in Table 3, where it is evident that the incorporation capability of all the studied formulations is very high.

Formulation Name	Drug	Entrapment efficiency(%)
L64	Diclofenac	38.00±2.81
L64-L64$_{Fun}$	Diclofenac	43.00±1.66
L64-L64$_{Fun}$P	Diclofenac	63.00±1.57
L64$_{Fun}$	Diclofenac	50.00±2.55
L64$_{Fun}$P	Diclofenac	67.00±2.01

Table 3. Entrapment efficiency of drug-loaded vesicular systems.
Values represent mean ± S.D. (n=3).

The L64 and L64-L64$_{Fun}$ formulations encapsulated almost similar percentage of the drug (38% and 43% respectively). However 50% of Diclofenac was encapsulated in the L64$_{Fun}$ formulation. This suggest that the increase in the amount of L64$_{Fun}$ led to an increase of Diclofenac incapsulation and this is probably due to good affinity between niosomal matrix and drug.

Moreover the encapsulation efficiency of L64-L64$_{Fun}$P was higher than the non-polymerized ones (63%), as found for the L64$_{Fun}$ and L64$_{Fun}$P formulations (50% and 67% respectively): probably the rigid and robust structure of polymerized niosomes have better affinity for the Diclofenac than the non-polymerized ones and could increased stability and protection of drug.

These results confirm that the entrapment of water-soluble molecules generally depend on the composition of the bilayers.

3.3 Transdermal permeation study

The slow and controlled release of encapsulated material is one of the requirements for the delivery of drugs [29]. In vitro percutaneous permeation of Diclofenac from different formulations was carried out by using Franz diffusion cell and Fig.5 shows the results of our study. As reported the permeation of Diclofenac from the solution through the stratum cornem was lower than that obtained from vesicles. This is due to the fact that the bilayer structure of vesicles is made up of surfactant that can behave as penetration enhancers thus allowing a temporary charge in packing order of stratum corneum, enabling drug passage across the skin.
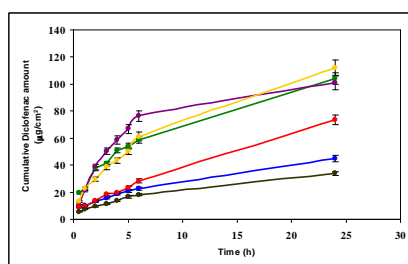
Fig.5. Cumulative amount versus time of permeated Diclofenac: (●) L64, (●) L64-L64$_{Fun}$, (●) L64-L64$_{Fun}$P, (●) L64$_{Fun}$, (●) L64$_{Fun}$P and (●) Diclofenac.

Significant changes in cutaneous permeation were observed with change in surfactant content in the bilayer of niosomes: L64 sample released 43% of the encapsulate drug in 24 hours, however, L64-L64$_{Fun}$ and L64$_{Fun}$ formulations released 18% and 20% respectively of Diclofenac in the same time. Polymerized samples (L64-L64$_{Fun}$P and L64$_{Fun}$P) show an increase of released Diclofenac as compared to non-polymerized ones. The permeation of drug was about 41% and 46% respectively within 24 h.

It is evident from these data that the polymerized niosomes improve the permeation of Diclofenac as compared to L64, L64-L64$_{Fun}$ and L64$_{Fun}$ samples; most likely the polymerization of monomer involved the formation of elution channels within the niosomal matrix structure, thereby the drug incorporated can be released rapidly, whereas the drug, entrapped in the internal aqueous core of

34

non polymerized vesicles, permeated more slowly, since it had first to overcome the acrylic moieties barrier of the bilayer, free to move.

The percutaneous permeation profile was found to be positively dependent from the interaction between skin and vesicles: in fact, the transdermal diffusion of Diclofenac from $L64_{Fun}P$, using synthetic membrane was the lowest, as shown in Fig.6.
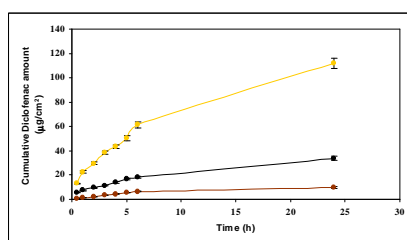
Fig.6. Cumulative amount versus time of released Diclofenac:
(●) $L64_{Fun}P$-membrane, (●) Diclofenac and (●) $L64_{Fun}P$-skin.

3.4 Release studies

The cumulative amount of Diclofenac released from free drug solution and niosomal formulations is shown in Fig.7.

In this study we reported only the formulations based on commercial L64, $L64_{Fun}$ and $L64_{Fun}P$ surfactant.
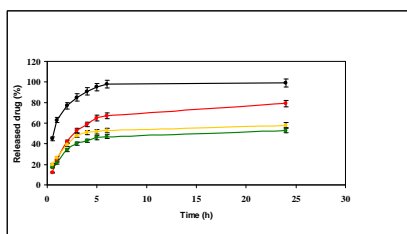
Fig.7 In vitro release profile of Diclofenac-loaded niosomes at pH 7.4:
(●) Diclofenac, (●) $L64_{Fun}$ (●), $L64_{Fun}P$ and (●) L64.

In vitro studies revealed that the cumulative release rate of Diclofenac from niosome preparations in simulate plasmatic fluid was significantly slowed down compared with free solution and percent of drug released was maximum for $L64_{Fun}$-based niosomes and minimum for both L64 and $L64_{Fun}P$-based niosomes. Fig.7 show that a slow release of Diclofenac from all samples was observed during the first h. By 3h, about 85% of Diclofenac was released from free solution, while all the niosomal formulations showed about 50% of release. When the test is over, about 100% of solute was released from free solution while only 53, 58 and 79% of drug was released from L64, $L64_{Fun}P$ and $L64_{Fun}$ niosomal formulations respectively.

35

This may confirm the possible molecular conformation assumed by the modified surfactant before the polymerization. In fact the in vitro cumulative release depends on the drug diffusion coefficient across the niosomal bilayer and $L64_{Fun}$ based niosome is the sample with the higher drug amount released.

The release experiments clearly indicate that the amount of drug released from niosomal formulations is effectively retarded.

3.5 Effect of niosomes on vitality of RAT-1 cells.

In order to examine the cytotoxic effect of the different niosomal formulations on RAT-1 cells vitality, the cells were cultured with all niosomal formulations in a concentration range from 0 to 10 μM for 24 h as described in section 2.10, and MTT assay was carried out with cells cultured in niosomes-free media as control. No significant change in viability was observed in RAT-1 treated in a range of 0-0.1 μM for L64, $L64$-$L64_{Fun}$ and $L64$-$L64_{Fun}$ P (Fig.8a, 8b, 8d), while no change was appreciated in cell viability for $L64_{Fun}$P (Fig.8e) in a concentration range of 0-1.0 μM. On the contrary, a reduction of vitality was found in the cells incubated with L64, $L64$-$L64_{Fun}$ and $L64$-$L64_{Fun}$P at 1 μM of 25%, 30% and 15% respectively (Fig.8a, 8b, 8d). A significant reduction of 25% in vitality was found in the cells incubated with $L64_{Fun}$ at concentrations of already 0.1 μM increasing to 40% at 1 μM (Fig.8c). After exposure to 10 μM concentrations cell viability was less than 50% for L64 and $L64$-$L64_{Fun}$P, about 70% for $L64_{Fun}$ and $L64$-$L64_{Fun}$ and less than 65% for $L64_{Fun}$P (Fig.8e).

Fig.8 Influence of niosomal formulation on RAT-1 cell line: a) L64, b) $L64$-$L64_{Fun}$, c) $L64_{Fun}$P, d) $L64$-$L64_{Fun}$P and e) $L64$-$L64_{Fun}$P.

The present results show that niosomes had a dose-dependent effect on viability of RAT-1 cells and were well tolerated for exposition at concentration up to 1 μM.

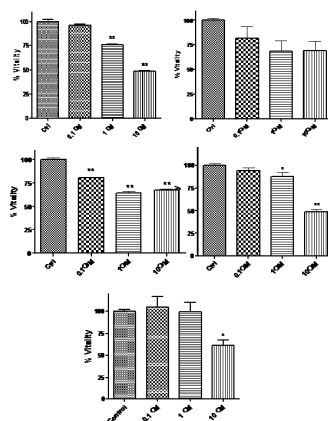In summary in this paper new niosomal formulations based on commercial and modified Pluronic surfactant were introduced and the effects of polymerizable groups on the vesicles particle sizes, morphology, in vitro model drug release and percutaneous permeation were illustrated.

The results show that dimensional and physicochemical properties can be modulated by varying the bilayer composition of vesicles: a systematic increase in niosomes size was observed with an increase of acrylic moieties amount. Also the entrapment efficiency of Diclofenac was enhanced by the presence of polimerizable groups.

Increased percutaneous permeation across rat skin as compared to control drug solution suggests that niosomal formulation has potential for transdermal delivery and enhanced drug release recommend them as possible novel long-circulating carriers for drug delivery.

These findings naturally lead to more diversified applications in pharmaceutical fields.

References
[1] Alexandridis, P., 1997. Poly(ethylene oxide)/poly(propylene oxide) block copolymer surfactants. Curr Opin Coll Polym Sci. 2:478–89.
[2] Koffi, A.A., Agnely, F., Ponchel, G., and Grossiord, J.L., 2006. Modulation of the rheological and mucoadhesive properties of thermosensitive poloxamer-based hydrogels intended for the rectal administration of quinine. Eur. J. Pharm. Sci. 27:328-35.
[3] Dumortier, G., El Kateb, N., Sahli, M., Kedjar, S., Boulliat, A., and Chaumeil, J.C., 2006. Development of a thermogelling ophthalmic formulation of cysteine. Drug Dev. Ind. Pharm. 32:63-72
[4] Dumortier, G., Zuber, M., Barges, N., Chast, F., Dutertre, H., and Chaumeil, J.C., 1994. Lacrimal and plasmatic kinetics of morphine after an ophthalmic delivery of three different formulations. Drug Dev. Ind. Pharm. 20:1147-158.
[5] Jeon, S.I., Lee, J.H., Andrade, J.D.,. Gennes, P.G.D., 1991. Protein-surface interactions in the presence of polyethylene oxide: I. Simplified theory. J.Colloid Interface Sci. 142:149-58.
[6] Moghimi, S.M., 1999. Re-establishing the long circulatory behaviour of poloxamine-coated particles after repeated intravenous administration, applications in cancer drug delivery and imaging. Biochim. Biophys. Acta 1472:399-403.
[7] Moghimi, S.M., 2003. Modulation of lymphatic distribution of subcutaneously injected poloxamer 407-coated nanospheres. FEBS Lett. 540:241-44.
[8] Fowler, E.B., Cuenin, M.F., Hokett, S.D., Peacock, M.E., McPherson, J.C., Dirksen, T.R., Sharawy, M., and Billman, M.A., 2002, Evaluation of pluronic polyols as carriers for grafting materials, study in rat calvaria defects. J. Periodontol.73:191-97.
[9] Clokie, C.M., and Urist, M.R., 2000. Bone morphogenetic protein excipients, comparative observations on poloxamer. Plast. Reconstr. Surg. 105:628-37.
[10] Kostarelos, K., Luckham, P.F., Tadros, Th.F., 1995. Addition of block copolymers to liposomes prepared using soybean lecithin. Effects on formation, stability and the specific localization of the incorporated surfactants investigated J. Liposome Res. 5:117-30.
[11] Kostarelos, K., Luckham, P.F., Tadros, T.F., 1998. Steric stabilization of phospholipid vesicles by block copolymers Vesicle flocculation and osmotic swelling caused by monovalent and divalent cations. J. Chem. Soc. Faraday Trans. 94:2159-168.

[12] Kostarelos, K., Tadros, T.F., Luckham, P.F., 1999. Physical Conjugation of (Tri-) Block Copolymers to Liposomes toward the Construction of Sterically Stabilized Vesicle Systems. Langmuir. 15:369-76.

[13] Jamshaid, M., Farr, S.J., Kearney, P., Kellaway, I.W., 1988. Poloxamer sorption on liposomes: comparison with polystyrene latex and influence on solute efflux. Int. J. Pharm. 48:125-31.

[14] Khattab, M.A., Farr, S.J., Taylor, G., Kellaway, I.W., 1995. The in vitro characterization and biodistribution of some non-ionic surfactant coated liposomes in the rabbit. J. Drug Target. 3:39-49.

[15] Woodle, M.C., Newman, M.S., Martin, F.J., 1992. Liposome leakage and blood circulation, comparison of adsorbed block copolymers with covalent attachment of PEG. Int. J. Pharm. 88:327-34.

[16] O'Brien, D.F., Whitesides, T.H., Klingbiel, R.T., 1981. The photopolymerization of lipid-diacetylenes in bimolecular-layer membranes. J. Polym. Sci: Polym. Lett. Ed. 19:95-01. [17] Regen, S.L., Singh, A., Oehme, G., Singh, M., 1982. Polymerized Phosphatidylcholine Vesicles. Synthesis and Characterization. J. Am. Chem. Soc. 104:791-95.

[18] Sadownik, A., Stefely, J., Regen, S.L., 1986 Polymerized liposomes formed under extremely mild conditions. J. Am. Chem. Soc. 108:7789-791.

[19] Georger, J. H., Singh, A., Price, R. R., Schnur, J.M., Yager, P., Schoen, P.E., 1987. Helical and tubular microstructures formed by polymerizable phosphatidylcholines. J. Am. Chem. Soc. 109:6169-175.

[20] Jeong, J.M., Chung, Y.C., Hwang J.H., 2002. Enhanced adjuvantic property of polymerized liposome as compared to a phospholipid liposome. J Biotech. 94:255-63.

[21] Okada, J., Cohen, S., Langer, R., 1995. In vitro evaluation of polymerized liposomes as an oral drug delivery system. Pharm. Res. 12:576-82.

[22] Sivakumar, P.A., Panduranga Rao, K., 2001. Stable polymerized chlolesteryl methacrylate liposomes for vincristine delivery. 3:143-48.

[23] Kweon, H.Y., Yoo, M.K.,.Lee, J.H., Wee, W.R., Han, Y.G., Lee, K.G., Cho, C.S., 2003, Preparation of a Novel Poloxamer Hydrogel, J. Appl Polym. Sci. 88:2670-76.

[24] El Maghraby, G.M.M., Williams, A.C., Barry, B.W., 1999. Skin delivery of oestadiol from deformable and traditional liposomes: mechanistic studies. J. Pharm. Pharmacol. 51:1123–134.

[25] Cevc, G., and Blume, G., 2001. New highly efficient formulation of Diclofenac for the topical, transdermal administration in ultradeformable drug carriers, Transferosomes. Biochim. Biophys. Acta 1514:191–205.

[26] Boinpally, R.R., Zhou, S.L., Poondru, S., Devraj, G., Jasti, B.R., 2003. Lecithin vesicles for topical delivery of Diclofenac. Eur. J. Pharm. Biopharm. 56:389–92.

[27] Cevc, G., and Blume, G., 1992. Lipid vesicles penetrate into intact skin owing to the transdermal osmotic gradients and hydration force. Biochim. Biophys. Acta 1104:226–32.

[28] Cevc, G., 1996. Transfersomes, liposomes and other lipid suspensions on the skin: permeation enhancement, vesicle penetration, and transdermal drug delivery, Crit. Rev. Ther. Drug. Carrier Syst. 13:257–388.

[29] Langer, R., 1993. Polymer-controlled drug delivery systems. Acc. Chem. Res. 26:537-42.

2.4.2 New sucrose cocoate based vesicles: preparation characterization and skin permeation studies

Lorena Tavano, Rita Muzzalupo, Roberta Cassano, Sonia Trombino,

Teresa Ferrarelli, Nevio Picci.

Department of Pharmaceutical Sciences, Calabria University, Ponte P. Bucci,

Ed. Polifunzionale, 87030 Rende, Italy

Abstract.

A commercial sucrose cocoate surfactant was used to obtain a new vesicular system for transdermal drug delivery. The preparation, the dimensional and morphological characterizations and the skin permeation profile of these new niosomes were evaluated. Moreover we studied the possible employment of mixture of sucrose cocoate and cholesterol at different weigh ratios for the vesicles preparation and we analyzed the influence of cholesterol on niosomes properties. Diclofenac and Sulfadiazine were used as model drugs.

Results suggest that sucrose cocoate was able to form vesicles in the presence or not of cholesterol and the addition of cholesterol leads to a variation of size: larger vesicles were obtained in the absence of cholesterol both in empty and drug-loaded niosomes. All vesicles were spherical and regular in shape.

In vitro skin permeation profiles were significantly higher than the free drug solution, indicating the favourable relations between skin and niosomes. The faster release of the drug was found for niosomes with no cholesterol or with a reduced amount of this membrane additive, in particular the optimal formulation was that in which the cholesterol content was about 27% wt of total lipid amount: probably this value is a good compromise between the membrane stability and its deformation capacity, allowing a higher drug permeation across the skin.

1. Introduction.

Despite of the significant number of publications on sugar fatty acid esters (SFAE) beginning in the mid-1950s, there is a renewed interest in these compounds with a noteworthy increase of studies in the last two decades. These studies have been motivated by their properties such as biodegradability, biocompatibility, low toxicity and their derivation from renewable sources [1-6]. Sugar fatty acid esters have a large number of applications in many fields such as cosmetic and pharmaceutic [7,8]. They are widely used in cosmetic products due to their low irritating properties and to the improvement of the sensorial characteristic of formulations in terms of skin feel and

mildness. Moreover they can be applied in pharmaceutical technology as emulsifiers, solubilizing agents, lubricants, penetrating enhancers and pore forming agents [9-15]. Also the raw materials involved in their synthesis are low-cost and easily available.

Sucrose esters exhibit also important pharmacological properties: as reported in literature, in fact, they are claimed to show antimicrobial and antimycotic activity [16-20]. Recently they were classified as a new class of inhibitors of cancer development because they inhibited TNF-alpha release from KATO III cells [21] and also exhibited significant anti-tumor-promoting effects [22].

Thus, this study was designed to evaluate the suitability of a commercial sucrose cocoate surfactant based niosomes as permeation enhancers for transdermal drug delivery. In this light we evaluated the possible employment of mixture of sucrose cocoate and cholesterol at different molar ratios for the vesicles preparation. The size, morphology, drug encapsulation efficiency and loaded-drug percutaneous permeation profile *in vitro* were investigated. Non-steroidal anti-inflammatory drug as Diclofenac sodium, widely used for the treatment of local and chronic inflammatory, and an antibiotic such as Sulfadiazine, used for the topical cure of infected burns, were used as model drugs.

2. Materials

Sucrose cocoate (TEGOSOFT LSE 65K®) was obtained from A.C.E.F. s.p.a. Diclofenac sodium salt and Sulfadiazine sodium salt were obtained from Sigma and used as received. All the other reagents were of analytical grade and were purchased from Sigma. The content of drug in the release studies was analyzed by UV-VIS JASCO V-530 spectrometer using 1 cm quartz cells at appropriate wavelengths.

3. Results

The aim of this work was the preparation of new sucrose cocoate based niosomal carriers suitable for percutaneous permeation. Their ability to form vesicles with different amounts of cholesterol was also evaluated. In fact, cholesterol is one of the most common additive included in vesicular formulations in order to improve their stability, to reduce or prevent leakage of drug and to maximize their longevity [23-26]. The study of the effects of cholesterol on the physical and structural properties of vesicular bilayers is important for understanding the mechanism of interaction between cholesterol and non-ionic surfactants in vesicular systems, that could influence the niosomes properties such as ion permeability, enzymatic activity, aggregation, fusion processes, elasticity, size and shape.

Table 1 shows the composition of different niosomal formulations.

Sucrose cocoate is a mixture of fatty acid sucrose esters, produced through the chemical esterification of coconut oil with sucrose. Coconut oil contains fatty acid chains of different lengths, as reported elsewhere [27]. Due to an inability to know exactly the sucrose cocoate molecular weight, we decide to test different weight of the surfactant to find the optimal amount for obtaining usable niosomes. All preparations were stable when kept at ambient temperature (25°C) over a period of 8 months.

Formulation Name	Surfactant mg	Ch mg	Ratio Surf/Ch	Ch %
T1	36.9	0	1:0	--
T2	29.5	11.2	1:0.37	27
T3	24.8	18.1	1:0.73	45

Table 1. Composition of the vesicular systems

3.1 Size and distribution analysis

Addition of cholesterol into these vesicular suspensions leads to a variation of size: larger vesicles were obtained in the absence of chlolesterol.

When the cholesterol amount was elevated from 1:0 to 1:0.73 (weight ratio Surf/Ch, 0-45% Ch weight) a systematic decrease in niosomes size was observed. A 40% decrease in size was seen when the weight ratio Surf/Ch was 1:0.37 (211 nm). Additional 20% decrease in size was measured when the cholesterol content was further increased from 0.37 to 0.73 (Table 2).

The relationship observed between niosome size and bilayer composition (cholesterol content) has been attributed to the decrease in surface energy with increasing hydrophobicity [28] that results in smaller vesicles: T1 formulation have a much lower hydrophobicity than those containing cholesterol.

The polydispersity index was between 0,26 and 0,30: these values were considered as evidence of homogeneous distribution of colloidal vesiscles.

The dimensions of niosomes entrapping drug were similar to those of empty ones for all formulation, as reported in Table 3. Both in empty and drug-loaded niosomes, the size decrease with the presence of cholesterol.

41

Formulation name	Diameter Nm	Polydispersity Index
T1	341±15	0.262
T2	211±15	0.259
T3	157±20	0.304

Table 2. Hydrodynamic diameter and polidispersity index of the empty niosomes

Formulation Name	Drug	Diameter (nm)
T1d	Diclofenac	314±10
T2d	Diclofenac	162±20
T3d	Diclofenac	150±20
T1s	Sulfadiazine	335±10
T2s	Sulfadiazine	234±15
T3s	Sulfadiazine	218±15

Table 3. Hydrodynamic diameter of loaded niosomes

This behavior is due both to the increased hydrophobicity of the systems and to the favourable interactions (hydrogen bonding or Van der Waals forces) between niosomial matrix and drugs.

3.2 Drug entrapment efficiency

Under analogous preparation conditions, equal level of drug were added with the aim to test the effect of molecular structure on entrapment efficiency. Niosomes without cholesterol has certain encapsulation and the quantity of entrapped Diclofenac or Sulfadiazine increased with increasing cholesterol content (Table 4): this suggests that the increase in the amount of this additive led to an increase of vesicle drug incorporation. Probably the rigid structure and low permeability could prevent drug leak from T3 formulation. Moreover when vesicles were loaded with Sulfadiazine, the E% values were lower than niosomes containing Diclofenac: in this case, the amount of drug

entrapped into niosomes, could be dependent on its affinity toward surfactant, confirming that the entrapment of water-soluble molecules generally depend on the bilayers composition [29].

Formulation Name	Drug	E%
T1d	Diclofenac	36.20±1.90
T2d	Diclofenac	40.66±1.85
T3d	Diclofenac	43.86±1.75
T1s	Sulfadiazine	13.60±2.70
T2s	Sulfadiazine	17.26±2.50
T3s	Sulfadiazine	18.60±2.25

Table 4. Entrapment efficiency (E%) of the loaded niosomes.

3.3 Trasmission electron microscopy (TEM)

The scanning electron microscopy images of the niosomes, prepared from different formulations, were found to be spherical and regular in shape: Fig.1 reported T1 formulation as example.
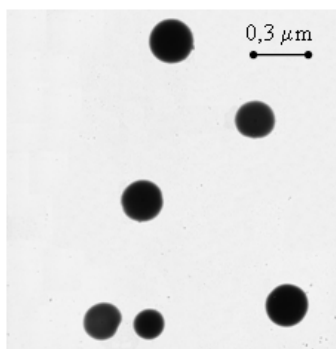
Fig.1 TEM photomicrographs of T1 niosomal formulations.

3.4 In vitro permeation studies

For hydrophilic drugs, the penetration enhancing effect seems to play a more important role in the enhanced skin delivery than in the case of lipophilic drugs (as for many penetration enhancers), since permeation of hydrophilic molecules tends to be relatively slower [30-34].

Diclofenac release from niosomes is analogous to that of Sulfadiazine and this trend is probably due to their similar weight and interactions between them and skin. As shown in Figures 2 and 3, the drugs release rates, loaded in vesicles across the skin, is significantly higher than the free drug solution, showing the favourable relations between skin and niosomes may be an important contribution to the improvement of transdermal drug delivery.

The faster release of the drug was found for niosomes with no cholesterol or with a reduced amount of this membrane additive (T2, ratio Surf/Ch 1/0.37); the increase of cholesterol content (T3, ratio Surf/Ch 1/0,73) resulted in a reduction of membrane permeability, which led to lower drug elution from the vesicles [35,36]. Cholesterol in fact is know to abolish the gel to liquid phase transition of niosomal systems, resulting in niosomes that are less leaky [37].
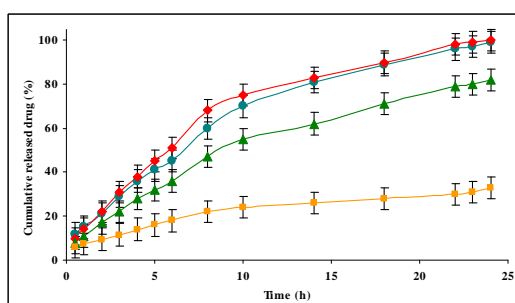
Fig.2. In vitro percutaneous permeation of Diclofenac-loaded niosomes: free solution (■), T1d (●), T2d (♦) and T3d (▲) formulations.
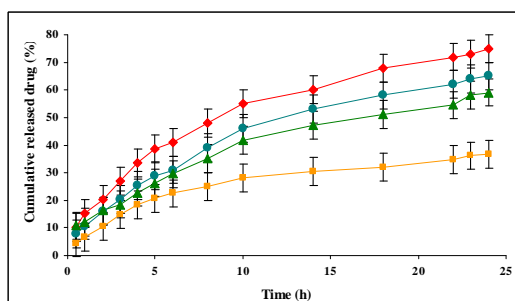
Fig.3. In vitro percutaneous permeation of Sulfadiazine-loaded niosomes: free solution (■), T1s (●), T2s (♦) and T3s (▲) formulations.

Several mechanisms could be proposed to explain the ability of niosomes to modulate drug transfer across the skin: structure modification of the skin, due to the temporary loss of intercellular lipid barrier properties of the stratum corneum followed by an increase in permeability; adsorption and fusion of niosomes onto the surface of skin leading to high thermodynamic activity gradient of drug at the interface, which is the driving force for permeation of drug [38-41]. Furthermore, as reported in literature, the cholesterol content affects membrane elasticity, making it more rigid [42]. This

effect is most pronounced at determined cholesterol concentration range. Our optimal formulation was found to be which one the cholesterol content was the 27% of total lipid amount. For this formulation both the used model drug showed the higher cumulative permeation, in fact, during 24 h the released Diclofenac amount was total, while the Sulfadiazine released was more than 75% of the loaded one.

Indeed a higher content of cholesterol involves both greater stability and lower deformability of the niosomal membranes, which results into a lower release of the carried drug [42]. T3 formulation, in fact, showed a cumulative permeation percent of about 80% for Diclofenac and 60% for Sulfadiazine. This behaviour was probably due to the niosomes greater resistance to deformation that results in a higher vesicles stability, but this effect implies also a higher rigidity that reduce their flow through small capillaries in the microcirculation and through other small apertures, for instance hair follicles or sweat pores, and consequently their loaded drug release.

However all formulations can be considered as percutaneous permeation enhancers for the hydrophilic drugs used as models. Our devices were found to be particularly useful for transdermal release when the cholesterol content was about 27% wt of total lipid amount (T2 formulation): probably this value is a good compromise between the membrane stability and its deformation capacity, allowing a higher drug permeation across the skin.

4. Conclusion

The effects of different bilayer compositions (based on a commercial sucrose cocoate and cholesterol) on the niosomes physical-chemical properties and in vitro drug percutaneous permeation were illustrated. We found sucrose cocoate able to form vesicles both in the presence or not of cholesterol. Cholesterol, used as membrane stabilizer, strongly influenced the dimension, the Diclofenac and Sulfadiazine sodium salts entrapment efficiency and the percutaneous permeation profile. Increased percutaneous permeation across the rabbit skin, respect to control drug solution, suggests that niosomal formulation has potential for transdermal delivery and enhanced drug release from the carriers. In particular the formulation that was found to be a good compromise between niosomes stability and elastic properties of the vesicles was that containing the lower cholesterol amount. In fact, an higher quantity of this last substance reduces the drug release from niosomes.

References

[1] M.T. Garcia, I. Ribosa, E. Campos, J.S. Leal, Chemosphere 35 (1997) 545.
[2] I.R. Vlahov, P.I. Vlahova, R.J. Lindhart, J. Carbohyd. Chem. 16 (1997) 1.
[3] I. Johansson, M. Svensson, Curr. Opin. Colloid Interface 6 (2001) 178.
[4] V. Molinier, J. Fitremann, A. Bouchu, Y. Queneau, Tetrahedron: Asymmetry 15 (2004) 1753.

[5] B. A.I. Van den Bergh, J.A. Bouwstra, H.E. Junginger and P.W. Wertz, J. Control. Release 62 (1999) 367.

[6] I.J.A. Baker, B. Matthews, H. Suares, I. Krodkiewska, D.N. Furlong, F. Grieser and C.J. Drummond, J. Surfact. Deterg. 3(2000) 1.

[7] F. Ahsan, J.J. Arnold, E. Meezan, D.J. Pillion, Int. J. Pharm. 251 (2003) 195.

[8] K. Hill and O. Rhode, Fett-Lipid 101 (1999) 25.

[9] N. Kanikkannan and M. Singh, Int. J. Pharm. 248 (2002) 219.

[10] A. Abd-Elbary, H.M. El-Laithy and M.I. Tadros, Int. J. Pharm. 357 (2008) 189.

[11] G. CsÓka, S. Marton, R. Zelko, N. Otomo and I. Antal, Int. J. Pharm. 65 (2007) 233.

[12] R.P. Begwe, J.R. Kanicky, B.J. Palla and D.O. Shah, Crit. Rev. Ther. Drug Carrier Syst. 18 (2001) 77.

[13] I.F. Uchegbu and S.P. Vyas, Non Int. J. Pharm. 172 (1998) 33.|

[14] P.C. Lerk, H.H. Sucker and H.F. Eicke, Pharm. Dev. Technol. 1 (1996) 27.

[15] D. Ntawukulilyayo, C. Demuynck and J.P. Remon, Int. J. Pharm. 128 (1995) 73.

[16] A. Kato, and K. Arima.. Biochem. Biophys. Res. Commun. 42 (1971) 596.

[17] N. Kato, and I. Shibasaki. J.Ferment. Technol. 53 (1975)793.

[18] L.R. Beuchat, Appl Environ Microbiol 39 (1980) 1178.

[19] D.L. Marshall and L.B. Bullerman *J. Food Sci*., 51(1986) 468.

[20] H.M. Thérien, I. Gruda, L. Bouchard *and* I. Daigle Immunoph Immunotox 11 (1989) 603.

[21] S. Okabe, M. Suganuma, Y. Tada, Y. Ochiai, E. Sueoka, H. Kohya, A. Shibata, M. Takahashi, T. Matsuzaki and H. Fujiki Jpn. J. Cancer Res. 90 (1999) 669.

[22] M. Takasaki, T. Konoshima, S. Kuroki, H. Tokuda and H. Nishino Cancer Lett. 173 (2001) 133.

[23] T.J. O'Leary, Biochim. Biophys. Acta.731 (1983) 47.

[24] K. Tajima and N.L. Gersfeld, Biophys. J. 22, 489 (1978)

[25] S. Mabery, P.L. Mateo and J.M. Sturtevant, Biochemistry 17 (1978) 2464.

[26] R.P. Rand, V.S. Parsegian, J.A.C. Henry, L.J.Lis and M. McAlister, Can.J. Biochem. 58 (1980) 959.

[27] A.H. Ensminger, M.E. Ensminger, J.E. Kolande and J.R.K. Robson, Coconut oil. In: Food and Nutrition Encyclopedia Pegasus Press, Clovis, CA (1983) 440

[28] T. Yoshioka, B. Sternberg, A.T. Florence, Int. J. Pharm. 105 (1994) 1.

[29] I. Uchegbu and S.P. Vyas, 172 (1998) 33.

[30] A.C. Williams and B.W. Barry, Int. J. Pharm. 74 (1991) 157.

[31] A.C. Williams, Transdermal and Topical Drug Delivery (1st ed.), Pharmaceutical Press, London (2003).

[32] M. Manconi, D. Valenti, C. Sinico, G. Loy and A.M. Fadda, Int. J. Pharm. 234 (2002) 237.

[33] M. Manconi, D. Valenti, C. Sinico, F. Lai, G. Loy and A.M. Fadda, Int. J. Pharm. 260 (2003) 261.

[34] M. Manconi, C. Sinico, D. Valenti, F. Lai and A.M. Fadda, Int. J. Pharm. 311 (2006) 11.

[35] S. Vemuri, C.D. Yu, J.S. de Groot and N. Roosdorp, Drug Dev. Ind. Pharm. 16 (1990) 1579.

[36] J.A. Virtanen, M. Ruonala, M. Vauhkonen, P. Somerharju, Biochemistry 34 (1995) 11568.

[37] A. Rogerson, J. Cummings and A.T. Florence, J Microenc 4 (1987) 321.

[38] D. Vanhal, A. Vanrensen, T. Devringer, H. Junginger and J. Bouwstra S.T.P. Pharma. Sci. 6 (1996) 72.

[39] I.F. Uchegbu, S.P. Vyas, Int. J. Pharm. 172 (1998) 33.

[40] E. Touitou, H.E. Junginger, N.D. Weiner, T. Nagai, M. Mezei, J. Pharm. Sci. 83 (1994) 1189.

[41] S. Bandak, A. Ramu, Y. Barenholz and A. Gabuzon, Pharm Res. 16 (1999) 841.

[42] B. Nasseri, Effect of cholesterol and temperature on the elastic properties of niosomal membranes, Int. J. Pharm. 300 (2005) 95.

2.4.3 Vesicle-polymer system for drug controlled release

Filipe E. Antunes[2], Luigi Gentile[1], Cesare Oliviero Rossi[1],

Lorena Tavano[3], Giuseppe Antonio Ranieri[1]

[1] *Department of Chemistry, University of Calabria, Ponte P. Bucci, Cubo 14/D,*
87036 Arcavacata di Rende, Cosenza, Italy;

[2] *Department of Chemical Engineering, University of Coimbra, 3030-290 Coimbra, Portugal;*

[3] *Department of Pharmaceutical Science, University of Calabria, 87036 Arcavacata di Rende, Cosenza, Italy.*

(Manuscript in preparation)

Abstract

In this research project we decide to create a gel for a drug delivery systems in wich niosomal vesicles were mixed, but also to maximize the advantages of both systems. Our strategy consists of a liquid solution with the drug loaded into the vesicles that can be injected into the body and forms a gel at 37°C. Pluronic F127 (FDA approved) was used as thermosensitive polymer thanks its well know biocompatibility and Tween 60, widely used in pharmaceutical, cosmetic, chemical and food fields was used to obtained niosomes. Several techniques were used to characterize the novel systems and also to investigate the mechanisms that govern the thermogelation of the polymer (rheological measurements, Differential Scanning Calorimetry (DSC), Dynamic Light Scattering (DLS)), while vesicles were characterized in terms of morphological, dimensional and Diclofenac sodium entrapment efficiency analysis. To evaluate the sutability of the vesicle-polymer system new carrier as potential transdermal drug delivery systems, percutaneous permeation study across rabbit ear skin was performed used the Franz cells. Results suggest that drug permeates faster when the drug is entrapped in vesicles alone solution and the permeation decreases with increasing the polymer concentration. This finding is ascribed to the fact that the drug loaded in the vesicles-polymer systems has to overcome the niosomes bilayer barriers and then the polymeric gel networks. In particular as confirmed by the rheological data, the gel network gets stronger when the concentration of polymer increases, consequently the drug presents more difficulties to move around. In addiction the very slow Diclofenac percutaneous permeation showed by the system prepared with the 18% of polymer was probably due to the worst affinity toward skin structure. These results confirmed that the systems based on Tween 60 vesicles and F127 could increase the percutaneous permeation of an hydrophilic drug, such as Diclofenac across the rabbit skin, when the amount of polymer was only about 15%: the increase of polymer content made the permeation slower than the free drug solution. These findings naturally lead to more diversified applications in trandermal drug delivery.

Materials and Methods

Pluronic F127 mixtures. Pluronic F127, $(EO)_{97}(PO)_{69}(EO)_{97}$, was a generous gift from BASF (Ludwigshafen, Germany) and was used without any further purification.

Doubly distilled, filtered and deionized water was used. The samples were prepared by weighing the desired polymer and the water amounts in vials containing a small magnetic stirring bar. The concentrations are given in percentage by weight of polymer (wt% F127) and range from 0.1 to 30 wt% of F127. The vial was sealed with an screw cap, which was fitted with a Teflon-lined septum to prevent any loss from solution, then were mixed in vortex. The prepared vials were placed in a water bath at 5 °C where the mixtures were left for 1 week before measurements.

Vesicle-F127 Polymer mixtures

The polymer mixtures were prepared by dissolving the desired amount of polymer in the stock solutions of vesicles. The concentrations are given in terms of weight percentage of F127 and range from 0.1 to 30 wt% of F127. All samples were stored at 5℃ for 1 week before performing the experiments. All the prepared mixtures are listed and labeled in table 1.

Tween 60 vesicle-polymer systems	Polymer Concentration (wt%)	Labels
Pluronic F127	12	F127
Pluronic F127	15	
Pluronic F127	18	
Pluronic F127 + Tween 60 vesicles	12	VT-F127
Pluronic F127 + Tween 60 vesicles	15	
Pluronic F127 + Tween 60 vesicles	18	
Pluronic F127 + drug entrapped Tween 60 vesicles	15	VT-F127*
Pluronic F127 + drug entrapped Tween 60 vesicles	18	

Table 1: Prepared vesicle-polymer mixtures.

Rheological measurements were conducted using a shear strain controlled rheometer RFS III (Rheometrics, USA) equipped with a couette, cylinder geometry (gap 1.06 mm, external and inner radius 17 and 7 mm, respectively). The temperature was controlled by a water circulator apparatus (±0.2°C). To prevent errors due to evaporation, measuring geometry was surrounded by a solvent trap containing water.

All the experiments were performed during heating. The rheological behavior at different temperatures was investigated by a time cure test at 1Hz with a heating ramp rate of 1°C/min. The

small amplitude dynamic tests provided information on the linear viscoelastic behaviour of materials through the determination of the complex shear modulus [1]:

$$G^*(\omega) = G'(\omega) + iG''(\omega) \tag{1}$$

or in terms of complex viscosity,

$$\eta^* = G'\omega/\omega \tag{2}$$

where $G'(\omega)$ is the in phase (or storage) component, $G''(\omega)$ is the out-of-phase (or loss) component, and i is the imaginary unit of the complex number. $G'(\omega)$ is a measure of the reversible, elastic energy, while $G''(\omega)$ represents the irreversible viscous dissipation of the mechanical energy. The dependence of these quantities on the oscillating frequency gives rise to the so-called mechanical spectrum, allowing the quantitative rheological characterization of studied materials. The applied strain amplitude for the viscoelastic measurements was reduced until the linear response regime was reached. This analysis was made by performing strain sweep tests in all temperature range investigated. Weak Gel Model [1] was also applied to some of the oscillatory spectra:

$$\left| G^*(\omega) \right| = \sqrt{G'(\omega)^2 + G''(\omega)^2} = A\omega^{\frac{1}{z}} \tag{3}$$

where "A" is interpreted as the interaction strength between the rheological units: a sort of amplitude of cooperative interactions, and "z" as the coordination number, which corresponds to the number of flow units interacting with each other to give the observed flow response [2].

The rheological characterization of the samples was also carried out by using a generalised Maxwell model [3] In such a scheme, the material's viscoelastic behavior is modeled by a number of Maxwell elements in parallel. A Maxwell element consists of a spring and a dashpot in series, characterized by a spring modulus $G°$ and a relaxation time λ. In a dynamic shear experiment, the generalized Maxwell model results into an equation for $G'(\omega)$ and $G''(\omega)$ of the form [3]:

$$G'(\omega) = \sum_i \frac{\omega^2 \lambda_i^2 G_i°}{1 + (\omega\lambda_i)^2} \tag{4}$$

$$G''(\omega) = \sum_i \frac{\omega\lambda_i G_i°}{1 + (\omega\lambda_i)^2} \tag{5}$$

49

In this study, appropriate spectra of the relaxation times ($G°_i$, λ_i) were obtained by a best fit of the observed viscoelastic moduli to equations (3) and (4). $G°$ and λ have been used as adjustable parameters in an iterative procedure that minimizes the overall standard deviation, $\sigma(G')+\sigma(G'')$. The relaxation times were calculated with an accuracy of ±5%.

Differential scanning calorimetry (DSC)

Differential scanning calorimetry (DSC) measurements were performed by using a Setaram micro DSC 131 instrument. Samples (20-30 mg) were sealed in aluminium-cells and brought to the initial temperature. As a reference, a sealed pan with the corresponding amount of water was used. To check water evaporation, the pans were weighed before and after the DSC measurements. The DSC thermograms were recorded in the temperature range from 10 to 90ºC. The heating rate was 1ºCmin⁻¹. Thermograms were digitized and phase transition temperatures with the associated heat changes were determinate by the use of the commercial software Origin 7.5 (OriginLab, MA USA).

Results and Discussion

The phase diagram of F127 in water is reported in literature [5,6]. Micellar and cubic phases lie within composition range 0.01 wt% $< c <$ 30 wt% of F127 and temperature range 10-90 ∘C. The findings agree with previous reported studies [7,8].

According to previous observations, the aqueous mixtures at 15 and 18 wt% of F127 are liquid-like at low temperature (15 °C) whilst they are gel-like at higher temperature (37°C). That means they do not flow under their own weight. All the polymer mixtures with concentration below 15 wt% are a liquid-like over the entire investigated temperature range.

Figure 1 shows images of selected polymer (1a) and vesicles-polymer solutions (1b) at 25°C and 37°C. The mixtures with vesicles are opaque. From a systematic visual observations thermal gelation process seems to be not affected by the presence of the vesicles. This means the gel phase covers the same temperature and polymer concentration ranges.

In order to understand the effects of vesicles on the mechanical properties of gel matrix, a deep rheological characterization was made.

50
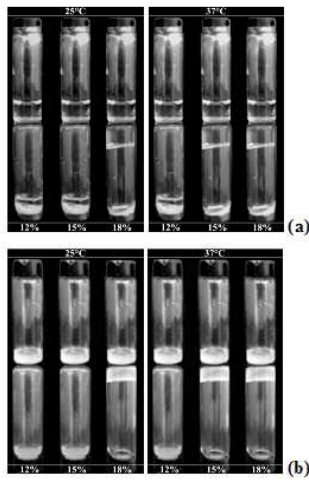
Figure 1: (a) Pictures of selected F127 polymer solutions; from left to right: 12, 15, 18 wt%; (b) Pictures of selected mixed F127-Tween 60 vesicles solutions; from left to right: 12, 15, 18 wt% of polymer.

Figure 2 shows mechanical spectra of F127 solutions with (2b) and without (2a) vesicles. The dynamic rheological response evidences a pronounced change from liquid to solid with increasing polymer concentration in both cases. This can be interpreted in terms of transition from dilute to semi-dilute regime, since the cubic phase is formed according to the phase diagram of F127/Water system.
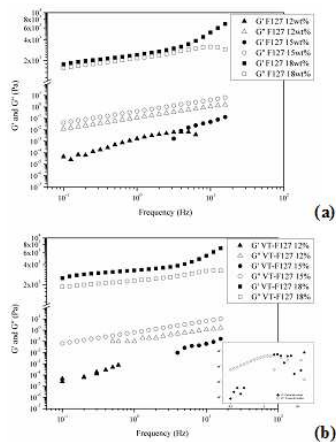
Figure 2: (a) Frequency dependence of the storage modulus (G') and loss modulus (G''), at different F127 concentrations (b) Frequency dependence of the storage modulus (G') and loss modulus (G''), for different polymer concentrations in polymer-vesicle mixtures. All mechanical spectra are performed at 25°C. The inset represents the mechanical spectrum of stock vesicles dispersion at 25°C.

The vesicle dispersion alone (stock solution) has a strongly liquid-like response in all investigated temperature range (see inset of the figure 2b) with low viscosity values (10^{-3} Pas at 25°C). Obviously the addition of polymer has marked differences: the vesicle system acquires the gel-like properties of the polymer alone.

It is worthy to note that the polymer network is affected by the polymer-vesicles interactions. The network becomes more solid with the addition of the surfactant aggregates. In fact the storage modulus is higher when the vesicles are added to the polymer solutions. This effect is more evident by considering the only G' values.

The mechanical relaxation times were extracted from frequency sweep experiments by fitting the experimental data to the equations 3 and 4. A home-made software package was used for the purpose calculation of those parameters. The relaxations times comparison between solutions with or without vesicles at 18 wt% of F127 are shown in figure 3. While the elastic moduli are related to the density of active links, the relaxation times are associated with the strength of those active links. The relaxation spectra obtained for the mixture at 18 wt% of polymer are dominated by relaxation times on the order of 1-1000 s. However, on the time scale of few milliseconds, a relevant second region of relaxation times is present. In accordance with the analysis on the relaxation processes this region refers to the local motion of a part of the polymer chain of the order of the entanglement length. The addition of vesicles seems to affect lightly relaxation spectrum: the weight of the long relaxation times (1-100 s region) is higher than one obtained for the analogues vesicles-free polymer solution (figure 3).

Temperature	Diameter (nm) of VT-F127 15wt%		Diameter (nm) of VT-F127 15wt%	
	Micelle	Vesicle	Micelle	Vesicle
15 °C	12	438	12	442
20 °C	18	512	18	546
25 °C	24	554	24	563

Figure 3: Structural relaxation times of samples at 18 wt% of polymer for F127 solution and for VT-F127 solution at 25°C by a fitting of the generalized Maxwell equations.

Even though the addition of vesicles does not affect the polymer association process. The cubic phase keeps his "phase existence range" [9], it seems that it makes stronger contacts (active links). This could be due to more favorable interactions both among surfactant molecules and among polymer-surfactant molecules.

Furthermore the effect of temperature has a strong impact in the dynamics of the system.

The dynamic mechanical analysis (DMA) ability to give complex viscosity and G' and G'' values for each point in a temperature scan allows one to estimate the transition temperature and the mechanical behavior.

This has the advantage of telling how much fluid the material is at any given temperature, so one can determine mechanical moduli values change with temperature and transitions in materials. This includes not only the phase transitions, but also other transitions that occur in the polymer matrix.

In figure 4 the temperature dependence of complex dynamic viscosity for selected mixed vesicle-polymer solutions is shown. Both systems present similar cure profiles but the system containimng vesicles shows higher viscosity values.
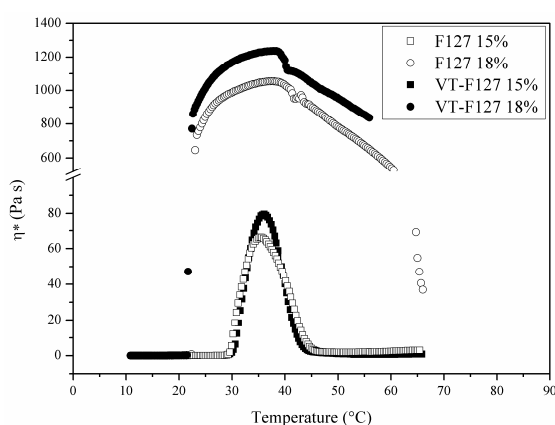
Figure 4: Linear viscoelastic thermograms for F127 and VT-F127 solutions. Temperature scan of complex viscosity, obtained by a time-cure test frequency = 1 Hz. Heating rate of the experiment was of 1°C/min.

Calorimetric measurements showed that the F127-containing gels (semidiluted region) do not present any change in the enthalpy at the gelation temperature.

No vesicle phase transition was detected within the studied temperature range, indicating that vesicles are stable. The scans of a VT-F127 and F127 mixtures at 18 wt% are shown in figure 5. The plots show the occurrence of an intense and broad peak centered at 15°C, ascribed to micellar formation process [5]. This can be considered complete at 24°C. Consequently from this temperature value, the increase of the complex viscosity can be interpreted in terms of the micellar growth.

The F127 and VT-F127 solutions show a Newtonian behavior in the liquid region, (characterized by an independency of viscosity with shear rate). In the figure 6 we show the temperature dependence of the Newtonian viscosity for both systems. Two relevant features emerge: low viscosity values and a progressive increase with increasing temperature. These findings clearly suggest the presence

53

of a molecular solution at low temperature and its transformation in a micellar phase with spherical aggregates that progressively grows upon a further increase of temperature. The mixtures, located near the cubic phase, show also a Newtonian . but the viscosity is too high to correspond to a small spherical aggregate (0.06 Pa s) and then it should have a structure of big globular micellar aggregates that become gel network in the cubic phase.
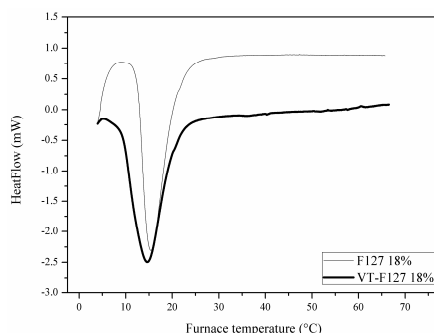
Figure 5: DSC upscans of vesicle-F127 and F127 alone samples at 18 wt% of polymer. Heating rate: 1.0 ∘C/min.
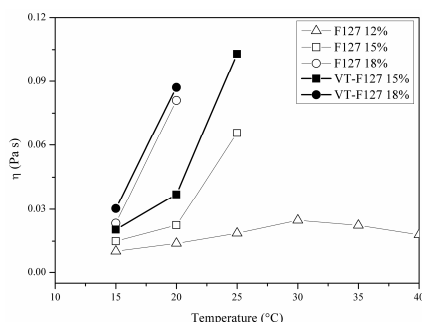
Figure 6: The Newtonian viscosity as a function of the temperature for F127 and VT-F127 mixtures.

On the contrary in cubic phase the shear viscosity is a function of the applied shear rates. The decrease of the viscosity with the increasing of the shear rate is observed and it results in a shear-induced orientation and deformation of the lyotropic domains, with deformed and elongated micelles aligned parallel to direction of the shear field.

Weak Gel Model

The table 2 shows the composition and temperature dependence of weak gel model parameters, z and A, as obtained by fitting the viscoelastic data to eqn. 3.

Temp. (°C)	A (± 0.1)			
	F127 15%	VT-F127 15%	F127 18%	VT-F127 18%
15	0.1	0.1	0.2	0.1
20	0.2	0.3	0.4	0.1
25	0.4	0.7	3448.0	3211.0
30	6.3	94.5	3913.0	3740.0
35	253.0	362.1	4316.0	6881.0
40	172.3	240.2	4519.0	6728.0
45	114.0	206.7	4033.0	6092.0
50	126.0	253.2	3223.0	5048.2
55	132.0	269.3	2429.0	4503.4
60	72.0	161.6	1480.0	3802.0
65	37.0	86.0	833.0	1432.1
70	10.0	23.5		
	z (± 0.01)			
15	1.11	1.08	1.04	1.02
20	1.04	1.02	1.00	1.00
25	1.00	1.00	5.00	7.14
30	1.49	4.35	9.09	9.09
35	6.06	6.11	10.00	11.11
40	5.38	5.69	11.13	12.50
45	5.26	5.00	11.12	12.69
50	6.69	6.17	11.11	12.67
55	6.25	6.76	11.11	12.67
60	7.14	7.69	11.11	12.67
65	3.85	3.67	10.00	11.89
70	3.85	3.04		

Table 2: Weak gel model parameters for different f127 and VT-F127 mixtures

Both systems exhibit a high flow coordination number, z, and high interaction strength values, A, in the cubic phase. Additionally, the data confirms the presence of a gel that becomes stronger with increased polymer concentration. The flow coordination number jumps from value close to unity up

to about 6 or 12 for mixtures at 15 wt% or 18 wt% respectively when cubic phase is formed. This means a hardening of the gel network and a different structural organization in the cubic phase marked by the increasing of A and z respectively.

Additionally it is worth noticing that:

- A values increase both with polymer and vesicles addition in a gel phase respectively;
- z values increase with polymer addition while they appear rather constant with the vesicles addition;

This means a hardening of the gel network but not an increasing of the flow units, that in turn means similar structural organization with the used vesicle concentration.

Polymer impact on Vesicle stability. The figure 7 shows the change in the size of the aggregates in vesicles-polymer solutions, determined by NNLS analysis of the light scattering data. Two distinct populations of aggregates of greatly differing size were observed and for each of them an average diameter was computed.

Interestingly, the size of the larger of the two co-existing populations (assumed to be vesicles) changes with the addition of polymer. This observation suggests that polymer F127 partitions into the vesicles and either causes fusion of the vesicles and/or swells their volume. In contrast, the smaller aggregates, assumed to be mixed F127/Tween 60 micelles, changes relatively little in size upon increasing the concentration of polymer as reported in literature for the vesicles free system [7]. The sizes of these aggregates were not much larger than the size of polymer micelles at a similar concentration (i.e. 18 nm radius at 20°C for 18 wt% mixture). However, depending upon the number of molecules incorporated into each micelle due to the low Tween 60 concentration, such changes may be relatively small and not observable in the light scattering data.

Temperature	Diameter (nm) of VT-F127 15wt%		Diameter (nm) of VT-F127 15wt%	
	Micelle	Vesicle	Micelle	Vesicle
15 °C	12	438	12	442
20 °C	18	512	18	546
25 °C	24	554	24	563

Table 3: Weak gel model parameters for different f127 and VT-F127 mixtures

These findings are in agreement with the DMA analysis. The micellar aggregates grow with temperature from 12 up to 24 nm within 15-25°C. This observation is in agreement with the data reported in the references [5,7]. Besides the vesicles show an more pronounced increase in the size at lower temperature.

Transdermal permeation study

The success of a transdermal drug delivery system depends on the ability of the drug to permeate the skin in sufficient quantity to maintain the therapeutic levels. An ideal drug candidate would have sufficient lipophilicity to partition into the Strateum Corneum, but also sufficient hydrophilicity to enable the second partitioning step into the viable epidermis and, eventually, the systemic circulation. Furthermore a slow and controlled release of encapsulated molecules is one of the requirements for the delivery of drugs [10].

Percutaneou permeation profiles across rabbit ear skin of Diclofenac as well as drug incorporated in niosomesn or in polymer-vesicles mixtures are reported in figure 7. Skin should be exposed to the drug for a maximum of 24 h because of deterioration of skin integrity with time.

According to the literature [11-13], a controlled and prolonged permeation effect of niosomes formulations in comparison with simple drug solutions has been found. Several mechanisms could be proposed to explain the ability of niosomes to modulate drug transfer across the skin: structure modification of the skin, due to the temporary loss of intercellular lipid barrier properties of the stratum corneum followed by an increase in permeability; adsorption and fusion of niosomes onto the surface of skin leading to high thermodynamic activity gradient of drug at the interface, which is the driving force for permeation of drug [14,15].
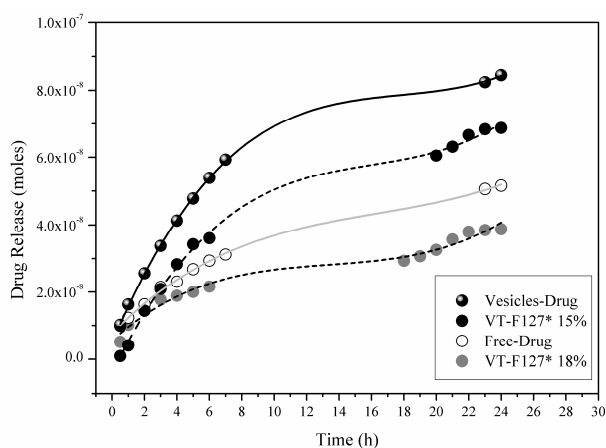
Figure 7: In vitro percutaneous permeation profile of Diclofenac loaded systems at 37°C.

Moreover, the figure 7 clearly shows that drug permeates faster when the drug is entrapped in vesicles alone solution. The permeation decreases with increasing the polymer concentration.

This finding is ascribed to the fact that the drug loaded in the vesicles-polymer systems has to overcome the niosomes bilayer barriers and then the polymeric gel networks. In particular as discussed analysing the rheological data, the gel network gets stronger when the concentration of polymer increases, consequently the drug presents more difficulties to move around. In addiction

the very slow Diclofenac percutaneous permeation showed by the system prepared with the 18% of polymer was probably due to the worst affinity toward skin structure. These results confirmed that the systems based on Tween 60vesicles and F127 could increase the percutaneous permeation of an hydrophilic drug, such as Diclofenac across the rabbit skin, when the amount of polymer was only about 15%: the increase of polymer content made the permeation slower than the free drug solution. These findings naturally lead to more diversified applications in trandermal drug delivery: the systems prepared with the lower polymer content could act as percutaneous permeation enhancers, while systems containing the 18% of polymer could be recommend as retarded drug delivery systems.

References
[1] D. Gabriele, B. d. Cindio, and P. D'Antona, Rheologica Acta 40, 120 (2001).
[2] L. Coppola, R. Gianferri, C. Oliviero, I. Nicotera, and G. A. Ranieri, Physical Chemistry Chemical Physics 6, 2364 (2004).
[3] M. R. Mackley, R. T. J. Marshall, J. B. A. F. Smeulders, and F. D. Zhao, Chemical Engineering Science 49, 2551 (1994).
[4] H. Z. Cummins, N. Knable, and Y. Yeh, Phys. Rev. Lett. 12, 150 (1964).
[5] G. Wanka, H. Hoffmann, and W. Ulbricht, Macromolecules 27, 4145 (1994).
[6] R. Ivanova, P. Alexandridis, and B. Lindman, Colloids and Surfaces A 183-185, 41 (2001).
[7] J. Zhang, C. Burger, and B. Chu, Electrophoresis 27, 3391 (2006).
[8] L. Wang, X. Chen, J. Zhao, Z. Sui, W. Zhuang, L. Xu, and C. Yang, Colloids and Surfaces A 257-258, 231 (2005).
[9]G. Horváth-Szabó, J. H. Masliyaha, and J. Czarneckib, Journal of Colloid and Interface Science 257 (2), 299 (2003).
[10] R. Langer, Acc. Chem. Res. 26 (10), 537 (1993).
[11] B. W. Barry, European Journal of Pharmaceutical Sciences 14 (2), 101 (2001).
[12] H. Schreiera and J. Bouwstrab, J. Control Rel 30 (1), 1 (1994).
[13] G. Gregoriadis, Liposomes as Drug Carriers: Recent Trends and Progress. (John Wiley, Chichester, 1988).
[14] I.F. Uchegbu, S.P. Vyas, Int. J. Pharm. 172 (1998) 33.
[15] E. Touitou, H.E. Junginger, N.D. Weiner, T. Nagai, M. Mezei, J. Pharm. Sci. 83 (1994) 1189.

2.4.4 Niosomes from α,ω-trioxyethylene-bis(sodium 2-dodecyloxy-propylenesulfonate): preparation and characterization

Rita Muzzalupo[a], Lorena Tavano[a], Sonia Trombino[a],

Roberta Cassano[a], Nevio Picci[a], Camillo La Mesa[b]

a Department of Pharmaceutical Sciences, Calabria University, Ponte P. Bucci, 87030 Rende, Italy

b Department of Chemistry, "La Sapienza" University, Piazzale A. Moro, 00185, Rome, Italy

Abstract

The synthesis and characterization of new surfactants with peculiar physical-chemical properties are amongst the most promising and expanding issues in pharmacological colloid science. The most used vesicular carriers are liposomes prepared from a wide variety of natural and synthetic phospholipids, but several ionic and non-ionic amphiphiles have been used to form multilamellar and/or unilamellar vesicles.

In the present study the synthesis of α,ω-trioxyethylene-bis(sodium 2-dodecyloxy-propylenesulfonate), an anionic Gemini surfactant, and its ability to form niosomes are elucidated. The compound forms vesicles with and without added cholesterol. The vesicular systems were characterized by size, shape and drug entrapment efficiency. The compounds to be incorporated are β-carotene and ferulic acid, as antioxidants, acetyl salicylic acid, as FANS, and the antineoplastic 5-Flurouracil, widely used in dermatological disorders. The results of this study show that α,ω-trioxyethylene-bis(sodium 2-dodecyloxy-propylenesulfonate) can be used for the preparation of niosomes entrapping lypophilic, amphiphilic or hydrophilic substances. These niosomes may be promising candidates as percutaneous carriers for the aforementioned drugs.

1. Introduction

Vesicular systems, such as liposomes and niosomes, are uni- or multilamellar spheroidal structures composed of amphiphilic molecules assembled into bilayers. They are considered primitive cell models, cell-like bioreactors and matrices for bioencapsulation. They play an increasingly important role in drug delivery or drug toxicity reduction, modify pharmacokinetics and bioavailability and are applied for the continuous release (1–5) or the targeted delivery of drug molecules (6–11). For the above reasons, vesicles are successfully applied in cosmetics and pharmaceutics (12-18). Compared to other vesicular systems, niosomes are preferred in topical delivery because they are chemically stable, show low toxicity, improve drug performances through better availability and

controlled delivery at a particular site, are biodegradable, biocompatible and non-immunogenic (19). In addition, the great chemical stability, ease of production and the extremely low costs make niosomes attractive colloidal carriers. Niosomes are interesting drug delivery systems in the treatment of dermatological disorders (20), enhance the residence time of drugs in the stratum corneum and epidermis and improve penetration of the trapped substances across the skin. In addition, these systems have been reported to decrease side effects and to give a considerable drugs release. (21).

The essential constituents of niosomes are membrane additives, such as cholesterol, in mixtures with sugar-based, polyoxyethylene-based, polyglycerol, or crown-ether based surfactants or with Gemini ones. The properties of the latter species have attracted the attention of chemists as far as possible changes in molecular structure of the constituents are concerned and led to preparation of new generation surfactants. Gemini surfactants consist of two hydrophilic head groups and two hydrophobic chains linked covalently by a spacer close to the head groups or joining together two points of the respective alkyl chains (22). (Fig.1).
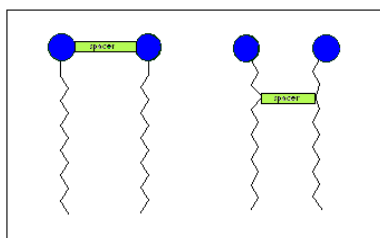
Fig.1 Schematic drawing of Gemini surfactants, indicating joints between polar head groups, on the left, or in selected positions along the main hydrocarbon chains.

The spacer can vary in length and chemical structure, be flexible or rigid, hydrophilic or hydrophobic, etc (23). Based on the polar head group nature, Gemini are classified as cationic, anionic, non-ionic and zwitterionic species. Anionic Gemini, in particular, have significant water solubility, form micelles and substantially lower the surface tension compared to conventional anionic homologues (24). Because of their high surface activity, sulfonated Gemini are used as emulsifiers, dispersants or hydrotropic agents in washing and cleaning technologies, laundry and detergent formulations, soil clean up, and enhanced oil recovery (27).

Gemini are mild products to be used in personal care (26), and are effective in the formulation of cosmetics, shampoos, etc. (25). From such a viewpoint, the low CMC of Gemini ensures less skin and eye irritation (28). Sulfoesther-based anionic Gemini, in particular, give rise to moderate protein denaturation and no cases of redness or skin rashes have been reported (29). Sulphated Gemini surfactants do not show irritancy on the abdominal region of guinea pigs (30).

Dispersed in water, Gemini surfactants form bilayer sheets and are organized in such a way that the ionic groups reside on the outside while the hydrocarbon tails extend into water-depleted bilayers (31). For the above reasons Gemini are useful for drug entrapment and percutaneous release.

In this work the synthesis and characterization of an anionic Gemini surfactant, α,ω-trioxyethylene-bis(sodium2-dodecyloxy-propylenesulfonate), termed EO_3S_2, are dealt with. EO_3S_2 was previously investigated by some of us and its thermodynamic properties in water or with progressive amounts of different polymers were investigated (32). EO_3S_2 is similar to the analogue obtained by Renoulf et al. (33,34) but presents an oxyethylene spacer connecting the two surfactant moieties.

In this work we evaluated the ability of EO_3S_2 to form vesicular systems in the presence of membrane additive, such as cholesterol (CH), and studied their capacity to entrap hydrophilic or lipophilic drugs. Ferulic acid and β-carotene, acetyl salicylic acid and antineoplastic 5-Flurouracil were dissolved in such vesicular systems. β-carotene is a well-known lipophilic antioxidant showing preventive effects in animals and humans against cancer, cardiovascular pathologies, atherosclerosis, macular degeneration and age related diseases (35,36). Ferulic is an hydroxycinnamic acid, largely present in nature. Its biological properties and antioxidant activity are well acquainted (37,38). Ferulic acid is a photoprotective ingredient in skin lotions and sunscreens. Acetyl salicylic acid (Aspirin) has antiplatelet activity. Its long-term use, at low doses, prevents heart attacks and thrombus formation in hypercoagulable states. 5-Fluorouracil (5-FU) is an anticancer agent used in the treatment of proliferated skin diseases, in actinic keratoses (39) superficial basal cell carcinomas (40) and psoriasis (41). In this paper we suggest conjugating innovative colloidal carriers from pharmaceutical nanotechnology and therapeutically effective natural compounds by traditional medicine, to be used in pharmaceutical and cosmetic formulations. The vesicular systems obtained in this work are characterized by transmission electron microscopy (TEM) to account for vesicles shape and morphology, by dynamic laser light scattering, (DLS) to detect mean vesicle sizes and size distribution and by HPLC to determine entrapment efficiency. Additional electrophoretic mobility experiments give indications on the stability of such biologically relevant colloidal dispersions.

2. Materials

2.1 Chemicals

All reagents from Sigma-Aldrich (St. Louis, MO, USA), were used without further purifications. The solvents are of high performance liquid chromatography grade.

2.2 Synthesis of □ α,ω-trioxyethylene-bis(sodium2-dodecyloxy-propylenesulfonate)

The□ α,ω-trioxyethylene-bis(sodium2-dodecyloxy-propylenesulfonate), (**I**) Gemini surfactant, was synthesized by following the procedure reported in literature (33,34) (Scheme 1) .
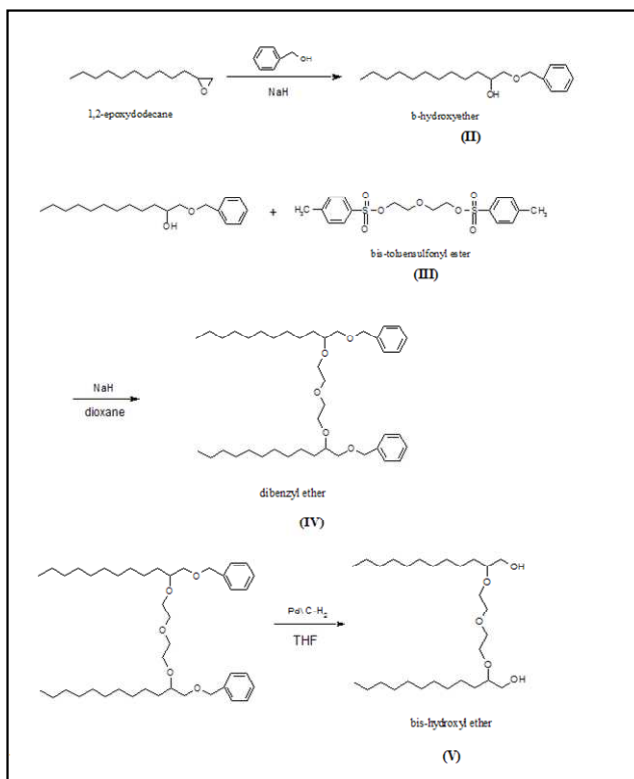
Scheme 1. Gemini synthesis

Briefly, Gemini (**I**) was obtained starting from 1,2-epoxydodecane that, after basic solvolysis of the oxirane in benzyl alcohol, produced the β-hydroxyether (**II**). Condensation of two equivalents of the secondary alcohol (**II**) with bis-toluensulfonyl esther (**III**), in refluxing dry dioxane, provided the dibenzyl ether (**IV**). Debenzylation by hydrogenolysis over Pd/C produced the bis-hydroxyl compound **V**. The sulfonated compound (**I**) was directly prepared by reacting the diol (**V**) with propane sultone and sodium hydride in refluxing dioxane. Major synthetic details are reported in the Appendix.

2.7 Drug entrapment efficiency

The amount of drug entrapped by niosomes was evalueted as drug mole fraction per cent (MF%), partitioned into the drug-loaded niosomes and the total amount of lipid, as reported elsewhere. (42) It was determined by HPLC after vesicles disruption with methanol. The drug content of the

samples was analyzed, at the respective wavelengths, by reverse-phase HPLC with spectrophotometric detection on a Perkin-Elmer LC-295 detector. The column was packed with Alltech C18 Adsorbosphere HS material, 3 μm in size, in a 15 cm × 0.46 cm cartridge format (Alltech Associates, Deerfield, IL). A 1-cm cartridge precolumn, containing 5- μm C18 Adsorbosphere packing was used. Mobile phases and flow rates for each drug are reported in Table 1.

Drug	Mobile phases	Flow rate
5-Fluorouracil	90% methanol 10% phosphate buffer 5mM-pH 6.8	0,5 ml/min
β-carotene	60% acetonitrile 10% methanol 30% isopropanol	1 ml/min
Acetyl salicylic acid	25% acetonitrile 75% water adjusted to pH 2.5 with phosphoric acid	2 ml/min
Ferulic acid	95 % methanol 5% formic acid	1 ml/min

Table 1. HPLC analysis conditions. Indication of the mobile phases used to detect different drugs and the respective flow rates.

3. Results and Discussion

Some niosomal formulations (G1, G2, G3) with Gemini (EO_3S_2) and different amounts of cholesterol were prepared (Table 2). The total concentration of surfactant and cholesterol was $1x10^{-2}$ M.

Formulation Name	Gemini (mg)	CH (mg)	Ratio CH/Surf
G1	76.20±0.02	0	0.0/1.0
G2	45.72±0.03	12.87±0.08	0.5/1.0
G3	38.10±0.05	19.33±0.08	1.0/1.0

Table 2. Composition of the vesicular systems used.

The results reported in Table 2 indicate that no cholesterol is required to form vesicles with EO_3S_2. All formulations are stable at room temperature over about twelve months. No sedimentation, creaming or flocculation can be inferred. This is a direct consequence of the vesicles surface charge

63

density. Table 3 indicates the results from laser light scattering and zeta potential measurements. According to the literature (43), the hydrodynamic diameter is influenced by the amount of cholesterol.

Name of the Formulation	Ratio CH/Gem	Hydrodinamic diameter/nm	Zeta potential (ζ) mV
G1	0.0/1.0	380 ±23	-51.5±1.6
G2	0.5/1.0	320 ±14	-30.9±2.5
G3	1.0/1.0	240 ±18	-38.0±2.3

Table 3. The hydrodynamic diameter (nm) and the zeta potential (mV) of the vesicular systems at 25.0 °C.

The formulation with the highest CH amount (G3) forms niosomes of lower size compared to the others; this effect is probably ascribed to the condensing effect of cholesterol (44). Significant amounts of the sterol, in fact, modify the molecular conformation of the surfactant and promote their more or less compressed state. In addition, the β-OH group of CH could form intermolecular hydrogen bonds with Gemini and enhance, thus, the bilayer stability (45) and membrane cohesion.

As expected, direct proportionality exists between zeta potential values and the vesicle charge density. The latter quantity decreases in proportion to the amount of added cholesterol. It is worth noticing that G2 e G3 formulations have comparable zeta potential values, quite lower than vesicles made of EO_3S_2 only. Perhaps, the zeta potential values are such to ensure a significant stability to all niosome dispersions. Even tiny amount of neutral electrolytes do not modify the above behaviour. It is also reasonable to suppose the occurrence of links between surface charge density (denoted by the modulus of zeta potential) and cholesterol amount in niosomes. It is well acquainted that the sterol gives rise to an increase in niosome (vesicle) rigidity. Much less is known on its effect on the surface charge. However, thanks to the overlapping of hydrogen bond effects and changes in surfactant packing, it is possible to modulate the surface charge density with some accuracy. This is, at present, a tentative hypothesis, since such viewpoint requires the independent determination of, at least, ionic conductivity and ion activity and is actually outside the purposes of the present paper.

Because of their stability and size, G3 formulations only were extensively used to incorporate the different drugs. Niosomes containing, in order, β-carotene, ferulic acid, acetyl salicylic acid and 5-FU could be used for percutaneous formulations. It has been reported, on this regard, that drug transport by niosomes decreases side effects, gives release and improves the penetration of trapped substances through the skin (46).

In Table 4 are reported the entrapment efficiency data, expressed as drug mole fraction per cent (MF%), and the hydrodynamic diameter of niosomes for Cholesterol/Gemini 1.0/1.0 ratios.

Name of the Formulation	Drug	Hydrodynamic diameter (nm)	MF %
G3-a	5-FU	195±16	0.69±0.05
G3-b	β-carotene	256±21	0.14±0.02
G3-c	Acetyl salicylic acid	234±24	0.071±0.007
G3-d	Ferulic acid	214±21	0.023±0.003

Table 4. The hydrodinamic diameter and the entrapment efficiency of selected G3 formulations.

The chemical structure of encapsulated drugs may strongly influence niosomes size, because highly lipophilic β-carotene may intercalate into vesicles bilayer, together with cholesterol. This is why G3-b formulations show larger hydrodynamic diameters compared to other. The partitioning and location of other species into niosomes can be largely different from the aforementioned one.

The amount of drug entrapped into niosomes, is dependent on its affinity toward Gemini. As indicated in Table 4, formulations containing β-carotene and 5-Fluorouracil, which are by far the most lipophilic and hydrophilic drugs, respectively, show high entrapment efficiencies. Probably, the latter effect depends on pKa values of 5-FU. Such molecules are unionized in the present experimental conditions. Hence, unfavorable electrostatic interations with EO_3S_2 could occur. Conversely, ferulic and acetyl salicylic acids suffer for a much lower trapping efficiency.

The vesicular systems were characterized by transmission electron microscopy (TEM) and light scattering. Transmission electron micrographs confirm the formation of vesicular structures, Fig. 2-A and Fig.2-B, whereas laser light scattering ones (Fig. 3), allowed to determine the particle size and the size distribution, as well.

According to both TEM and DLS, size polydispersity is significant in almost all vesicular systems which have been investigated, even though the effect is by far less relevant in G3-based formulations.
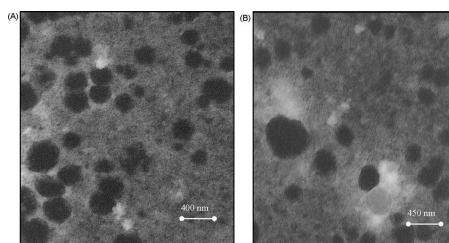

Fig 2. Photomicrographs of G3 formulations as seen by TEM (transmission electronic microscopy). The micrograph indicated as A refers to vesicles containing 5-FU (A), that indicated as B, conversely, contains□ β-carotene.

The latter, thus, are considered the most efficient mixtures for pharmaceutical niosome-based formulations. In particular, the packing efficiency and the moderate sizes, as well, ensure the attainment of high yields in the trapping efficiency of lipophilic drugs.
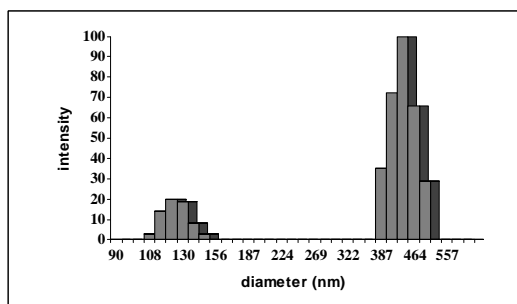

Fig 3. Bimodal vesicle size distribution of niosomal dispersions, inferred by a statistical cumulant analysis based on DLS findings. Data refer to mixtures belonging to the G3-b family, at 25.0 °C.

4. Conclusions

An anionic Gemini surfactant (EO_3S_2) was synthesized and its ability to form niosomes was evaluated. EO_3S_2-based vesicular systems were prepared with and without cholesterol. Smaller sizes are observed by G3 formulation, which is prepared in mixtures with the highest cholesterol/surfactant ratio. In such vesicles several drugs were encapsulated: the highest trapping efficiency is observed for formulations containing 5-FU and □-carothene. Niosomes prepared with EO_3S_2 are promising candidates as percutaneous carriers of lipophilic and hydrophilic drugs.

References

[1] H. Schreier, M. Levy, P. Mihalko, J. Control. Release, 5, (1987),187.
[2] V.M. Knepp, R. S. Hinz, F. C. Jr. Szoka, R.H. Guy, J. Control. Release 5, (1988), 211.
[3]. V.M. Knepp, F. C. Jr. Szoka, R. H. Guy, J. Control. Release 12, (1990), 25.
[4] G. Blume, G. Cevc, Biochim. Biophys. Acta, 91, (1990), 1029.
[5] P. Arunothayanum, J. A. Turton, I. F. Uchegbu, A.T. Florence, J. Pharm. Sci. 88, (1999), 34.
[6] H.H. Spanjer, G. Scherphof, Biochim. Biophys. Acta 734, (1983), 40.
[7] V.P. Torchilin, CRC Crit. Rev. Ther. Drug Carrier Syst. 2, (1985), 65.
[8] D. Papahadjopoulos, A. Gabizon, in "Targetting of Drugs 2. Optimizing Strategies" (G.Gregoriadis, A. C. Allison, G. Poste, Eds.), Plenum Publishing Co., New York, NATO ASI Ser. 199, (1991), 95.
[9] K. Yagi, "Medical Application of Liposomes." Japan Scientific Society Press, Tokyo, 1986.
[10] H. Kiwada, H. Niimura, Y. Kato, Chem. Pharm. Bull. 33, (1985), 2475.
[11]I.F. Uchegbu, J.A. Double, J.A. Turton, A.T. Florence, Pharm. Res. 12, (1995), 1019.
[12] R.M. Handjani-Vila, A. Riber, B. Rondot, G. Vanlerberghe, Int. J. Cosmet. Sci. 1, (1979), 303.
[13] J.-Y. Fang, C.-T. Hong, W.-T. Chiu, Y.-Y. Wang, Int. J. Pharm. 219, (2001), 61.
[14] M.N. Azmin, A.T. Florence, R.M. Handjani-Vila, J.F.B. Stuart, G. Vanlerberghe, J.S. Whittaker, J. Pharm. Pharmacol., 37, (1985), 237.

[15] H.E.J. Hofland, R. Van der Geest, H.E. Bodde, H.E. Junginger, J. A. Bouwstra, Pharm. Res. 11, (1994), 659.

[16] A.B. Mullen, A.J. Baillie, K.C. Carter, in, "Synthetic Surfactant Vesicles: niosomes and other non-phospholipid vesicular systems", I.F. Uchegbu (ed), Harwood Academic Publishers, Amsterdam, The Neitherlands, 6, (2000), 97.

[17] G.K, Pillai, M.L. Salim, Int. J. Pharm., 193, (1), (1999), 123.

[18] R. Agarwal, O.P. Katare, S.P. Vyas, Int. J. Pharm., 228, (2001), 43–52.

[19] S.S. Biju, S. Talegaonkar, P.R. Mishra, R.K. Khar, Indian J. Pharm. Sci., 68, (2), (2006), 141.

[20] M. Manconi, C. Sinico, D. Valenti, F. Lai, A.M. Fadda, Int. J. Pharm., 311, (2006), 11.

[21] H. Schreier, J. Bouwstra, J. Control. Rel., 30, (1994), 1.

[22] F.M. Menger, C.A. Littau, J. Am. Chem. Soc., 115, (1993), 10083.

[23] R. Zana, in "Structure-Performance Relationships in Surfactants", K. Esumi, M. Ueno (Eds.), Dekker, New York, (1997), 255.

[24] D. Shukla, V.K. Tyagi, J.Oleo. Sci., 55, (5), (2006), 215.

[25] K. Kwetkat, U. Giacobs, S. Scholz, Chem. Abstr, 128, (1998), 169006d.

[26] R. Li, D.J. Tracy, Chem. Abstr. 131, (1999), 215860.

[27] A. Von Zon, J.T. Bouman, H.H. Deuling, S. Karaborni, J. Karthaeuser, H.T.G. A. Mensen, N. M. Van Os, K.H. Raney, Tenside Surfactants, Deterg, 36 (2), (1999), 84.

[28] L. Liu, M.J. Rosen, in "Surfactants and Interfacial Phoenomena", 2nd edn, John Wiley, New York, (1989), 84.

[29] T. Okano, M. Fukuda, J. Tanabe, M. Ono, Y. Akabane, H. Takahashi, N. Egawa, T. Sakotani, H. Kanao, Y. Yoneyanna, U.S. Patent (1997), 5681803.

[30] T. Kitsubi, M. Uno, K. Kita, Y. Fujikura, A. Nakano, M. Tosaka, K. Yahagi, S. Tamura, K. Maruta, U.S. Patent 5, (1998), 714457.

[31] F.M. Menger, C.A. Littau, J. Am. Chem. Society, 113, (1991), 1451.

[32] R. Muzzalupo, M.R. Infante, L. Perez, A. Pinazo, E.F. Marques, M.L. .Antonelli, C. Strinati, C. La Mesa, Langmuir, 23, (2007), 5963.

[33] P. Renoulf, C. Mioskowski, L. Lebeau, Tetrahedron Lett., 39, (1998), 1357.

[34] P. Renoulf, D. Hebrault, J. R. Desmurs, J. M. Mercier, C. Mioskowski, L. Lebeau, Chem. Phys. Lipids, 99, (1999), 21.

[35] S.T. Mayne, FASEB J. 10, (1996), 690.

[36] P. Palozza, R. Muzzalupo, S. Trombino, A. Valdannini, N. Picci., Chem. Phys. Lipids, 139, (2006), 32.

[37] S.Trombino, S. Serini, F. Di Nicuolo, L.Celleno, S. Andò, N.Picci, G. Calviello, P. Palozza, J. Agric. Food Chem., 52, (2004), 2411.

[38] E. Graf, Free Radic. Bil. Med. 13, (1992), 435.

[39] G.J. Butler, R. Neale, A.C. Green, N. Pandeya, D.C. Whiteman, J. Am. Acad. Dermatology, 53, (2005), 966.

[40] E. Epstein, Arch. Dermatol., 121, (1985), 207.

[41] T. Tsuji, T. Sugai, Arch. Dermatol., 105, (1972), 208.

[42] S. Benita, P.A. Poly, F. Puisieux, J. Delatore, J. Pharm. Sci., 73, (1984), 1751.

[43] A. Monosroi, P. Wongtrakul, J. Monosroi, H. Sakai, F. Sugawara, M. Yuasa, M. Abe, Colloids Surf. B: Biointerfaces, 30, (2003), 129.

[44] K. Kamio, M. Sakai, A. Kaminaga, I. Satake, K. Hayakawa, Colloid Polym. Sci., 280, (2002), 78.

[45] B. Nasseri, Int. J. Pharm., 300, (2005), 95.

[46] B.W. Barry, Eur. J. Pharm. Sci. 14, (2001), 101

2.4.5 N,N'-hexadecanoyl l-2-diaminomethyl-18-crown-6 surfactant: Synthesis and Aggregation Features in Aqueous Solution

L. Tavano[1], R. Muzzalupo[1], S. Trombino[1], I. Nicotera[2], C. Oliviero Rossi[2], C. La Mesa[3]

1) Department of Pharmaceutical Science, Calabria University, Edificio Polifunzionale,

87036 Arcavacata di Rende, Cosenza, ITALY;

2) Department of Chemistry, Calabria University, Via P. Bucci, Cubo 14/D,

87036 Arcavacata di Rende, Cosenza, ITALY;

3) Department of Chemistry, La Sapienza University, P.le A. Moro 5, 00185 Rome, ITALY.

Abstract

Bolas surfactants can be inserted into bi-layers and may operate as permanent holes in such membranes. Significant synthetic work and an exhaustive characterisation of their properties in the bulk was performed. On this purpose the phase diagram of the system composed by water and 1,16-hexadecanoyl-bis-(2-aminomethyl)-18-crown-6 (termed *Bola A16*) was investigated in a wide temperature and concentration range. No liquid crystalline phases were observed and a large micellar solution is present, up to about 50 surfactant wt%. Surface tension experiments defined adsorption and micelle formation The low observed *cmc* value is important for pharmacological applications, in fact, considering intravenous administration, only micelles with low *cmc* value can exist in blood. Nuclear magnetic resonance experiments determined both water and surfactant self-diffusion. According to the aforementioned experiments, slight, if any, modifications in the structure of micelles were inferred on increasing *Bola A16* content.

Dynamic rheological experiments probed the solution micro-structure. The observed rheological behaviour is newtonian. The solution viscosity and the shear relaxation processes were rationalized assuming the presence of spherical aggregates, occurring up to high surfactant content. The viscometric behaviour was rationalised in terms of a former theory of flow as a cooperative phenomenon. The number of micelles coordinated each other during the viscous flow and the interaction strength between them was obtained as a function of *Bola A16* concentration. Such value is close to unity and practically independent on surfactant content in the whole concentration range we investigated. This behaviour points out that little, or not, interactions among micellar aggregates occur.

The absence of shear induced changes in the aggregate shape implies no change in drug delivery properties under flow, this is useful in the pharmaco-dynamics field, since drug delivers usually operate in mechanically stressed conditions.

Thanks to the above properties, the material results particularly suitable for application in pharmaceutical field, may solubilize lipid membranes and selectively transport ions across them. Ancillary effects, such as the uptake of counter-ions in the crown ether, are to be considered.

1. INTRODUCTION

Surfactants are known to play a vital role in many processes of interest in both fundamental and applied science. One important property of surfactants is the formation of colloidal-sized clusters in solutions, known as micelles, which have particular significance in pharmacy because of their ability to increase the solubility of sparingly soluble substances in water [1].

Micelles are known to have an anisotropic water distribution within their structure. In other words, the water concentration decreases from the surface towards the core of the micelle, with a completely hydrophobic (water-excluded) core. Consequently, the spatial position of a solubilized drug in a micelle will depend on its polarity: nonpolar molecules will be solubilized in the micellar core, and substances with intermediate polarity will be distributed along the surfactant molecules in certain intermediate positions.

Furthermore, numerous drug delivery and drug targeting systems have been studied in an attempt to minimize drug degradation and loss, to prevent harmful side effects and to increase drug bioavailability [2-6].

Within this context, the utilization of micelles as drug carriers presents some advantages when compared to other alternatives such as soluble polymers and liposomes. Micellar systems can solubilize poorly soluble drugs and thus increase their bioavailability, they can stay in the body (blood) long enough to provide gradual accumulation in the required area, and their sizes permit them to accumulate in areas with leaky vasculature [7].

The synthesis and characterisation of new surfactants with peculiar physical-chemical properties are among the most promising and expanding issues in pharmacological colloid science. Particularly interesting, on this regard, are species having crown ethers as polar head groups joined to long alkyl chains. The reasons for using crown ether based surfactants are many-fold and find application in highly saline media, because of their selective capacity to complex ions. Crown ethers, in fact, are macro-cycles possessing an outstanding capacity to complex ions or small organic molecules and to selectively extract such species from multi-component mixtures, according to a key-lock

mechanism. The process is controlled by the respective sizes of the crown cavity and of the incoming species.

The first reports on crown ethers were published more than forty years ago [8, 9]**.** From a surfactant science viewpoint, crown ethers functionalised with pending alkyl groups are special ionophores allowing ion transport across lipophilic barriers [10]. In the last years developments in supra-molecular sciences resulted in significant progresses of crown ethers chemistry. In supra-molecular sciences, the stabilising effects are played by a combination of non-covalent contributions, due to hydrogen bonds, hydrophobic and electrostatic interactions, etc., which are responsible for the formation of associated species, combining high stability and flexible geometry.

Addition of lipophilic long-chain alkyl groups to crown ethers results in the formation of crown ether-based surfactants, forming micelles or complex supra-molecular structures in water [11-14]. The production of new compounds possessing in the same molecule hydrophilic and lipophilic parts, or regions of different polarity, is of great interest for both scientific and industrial purposes. For instance, the supra-molecular structures formed by different ligands (such as calix[*n*]arenes, cryptands, crown ethers) and inclusion complexes containing cyclodextrins, polyrotaxanes, and molecular nano-tubes, are currently studied for potential use in host-guest chemistry [15-18].

Surfactants presenting two polar head groups bridged together by a long hydrophobic chain are defined bolaform [19-25]. These compounds have been the subject of extensive research in the past for their interesting properties [26-30]. Efforts were made to design and synthesize bolaform molecules with different structures and to characterise their aggregation behaviour in aqueous solution [31-36]. When dispersed in water, these molecules organise into self-assembled vesicles, which are stable over long times, insensitive to changes in temperature or ionic strength and can be used in membrane mimetic chemistry. The fundamental physicochemical aspects of these compounds (such as micelle formation and surface activity) have been extensively investigated. Usually, the surface tension of bolaform surfactants is higher and the aggregation number is lower than conventional ones [37-39]. Compared to common surfactants, bolaforms occupy large areas at the air/water interface, because, very presumably, their alkyl chains adopt a looped conformation [40-42]. This hypothesis is currently accepted for alkyl chains longer than twelve carbon atoms [43].

Understanding the phase behaviour of bolaform-surfactant systems in water is important for elucidating and controlling the component reconstitution of biological membrane, as well as in the optimisation of vesicular drug delivery. Some of us have formerly investigated this synthetic

bolaform surfactant, as an antineoplastic drug delivery in vesicular system, and the results are reported in previous work [44].

Technical applications of crown ethers and of derived surfactants, including Bolas, in bio-chemically oriented studies are many-fold and find applications as ion carriers through lipid bilayers,[45-47] and in a lot of membrane mimetic chemistry effects.[48,49] Due to their peculiar molecular properties, it is expected that alkyl crown ethers may work in ion transport across membranes, by flip-flop mechanism.[50,51]. Bolas, very presumably, keep their position into bilayers and, thus, may operate as permanent holes in the membrane. These are interesting aspects to clarify and require, perhaps, significant synthetic work and an exhaustive characterisation of their properties in the bulk. In particular, work is in progress to determine whether, and to what extent, they are soluble into lipid membranes, and what it the selectivity in ion transport. Ancillary effects, such as the uptake of counter-ions, are far to be solved, for instance. Thus, the promising properties of such compounds need to be fully investigated. As a preliminary work, let us report here the synthesis and some solution properties of a novel surfactant, 1,16-hexadecanoyl-bis-(2-aminomethyl)-18-crown-6, hereafter termed *Bola A16*. The results, obtained through an investigation of the binary phase diagram, surface tension, differential scanning calorimetry (*DSC*), *NMR* self-diffusion and different rheological methods indicate the occurrence of an extended micellar solution. The observed properties indicate moderate changes in micelle size and little, if any, inter-micellar interactions up to relatively high surfactant content. This behaviour is particularly evident in the rheological experiments, which have been performed in a wide temperature and concentration range.

2 MATERIALS AND METHODS

2.1 Materials

Chemicals and reagents were from Sigma Aldrich and used without further purifications. The 1,16-hexadecanoyl-bis-(2-aminomethyl)-18-crown-6, *Bola A16*, was synthesized by following previously reported routes [20,52], as shown in the following Scheme:
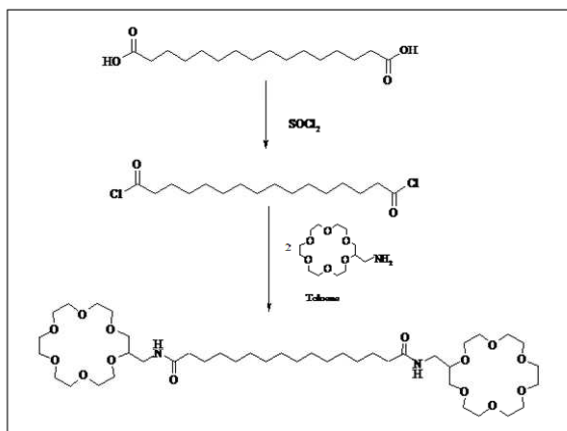
Scheme: Simplified reaction scheme inherent to Bola A 16 synthesis.

The α,ω-hexadecane-dioic acid (1.70 mmol, 0.488 g) was transformed, under stirring in refluxing conditions for several hours, in the corresponding diacyl chloride by adding 5.0 ml $SOCl_2$. 0.55 g (yield 91.4%) of the diacyl chloride were evaporated and dried. *IR* spectra were recorded on a *FT-IR* Jasco 4200 spectrometer. *IR v* □values (on *KBr*): are 2928, 1795, and 1211 cm^{-1}. The diacyl chloride (1.55 mmol, 0.55 g), dissolved in dry toluene, was added drop-wise to a solution of 2-aminomethyl-18-crown-6 (3.42 mmol, 1.00 g) in toluene, containing a nearly equivalent amount of triethyl-amine (3.10 mmol, 0.314 g), at room temperature under stirring for 20 h. The suspension is refluxed for 24 h.

The final diamide was extracted with dichloromethane, washed with *HCl* (20 ml, 3M), Na_2CO_3 (20 ml, 3M) and, finally, with distilled water. The residual organic layer is dried over $MgSO_4$ and evaporated under reduced pressure. The crude residue is purified by chromatography on alumina (with 3:7 2-propanol:hexane as eluent). The total final product yield was 78.2 %. The compound is a viscous yellow liquid at room temperature.

A 300-MHz Bruker determined ^1H *NMR* spectra of the product. The chemical shift□ values of the protons (in ppm) are: 6.40 (s, 2 protons, NH), 3.23-3.69 (m, 32 oxy-ethylene chain protons), 2.78 (s, 8 protons), 2.80 (s, 2 protons), 2.03-2.08 (t, 4 protons) 1.49 (t, 4 protons) 1.12-1.46 (m, 20 aliphatic protons). *IR* □□ *v* (in□ film): 3033, 2882,1124-1049 cm^{-1}.

2.2 Methods

2.2.1 Surface tension measurements

Surface tension measurements, τ (mN m^{-1}), were performed by a Du Noüy ring tensiometer, Nima, whose measuring vessel is thermostated to ±0.1 °C by circulating water.

The uncertainty on τ values is ± 0.2 mN m^{-1}. The surface tensions of doubly distilled water and absolute ethanol, at 25.0 °C, were used as calibration standards. The time required to get stable surface tension values is less than 5 min. The critical micellar concentration, *cmc*, is determined from abrupt changes in the surface tension *vs.* ln (m) plots. The accuracy on *cmc* is 3%. To test the surfactant purity, several independent runs of τ vs. ln (m) plots were performed. The absence of surface-active contaminants in the product is ensured by the absence of minima in τ values close to the *cmc* [53, 54].

2.2.2 Rheological techniques

Rheological measurements were performed by using a shear strain controlled rheometer RFS III (Rheometrics, USA) equipped with a concentric cylindrical geometry (inner radius 17 mm, gap 1.06 mm). A liquid circulator, JULABO F32 (Houston, USA), controlled the temperature. Samples were fully homogeneous and free from air bubbles during the rheological experiments. More details on the apparatus and the measuring procedures are given elsewhere [55]. Steady flow experiments were performed in the shear rate range 0.02-1700 s^{-1}. To ensure steady flow conditions, the required equilibration time was determined by transient experiments, according to step-rate tests. 10 s perturbations ensured steady flow conditions in the system for the whole shear rate range.

Dynamic shear experiments were performed in the frequency range 0.1-15.9 Hz. A strain sweep test was carried out before the frequency sweep, to ensure the linear visco-elastic behaviour during the sweep test. All samples were sheared for 60 s at 10 s^{-1}. Rheological experiments were performed immediately before and after the steady shear. No significant changes in viscosity were observed by application of the steady shear treatment.

2.2.3 NMR measurements.

^{1}H-NMR self-diffusion studies were performed using a Bruker Avance 300 NMR spectrometer, working at a resonance frequency of 300 MHz. Self-diffusion measurements were performed by Fourier Transform PGSE techniques [56]. The experimental errors on self-diffusion coefficients are below ± 4%. An airflow regulator, yielding a stability of ± 0.3 °C, controlled the temperature in the measuring chamber. A spin-echo signal is induced by a 90°-τ-180° radio frequency pulse sequence. A magnetic field gradient of intensity *g* is applied during a time δ, as a twin pulse separated by a time Δ, before and after the 180° pulse. The gradient strength was calibrated with pure water, for

which the self-diffusion is known. The attenuation of the echo amplitude is represented by the equation [57]:

$$A(g) = \exp\left[-\lambda^2 g^2 D\delta^2 \left(\Delta - \frac{\delta}{3}\right)\right]$$

(1)

where D is the self-diffusion coefficient and γ the protons nuclear gyro-magnetic ratio. The diffusive term in the equation is proportional to the mean-squared displacement of the molecules over an effective (Δ- δ/3 time scale. The experimental parameters Δ and δ were 30 and 1 ms, respectively, and the gradient amplitude, g, varied from 10 to 200 Gauss cm^{-1}.

2.3.4 Optical methods.

Homemade polarizing units were used. The investigation was performed in a thermostatic bath. The samples were sealed in glass tubes, equipped with small magnetic stirrers. The temperature was controlled to $\pm$ 0.1 °C. A Heto programmable thermostatic unit controlled heating and cooling modes. Additional experiments were performed by sealing small amounts of samples in thin glass capillaries, which were flame sealed. A Ceti optical polarizing microscope, equipped with a heating stage, performed additional studies. A Leitz microscope, equipped with a rotating stage, operating in polarising mode or with Bertrand lenses, was also used. Details on the apparatus set-up and measuring procedures are given elsewhere [58].

3 RESULTS AND DISCUSSION

Phase diagram and Thermodynamic Characterisation.

In Figure 1 is sketched the phase sequence for the *Bola A16*-H$_2$O system. No lyotropic liquid crystalline phases are observed and a wide micellar region follows the molecular solution one. At low surfactant content the solutions have the same viscosity as water.
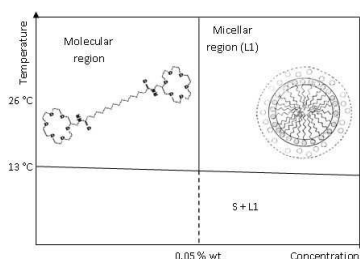

Figure 1: Schematic picture showing the phase sequence observed in the *Bola A16*-H$_2$O system.

74

When *Bola A16* concentration exceeds 0.5 weight percent (wt%), the viscosity gradually increases. Some modifications in water self-diffusion were observed in the same concentration range. The molecular and micellar region have significantly different transport and rheological properties. The solutions are fluid and easily flowing; at concentrations below, or close to, the *cmc,* they have the same viscosity as neat water.

Thermodynamic information associated with the onset of upper consolute boundaries [59, 60] in *Bola A16*-water mixtures were inferred by *DSC*. Scans on selected mixtures, at concentrations below, close to or above the *cmc* are reported in Figure 2.
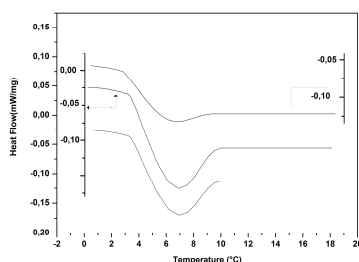
Figure 2: *DSC* thermograms, reported as heat flow (in mw mg^{-1}) *vs*. T (°C) are relative to, 10.0 wt% (a) 0.5 wt% (b) and 0.023 wt% (c) *Bola A16* (from the bottom),. The heating rate is 1 °C min^{-1}.

At high surfactant content the occurrence of a sharp transition peak is observed by *DSC*. It is ascribed to the melting enthalpy of hydrated *Bola A16* (which is an oil) and to the subsequent formation of the solution phase. As the surfactant concentration approaches the regimes pertinent to the molecular solution, the *DSC* peak vanishes and is hardly detected (Figure 2c). More information on the transition enthalpies and on the related temperatures are given in Table 1. The transition temperature, T_{tr}, inferred by optical methods is close to the one inferred by *DSC*. T_{tr} is a cloud point defining a phase boundary between the one and two-phase regions. Hereafter it is identified as a critical solution temperature.

Bola A 16 (wt%)	ΔH_{tr} (kJ mol^{-1})	T_{tr} (K)
2.0 10^{-2}	-3.32± 0.01	279.7± 0.1
0.5	-5.43± 0.01	279.9± 0.1
10.0	-6.65± 0.01	280.1± 0.1

Table 1: Transition enthalpies, ΔH_{tr}, and temperatures, T_{tr}, for selected Bola A 16-water mixtures.

In Figure 3 is reported the surface tension, τ *vs*. ln (*m*) plot. As can be seen, *Bola A16* is adsorbed at the air/water interface and the surface tension decreases up to the critical micellar concentration. At this point, micelle formation competes with interfacial adsorption and the slope of the plot abruptly

decreases. The break point, represented by the intersection of two straight lines, defines the *cmc* and is close to 4.7×10^{-3} mol kg^{-1} (about 0.5 wt%). The lower is the *cmc* value of a given surfactant, the more stable are the micelles. This is especially important from the pharmacological point of view, since upon dilution with a large volume of the blood, considering intravenous administration, only micelles of surfactants with low *cmc* value still exist, while micelles from surfactants with high *cmc* value may dissociate into monomers and their content may precipitate in the blood [61]

The surface tension above the *cmc* is nearly constant.
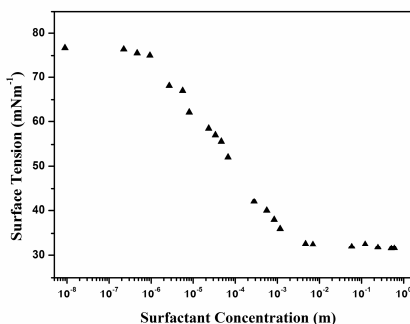
Figure 3: Surface tension, τ, in mN m^{-1}, as a function of *Bola A16* concentration, *m* (mol kg^{-1}), at 25 °C.

The links between the chemical structure and the micelle formation in systems containing surfactants different from the mono-alkyl chain type are not always immediately rationalised by an univocal *cmc* value. In an effort to bring to convergence the behaviour of structurally complex surfactants, Zana derived a unified approach to define the *cmc* in all surfactant systems, independently from the number of chains, polar head groups and counter-ions, whatever their charge is [62,63]. Accordingly, the standard Gibbs energy of micelle formation, ΔG_M^0, is defined by the generalised equation

$$\Delta G^{\circ}{}_{M} = RT \left[\left(\frac{1}{j} + \beta \frac{i}{j} \left| \frac{z_s}{z_c} \right| \right) \ln cmc \right.$$
$$\left. + \left(\frac{i}{j} \left| \frac{z_s}{z_c} \right| \beta \ln \left(\frac{i}{j} \left| \frac{z_s}{z_c} \right| \right) - \frac{1}{j} \ln j \right) \right] \qquad (2)$$

where i is the number of charged (or ionisable) groups and j that of alkyl chains, β the counter-ion binding degree, z_s and z_c the valency of surfactant ion and counter-ion, respectively. In non ionic surfactants, as in the present case, Equation (2) reduces to the form predicted by the pseudo-phase separation model [64]. The above equation has perhaps a significant predictive capacity in case of ionisation of crown ether bolas, because the Gibbs energy terms associated with charging the polar

76

groups can be significant. It is expected that ionised crown-ether based *Bolaforms* have *cmc* values largely different from those pertinent to the non ionic form [23,25]. When the crown ether *Bolas* complexes sodium ions in aqueous NaCl solutions, Equation (2) reduces to

$$\Delta G^{\circ}{}_M = RT[(1 + 2\beta)\ln cmc + 2\beta \ln 2]$$

(2')

and reasonable estimates of the electrostatic contribution to the Gibbs energy changes, associated with micelle formation, $\Delta G_{M,el}$, can be made (provided β is known).

The questions pointed out above are crucial in the analysis of crown ether *Bolas*, since ion uptake in their cavity is a true complexation equilibrium and is controlled by the amount of free electrolyte in the bulk. Actually, we do not know as to whether partial ionisation of nitrogen groups in the crown ether units is effective, or residual sodium ions are trapped in the aza-crown cavities. The crown ether charging process (subsequent to complexation) and counter-ion binding, as well, depend on the amount of salt in the bulk and can be ruled out in the present experimental conditions. Complete or un-complete ion uptake by crown ether surfactants, and *Bolas* as well, control the consolute boundaries observed in selected systems [65]. No information on the occurrence of such consolute phenomena could be observed in the temperature region investigated in the present work, up to about 50 °C.

NMR Self Diffusion measurements.

Fourier transform *NMR* self-diffusion provides insight into the solution micro-structure by determining the long-range mobility of the components. Detection of motions over much longer distances compared with molecules or micelles (some nm large), provides a sensitive probe for the state of aggregates [66]. Owing to the long transverse relaxation times of *Bola A16* protons, the surfactant self-diffusion values could be measured in the whole investigated concentration range by using a simplified relation, Equation (1). Selected self-diffusion coefficients of the surfactant as a function of *Bola A16* concentration, at different temperatures, are reported in Figure 4.
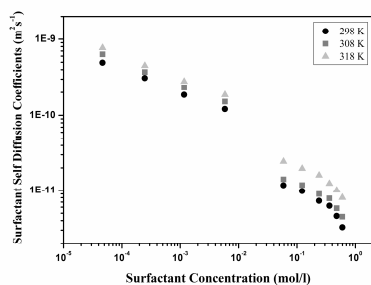

**Figure 4: Surfactant self-diffusion coefficient, *D*s, *vs. Bola A16* concentration, (mol l⁻¹),
at 25.0 (diamonds), 35.0 (grey squares) and 45.0 °C.**

Typical values of the molecular surfactant are close to 10^{-10} m^2 s^{-1}. At concentrations close to the *cmc* changes in the diffusive trends are observed. Thereafter the self diffusion values decrease more significantly and the contribution ascribed to the molecular species progressively vanishes. The decrease in self-diffusion becomes more pronounced at higher concentration and is due to the formation of aggregates. Concerning micelle diffusivity, an apparent micelle radius, *r*, of 10.0 ±0.5 nm may be inferred by the Stokes–Einstein equation, according to:

$$ r = \left[\frac{K_B T}{6\pi D_{mic} \eta} \right] $$

(3)

where η is the solvent viscosity at the given temperature. Very presumably, *r* values from self-diffusion include a significant amount of bound (hydration) water. Such values refer to the low concentration limit, when inter-micellar interactions are negligible.

The big size of the micelles formed by this surfactant offers a big advantage for solubilization of the drugs. In fact it was observed that for alkyl sodium sulfates and alkyl trimethylammonium bromides, the solubilization of β-Arteether increases with the increase in the alkyl chain length, due to the larger micellar size[67].

According to viscosity findings, (see below), micelle sizes are not expected to change much with composition.

Water self-diffusion in surfactant solutions is influenced by hydration and obstruction effects due to micelles [68]. The increase in volume fraction of the dispersed phase, in aggregate size ad in micelle hydration, as well, are concomitant to a decrease in water self-diffusion. In Figure 5 the normalised water self-diffusion coefficients are reported as a function of surfactant content.

The results indicate the occurrence of two different composition ranges: up to *cmc* and above that limit, respectively.
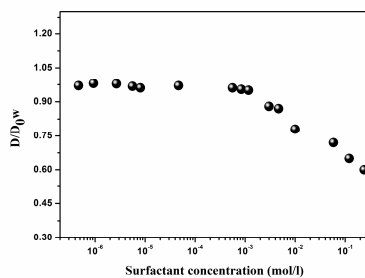

Figure 5: Normalized water self-diffusion coefficients, *D*w/D$_0$w, *vs. Bola A16* concentration, (mol l^{-1}), at 25.0 (diamonds), 35.0 (grey squares) and 45.0 °C

The observed behaviour is reproducible and implies the occurrence of significant variations in the hindrance to diffusion. Concerning water diffusion, its self diffusion coefficient slightly decreases with surfactant content (when no aggregates are present), and a significant change in slope occurs at the *cmc*, because of the presence of micelles. From that point onward changes in relative water self-diffusion values are analysed by assuming the overlapping of hydration with micelle size and shape effects. In accordance with the 'cell-diffusion model' the measured water self-diffusion coefficient, D_W, can be interpreted according to a two-site approach as [69,70 53, 54]:

$$D_W = f(1 - P)D_f + PD_b$$

(4)

where the observed D_W is the mean average value resulting from the contributions due to free, D_f, and bound, D_b, water molecules. It is modulated by the relative amounts of bound water, P, and by the obstruction factor, f as well. The aforementioned relation is the time average value resulting from matter exchange from free to bound states, invariant with time. Changes in the above trends may imply size transitions. As demonstrated in the rheological section, shape transition can be ruled out, since the micelles keep a spherical shape with increasing the surfactant content.

Rheological Results.

In Figure 6 the dependence of viscosity, η, on shear rate, γ, for samples at different surfactant concentrations is given. A newtonian behaviour is observed for all mixtures, even though the viscosity can be one order of magnitude higher than water, or more. In all cases reported here the behaviour is newtonian, i.e. independent of shear rate.
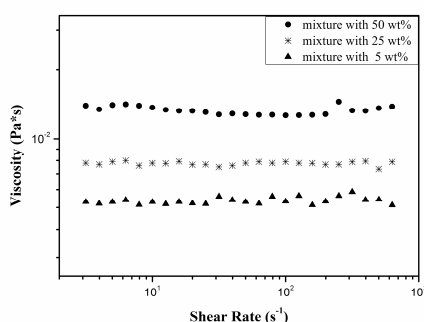
Figure 6: Viscosity (Pa s) *vs*. shear rate (s⁻¹) for *Bola A16*-water mixtures containing 5.0, 25.0 and 50.0 wt% of surfactant at 25.0 °C.

The structural organisation in the above system is presumably due to spherical and mono-disperse micelles. According to the present findings no direct evidence of micelle growth can be inferred. In addition, no flow-orientation phenomena were observed (and no dependence of viscosity on shear

rates). Thus, spherical aggregates very presumably occur and no micelle entanglement, with subsequent orientation phenomena in the flow, is observed. The high η values and the independence of viscosity on shear rate demonstrate that micelles soon grow above the cmc (i.e. no intermediate association stages occur) and retain a grossly spherical shape.

Therefore it is worth underlining that in this micellar solution the molar drugs solubilization capacity does not change under different flow conditions because of no changes in the shape. The extent of the drugs solubilization into a particular micelle depends upon the locus of the solubilization and therefore the shape of the micelle. This makes this surfactant extremely versatile like drugs carriers [71].

The dynamic strain sweep tests provide information on the linear visco-elastic behaviour of the materials determining the complex shear modulus, defined as [72]:

$$G(\omega) = G'(\omega) + iG''(\omega)$$ (5)

where $G'(\omega)$ is the in-phase (or storage) and $G''(\omega)$ the out-of-phase (or loss) component, respectively. The use of a generalised Maxwell model allows determining the rheological properties of the solutions. The visco-elastic behaviour is modelled by a number of Maxwell elements in parallel. Each element consists of a spring and a dashpot in series, and is characterised by a spring modulus, G^o, and a relaxation time, λ. In dynamic shear experiments, the generalized Maxwell model gives the following equations for $G'(\omega)$ and $G''(\omega)$ [73]:

$$G'(\omega) = \sum_i \frac{\omega^2 \lambda_i^2 G_i^0}{1 + (\omega\lambda_i)^2}$$ (6)

$$G''(\omega) = \sum_i \frac{\omega\lambda_i G_i^0}{1 + (\omega\lambda_i)^2}$$ (7)

where ω is the applied frequency.

The relaxation amplitudes and times were obtained by a best fit of the observed visco-elastic moduli in Equations (6) and (7). The real and imaginary amplitudes in the above equation were used as adjustable parameters in an iterative procedure minimising the overall standard deviation, expressed as $\sigma(G') + \sigma(G'')$. The accuracy on relaxation times is ±5%.

The experimental data were analysed according to the "weak gel" model, which considers flow as a co-operative phenomenon [74]. The theory provides a link between the solution microstructure and its rheological properties. The most important parameter introduced by the weak gel model is the 'co-ordination number', z, indicating how many flow units interact with each other in the process, and quantifies how much co-operative is the flow response. It can be demonstrated, on this regard, that [75]

$$G*(\omega) = A\omega^{\frac{1}{z}}$$ (8)

where A is a proper constant, related to the 'interaction strength' between the rheological units in the flow process. The micellar solution is modelled as an ensemble of such units, interacting each other to establish a transient structure during the flow process. The co-ordination number (z) and the amplitude of such interactions were obtained from $G*$ $vs.$ ω plots, according to Equation (8). Quite unexpectedly, no coordination is present among flow units, since the coordination number is close to unity and does not change much with *Bola A16* content. This is a preliminary, but strong, evidence that micelles retain the same shape in the whole concentration range that has been investigated.

The visco-elastic properties of *Bola A16*-water mixtures were analysed by oscillatory experiments in frequency and temperature sweep modes. To define the linear visco-elastic conditions several strain-sweep tests were performed by applying small strain amplitudes to the solutions. Pre-shear tests ($\approx$10 s^{-1} for 60 s) showed negligible effects on the visco-elasticity of such mixtures. The mechanical spectra as a function of frequency, at 25.0 °C, are shown in Figure 7 for different concentrations.
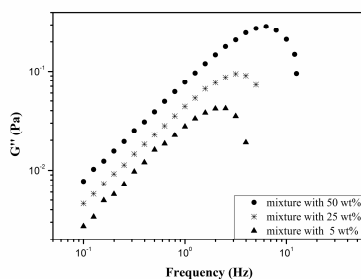
Figure 7: Frequency sweep test, reported as G" (Pa) *vs.* frequency, (Hz), at 25.0 °C. Data refer to 5.0 (crosses), 25.0 (grey circles) and 50.0 *Bola A16* wt%. The applied strain is 100 %.

Significant information can be inferred from the above rheological results. As previously mentioned, mixtures can be considered as purely newtonian fluids. In such liquids, the viscosity is shear-rate independent and no elastic contributions appear in the spectra. All mixtures are conform

to the above statements and no storage modulus can be measured, within the limits of the instrumental resolution. The micellar solutions made of *Bola A16* behave as single-element Maxwell fluids and their relaxation time is so short that much higher frequencies are required to observe Maxwell-type curves and to define their relaxation times accordingly. In addition, the absence of shear induced changes in the aggregate shape gives another reason for using this systems in the pharmacological field. The flow behaviour reflects structural modifications in the particles morphology and its determination is of fundamental relevance in pharmaco-dynamics, since drug delivers usually operate in mechanically stressed conditions.

CONCLUSIONS

As a result of combined investigation some structural information on the micellar solutions made by *Bola A16* were inferred. *DSC* measurements indicate the occurrence of consolute boundaries at low temperatures. The *cmc* is low and poorly dependent on *T*. Micelles retain a nearly globular shape in a wide composition range and their size is similar to normal surfactants. Such hypotheses are substantially supported by *NMR*.

At all concentrations the solutions are newtonian liquids and *Bola A16* micelles behave as rigid spherical aggregates. They are not deformed by the applied shear. On increasing the surfactant content the micelle structure is retained and spherical aggregates are still present. The very short relaxation times observed in the rheological experiments may be ascribed to the breaking/forming transient processes occurring during the application of shear stresses. The absence of visco-elastic effects supports the aforementioned hypotheses of spherical micelles and suggests that no inter-micellar interactions do occur.

Further developments in the characterisation could be important. In particular, given the strong complexing capacity of the crown ether units towards alkali ions, it is expected that *Bola A16* may form charged aggregates and the solution structure should be stabilised by electrostatic interactions. The rheological properties of these systems allow to improve their performances as drug delivers. The rheological results underline spherical shape in all flow conditions and suggest possible applications of such Bolas aggregates as colloidal lipophilic drug carriers.

References

[1] S. Mall, G. Buckton, D.A. Rawlins, J. Pharm. Sci., 85, (1996), 75.
[2] T.M. Allen, C.B. Hansen, D.E.L. Menenez, Adv. Drug Deliv. Rev., 16, (1995), 267.
[3] G.S. Canto, S.L. Dalmora, A.G. Oliveira, Drug Dev. Ind. Pharm., 25, (1999), 1235.
[4] R. Gref, Y. Minamitake, M.T. Peracchia, V.S. Trubetskoy, V.P. Torchilin, R. Langer,. Science, 263, (1994), 1600.
[5] M.C. Jones, J.C. Leroux, Eur. J. Pharm. BioPharm., 48, (1999), 101.

[6] V.P. Torchilin, V.S. Trubetskoy, K. R. Whiteman, P. Caliceti, P. Ferruti, F.M. Veronese, J. Pharm. Sci., 84, (1995), 1049.

[7] V.P. Torchilin, J. Control. Rel., 73, (2001), 137.

[8] C. J. Pedersen, J. Am. Chem. Soc., 89, (1967), 7017.

[9] J. M. Lehn, Angew. Chem. Int. Ed. 27, (1988), 89.

[10] E. D. Glendening, D. Feller, M. A. Thompson, J. Am. Chem. Soc., 116, (1994), 10657.

[11] J. LeMoigne, P. Gramain, J. Simon, J. Colloid Interface Sci., 60, (1977), 565.

[12] Y. Morio, E. Pramauro, M. Gratzel, E. Pelizzetti, P. Tundo, J. Colloid Interface Sci., 69, (1979), 341.

[13] I. Ikeda, S. Yamamura, Y. Nakatsuji, M. Okahara, J. Org. Chem., 45, (1980), 5355.

[14] P. L. Kuo, I. Ikeda, M. Okahara, Tenside Deterg., 19, (1982), 204.

[15] P. Lo Nostro, A. Casnati, L. Bossoletti, L. Dei, P. Baglioni, Colloids Surf. A, 116, (1996), 203.

[16] L. Dei, A. Casnati, P. Lo Nostro, A. Pochini, R. Ungaro, P. Baglioni, P. Langmuir, 12, (1996), 1589.

[17] L. Dei, A. Casnati, P. Lo Nostro, P Baglioni, Langmuir, 11, (1995), 1268.

[18] M. Ceccato, P. Lo Nostro, P. Baglioni, Langmuir, 13, (1997), 2436.

[19] J. H. Fuhrhop, R. Bach, Adv. Supramol. Chem., 2, (1992) 25.

[20] R. Muzzalupo, G. A. Ranieri, C. La Mesa, Langmuir, 12, (1996), 3157.

[21] La Mesa, C., In Novel Surfactants Conference; Robb, D., Ed.; Roy. Soc. Chem., Wrexham, UK, (1998), p 39.

[22] E. Caponetti, D. Chillura Martino, L. Pedone, J. Appl. Cryst., 36, (2003), 753.

[23] E. Caponetti, D. Chillura-Martino, C. La Mesa, R. Muzzalupo, L. Pedone, J. Phys. Chem. B, 108, (2004), 1214.

[24] R. Muzzalupo, S. Trombino, F. Iemma, F. Puoci, C. La Mesa, N. Picci, Colloids Surf. B: Biointerfaces, 46, (2005), 78.

[25] R. Muzzalupo, G. Gente, C. La Mesa, E. Caponetti, D. Chillura-Martino, L. Pedone, M.L. Saladino, Langmuir, 22, (2006), 6001.

[26] G. H. Escamilla, G. R. Newkome, Angew. Chem. Int. Ed. Engl., 33, (1994), 1937.

[27] J. H. Fuhrhop, J. Matthieu, Angew. Chem. Int. Ed. Engl., 23, (1984), 100.

[28] Q. Lu, H. F. Gong, M. H. Liu, Prog. Chem., 13, (2001), 161.

[29] J. Sirieix, V. N. de Lauth, M. Riviere, A. Lattes, New J. Chem., 24, (2000), 1043.

[30] M. Kolbel, T. Beyersdorff, I. Sletvold, C. Tschierske, J. Kain, S. Diele, Angew. Chem. Int. Ed. Engl., 38, (1999), 1077.

[31] M. Masuda, T. Shimizu, J. Carbohyd. Chem., 17, (1998), 405.

[32] L. M. Cameron, T. M. Fyles, C. W. Hu, J. Org. Chem., 67, (2002), 1548.

[33] J. Guilbot, T. Benvegnu, N. Legros, D. Plusquellec, J.C. Dedieu, A. Gulik, Langmuir, 17, (2001), 613.

[34] T. Shimizu, R. Iwaura, M. Masuda, T. Hanada, K. Yase, J. Am. Chem. Soc., 123, (2001), 5947.

[35] R. Iwaura, K. Yoshida, M. Masuda, K. Yase, T. Shimizu, Chem. Mater., 14, (2002), 3047.

[36] R. Buller, H. Cohen, T. R., Jensen, K. Kjaer, M. Lahav, L. Leiserowitz, J. Phys. Chem. B, 105, (2001), 11447.

[37] R. Zana, H. Levy, J. Colloid Interface Sci., 170, (1995), 128.

[38] R. Zana, Y. Muto, K. Esumi, K. Meguro, J. Colloid Interface Sci., 123, (1988), 502.

[39] I. Satake, T. Morita, T. Maeda, K. Hayakawa, Bull. Chem. Soc. Jpn., 70, (1997), 761.

[40] F. M. Menger, J. F. Chow, J. Am. Chem. Soc., 105, (1983), 5501.

[41] S. K. Abid, S. M., Hamid, D. C., Sherrington,. J. Colloid Interface Sci., 120, (1987), 245.

[42] T. W. Davey, W. A. Duck, A. R. Hayman, J. Simpson, Langmuir, 14, (1998), 3210.

[43] J. H. Fuhrhop, T. Wang, Chem. Rev., 104, (2004), 2901.

[44] R. Muzzalupo, F.P. Nicoletta, S. Trombino, R. Cassano, F.Iemma, N. Picci, Colloids and Surfaces B: Biointerfaces 58, (2007), 197

[45] H. Matsuda, Y.Yamada, K. Kanamori, Y. Kudo, Y.Takeda, Bull. Chem. Soc. Jap., 64 (1991), 1497.

[46] M. Szogyi, T. Cserhati, F. Tolgyesi, Lipids, 28, (1993), 847.

[47] B. Sesta, A. D'Aprano, Colloids Surf. A., 140, (1998), 119.

[48] J.H. Fendler, Chem. Rev. 87, (1987), 877.

[49] J.H. Fendler, Am. Chem. Soc. Symp. Ser. 83, (1987), 342.

[50] G.R. Thuduppathy, J.W. Craig, V. Kholodenko, A. Schon, R.B. Hill, J. Mol. Biol. 359 (2006), 1045.

[51] S. Keller, H. Heerklotz, A.J. Blume, J. Am. Chem. Soc. 128, (2006), 1279.

[52] S. Munoz, J. V. Mallen, A. Nakano, Z. Chen, I. Gay, L. Echegoyen, G. W. Göckel, J . Am. Chem. Soc., 115, (1993), 1705.

[53] C. La Mesa, G. A. Ranieri, Ber. Bunsen-Ges. Phys. Chem., 97, (1993), 620.

[54] R. Muzzalupo, G.A. Ranieri, C. La Mesa, Colloids Surf. A, 104, (1995), 327.

[55] L. Coppola, R. Gianferri, C. Oliviero, I. Nicotera, G. A. Ranieri, Phys. Chem. Chem. Phys., 6, (2004), 2364.

[56] P. Stilbs, Prog. NMR Spectrosc., 19, (1987), 1.

[57] E. D. Stejskal, J. E. Tanner, J. Chem. Phys., 42, (1965), 288.

[58] M. G. Bonicelli, G. F. Ceccaroni, C. La Mesa, Colloid Polym. Sci., 276, (1998), 109.

[59] B. Faucomprè, B. Lindman, J. Phys. Chem., 91, (1987), 383.

[60] C. Whiddon, O. Söderman, P. Hansson, Langmuir, 18, (2002), 4610.

[61] M.Yokoyama, CRC Crit Rev Ther, Drug Carrier Syst, 9, (1992), 213.

[62] R. Zana, Langmuir, 12, (1996), 1208.

[63] R. Zana, J. Colloid Interface Sci., 248, (2002), 203.

[64] P. Mukerjee, Adv. Colloid Interface Sci., 1, (1967), 241.

[65] G. J. T. Tiddy, Phys. Rep., 57, (1980), 1.

[66] O. Söderman, B. Lindman, P. Stilbs, in "Nuclear Magnetic Resonance"; G. A. Webb, Ed.; Roy. Soc. Chem., London, (1983), Vol. XII, p 302.

[67] A.K. Krishna, D.R. Flanagan, J. Pharm. Sci., 78, (1989), 574.

[68] P. G. Nilsson, B. Lindman, J. Phys. Chem., 87, (1983), 4756.

[69] B. Lindman, O. Söderman, H. Wennerström, In Surfactant Solutions: New Methods of Investigation; R. Zana, Ed.; Marcel Dekker: New York, 1987; Chapter VI, p 295.

[70] B. Jonsson, H. Wennerstrom, P.G. Nilsson, P. Linse, Colloid Polym. Sci. 264, (1986), 77.

[71] M.J.Rosen, M.J. Surfactants and interfacial phenomena, 2ed., John Wiley & Sons, New York, 1989.

[72] J. D. Ferry, in "Viscoelastic Properties of Polymers", 3rd Ed., Wiley, New York, (1980).

[73] M. R. Mackley, R. T. J. Marshall, J. B. A. Smeulders, F. D. Zhao, Chem. Eng. Sci., 49, (1994), 2551.

[74] L. Bohlin, J. Colloid Interface Sci., 74, (1980), 423.

[75] D. Gabriele, B. De Cindio, P. D'Antona, Rheol. Acta, 40, (2001), 120.

2.4.6 Novel Glucuronic acid-based surfactant as new approach for cancer therapy: Synthesis, characterization and preparation of targeted niosomal formulation

(<u>Work in progress</u>).

Drugs used in humans to treat cancers are cytotoxic because kill normal cells as well as cancerous cells. Furthermore, because of the blood circulation in the body only a small fraction of the drug gets to the target tumor; most of drug acts on normal tissues or is rapidly eliminated. Therefore, to obtain a therapeutic effect, a relatively high dose of drug must be administered and usual formulations are a balance between killing the tumor (efficacy) and killing the patient (toxicity). One way to reduce the toxicity of the drug to the normal tissue is to direct the drug to the tumor cells with a drug delivery system. This is similar in concept to the use of a cruise missile to only destroy a military target. The bomb in this research is called a niosome and since malignant cells are known to have accelerated metabolism, high glucose requirements, and increased glucose uptake compared with healthy cells, we propose to turn the niosome into a 'smart bomb' by attaching a carbohydrate molecule (a sugar) to an alkylic chain and using this new surfactant to obtained target niosomes. The sugar could target the liposome to the tumor.

Herein we report novel nonionic glucuronic acid-based surfactant, obtained by selective amidation of previously synthesized N-decanoylesamethilendiammine and 1,2,3,4-tetraacethoxy- glucuronic acid (Fig 5). The obtained molecule was characterized by infrared (FT-IR) and ^{1}H-NMR spectroscopies and a preliminary study of its aggregation behaviour has been made. Moreover in this study the suitability of this new glucuronic acid-based surfactant to form niosomes was evaluated. Our results suggest that this surfactant was able to form niosomes without membrane additives, such as cholesterol and morphological and dimensional analysis also suggest that vesicles were regular and spherical in shape and show a diameter of 350 nm.

Now we are evaluating the entrapment efficiency of an antitumoral model drug (X) widely used in the treatment of breast cancer, and after these carriers will be tested *in vitro* in different tumor cell lines. In particular, studies will be done to assess the cytotoxic and antiproliferative activity of niosomes, their compartmentalisation at the cellular level, and using different methods, the degree of apoptotic induction will be studied**.** Moreover the applicability of the obtained new nanomaterials, will be evaluated by testing the release of carried active molecules in the different districts of the body.

2.4.7 Niosomes as photostability systems for Nifedipine and Barnidipine liquid oral dosage forms

(**Work in progress**).

Nifedipine and Barnidipine, belonging to the 1,4-dihydropyridine class of antihypertensive drugs, are photosensitive since light catalyzes their oxidation to pyridine derivatives, lacking any therapeutic effect. Accordingly, many new technology-based pharmaceutical systems are proposed in order to enhance stability, such as vesicular systems. Nifedipine and Barnidipine are usually administered as solid oral dosage forms and not many liquid formulations are available. In this light we decide to carry out a scientific collaboration with the research group of Prof. Ragno, (Department of Pharmaceutical Science, University of Calabria) involved in the study of photodegradation of 1,4-dihydropyridine class of antihypertensive drugs, for the design of an innovative Nifedipine and Barnidipine liquid oral dosage forms based on niosomes. We characterized these systems in terms of dimensional and morphological analysis and entrapment efficiency. Results suggest that vesicle were regular and spherical in shape, they showed diameter of about 200-300 nm and the polydispersity index values (0.21) were considered as evidence of homogeneous distribution of colloidal vesiscles. Nifedipine and Barnidipine-containing niosomes were subjected to stressed degradation studies, according to the ICH (International Conference on Armonization) rules, by comparison of their degradation kinetics to that of the drug in solution and analytical determination of drugs was performed by measuring the absorbance at the maximum peak in the zone 350-370 nm, that is a typical signal of the 1,4-dihydropyridine structure. Preliminary results showed that the drug entrapment into niosomes strongly reduced the photodegradation process, both in the case of Nifedipine and Barnidipine niosomes. All the studied systems have shown a high degree of protection, with a degradation rate always lower than in the drug solution. In particular niosomal systems may double the drug half-life. Now we are optimizing the properties of these vesicular systems and the applicability of these new nanomaterials, will be evaluated by testing the release of drugs *in vitro* in fluid simulating the gastrointestinal tract.

3

Polymeric materials

This section reviews the polymeric materials (gels, fibbers or polymers) generated during my PhD research, including a first part in which I briefly introduced this class of drug carriers.

3.0 A brief introduction on Polymeric materials in Drug Delivery

Polymers find broad uses in drug delivery applications. Reasons include their surfaces activity, which makes them efficient stabilizers of colloidal drug delivery systems, their gel forming capacity, which allows many opportunities in drug delivery, and their formation of self-assembly structures analogous to those formed by low molecular weight surfactant.[1]

Moreover polymeric materials exhibit several desirable properties for drug carrier use including biocompatibility, biodegradability, and functionalization capability. Through functionalization and structural manipulation of polymer materials, drug molecules can be incorporated within the polymer. Entrapping or encapsulating the drug within a polymer allows for greater control of its pharmacokinetic behaviour that maintains more appropriate steady levels of the drug at the site of delivery.[2] Techniques that are used to couple the drug with the polymer include sequestering, conjugation, and micelle formation.[3] Nanostructure formation of polymers has been accomplished through mold replication,[4] colloidal lithography,[5] interfacial polymerization, nanoprecipitation, multiple solvent emulsion evaporation[6] and electrospinning.[7]

This class of materials presents seemingly endless diversity in topology and chemistry[8]: besides the several class of polymeric materials used in drug delivery, block copolymer, consisting of blocks of two or several polymers, and the polysaccharides have found widespread use in pharmaceutical field. In the last case this is due to the formation of gels in aqueous solution containing also low amounts of polymer. In addition the classification is not complete without mentioning hybrid materials such as modified biopolymers (e.g. modified chitosans or cellulose) or modified synthetic polymers (e.g. polymer peptide conjugates). Many of these polymers were designed in such a way that their natural and positive properties remains constant throughout an application.[1]

The field is usually characterised by the terms 'polymer therapeutics' or 'nanomedicines'.[9-11]
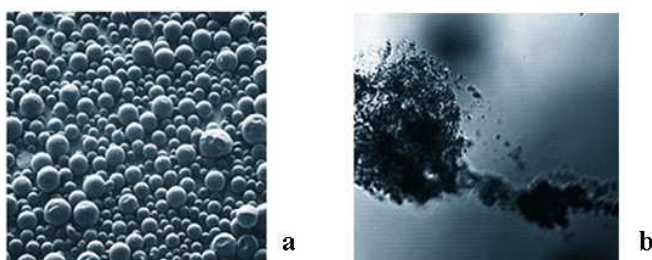

Fig.3.1 Examples of nanoparticles (a) and bio-degradable matrices (b).

Polymeric materials are being used as drug delivery systems as a polymeric drug itself or in combination with small molecule drugs or with biomacromolecules.

If the polymer is not a drug itself, it often provides a passive function as a drug carrier, reducing immunogenicity, toxicity or degradation, whilst improving circulation time and potentially a passive targeting function. In this case the polymer has to be water-soluble, non-toxic, non-immunogenic and it needs to be safe at all stages of the drug delivery process (e.g. before and after the drug has been released) including a safe excretion.

An aspect which has been highlighted in the relation to the use of polymers in drug delivery is their biodegradation, due the possibility to control the degradation rate of polymers over wide ranges through, e.g., the polymer structure and composition , biodegradation has been found to provide an interesting way to obtain a controlled drug release over a prolonged time, and to protect sensitive compound from harsh environment, e.g., in the stomach. If the polymer is non-degradable (e.g. poly(meth)acrylates), the size needs to be below the renal threshold ensuring that it is not accumulated in the body. If the polymer is degradable (e.g. polyesters), the toxicity and/or immune response of the degradation products have to be considered as well.[12]

Besides its application in a passive fashion, synthetic polymers often adopt a more active role such as releasing a drug molecule, peptide or oligo/poly(nucleic acid) upon an external stimulus.[13] In this case, we consider these polymers as stimuli responsive polymers. Stimuli-responsive polymers mimic biological systems in a crude way where an external stimulus (e.g. change in pH or temperature) results in a change in properties.[14] This can be a change in conformation, change in solubility, alteration of the hydrophilic/hydrophobic balance or release of a bioactive molecule (e.g. drug molecule). This also includes a combination of several responses at the same time. In medicine, stimuli-responsive polymers and hydrogels have to show their response properties within the setting of biological conditions, hence there is a large variety of different approaches.

Typical stimuli are temperature,[15] pH,[16,17] light[18] and redox potential.[19,20] The obvious change in pH along the GI tract[21,22] from acidic in the stomach (pH=2) to basic in the intestine (pH=5–8) has to be considered for oral delivery of any kind of drug, but there are also more subtle changes within different tissue. Certain cancers as well as inflamed or wound tissue exhibit a pH different from 7.4 as it is in circulation.[23]
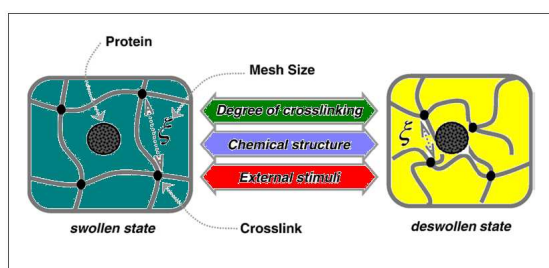
Fig.3.2 Example pH-responsive system.

In addition, the combination of a pH-responsive system with a thermo-responsive polymer can further alter the hydrophilic/hydrophobic balance. This allows a polymer to become membrane active at a specific temperature[24] and/or a specific pH.[25-28]

References

[1]Malmsten M., Drugs and Pharmaceutical Sciences, New York: Marcel Dekker, Surfactants and Polymers in Drug Delivery, 2002.

[2] G.A. Hughes Nanomedicine: Nanotechnology, Biology, and Medicine, 1, (2005), 22.

[3] Duncan R., Nat Rev Drug Discovery, 2, (2003), 347.

[4] Li Y.Y., Cunin F., Link J.R., Cao T., Belts R.E., Reiver S.H., Science, 299, (2003), 2045.

[5] Dalby M.J., Berry C.C., Riehle M.O., Sutherland D.S., Agheli H., Curtis A.S.G., Exp Cell Res, 295, (2004), 387.

[6] Couvreur P, Barratt G, Fattal E, Legrand P, Vauthier C. Crit Rev Ther Drug Carrier Syst, 19 (2002), 99.

[7] Frenot A., Chronakis I.S., Curr Opin Colloid Interface Sci 8, (2003), 64.

[8] Li Y.Q, You H.B., Pharm Res, 23, (2006), 460.

[9] Duncan R., Nat Rev Drug Discov, 2, (2003), 347.

[10] Twaites B., de las Heras Alarcon C., Alexander C., J. Mater. Chem. 15, (2005), 441.

[11] M. Ferrari, Nat Rev, Cancer, 5, (2005), 161.

[12] Schmaljohann D., Adv Drug Del Rev, 58, (2006), 1655.

[13] Miyata T., Uragami T., Polymeric Biomaterials, in: S. Dumitriu (Ed.), 2nd ed., Marcel Dekker, New York, 2002.

[14] Ottenbrite R.M., Kim S.W., (Eds.), Polymeric Drugs and Drug Delivery Systems, CRC Press, Boca Raton, 2001.

[15] Chen G., Hoffman A.S., Nature, 373, (1995), 49.

[16] Tanaka T., Nishio I., Sun S.T., Ueno-Nishio S., Science, 218, (1982), 467.

[17] Osada Y., Okuzaki H., Hori H., Nature, 355, (1992), 242.

[18] Suzuki A., Tanaka T., Nature, 346, (1990), 345.

[19] Hoffman A.S., Polym Gels, 268, (1991), 82.

[20] De las Heras Alarcon C., Pennadam S., Alexander C., Chem Soc Rev, 34, (2005), 276.

[21] Florence A.T., Attwood D., Physicochemical Principles of Pharmacy, 3rd ed., Macmillan Press, London, 1998.

[22] Dissemond J., Witthoff M., Brauns, T.C. Harberer D., Gros M., Hautarzt 54, (2001), 959.

[23] Rofstad E.K., Mathiesen B., Kindem K., Galappathi K., Cancer Res, 66, (2006), 6699.

[24] Ringsdorf H., Venzmer J., Winnik F.M., Angew Chem, Int Ed Engl, 30, (1991), 315.

[25] Kusonwiriyawong C., Wetering P., Hubbell J.A., Merkle H.P., Walter E., Eur J Pharm Biopharm, 56, (2003), 237.

[26] Barker S.L.R., Ross D., Tarlov M.J., Gaitan M., Locascio L.E., Anal Chem, 72, (2000), 5925.

[27] Cunliffe D., De las Heras Alarcon C., Peters V., Smith J.R., Alexander C., Langmuir, 19, (2003), 2888.

[28] Dong L.C., Hoffman A.S., J Contr Rel 15, (1991), 141.

Research Projects

on polymeric materials
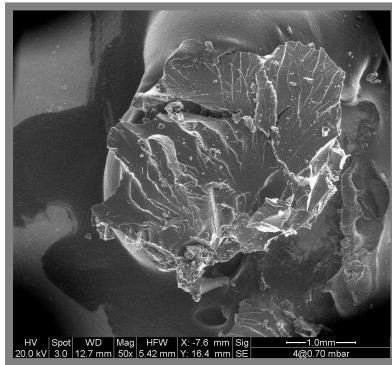
3.1.1 Synthesis and properties of methacrylic functionalized Tween[TM] monomer networks

Rita Muzzalupo,[,§] *Lorena Tavano,*[§] *Cesare Oliviero Rossi,*[†]

Roberta Cassano,[§] *Sonia Trombino,*[§] *and Nevio Picci*[§]

[§]*Department of Pharmaceutical Science, Calabria University, Edificio Polifunzionale,*

87036 Arcavacata di Rende, Cosenza, ITALY;

[†]*Department of Chemistry, Calabria University, Via P. Bucci, Cubo 14/D,*

87036 Arcavacata di Rende, Cosenza, ITALY;

Abstract

Tween[TM] surfactants possess very interesting properties such as biodegradability, biocompatibility and low toxicity. The synthesis of acrylate monomers by means of the chemical modification of polysorbate surfactants Tween 20, 40, 60[TM] with unsaturated groups is described. Monomers were obtained owing to the reaction of methacrylic anhydride with different grades of Tween[TM] surfactants. Further polymerization was carried out in tetrahydrofuran, dimethylformamide and a mixture of water-tetrahydrofuran. Physical-chemistry properties of the polymer networks were investigated and the obtained results reveal that they strongly depend on the type of solvent used during the polymerization, as well as on the concentration of the casting solution. In particular, our study demonstrated that, depending on the solvent boiling point, i.e. the facility to remove the solvent from the polymer matrix, it is possible to predict properties of the network morphology.

Moreover, *in vitro* studies on controlled release were accomplished to demonstrate the possibility of utilizing these new materials as drug delivery systems.

All resulting networks represent a novel class of cross-linked polymeric materials useful both in pharmaceutical and chemical applications.

1. Introduction

Polysorbates are a group of non-ionic surfactants that consist primarily of fatty acid esters of sorbitol-derived cyclic ethers (sorbitans and sorbides) condensed with approximately 20 mol of ethylene oxide per mol (polyethoxy sorbitan). The introduction of ethylene oxide improves their water solubility, thereby expanding their applications.

The use of polysorbate surfactants depends on their chemical nature, as dictated by the structure of the sorbitol derivative core, the alkyl chain length of the fatty acid, the degree of esterification, and the number of polymerized oxyethylene residues.

These polysorbates are marketed under a variety of trade names such as Sorlate[TM], Tween[TM], Monitan[TM] and they find widespread use as emulsifiers, defoamers, dispersants, and stabilizers in food and cosmetics, to solubilise essential oils into water based products and biodegradation media [1,2]. In particular Tween[TM] surfactants are used successfully as additive to many food as well as cosmetic preparations. Properties such as emulsification, foaming, water binding capacity, spreading and wetting are efficiently utilized in industry [3-5].

In addition, to their well established chemical applications like remediation of toluene-contaminated groundwater,[6] they are also being tested for novel medical and pharmaceutical applications, such as drug delivery devices due to their very interesting properties of biodegradability, biocompatibility, low toxicity and moreover they show derivation from easily available materials [7,8].

Many surfactants, in particular conditions (such as concentration or temperature) or upon functionalization form gels that could find widespread applications in industry. Gels defined in terms of rheological characteristics as described elsewhere [9,10] can be considered as two component systems exhibiting a solid-like behaviour under small deformation.

In general, polymer gels are found in industrial and domestic applications such as in ion exchangers, coatings, diapers, etc., and in analytical equipment (e.g., in gel permeation chromatography); they are also interesting for medical applications such as drug delivery devices, artificial muscle and organs, chemical memories and valves [11,14] (e.g., for eye drops, skin care products, insulin controlled delivery, etc.). Additionally the use of polymeric materials as chemical sensors for the control of air pollution (NO, NO_2, H_2S, CO, etc.) or for storage purposes (freshness of food, by detection of alcohols, esters, amines, etc.) was widely investigated [15-20].

In this light, we decided to carry out the chemical modification of some grades of Tween[TM] surfactants by introducing unsaturated groups and these molecules were used as monomers for obtaining networks owing to a radical polymerization.

Hence, one would expect that these new Tween[TM]-based networks keep on one side the important bio-affinity characteristics of precursor monomers and on the other side the great advantages typical of gel systems.

For these reasons, the physical-chemistry properties (e.g. mechanical properties, solvent affinity, morphology) of these novel networks were characterized to evaluate their employment in pharmaceutical and medical fields. SEM images and NMR analysis allowed obtaining information on the morphology of the polymer networks and on the interactions network/solvent.

In particular, this paper concerns with a deep characterization of the Tween 60[TM]-based polymer network and this study is preliminary of a further wider characterization of other grades Tween[TM]–based polymer gels.

2. Materials and methods

2.1 Materials

Chemicals and reagents, Tween 20[TM], Tween 40[TM], Tween 60[TM], ethanol, acetone, dimethylformamide (DMF), chloroform, isopropanol, ferulic acid, toluene and benzene were supplied by Sigma Aldrich and used without further purifications. Methacrylic anhydride (MA) was distilled before using. Triethylamine, (Et_3N), azobis(isobutyronitrile) (AIBN), ammonium persulphate (PA), diethyl ether were supplied by Sigma Aldrich and used after purifications.

2.2 Synthesis of the monomers

Different grades of Tween[TM] surfactants were modified by the reaction with methacrylic anhydride (MA), in order to obtain methacrylate monomers as precursors of polymer networks.

Details on synthesized monomers as well as the solvents and the additive used are listed in Table 1. Labels indicating the samples will be used throughout the text.

Samples	Surfactant	Surfactant mol·10^{-2}	Trietylamine mol·10^{-2}	MA mol·10^{-2}	Surf/MA mole ratio
A2	Tween 20[TM]	0.65	1.30	1.30	1:2
A3	Tween20[TM]	0.65	1.90	1.90	1:3
A4	Tween 20[TM]	0.65	2.60	2.60	1:4
B2	Tween 40[TM]	0.62	1.24	1.24	1:2
B3	Tween 40[TM]	0.62	1.86	1.86	1:3
B4	Tween 40[TM]	0.62	2.48	2.48	1:4
C2	Tween60[TM]	0.61	1.22	1.22	1:2
C3	Tween 60[TM]	0.61	1.86	1.86	1:3
C4	Tween 60[TM]	0.61	2.48	2.48	1:4

Table 1. Details on the type and concentration of reagents used for the synthesis of the monomers

The procedure for the synthesis of methacrylic functionalized Tween[TM] monomers is shown in the Scheme 1.

Dry triethylamine (Et_3N) was added to the stirred solution of Tween[TM] in 100 ml of dry diethyl ether at 25°C. After 30 min a quantity of MA equimolar to the amount of Et_3N was added dropwise to the Tween[TM] solution at 0°C and the reaction was left to proceed by stirring for 24 hours at 25°C.

The final product was extracted by diethyl ether and washed with 50 ml of a 3M HCl solution, then with 50 ml of a 3M Na_2CO_3 solution, finally with water up to neutralization.
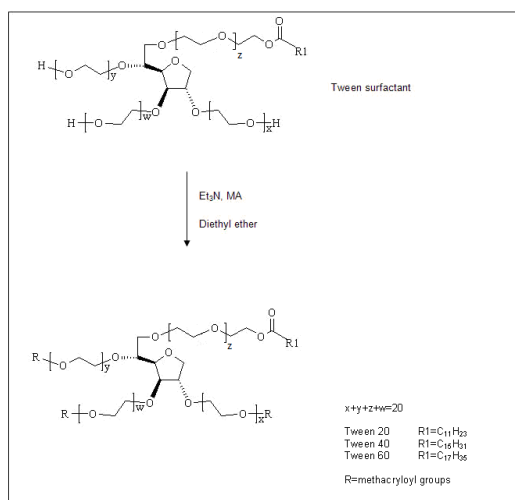
Scheme 1. Schematic representation of the synthesis of methacrylic monomers.

Afterwards, the resulting organic solution was dried over Na_2SO_4 and left alone overnight and finally evaporated under reduced pressure. The obtained functionalized Tween[TM] monomer was a quite viscous ivory-like liquid at room temperature. The yields of the reactions were 85%, 70%, and 86% for Tween 20[TM], Tween 40[TM] and Tween 60[TM], respectively. IR values (on KBr) are 3107, 1785, 947 cm^{-1}. These peaks are significant for the formation of functionalized Tween[TM], in fact 3107 cm^{-1} is the terminal olefins stretching, 1785 cm^{-1} is the stretching C=O of new esteric bonds and 947 cm^{-1} is the typical methacrylic band. (Supporting Information)

The chemical shift values of the Tween 60[TM] monomer protons (in ppm) are: (CDCl$_3$, 300 MHz), 6.15 (m, 3H), 5.68 (m, 3H), 4.1 (m, 8H), 3.60-3.45 (m, 84H), 2.15 (t, 2H), 1.87 (d, 9H), 1.77 (m, 2H), 1.1 (m, 28 H), 0.74 (t, 3H).

The others Tween[TM] NMR spectra are similar to Tween60[TM] ones. The only difference is the alkylic chain protons number, in fact the chemical shift at 1.1 ppm is a multiplet of 16H and 24H for Tween 20[TM] and Tween 40[TM], respectively.

2.3 Polymerization of functionalized monomers

The polymerization of the functionalized monomer was carried out in different solvents as well as their mixture, under a nitrogen atmosphere using 2,2-azobisisobutyronitrile (2.4×10^{-5} mol, AIBN) before recrystallization from methanol. In the case of water and THF mixture, ammonium persulphate (1.3×10^{-5} mol, AP) was used as initiator. The reactions were carried out for 3 hours at

temperatures reported in Table 2. The obtained gels were crushed, purified and washed several times with (in the order), chloroform, ethanol, water and acetone and furthermore dried under reduced pressure at room temperature for at least 24 h.

Details on the experimental conditions used for the polymerization process are listed in Table 2.

Monomer samples	Monomer mol 10^{-3}	Solvent	Initiators	Cross-linking Temperature °C	Networks Samples
A4	1.62	DMF	AIBN	85	A4N1
A4	1.62	THF	AIBN	65	A4N2
A4	1.62	THF-Water	A. P.	80	A4N3
B4	1.55	DMF	AIBN	85	B4N1
B4	1.55	THF	AIBN	65	B4N2
B4	1.55	THF-Water	A. P.	80	B4N3
C4	1.52	DMF	AIBN	85	C4N1
C4	1.52	THF	AIBN	65	C4N2
C4	1.52	THF-Water	A. P.	80	C4N3

Table 2. Details on the type and concentration of reagents used for the synthesis of the networks.

2.4 Differential Scanning Calorimetry (DSC)

Thermal stability of the networks was checked by DSC. The experiments were performed by using a Setaram DSC-131 instrument, using indium to calibrate the temperature and the energy scales. Samples (20–30 mg) were sealed in aluminium-cells and heated to the initial temperature. An empty pan was used as reference for the measurements. Samples were heated from -30 °C at 150 °C and the scan rate temperature was 10 °C min^{-1}. Before each test, the samples were carefully dried for 72 hours under vacuum in the presence of P_2O_5. The glass transition temperature, Tg, was determined as the temperature corresponding to the slope change in the specific heat-temperature plot.

2.5 Morphological analysis

Surfaces of the polymer networks were observed by a Scanning Electron Microscope (SEM) (Cambridge Stereoscan 360) at 20 kV. The analyzed samples were not subjected to any drying process in order to remove the residual solvent. Therefore, a certain amount of solvent is retained in the bulk of the polymer network. Sample specimens were cryogenically fractured in liquid nitrogen to guarantee a sharp brittle fracture, and were successively sputter coated with a thin gold film prior to SEM observation. The dimensions of the observed peculiarities on the surface were directly read from the SEM image.

2.6 Rheological measurements

The polymerization temperatures of the monomers, dispersed in different solvents, were evaluated by dynamic rheological measurements.

Rheological measurements were conducted using a shear-strain controlled rheometer RFS III (Rheometrics, USA) equipped with a concentric cylinder geometry (inner radius 17 mm, gap 1.06 mm). The temperature was controlled by a water circulator heating apparatus (± 0.1°C). To prevent errors due to evaporation, the measuring geometries were surrounded by an evaporation trap. Measurements were obtained by imposing a sinusoidal deformation (γ) $\gamma 0 \sin \omega t$) to the samples, where ω is the frequency and γ_0 the maximum strain amplitude. The resulting stress component in phase with the deformation defines the storage or elastic modulus, G′, whereas the stress component out-of-phase with the strain defines the loss or viscous modulus, G″. The applied strain amplitude for the viscoelastic measurements was reduced until the linear response regime was reached. This analysis was made by performing strain sweep tests in all temperature range investigated. All the samples, in fact, were tested by strain sweep tests at 1 Hz, to define the presence of a linear sweep-strain range.

2.7 Relaxation time measurements

NMR relaxation experiments were performed on the Bruker NMR spectrometer (AVANCE 300 Wide Bore) working at 300 MHz on ^{1}H, equipped with a 25 mm (inner diameter) radio frequency bird-cage coil. The experimental conditions were: 9 μs for the 90° radio-frequency pulses, 1.5 kHz spectral width, 1.9 kHz filter bandwidth, acquisition of 1024 complex data point per transient (in 8 s), accumulation of 128 free induction decays. ^{1}H-NMR relaxation times (T_2) were obtained from DMF *N*-methyl protons and THF (3.4 methylen) protons by means of signal decay on Hahn spin echo sequences[21].

In the case of NMR relaxation experiments the polymerization of the functionalized monomer was carried out in DMF and THF solvents using AIBN as initiator with 1:2, 1:0.5 and 1:0.25 mass ratios be Tween[TM] monomer and solvent. Vial containing approximately 10 g of sample was sealed off, to prevent loss of solvent, hence it was heated at appropriate cross-linking temperatures and then was placed in the NMR probe and directly analyzed.A nonlinear least-squares fitting procedure was used to get T_2 values. The temperature was controlled to ± 0.5 °C and calibrated with a copper–constantan thermocouple. Sample rotation was set at 20 Hz.

2.8 Gel behavior to swell.

Aliquots (170-200 mg) of the dried networks were placed in tared 5 ml sintered glass filters (diameter 10 mm; porosity, G3) and left to swell by immersion in a beaker containing the solvent. After different times (1, 3 and 24 h), the excess of solvent in the filters was removed by percolation at atmospheric pressure, then filter were centrifuged at 3500 rpm for 15 min and weighed. Weights recorded were averaged and used to give the weight gain (WG) by the following equation:

$$WG(\%) = (\frac{W_s \quad W_d}{W_d}) \times 100 \tag{1}$$

Where W_s and W_d are the masses of the swollen and dried networks respectively. Each experiment was carried out in triplicate and the results were in agreement within ±4% standard error.

2.9 Drug loading efficiency

Ferulic acid was used as model drug to evaluate the drug loading efficiency of the gel network. Incorporation of drug into gel was performed as follows: 500 mg of C4N1 dry gel (prepared as described above) was wetted with 25ml in chloroform solution of drug (2.2×10^{-3} M). After 3 days, under slow stirring at 37 °C, the gel was filtered and dried at reduced pressure in presence of P_2O_5 to constant weight. The loading efficiency percent (LE, %) of sample is determined by UV/VIS spectrometer analysis at wavelength of 311 nm of filtered solvent. Loading efficiency percent is expressed as the percentage of the drug trapped in dried gel referred to the total amount of drug used in according to Eq.(2).

$$LE(\%) = \frac{C_i \quad C}{C_i} \times 100 \tag{2}$$

Here C_i was the concentration of drug in solution before the loading study, C the concentration of drug in solution after the loading study.

2.10 Drug release

In order to study the drug release profile, solutions at pH 1.0, 6.8 and 7.4 were prepared, to reproduce the physiological conditions of the gastrointestinal tract. Pre-weighed drug loaded sample was placed in each water solution at a proper pH and continuously stirred at the physiological temperature of 37 °C. At scheduled time intervals, 2ml of solution is withdrawn and an equal volume of the same type of solution is added to the mother solution to maintain a constant volume. The drug release percent was determined using the following equation:

$$Drug\ release(\%) = (M_t / M_i) \times 100 \tag{3}$$

where M_i and M_t are the initial amount of drug entrapped in the gel network and the amount of drug released at the time t. All the experimental procedure was repeated three times. The release of the free drug was also investigated in the same way, but the ferulic acid solution was preliminary transferred into Visking dialysis tubes (20/30), and then placed into the different water media. Release profiles of the drug from the gel, determined by UV/VIS spectrometer analysis at wavelength of 311 nm, were obtained by plotting the amount of released ferulic acid (moles) as a function of time (h).

3. Results and discussion

3.1 Polymerization of functionalized monomers

The cross-linking temperature strongly depends on the solvent type as will explained later, in fact, rheological temperature ramp tests allowed to investigate the polymerization process and to determine its temperatures for each solvent.

As confirmed by IR and NMR spectroscopic analysis, R groups of A4, B4, C4 monomers were only methacryloyl groups. Indeed, IR spectra of the samples do not show the typical peak of the free OH group.

It is worthy emphasizing that only A4, B4, C4 monomers ensure a complete formation of the polymer networks, as a consequence we focused our attention on these monomers prepared with a mole ratio of 1/4 surfactant/MA.

The polymerization of monomers was studied in different conditions to investigate how both solvents and their amounts influence the physical-chemical properties of the gels systems.

For the purpose of this study we will focus on the C4 series as it seems to be the most representative of the whole class of these new materials. A complete characterization involving the other series will be performed in the future.

As example, the polymerization of C4 monomer carried out with 1:2, 1:0.5 and 1:0.25 mass ratios between monomer and solvent respectively, was shown in Table 3.

3.2 C4N series characterizations.

3.2.1 NMR characterization

C4N networks were characterized by NMR spectroscopy in order to evaluate the spin-spin relaxation times (T_2) of all protons present in the sample and self-diffusion of DMF and THF still present in the networks after the polymerization process. NMR parameters are resumed in Table 3 where T_2 and solvent self diffusion coefficients (D) are reported for different samples at 25°C.

T_2 is predominantly affected by interactions and motion over short distances. Long T_2 times are to ascribe to the absence of static dipole-dipole interactions which means that in a short time, compared to the inverse of dipole-dipole interaction, the proton vectors take up all direction with respect to the external magnetic field.

Solvent	Network:Solvent mass ratio	T_2 ms	D cm^2/s	Label
DMF	1:2	680	$3.56\ 10^{-6}$	C4N1
DMF	1:0.5	430	$1.18\ 10^{-6}$	C4N1a
DMF	1:0.25	160	$2.51\ 10^{-7}$	C4N1b
THF	1:2	210	$4.70\ 10^{-7}$	C4N2
THF	1:0.5	37	$4.09\ 10^{-7}$	C4N2a
THF	1:0.25	20	-	C4N2b

Table 3. Relaxation times and diffusion coefficients of C4N networks in different solvents.

In fact, T_2 results in a loss of phase coherence and a decay of the NMR signal. The rate of relaxation is sensitive to the magnitude of the various spin interactions and also to their rate of fluctuation. C4N1 sample presents high relaxation time (680 ms). This value is comparable to T_2 of the pure solvent (700 ms). It means that the motion over short distances is completely free, namely, network matrix is solvated by a small fraction of solvent whilst the most part is free and it behaves as in bulk solvent. A decrease in solvent leads to a decrease in the T_2. The structure becomes more compact and the motion of proton vector is blocked. The same trend is observed for networks obtained from THF. In this case C4N2 sample shows a T_2 value lower than that of pure solvent (645 ms). This suggests that THF solvent once entrapped in the polymer matrix is hard to remove. The strong interaction between THF and the polymer matrix is also confirmed by the low self-diffusion values.

3.2.2. Rheological and mechanical properties
The dynamic mechanical analysis (DMA) ability to give complex viscosity and G' and G'' viscosity and modulus values for each point in a temperature scan allows one to estimate the polymerization temperature and the kinetic behaviour as a function of the viscosity.
This has the advantage of telling how much fluid the material is at any given temperature, so one can determine mechanical moduli values change with temperature and transitions in materials. This includes not only the glass transition and the melt, but also other transitions that occur in the polymer matrix.

The cast solution cure profiles for C4N1 and C4N2 using DMF and THF as solvents in the mass ratio of 1:2 are shown in Figure 1.
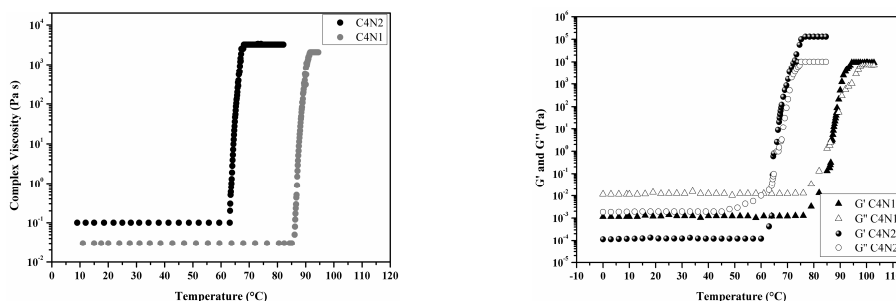

Figure 1. Complex viscosity (Pa s) vs. temperature (°C) for C4N1 (grey circle) and C4N2 (black circle). Linear viscoelastic thermogram for C4N1 and C4N2. Temperature scan of storage modulus G' and loss modulus G' obtained by a time-cure test frequency = 1 Hz. Heating rate of the experiment was of 1 °C/min and the equilibration time of 2 s.

From these scans one can determine the minimum viscosity (η*min), the temperature to η*min the onset of cure and the point of gelation where the cast solution changes from a viscous liquid to a solid network.

As the viscosity begins to increase, we can see an inversion of the G″ and G′ values as the material becomes more solid-like. This crossover point is taken to be the main cross-linking point, where the cross-links have progressed to form a long network across the specimen. At this point, the sample will no longer dissolved in the solvent. The observed polymerization temperatures were 85 and 65 °C for C4N1 and C4N2 networks respectively (Figure 1).

In brief, DMA gave information about the polymerization temperatures for different solvents that are listed in Table 2.

The storage modulus G' values are almost constant when the polymer networks are formed as expected. The plateau value seems to depend on the solvent type. Taking in account the effect of the studied solvents, it decreases in according to the boiling point of the solvent, in fact the lower the boiling point is the more solid the network becomes. In agreement with this, the plateau of G' of the C4N gel obtained without solvent is the highest as a consequence of a collapse of the structure when the polymerization starts (data not shown). This can be ascribed to the higher number of formed cross-linkers.

3.2.3. Morphology characterization

It is well known[22] that the morphology of a polymer network strongly depends on both the type of solvent used for the polymerization of the precursor monomer and on the cross-linking temperature.

101

In this light, the first investigation of the networks obtained from the systems C4N/DMF and C4N/THF at 85 and 65°C respectively, regarded the study of their surface morphology in conjunction with the solvents used for the polymerization.

Figure 2a shows the SEM photograph of the C4N gel obtained without solvent. In this case, the gel surface shows regular and spaced protuberances probably due to the formation of N_2 during the thermal polymerization of the monomer using AIBN as initiator. The surface morphology of the gel systems strongly varies as a function of the type and amount of the solvents used. Indeed, both dense and very wrinkle networks are obtained. In particular, totally dense surface was obtained by using DMF as solvent in the mass ratio 1:2 (Figure 2c).
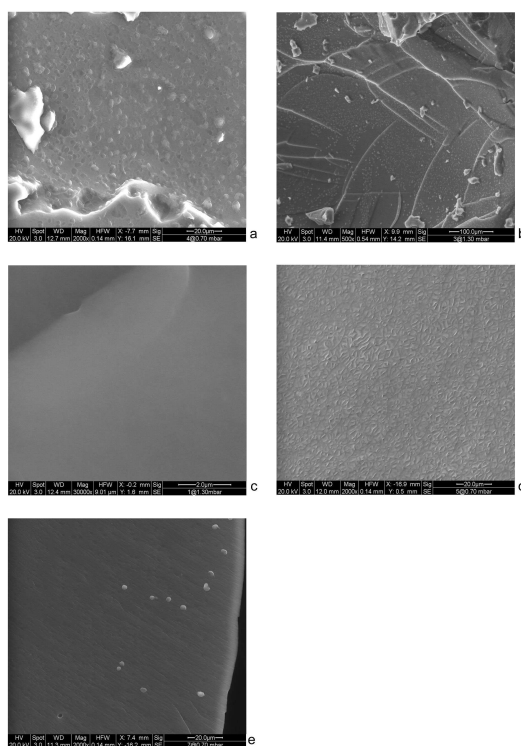

Figure 2. SEM images of surface of network from without solvent (a), from DMF in solvent mass ratio 1:0.25 (b), from DMF in solvent mass ratio 1:2 (c), from THF in solvent mass ratio 1:0.25 (d), from THF in solvent mass ratio 1:2 (e)

Apparently the complete swelling of the polymer network by DMF created a perfectly dense surface which presents defects typical of the solvent-free network when the concentration of the solvent is low, mass ratio 1:0.25. Hence, with the decreasing of the solvent concentration, some flakes start to appear (Figure 2b). On the contrary, in the case of THF as solvent, wrinkle surfaces were always obtained independently from the solvent concentration (Figure 2d and 2e).

The different effect of DMF and THF on the network morphologies is probably to ascribe to their different boiling points (BP): 153 °C and 65 °C respectively. The cross-linking temperature is an important parameter to consider in order to understand the solvent behaviour within and on the surface the polymer matrix and the resulting morphology of the network. In the case of THF, the solvent is removed easily from the network surface since the temperature of cross-linking is 65 °C. Analogously, in the case of DMF, the cross-linking temperature was lower than its BP, consequently the solvent is entrapped inside the matrix. The lower BP of THF allow its faster removal from the polymer matrix resulting in a rapid increase of the monomer concentration and, consequently, in the formation of wrinkles and defects. At the same way, the slow diffusion of DMF through the polymer matrix arises to a dense or nearly dense surface structure.

Further information about gel structure was obtained by DSC. The thermograms showed the absence of melting peaks both in the sample C4N1 and C4N2. In fact, they are in the amorphous state and the Tg values are of 17.0 °C and independent of the solvent utilized during the polymerization.

3.2.4 Swelling of C4N networks series.

The swelling and deswelling behaviours of the obtained materials were studied under the influence of water at different pH values and many solvents (as DMF, toluene and isopropanol) at room temperature. The variation of the swelling ratio with time is shown in Tables 4a and 4b.

Samples	A[a]	B[a]	N[a]
C4N1	45	510	91
C4N2	43	869	64
C4N3	39	377	38

Table 4a. Weight gain (WG%) of C4N network series in different water media.
[a] A at pH=1.0, B at pH=7.4 and N at pH=6.8

Samples	DMF (%)	Toluene (%)	Isopropanol (%)
C4N1	367	298	48
C4N2	657	379	67
C4N3	307	218	112

Table 4b. Weight gain (WG %) of C4N networks series in various organic media.

The swelling ratios at various pH environments depend upon the available free volume of the expanded polymer networks, polymer chain relaxation, and availability of ionizable groups able to form hydrogen bonds with water.

As show in Table 3a, C4N1, C4N2 and C4N3 swelled more in alkaline conditions rather than in acid or neutral ones: for example, for C4N2 sample, the swelling ratios of the gel increases from 43 to 869 weight percent (wt%) with the increase of the pH.

Probably this is due to the partial basic hydrolysis of ester bonds: in fact, as reported in literature, methacryloyl/acryloyl functionalized lipids are susceptible to hydrolysis [23].

In order to confirm this hypothesis, we performed FT-IR spectra of network gels after swelling: in the case of alkaline media the characteristic band of –COO$^-$ group at 1550 cm^{-1} is present (Figure 3c), whist no bands are evident in both acid or neutral ones (Figure 3a,b). This is an indication of partial hydrolysis of ester bond and consequent formation of carboxyl anion.

The C4N gels are expanded in alkaline conditions, since –COOR groups are dissociated into carboxyl anion resulting in ionic repulsions among anionic groups and consequently in the conformational stretching.
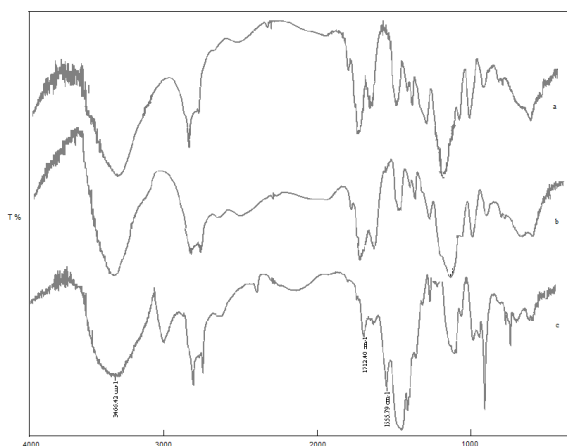

Figure 3. FT-IR spectra in (a) acid, (b) neutral and (c) alkaline media.

Hence, C4N network series are pH sensitive devices. This suggests that they could be used as colon-specific oral delivery system. They may encapsulate drug almost protected in acidic and neutral environment due to minimum swelling, then release the maximum amount of drug when the pH is slightly alkaline. In order to confirm this, the release of drug-loaded C4N1 samples was studied in media at pH 1.0, and 6.8 and 7.4 at 37 °C as discussed below.

Therefore, these new devices can be potentially used as chemical sensors for the control of air pollution, as bio-remediation tools of organic compounds contaminating groundwater or for storage purposes.

As shown in Table 4b, the swelling ratio for organic solvent is higher than that one observed for water, probably due to a better affinity between functional groups of gel and solvent. In particular, all the samples showed the most notable weight gain (WG%) when the DMF solvent was used as medium, with toluene producing a remarkable swelling ratio as well.

In order to confirm this, a simple experiment was carried out: an amount of dried C4N samples was put in atmosphere of toluene or benzene vapours for 24h, following the same procedure indicated for the determination of swelling behaviour in liquid medium. Afterwards, the organic solvent vapours absorption property was evaluated. Results show that C4N series samples were able to capture remarkable amount of the aromatic compound (Table 5).

Samples	Toluene vapour (%)	Benzene vapour (%)
C4N1	42.13	172.5
C4N2	47.88	186.34
C4N3	42.34	123.80

Table 5. Weight gain% (WG%) of C4N networks series in various organic vapour media after 24 hours.

3.2.5. Loading efficiency of C4N1 network

In order to evaluate the possibility to use our networks as colon-specific oral delivery systems and as encapsulating agent for a model drug (ferulic acid), its in vitro release rates were preliminary studied for C4N1 sample and its loading efficiency percent was 34.83%.

The nature of the drug influences its loading efficiency and it is strongly dependent on its affinity toward polymeric matrix sample.

In the present case, as the drug ferulic acid is hydrophilic in nature and rich in ionisable groups, such as -COOH, it could have happened that the low values of LE% were affected by unfavourable electrostatic interactions between the drug molecules and the functional groups present along the macromolecular chains inside the gel network.

3.2.6 Drug Release Study.

In the presence of anionic group, the swelling ratios increase in alkaline condition, which increase the released amount of drug. So, the swelling is the important rate-determining step in the controlled release processes in release systems.

In the C4N1 samples, it is found that the presence of alkaline media can affect the drug release rate significantly. In all the samples drug release increases, as the pH of the medium is increased from 1 to 7.4. This is consistent with the percentage of swelling which shows that water uptake by the network increases with increasing the pH of the medium. These observations are related to the anionic characteristics of the polymer networks. An increase in the pH of the release medium results in the basic hydrolysis of ester bonds in the monomers structure and the consequent repulsion between polymer chains. Then extensive ionization of the functional groups at pH 7.4 significantly influences the polymer chain relaxation and consequently, the drug transport mechanism.

The ferulic acid release was tested in selected conditions to simulate the pH and time intervals likely to be encountered during transit from stomach to colon. Results for the this simulation are reported in the Figure 4.
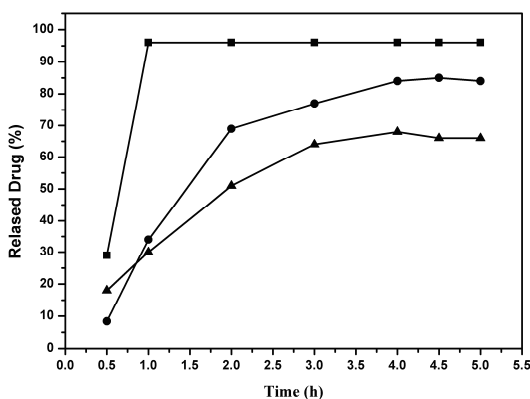

Figure 4. In vitro release profile of ferulic acid-loaded gels at 37°C under different pH conditions: pH 1 (▲), pH 6.8 (●) and pH 7.4 (■).

When the dry sample is placed in the medium of acidic pH we can see that a small release (30.0% of total release amount) is observed in 1 hour, because the diffusion of solvent into the interior structure of gel was restricted, consequently a limited drug release was observed. As expected, at pH 6.8, ferulic acid was released constantly and slowly for 1h (34% of total release amount). When the drug-loaded device is placed in the medium at pH 7.4, the hydrolysis of ester groups was observed along with the repulsion between the similarly charged –COO⁻ groups giving an increase of swelling ratio. Under these conditions, the drug molecules diffused at a fast rate into the media and in conjunction with a fast release of ferulic acid. When these samples were put in the pH 7.4 solution, the C4N1 kept the highest accumulative release percent (96%) in 1 hour.

In addition, it was not observed noticeable difference between the total released drug from C4N1 in the different media after 8 hours. Values of 66.0, 88.0 and 98.% were respectively measured.

The nature of the drug, encapsulated within the polymer matrix, obviously influences its release.

106

Ferulic acid is a hydrophilic molecule with a pK_a value equal to 4.8 and since the release experiments was carried at the pH 7.4 the probability of electrostatic interactions between the drug molecules and the gel is quite high. For this reason, ferulic acid molecules associated with the network, were quickly released from the formulation, which reflected repulsions between the drug, the gel and charged anionic groups.

Finally the release rates of drug from C4N1 samples were significantly lower than the one free in solution. In fact, the free drug in solution releases completely ferulic acid-loaded in acid media within two hours, while all devices release only 30% of loaded drug In vitro release profile of model drug implies that the C4N1 gels can be utilized as potential carriers for colon-specific retarded drug delivery.

4. Conclusions

Synthesis of new Tween^{TM}-based network gels, with good gel characteristics was achieved. Several physical chemistry properties were investigated in order to characterize their microstructure, stability and solvent affinity.

The mechanical properties confirmed the formation of robust and high cross-linked gels with strong elastic component with potential use in practical applications. Most importantly, it was observed that these gels can be used as drug delivery devices as well as drying agents for organic solvents.

It should be added that these networks represent a new class of cross-linked polymeric materials which have shown interesting properties for use in pharmaceutical field as well as organic vapours and humidity sensors.

It has been demonstrated that these novel gels can be potentially used for drug release applications in alkaline media and can be also used as "moisture" removing agents due to their good swelling capacity in organic solvents.

References
[1] Adamantini, P.; Vassilis, K. Int J Food Sc and Technology 1995, 30, 57-63.
[2] Ayorinde, F.O.; Gelain, S.V.; Johnson, Jr.; J.H., Wan, L. W. Rapid Commun Mass Spectrom 2000, 14, 2116-2124.
[3] Hoffman, W.L.; and Jump, A.A. J Immunol Methods, 1986, 94, 191–196.
[4] Feng, M.; Morales, A.B.; Poot, A.; Beugeling, T.; and Bantjes, A. J Biomater Sci Polym Ed, 1995, 7, 415–424.
[5] Charman, S. A.; Mason, K. L.; Charman, W. N. Pharm. Res. 1993, 10, 954-962.
[6] Lee, D.H.; Kim, E.S.; Chang, H.W. Geosciences Journal 2005, 9, 261-267.
[7] Hood, E.; Gonzalez, M.; Plaas, A.; Strom, J.; VanAuker, M. Int J Pharm 2007, 339, 222-230.
[8] Manosroi, A.; Wongtrakul, P.; Manosroi, J.; Sakai, H.; Sugawara, F.; Yuasa, M.; Abe, M. Colloids Surf B Biointerfaces 2003, 30, 129-138.
[9] Ross-Murphy, S.B. J. Rheo, 1995, 39, 1451-146.

[10] Rao, M. Rheology of Fluid and Semisolid Foods: Principles and Applications, Aspen Publishers: Gaithersburg, 1999.

[11] Bag, D.S. Proceedings of Polymer Research in Academy, Industry and R&D Organization: Calcutta; 1998

[12] Bag D.S.; Kandpal, L.D.; Mathur, G.N. Proceedings of Recent Advances in Polymers and Composites, ed Mathur, G.N., Kandpal, L.D., and Sen, A.K., New Delhi, Allied Publisher, 2000.

[13] Dagani, R. Chem. Eng. News 1997, 75, 26-37.

[14] Doyle, F.J.; Dorski, C.; Harting, J.E.; Peppas, N.A. American Control Conf 1995, 1, 776-780.

[15] Harsànyi, G. Polymer Films in Sensor Applications: Technology, materials, devices and their characteristics, Technomic Publishing AG: Basel, Switzerland, 1995; p 435.

[16] Osada, Y.; De Rossi, D.E., (Eds.), Polymer Sensors and Actuators, Springer: Berlin, 1999; p 420.

[17] De Wit, M.; Vanneste, E.; Geise, H.J.; Nagels, L.J. Sens. Act. B 1998, 50, 164-172.

[18] Musio, F.; Ferrara, M.C. Sens Act. B 1997, 41, 97-103.

[19] Partridge, A.C.; Jansen, M.L.; Arnold, W.M. Mat. Sci Eng 2000, 12, 37-42.

[20] Altamura, P.; Bearzotti, A.; D'Amico, A.; Foglietti, V.; Fratoddi, I.; Furlani, A.; Padeletti, G.; Russo, M.V.; Scavia, G. Mat. Sci Eng 1998, 5, 217-221.

[21] Sanders, J.K.M.; Hunter, B.K. Modern NMR Spectroscopy, Oxford University Press: Oxford, 1987; p 61.

[22] Kesting, R.E., Frietzsche, A.K., Polymeric gas separation membrane, Wiley: NewYork, 1993.

[23] Singh, A.; Schnur, J.M. Polymerizable phospholipids in Phospholipid handbook, Cevc, G., Ed.; Marcel Dekker: New York, 1993; p 233.

Supporting Information
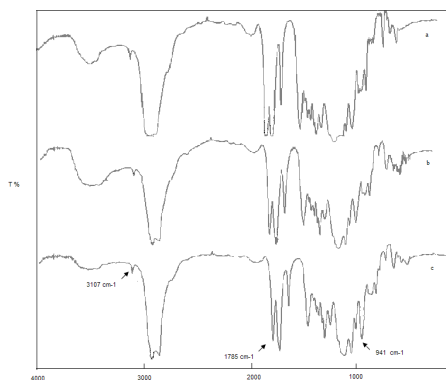
FT-IR spectra of Tween 20[TM] (a), Tween 40[TM] (b) and Tween 60[TM] (c) functionalized monomers.

This material is available free of charge via the Internet at http://pubs.acs.org.

3.1.2 Colon-specific devices based on methacrylic functionalized Tween monomer networks: swelling studies and in vitro drug release

Rita Muzzalupo, Lorena Tavano, Roberta Cassano,

Sonia Trombino, Alessia Cilea, Nevio Picci

Department of Pharmaceutical Science, Calabria University, Edificio Polifunzionale, 87036 Arcavacata di Rende, Cosenza, ITALY

Abstract

Colon-targeted delivery devices based on methacrylic functionalized Tween monomer networks, useful for 5-FU or Ferulic acid site-specific release, were synthesized. The basic design consists of methacrylic functionalized Tween monomer-based networks prepared with or without acrylic acid as co-monomer. The swelling behaviour and loaded drugs release from these gels was studied as a function of pH. The devices showed a strong pH-dependent swelling behaviour, allowing a maximum release at pH 7.4. The acrylic acid introduction increased the polymeric gels pores size, as evidenced by the loading efficiency increase, but also reduced the amount of released drug in basic media compared to analogous network not containing the co-monomer. This behaviour, already found in the matrix swelling, could be attributed to a slower hydrolysis kinetics of the ester bond in functionalized Tween monomers, which implies a reduced ability to absorb water from a basic medium, resulting in a lower capacity to release the loaded drug.

Since our device possesses a maximum drug release in the media at pH 7.4, it could be used for colon-targeted drug delivery of both 5-FU and Ferulic acid.

1. Introduction

In recent years, many efforts have been made to achieve drug selective delivery to the colon following oral administration. Colonic drug delivery may be useful for the local treatment of ulcerative colitis, irritable bowel syndrome and can also be used for colon cancer treatment or for systemic administration of drugs that are adversely affected by the upper gastro-intestinal (GI) tract [1-3].

Thus colon-specific drug delivery systems (CDDS) have been developed to improve drugs bioavailability, therapeutic efficacy and to reduce the necessary dose for optimal treatment and, at the same time, to decrease the amount of side effects normally encountered when these drugs are released and absorbed in the upper GI tract.

In addition, these systems offer various pharmacokinetic advantages such as maintenance of constant therapeutic levels over a prolonged period of time and reduction of the therapeutic levels fluctuation thus minimizing the risk of resistance especially in the case of antibiotics [4-8].

Oral colon targeting requires minimal drug release in the upper GI tract (stomach and small intestine) and a complete and rapid release in the colon [9]. Various approaches have been proposed for colon-targeted drug delivery, such as time-dependent delivery [10], pH-dependent systems [11, 12] and delivery systems based on utilization of bacteria (or enzymes produced by them) that specifically colonize the colon [13-26].

These hydrogels, three-dimensional polymeric networks, exhibiting a thermodynamic compatibility with water as determined by water swelling and crosslinking density, are suitable as drug carriers in the controlled release of pharmaceuticals [27]. In fact, the controlled release of active agents from the polymeric matrix to the GI tract has been carried out successfully by various scientists [28-33].

In our previous work, we synthesized and studied the swelling of methacrylic functionalized Tween monomer networks and we found that these gels show a natural, excellent pH-dependent swelling behaviour, thus exhibiting minimum swelling at pH 1.0 and maximum swelling in the pH range 7-8 of the external media. Based on the difference in pH throughout the GI tract, we proposed these pH-dependent devices for colonic targeting, to achieve the selective delivery of drugs to the colon.

The aims of this paper were to investigate: i) the influence of polymeric matrix composition, following the addition of acrylic acid, as pH-sensitive molecule; ii) the chemical structures influence of two different model drugs, Ferulic acid and 5-Fluoruracil (5-FU), on the swelling properties of the obtained hydrogels in aqueous medium and on the drug release profile at different pH of networks series based on functionalized Tween monomer.

Materials and Instruments

2.1 Materials and Instruments

Chemicals and reagents, Tween 20^{TM}, Tween 40^{TM}, Tween 60^{TM}, ethanol, acetone, dimethylformamide (DMF), chloroform, isopropanol, Ferulic acid, toluene and benzene were supplied by Sigma Aldrich and used without further purifications. All solvents were of high performance liquid chromatography grade. Methacrylic anhydride (MA) and Acrylic acid (AA) were distilled before use. Triethylamine, (Et$_3$N), 2,2-azobisisobutyronitrile (AIBN), ammonium persulphate (AP), diethyl ether were supplied by Sigma Aldrich and used after purifications. IR spectra were recorded on FT-IR Jasco 4200 spectrometer. ^{1}H NMR spectra of the products were

obtained by a 300-MHz Bruker instrument (AVANCE 300 Wide Bore). Absorption spectra were recorded with a UV±VIS JASCO V-530 spectrometer using 1 cm quartz cells.

2.2 Synthesis of the monomers

Methacrylic functionalized Tween monomers were synthesized by a previously reported procedure [34] as shown in Figure 1. The synthesis details are listed in Table 1.
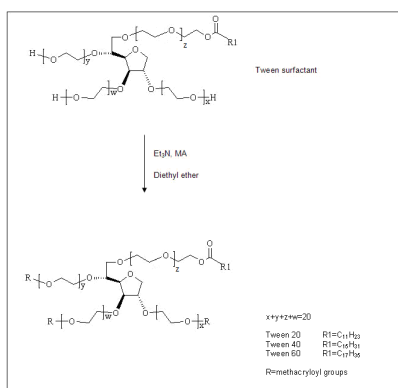

Fig.1 Schematic representation of the methacrylic monomers synthesis.

Surfactant	Surf mol 10^{-3}	Et$_3$N mol 10^{-3}	MA Mol 10^{-3}	Mole ratio Surf/MA	Label
Tween 20	6.5	2.60	2.60	1:4	A4
Tween 40	6.2	2.48	2.48	1:4	B4
Tween 60	6.1	2.44	2.44	1:4	C4

Table 1. Details on the type and concentration of reagents used for the monomers synthesis

Briefly, dry triethylamine (Et$_3$N) was added to a diethyl ether Tween solution at room temperature. After 30 min, a quantity of MA equimolar to the amount of Et$_3$N was added, at 0°C, to the Tween solution and the reaction was left to proceed by stirring for 24 hours at 25°C.

The methacrylate monomers were characterized by ^{1}H-NMR and FT-IR spectrometry and details are given elsewhere [34]. The complete Tween functionalization by MA was evident by FT-IR spectra. In fact, in these spectra the typical hydroxyl band at 3330 cm^{-1} is absent, whilst we found the terminal olefins stretching, the C=O stretching of new esteric bonds and the typical methacrylic band at 3107 cm^{-1}1, 785 cm^{-1} and 947 cm^{-1}, respectively.

2.3 Polymerization of functionalized monomers

Gels were prepared by the radical polymerization of functionalized Tween monomers both in the presence or not of AA, in different solvents, using 2,2-azobisisobutyronitrile (2.4×10^{-5} mol, AIBN) or ammonium persulphate (1.3×10^{-5} mol, AP) as initiators. In addition, the reactions were carried out for a period of 3 hours at appropriate temperatures, as shown in Table 2. The resulting semi-transparent gels were cut into small pieces, then washed several times with chloroform, ethanol, water and acetone and finally dried under vacuum for a period of 24 h until constant weight.

a)

Monomer	Monomer mol 10^{-3}	AA mol 10^{-3}	Initiator	Solvent	Cross-linking Temperature °C	Networks Samples
Tween 20^{TM}	1,62	-	AIBN	DMF	85	A4N1
Tween 20^{TM}	1,62	-	AIBN	THF	60	A4N2
Tween 20^{TM}	1,62	-	AP	THF-Water	80	A4N3
Tween 20^{TM}	1,62	0,61	AIBN	DMF	85	A4N1a
Tween 20^{TM}	1,62	0,61	AIBN	THF	60	A4N2a
Tween 20^{TM}	1,62	0,61	AP	THF-Water	80	A4N3a

b)

Monomer	Monomer mol 10^{-3}	AA mol 10^{-3}	Initiator	Solvent	Cross-linking Temperature °C	Networks Samples
Tween 40^{TM}	1,55	-	AIBN	DMF	85	B4N1
Tween 40^{TM}	1,55	-	AIBN	THF	60	B4N2
Tween 40^{TM}	1,55	-	AP	THF-Water	80	B4N3
Tween 40^{TM}	1,55	0,59	AIBN	DMF	85	B4N1a
Tween 40^{TM}	1,55	0,59	AIBN	THF	60	B4N2a
Tween 40^{TM}	1,55	0,59	AP	THF-Water	80	B4N3a

c)

Monomer	Monomer mol 10^{-3}	AA mol 10^{-3}	initiator	Solvent	Cross-linking Temperature °C	Networks Samples
Tween 60^{TM}	1,52	-	AIBN	DMF	85	C4N1
Tween 60^{TM}	1,52	-	AIBN	THF	65	C4N2
Tween 60^{TM}	1,52	-	AP	THF-Water	80	C4N3
Tween 60^{TM}	1,52	0,58	AIBN	DMF	85	C4N1a
Tween 60^{TM}	1,52	0,58	AIBN	THF	65	C4N2a
Tween 60^{TM}	1,52	0,58	AP	THF-Water	80	C4N3a

Tables 2a, b, and c. Details on the type and concentration of reagents used for the networks synthesis

2.4 Gel behaviour to swell

Swelling studies of the polymeric networks were carried out in aqueous medium by gravimetric method. Known amount of dried gel (0.5 g) were placed in tared 5 ml sintered glass filters (diameter 10 mm; porosity, G3) and immersed in excess of solvent for 24 h at room temperature to attain equilibrium swelling. At predetermined time intervals (1, 3 and 24 h) filters were taken out, wiped with tissue paper to remove excess of solvent, and weighed immediately after centrifugation at 5000 rpm for 15 min. The difference in weight of the gel after swelling correspond to the amount of water taken by the network. Swelling behaviour of the polymeric networks was studied as function of pH and swelling was taken as the difference between the initial and the final weight of polymers after fixed interval. The media for the swelling studies were 0.1 M HCl (pH 1.0) or phosphate-buffered solutions (pH 6.8 and 7.4),

Swelling characteristics of the networks were expressed as the weight gain (WG) as shown in the Equation 1 where W_s and W_d are the masses of the swollen and dried networks respectively. Each experiment was carried out in triplicate and the results were in agreement within ±4% standard error.

$$WG(\%) = (\frac{W_s - W_d}{W_d}) \times 100 \tag{1}$$

2.5 Drug loading efficiency

Loading of a drug onto gels was carried out by the swelling equilibrium method. Dried gels (500 mg) were allowed to swell in the drug solution of known concentration for 24 h at 37 °C and than dried to obtain the release device. Details on the experimental conditions used for the drug loading process are listed in Table 3.

Solvent	Drug	M drug solution mol/L 10^{-3}
Chloroform	Ferulic acid	2,28
Water	5-FU	2,28

Table 3. Details on the experimental conditions used for the drug loading process.

After 3 days, under slow stirring at 37 °C, the gel was filtered and dried at reduced pressure in the presence of P_2O_5 to constant weight. The sample loading efficiency percentage (LE %) was determined by UV/VIS spectrometer analysis at a wavelength of 311 nm (Ferulic acid) and 266 nm (5-FU) of filtered solvent. Loading efficiency percent was expressed as the percentage of the drug trapped in dried gel, referred to the total amount of drug used, according to Eq. 2:

$$LE(\%) = \frac{C_i \quad C}{C_i} \times 100 \qquad (2)$$

Here, C_i was the concentration of the drug solution before the loading study and C the concentration of the drug solution after the loading study. Each experiment was carried out in triplicate and the results are the mean of three determinations.

2.6 Drug release

The in-vitro release studies of entrapped drugs, Ferulic acid and 5-FU, were carried out by placing an accurate amount of the dried gel (0.5 g) loaded with the drug in a 200 mL solution of phosphate buffer (pH 6.8 and 7.4) or 0.1 M HCl (pH 1.0) solution, simulating gastrointestinal tract conditions. At periodic intervals, 2 mL of the release solution was withdrawn and the drugs release was determined using UV-VIS spectrophotometer, at λ_{max} 311 and 266 for Ferulic acid and 5-FU, respectively. The release media were replaced with an equal volume of fresh dissolution medium to maintain a constant volume. The amount of drug released from the matrix was determined using Eq. 3 where M_i and M_t are the initial amount of drug entrapped in the gel network and the amount of drug released at the time t, respectively.

Drug release(%) $= \left(M_t / M_i \right) \times 100$ \qquad (3)

Results are the mean of three determinations from three different experiments. The release of the free drug was also investigated in the same way, but the drug solution was preliminary transferred into Visking dialysis tubes (20/30), and then placed into the different water media.

3. Results and Discussion

Swelling studies.

The chemical structure of the polymer affects the swelling ratio of the network gels, which is directly related to the loading of drug into the polymers and to the release of the drug from the polymeric matrix.

The chemical structure and the behaviour depended upon the composition of the polymeric matrix: highly cross-linked gels have a tighter structure and will swell less compared to the same network with lower cross-linking ratios, because cross-linking hinders the mobility of the polymer chains.

In this work, the swelling behaviours of polymeric networks were studied at time interval of 24 h. The effect of medium pH on water uptake of these devices, prepared in the presence or not of acrylic acid, as ionisable molecules, is presented in the Table 4.

Samples	A	N	B
A4N1	39	44	1059
A4N2	59	61	1103
A4N3	36	38	507
A4N1a	29	38	805
A4N2a	32	38	884
A4N3a	22	31	335

**Table 4a. Weight gain (WG%) of Tween 20 network series in different water media.
A pH=1.0, N pH=6.8 and B pH=7.4**

Samples	A	N	B
B4N1	46	66	783
B4N2	19	29	957
B4N3	11	29	508
B4N1a	22	41	501
B4N2a	16	25	657
B4N3a	27	20	314

**Table 4b. Weight gain (WG%) of Tween 40 network series in different water media. A pH=1.0, N pH=6.8 and B
pH=7.4**

Samples	A	N	B
C4N1	45	91	510
C4N2	43	64	869
C4N3	38	39	377
C4N1a	19	20	193
C4N2a	33	41	275
C4N3a	62	80	122

**Table 4c. Weight gain (WG%) of Tween 60 network series in different water media.
A pH=1.0, N pH=6.8 and B pH=7.4**

In particular, it has been observed that the networks, due to their natural pH-sensitive properties, swelled more in alkaline condition than in acidic or neutral ones, either in the presence or absence of AA.

As previously reported, this behaviour can be attributed attributable to the natural partial hydrolysis of methacrylate monomers that leads to the generation of new water interaction centres and especially new ion dipole interactions in the polymer chains, resulting in significant changes in the water uptake of these networks. At lower pH, the hydrolysis reaction does not occur and hence, the –COOH groups are not present so the networks are in their collapsed state. By contrast, at high pH,

when a partial hydrolysis reaction takes place the networks are partially ionized, and the charged COO⁻ groups repel each other, leading to the polymer swelling [35]. Furthermore, as reported in Table 4, the gels without acrylic acid swelled more than the networks containing the co-monomer, although acrylic acid created a less tight structure that should be result in a higher swelling ratio. No difference between networks based on Tween 20, Tween 40 and Tween 60 was achieved: in all cases we found a remarkable diversity on swelling at pH 1 and pH 7.4.

Loading efficiency

Release profiles were made only for functionalized Tween 20 and Tween 60 monomer-based networks, since it was decided to test systems with different hydrophilic-lipophilic balance.

Loading efficiency (LE%) values for the tested networks are shown in Table 5. The drug content was found to be dependent from the network composition: in particular, samples based on Tween 60 functionalized monomer showed higher LE% than Tween 20 ones, and networks containing acrylic acid as co-monomer exhibited in all cases a more relevant loading efficiency than those prepared without this molecule.

Samples	LE% 5-FU	LE% Ferulic acid
A4N1	15.00±2.81	18.67±2.21
A4N1a	25.50±1.67	38.24±2.72
C4N1	19.13±2.04	34.83±1.45
C4N1a	42.13±1.98	65.9±2.25

Table 5. Loading efficiency of 5-FU and Ferulic acid in selected matrices.

This confirms the hypothesis of a less tight structure produced by the presence of the co-monomer. Moreover both formulations can load an higher amount of Ferulic acid than 5-FU: probably this is due to a major affinity of matrices for Ferulic acid chemical structure and to its higher solubility in the solvent used during the loading process.

Release

The release of water-soluble drugs, entrapped in a gel, occurs only after water penetration in the polymeric networks, by diffusion along the aqueous pathways to the surface of the device. Moreover the release of drug is closely related to the swelling characteristics of the networks, which is a function of the chemical architecture of the matrices.

As mentioned in our previous work, the proposed gel systems showed a natural pH-dependent swelling tendency probably due to the partial basic hydrolysis of ester bonds, thus exhibiting minimum swelling in the acidic pH and maximum in slightly alkaline one. In fact, the FT-IR spectra of polymeric networks after swelling showed, in the case of alkaline media, a characteristic band of –COO⁻ group at 1550 cm⁻¹, while no bands were evident in acidic or neutral ones. This is consistent with the percentage swelling which shows that water uptake by the polymer increases by enhancing the pH of medium.

In this paper, in addition to the behaviour studies performed on the networks obtained from Tween 20, Tween 40 and Tween 60, we introduced the acrylic acid, as pH sensitive co-monomer, to evaluated how the matrices changes their performances.

At lower pH values, the –COOH groups of the polymeric matrix do not ionize and keep the polymeric networks at their collapsed state. This restricts the movement of polymeric segments, discourages the diffusion of drug from the device and results in limited drug release. When the drug-loaded device is placed in the medium at pH 7.4, the solvent diffuses into the outermost surface and so macromolecular chains in the drug-loaded device undergo extensive chain-relaxation due to the electrostatic repulsion among the charged –COO⁻ groups. This produces an extensive device swelling, followed by release of the drug through water-filled macro pores of exterior swollen core.

As stated above, the effect of pH on the release pattern of two different drugs was studied in different pH media and the release kinetics from the networks obtained from functionalized Tween 20 and Tween 60 monomers were evaluated with and without acrylic acid. In particular, the network used were obtained by polymerization using DMF as solvent.

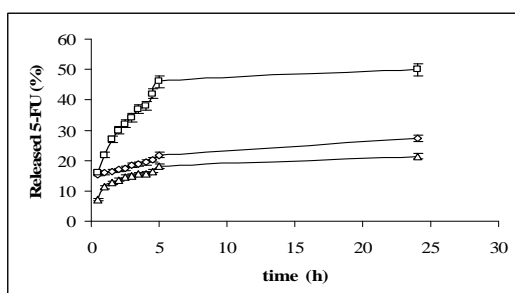In Figures 2 and 3 the release profile of 5-FU and Ferulic acid from A4N1 network are shown.

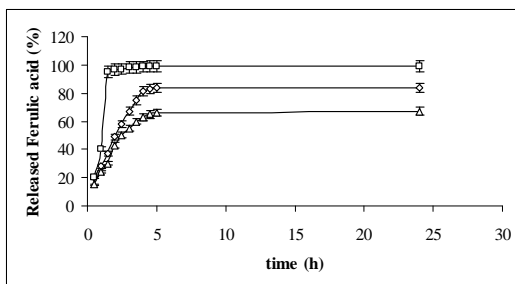**Fig.2 In vitro release profile of 5-FU-loaded gels A4N1 at 37°C under different pH conditions: pH 1(△), pH 6.8 (◊), and pH 7.4 (□).**

The 5-FU release from A4N1 was found to be in agreement with our expectation: when the dry sample is placed in the acidic medium, a small release (about 20.0%) occurs. This behaviour is due to the reduced solvent diffusion into the inner structure of the gel. As expected, at pH 6.8, 5-FU was released slowly (about 25%). When the drug-loaded device was placed in the medium at pH 7.4, the hydrolysis of ester groups occurred and, consequently, an increase of swelling ratio, due to the repulsion between the similarly charged –COO$^-$ groups, was observed. Under these conditions, the drug molecules diffused at a fast rate into the media resulting in a 5-FU fast release.

Fig.3 In vitro release profile of Ferulic acid-loaded gels A4N1 at 37°C under different pH conditions: pH 1(△), pH 6.8 (◊), and pH 7.4 (□)

When these samples were put in the pH 7.4 solution, the network kept the highest cumulative release percent (55%) in 24 hours. The Ferulic acid release showed a behaviour depending not only on the polymeric network but also on the nature of the loaded drug. Ferulic acid is a hydrophilic molecule with a pK_a value equal to 4.8 and since the release experiments were carried at pH 7.4 the probability of electrostatic interactions between the drug molecules and the gel is quite high. For this reason, the Ferulic acid kinetic release was faster than that of 5-FU one, with its pK_a value equal to 8.

Similarly, the release profile of 5-FU from the C4N1 devices was found to be pH-sensitive, as reported for A4N1 sample, with the highest cumulative release percent in basic media (about 54%) in 24 hours.
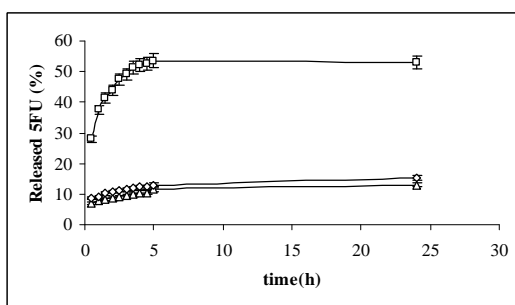

Fig.4 In vitro release profile of 5-FU-loaded gels C4N1 at 37°C under different pH conditions: pH 1(△), pH 6.8 (◊), and pH 7.4 (□)

Ferulic acid release from C4N1 was analogous to that obtained with A4N1, as reported in our previous work [34].

The introduction of acrylic acid as co-monomer in the polymeric network results in an improvement of the colon-specific properties of the gels, especially in the case of Ferulic acid. In particular, we observed that Ferulic acid release in acid and neutral media, was lower than that obtained in the case of a network prepared without acrylic acid. Therefore, we do not have relevant drug loss in the upper GI tract, but a drug colon specific release. On the contrary, when the loaded drug was the 5-FU, the presence of acrylic acid did not influence the network properties. In fact, the amount of 5-FU released or lost in acid or neutral media, from both networks, was low. This behaviour makes the system suitable for the colon-specific drug release but we did not observe the expected drug loss decrease in acidic or neutral media when the network contains acrylic acid, as reported in literature for hydrogels loaded with 5-FU, and including an acid co-monomer [35-37]

Moreover, both 5-FU and Ferulic acid release in basic media, from the networks obtained in the presence of acrylic acid, showed a cumulative release percent lower than the previously described network series. As reported in Figures 5 and 6, for A4N1a and Figures 7 and 8, for C4N1a, the cumulative release showed a pH-sensitive behaviour, but experimental data showed a lower total amount of released drug. In particular, at pH 7.4, values of 40, 23, 39 and 37, respectively in 24 h, were obtained.
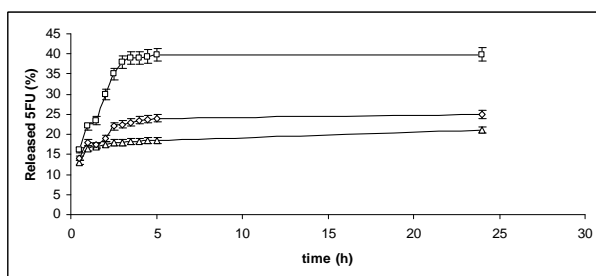

Fig.5 In vitro release profile of 5-FU-loaded gels A4N1a at 37°C under different pH conditions:
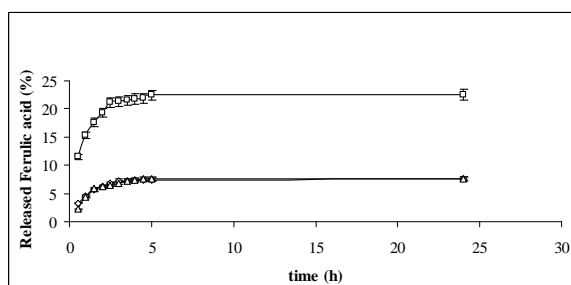**pH 1(△), pH 6.8 (◊), and pH 7.4 (□)**

Fig.6 In vitro release profile of Ferulic acid-loaded gels A4N1a at 37°C under different pH conditions:
pH 1(△), pH 6.8 (◊), and pH 7.4 (□)

119

Indeed, the introduction of acrylic acid increased the pores size of the polymeric gels, as evidenced by a higher loading efficiency, which is about twice that of corresponding networks that do not contain the co-monomer. This effect should also result in a higher release at least in basic medium. The obtained data, however, indicated that in the presence of acrylic acid the total amount of released drug in basic environment was lower than that released by the network missing the co-monomer. This behaviour, already found in the matrix swelling, could be attributed to a slower hydrolysis kinetic of the ester bond in functionalized Tween, which implies both a reduced ability to absorb water from a basic medium, and a low capacity to release the loaded drug. These findings suggest that the presence of acrylic acid, while giving the pH-sensitive characteristic to the studied material, limited the intrinsic properties of the methacrylate Tween, protecting it from the hydrolysis reaction or decreasing the hydrolysis kinetic reaction.
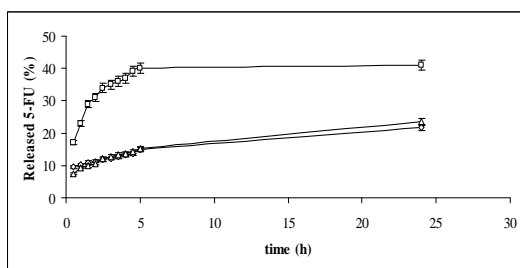

Fig.7 In vitro release profile of 5-FU-loaded gels C4N1a at 37°C under different pH conditions: pH 1(△), pH 6.8 (◊), and pH 7.4 (□)
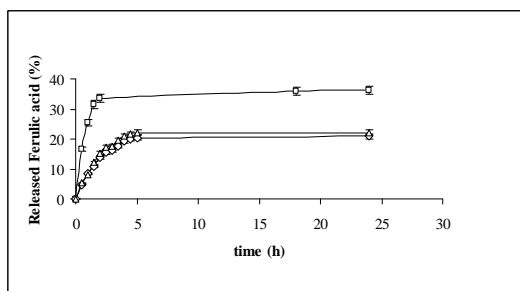

Fig.8 In vitro release profile of Ferulic acid-loaded gels C4N1a at 37°C under different pH conditions: pH 1(△), pH 6.8 (◊), and pH 7.4 (□)

Conclusions

Colon targeting requires minimal drug release in the upper GI tract (stomach and small intestine) and complete and rapid release in the colon.

In order to design new potential colon-targeted delivery devices, methacrylic functionalized Tween monomer networks were prepared through free radical solution polymerization also in the presence of acrylic acid, as co-monomer. The swelling ratios of different networks were studied as a function of pH, simulating the fluids in the gastrointestinal tract. Results indicated significant water uptake and suggest their use them as drug delivery devices. In this light the gels were loaded with Ferulic acid or 5-FU and the drug content was found to be dependent from the network composition. In particular, samples based on Tween 60 functionalized monomer showed higher LE% than Tween 20 ones and networks containing acrylic acid as co-monomer exhibited in all cases a more relevant loading efficiency than those prepared without this molecule.

All networks displayed a strong pH-dependent release of drug at physiological temperature: the matrices obtained only by functionalized Tween showed the highest cumulative percent drug release at pH 7.4.

The introduction of acrylic acid as co-monomer in the polymeric network results in an improvement of the colon-specific properties of the gels, especially in the case of Ferulic acid, since it did not give a relevant drug loss in the upper GI tract, but a colon-specific drug release, while no significant differences were found in the case of 5-FU.

The presence of acrylic acid decreased the cumulative percent drug release, because it seems to protect the networks from the reaction of hydrolysis or to decrease the hydrolysis kinetic reaction. Taken together, our results indicate that all the prepared Tween-based networks could be a potential pH-sensitive carrier for colon- specific drug delivery systems.

References

[1] Yang L, Chu J, Fix J, Colon-specific drug delivery: new approaches and in vitro/in vivo evaluation. Int J Pharm 2002;235:1-15.

[2] Saffarin M, Kumar GS, Savariar C, Burnham JC, Williams F, Neckers DC, A new approach to the oral administration of insulin and other peptide drugs. Science 1986;233:1081-1084.

[3] Ashford M, Fell T, Targeting drugs to the colon: delivery systems for oral administration. J Drug Target. 1994;2:241-258.

[4] Risbud MV, Bhonde RR, Polyacrylamide-chitosan hydrogels: In vitro biocompatibility and sustained antibiotic release studies. Drug Deliv 2000;7:69-75.

[5] Portero A, Remunan-Lopez C, Criado MT, Alonso MJ, Reacetylated chitosan microspheres for controlled delivery of anti-microbial agents to the gastric mucosa. J Microencap 2002;19:797-809.

[6] Mi FL, Wong TV, Shyu SS, Sustained-release of oxytetracycline from chitosan microspheres prepared by interfacial acylation and spray hardening methods. J Microencap 1997;14:577-591.

[7] Bittner B, Mader K, Kroll C, Borchert HH, Kissel T, Tetracycline–HCl-loaded poly(dl-lactide-co-glycolide) microspheres prepared by a spray drying technique: influence of gamma-irradiation on radical formation and polymer degradation. J Cont Rel 1999;59:23–32.

[8] Hejazi R, Amiji M, Stomach-specific anti-H. pylori therapy. II: Gastric residence studies of tetracycline-loaded chitosan microspheres in gerbils. Pharm Dev Technol 2003;8:253-262.

[9] Silva I, Gurruchaga M, Goñi I, Physical blends of starch graft copolymers as matrices for colon targeting drug delivery systems, Carbohyd. Polym.2009; 76**:** 593-601.

[10] Maroni A, Curto MDD, Serratoni M, Zema L, Foppoli A, Gazzaniga A, Feasibility, stability and release performance of a time-dependent insulin delivery system intended for oral colon release, Eur. J. Pharm. Bioph, 2009; 72: 246–251.

[11] Wang K, Fu SZ, Gu YC, Xu X, Dong PW, Zhao GGX, Wei YQ, Qian ZY, Synthesis and characterization of biodegradable pH-sensitive hydrogels based on poly(ε-caprolactone), methacrylic acid, and poly(ethylene glycol), Polym. Degr. Stab. 2009; 94: 730-737.

[12] Han J, Wang K, Yang D, Nie J, Photopolymerization of methacrylated chitosan/PNIPAAm hybrid dual-sensitive hydrogels as carrier for drug delivery, International Journal of Biological Macrom, 2009; 44: 229-235.

[13] Xi MM, Zhang SQ, Wang XY, Fang Q, Gu Y, Study on the characteristics of pectin-ketoprofen for colon targeting in rats. Int J Pharm 2005;298:91-97.

[14] Basit AW, Advances in colonic drug delivery. Drugs 2005;65:1991-2007.

[15] Chourasia MK, Jain S, Pharmaceutical approaches to colon targeted drug delivery systems. J Pharm Sci 2003;6:33-66.

[16] Chourasia MK, Jain SK, Polysaccharides for colon targeted drug delivery. Drug Deliv 2004;11:129-148.

[17] Yang L. Biorelevant dissolution testing of colon-specific delivery systems activated by colonic microflora. J.Control Release 2008;125: 77–86.

[18] Pozzi F, Furlani P, Gazzaniga A, Davis SS, Wilding IR, The Time-Clock ☐system: a new oral dosage form for fast and complete release of drug after predetermined lag time. J Cont Rel 1994;31:99-108.

[19] Steed KP, Hooper G, Monti N, Benedetti MS, Fornasini G, Wilding IR, The use of pharmacoscintigraphy to focus the development strategy for a novel 5- ASA colon targeting system (''Time Clock'' system). J Cont Rel 1997;49:115-122.

[20] Dew MJ, Ebden P, Kidwai NS, Lee G, Evans BK, Rhodes J, Comparison of the absorption and metabolism of sulphasalazine and acrylic-coated 5-amino salicylic acid in normal subjects and patients with colitis. Br J Clin Pharmacol 1984;17:474-476.

[21] Ashford M, Fell JT, Sharma HL, Woodhead PJ, An evaluation of pectin as a carrier for drug targeting to the colon. J Cont Rel 1993;26:213-220.

[22] Wakerly Z, Fell JT, Attwood D, Parkins D, Studies on drug release from pectin/ethylcellulose film-coated tablets: a potential colonic delivery system. Int J Pharm 1997;153:219-224.

[23] Minko T, Drug targeting to the colon with lectins and neoglycoconjugates. Adv Drug Deliv Rev 2004;56:491-509.

[24] Liu L, Fishman ML, Kost J, Hicks KB, Pectin based systems for colon specific drug delivery via oral route. Biomaterials 2003;24:3333-3343.

[25] Yang L, Chu JS, Fix JA, Colon-specific drug delivery: new approaches and in vitro/in vivo evaluation. Int J Pharm 2002;235:1-15.

[26] Sinha VR, Kumria R, Microbially triggered drug delivery to the colon. Eur J Pharm Sci 2003;18:3-18.

[27] Singh TRR, McCarron PA, Woolfson AD, Donn RF, Investigation of swelling and network parameters of poly(ethylene glycol)-crosslinked poly(methyl vinyl ether-co-maleic acid) hydrogels, Eur. Pol. J, 2009; 45: 1239-1249.

[28] Krogel I, Bodmeier R, Pulsatile drug release from an insoluble capsule body controlled by an erodible plug. Pharm Res 1998;15:474-481.

[29] Wilding IR, Davis SS, Bakshaee M, Stevens HNE, Sparrow RA, Brennan J, Gastrointestinal transit and systemic absorption of captopril from a pulsed-release formulation. Pharm Res 1992;9:654-657.

[30] Siegel RA, pH-Sensitive gels: swelling equlibrium, kinetics, and applications for drug delivery. In: J. Kost, Editor, Pulsed and Self-regulated Drug Delivery, CRC Press, Boca Raton 1990. p.129-157.

[31] Nam K, Watanabe J, Ishihara K, Modeling of swelling and drug release behavior of spontaneously forming hydrogels composed of phospholipid polymers. Int J Pharm 2004;275:259-269.

[32] Huang Y, Yu H, Xiao C, pH-sensitive cationic guar gum/poly (acrylic acid) polyelectrolyte hydrogels: Swelling and in vitro drug release. Carboidr Polym 2007;69:774-783.

[33] Basan H, Gümüşderelioğlu M, Tevfik Orbey M, Release characteristics of salmon calcitonin from dextran hydrogels for colon-specific delivery. Eur J Pharm Biopharm 2007;65: 39-46.

[34] Muzzalupo R, Tavano L, Oliviero Rossi C, Cassano R, Trombino S, Picci N, Synthesis and properties of methacrylic functionalized Tween monomer networks. Langmuir 2009;25:1800-1806.

[35] Singh A, Schnur JM, Polymerizable phospholipids in Phospholipid handbook, G. Cevc, Ed., Marcel Dekker: New York, 1993.

[36] Arias JL, Novel Strategies to Improve the Anticancer Action of 5-Fluorouracil by Using Drug Delivery Systems. Molecules 2008; 13: 2340-2369.

[37] Pitarresi G, Pierro P, Giammona G, Muzzalupo R, Trombino S, Picci N, Beads of acryloylated polyaminoacidic matrices containing 5-fluorouracil for drug delivery. Drug Delivery 2002; 9: 97-104

3.1.3 Rheological characterization of the thermal gelation of poly(N-isopropylacrylamide) and poly(N-isopropylacrylamide)co-Acrylic Acid

Filipe E. Antunes, Luigi Gentile, Lorena Tavano and Cesare Oliviero Rossi

1Department of Chemistry, University of Coimbra, Polo II - Pinhal de Marrocos, 3004-535 Coimbra, PORTUGAL;

2Department of Chemistry, Calabria University, Via P. Bucci, Cubo 14/D, 87036 Arcavacata di Rende, ITALY;

3Department of Pharmaceutical Science, Calabria University, Edificio Polifunzionale,

87036 Arcavacata di Rende, Cosenza, ITALY.

Abstract

The combined effect of charged addition and molecular weight (Mw) on the thermal gelation and gel dissolution of poly(N-isopropylacrylamide) chains was explored by using Rheological techniques. The synthesized charged derivative is poly(N-isopropylacrylamide co-Acrylic acid). The rheological behavior of the two macromolecules is clearly different: the thermal gelation of the high Mw and charged macromolecule is much more accentuated. This suggests that the gelation at high temperatures only occurs when the inter polymer aggregate distance is sufficiently short to allow polymer bridging; this situation can be achieved by different approaches, such as increasing polymer concentration and increasing polymer persistence length and polymer Mw.

Introduction

Some systems show high miscibility in water at low temperatures while they phase separate at high temperatures. Before the macroscopic phase separation there is a strong turbidity, defined as clouding [1,2]. At certain circumstances, namely above a critical concentration, the polymer system stays turbid with a gel-like appearance, without any macroscopic phase separation [3]. Gels defined in terms of rheological characteristics can be considered as two component systems exhibiting a solid-like behaviour under small deformation. Thermal reversible gelation upon heating is relatively rare and is reported in some nonionic polymer systems, such as hydroxypropylmethylcellulose [4-9], poly(N-isopropylacrylamide) derivatives [10-17], and block copolymers composed of poly(ethylene oxide) and poly(propylene oxide), known as Pluronics [18-22]. These macromolecules, containing both hydrophilic and hydrophobic segments, may build-up core-shell-like nanoparticles in polar solvents, consisting of a hydrophobic core surrounded by a hydrophilic shell.

Although many attempts have been made to clarify the mechanisms behind thermal gelation, this is still a controversial field. While it is clear that these polymers associate better at higher temperatures

[5, 23], the molecular details regarding the polarity change are not fully consensual. The thermogelation mechanisms include partial crystallization, coil-to-helix transition, hydrophobic association, and micelle packing [12, 22, 24, 25]. This leads to a temperature dependent polymer network formation and an increased viscosity [10, 12, 16].

This investigation reports the combined effect of charge and Mw on the thermal gelation. The selected polymer was Poly(N-isopropylacrylamide) (PNIPAA) and a charged derivative of PNIPAA, poly(N-isopropylacrylamide co-Acrylic acid) (PNIPAAcoAAc).

PNIPAA is a thermo responsive water-soluble polymer that exhibits a cloud point at approximately 32°C [24]. Because of the swelling and shrinking in response to environmental stimuli, PNIPAA belong to a category of polymers widely explored for many biomedical applications, including drug delivery and tissue engineering [24, 26], artificial organs [27], on–off switches [28], and other temperature-pH sensitive smart hydrogels [29-32]. At temperatures well below the cloud point, PNIPAA is hydrophilic, while at temperatures above the cloud point the polymer chain backbone becomes hydrophobic and collapses into globules or multichain aggregates [24]. Above this temperature, PNIPAA solutions have a turbid appearance and a more viscous solution is formed. This viscous solution may shrink if the polymer concentration is not sufficiently high. The cloud point of PNIPAA can be controlled by copolymerizing with other monomers with different hydrophobicity. The more hydrophobic the co-monomer, the lower the resulting cloud point.

The polymer association that drives the thermal gelation in aqueous solutions is of hydrophobic nature. Ordering PNIPAA in water results from some orientations required to hydrogen bond with the already arranged water molecules [33]. When PNIPAA gets more hydrophobic, the water molecules must reorient around nonpolar regions of the polymer, being unable to hydrogen bond with them. This is called the hydrophobic effect [34] and results in decreased entropy upon mixing. At higher temperatures, the entropy term dominates the enthalpy of the hydrogen bonds formed between the polymer polar groups and water molecules and the consequence is phase separation above the cloud point. At high polymer concentrations the replacement of polymer-water association with polymer-polymer and water-water association is seen by precipitation or gel formation [24].

Some studies confirmed this PNIPAA association at high temperatures. One of them deals with added pyrene as fluorescence probe into PNIPAA systems. Below the cloud point the pyrene spectra are identical to that of each probe in polymer-free solution, indicate that PNIPAA itself does not have any hydrophobic binding sites. However, an abrupt shift in pyrene emission spectra is seen in above the cloud point, suggesting that pyrene molecules are incorporated into the hydrophobic core region upon micellar aggregation [24].

Below the cloud point PNIPAA exists as a flexible but highly extended coil approaching a rod-like conformation in dilute aqueous solutions [35, 36]. While heated, it was reported that the apparent Mw increases 4.5 times upon increasing the temperature from 25°C to 33°C, which suggests polymer aggregation [35]. In very dilute solutions the polymer has a transition from coil to globule while heating [36]. Greater understanding of polymer conformation may be obtained by using the Mark-Houwink equation: $[\eta] = KM\ a$, $[\eta]$ being the intrinsic viscosity and M the molecular weight. This equation predicts the shape of polymer molecules in solution. When the exponent a is 0.50, the polymer is in theta conditions. When the exponent reaches 0.6-0.8 the polymer is stretched out in a good solvent, while an exponent higher than 1 means that the polymer is in rod-like conformation [37]. The coefficients found for PNIPAA, at low temperatures, are all above 0.5 [24]. Viscosity dependence on temperature of PNIPAA systems shows a peak around the cloud point. This was explained as being due to intermicellar association followed by contraction [10].

With this study we want to explore the thermal gelation of PNIPAA and the effect of charge addition and increased Mw by using a charged PNIPAA derivative, PNIPAAcoAAc. The incorporation of low amounts of charge and the increased of Mw was found to dramatically increase the magnitude of the thermal gelation.

2 Experimental

Materials

PNIPAA (average Mn=20000-25000), Acrylic Acid (AAc), and 2,2'-azobisisobutyronitrile (AIBN) were purchased from Sigma Chemicals (Steinheim, Germany). All Chemicals and reagents were used without further purifications.

Polymer synthesis

Polymers composed of NIPAA monomers with AAc (2 mol% in feed, Mw ~ 1000000KD) were synthesized by free radical polymerization of NIPAA in benzene with AIBN as initiator (7×10-3 mole/mole monomer). The monomer solutions were bubbled with dried nitrogen gas for 30 min. After the addition of AIBN, mixtures were degassed for 30 min by applying vacuum. The polymerization was performed at 60°C for 16 h under dried nitrogen gas pressure; polymers have precipitated in the solvent during polymerization. The precipitate was dissolved in a 90/10 v/v% acetone/methanol mixture, and it was precipitated in an excess amount of diethyl ether. Finally, it was dried in vacuum for 3 days. The high obtained average molecular weight was due to the radical chain transfer reaction to the solvent molecules during polymerization [38]. The relative acrylic acid content of PNIPAAcoAAc was 1.4 obtained by acid basic titration method.

126

Figure 1 shows the molecular structure of NIPAA and NIPAAcoAAc monomers.
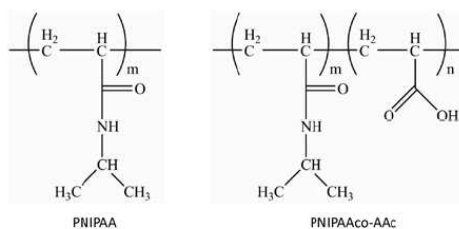

Figure 1 – Molecular structure of PNIPAA (left) and PNIPAAcoAAc (right) monomers.

Methods

Polymer solutions were prepared by weighting the desired amount of polymer and water in vials containing a small magnetic stirring bar. All the samples were mixed by a vortex 708 (ASAL, Italy) and were homogenized in a liquid state at 25°C. After homogenization the mixtures were stored at 5ºC for 1 week before being tested.

Rheological measurements were conducted using a shear strain controlled rheometer RFS III (Rheometrics, USA) equipped with a couette, cylinder geometry (gap 1.06 mm, external and inner radius 17 and 7 mm, respectively). The temperature was controlled by a water circulator apparatus (±0.2°C). To prevent errors due to evaporation, measuring geometries were surrounded by a solvent trap containing water. Two different kinds of experiments were carried out: a) Steady flow experiments; b) Dynamic shear experiments were performed in a frequency range between 0.1 and 15.9 Hz. The small amplitude dynamic tests provided information on the linear viscoelastic behaviour of materials through the determination of the complex shear modulus [39]:

$$G^*(\omega)=G'(\omega)+iG''(\omega) \qquad\qquad 1$$

or in terms of complex viscosity,

$$\eta^*=G'\omega/\omega \qquad\qquad 2$$

where $G'(\omega)$ is the in phase (or storage) component and $G''(\omega)$ is the out-of-phase (or loss) component. $G'(\omega)$ is a measure of the reversible, elastic energy, while $G''(\omega)$ represents the irreversible viscous dissipation of the mechanical energy. The dependence of these quantities on the oscillating frequency gives rise to the so-called mechanical spectrum, allowing the quantitative rheological characterization of studied materials. The applied strain amplitude for the viscoelastic

measurements was reduced until the linear response regime was reached. This analysis was made by performing strain sweep tests in all temperature range investigated. Weak Gel Model [39] was also applied to some of the oscillatory spectra:

$$\left| G^*(\omega) \right| = \sqrt{G'(\omega)^2 + G''(\omega)^2} = A\omega^{\frac{1}{z}}$$

$\qquad$ 3

where "A" is interpreted as the interaction strength between the rheological units: a sort of amplitude of cooperative interactions, and "z" as the coordination number, which corresponds to the number of flow units interacting with each other to give the observed flow response [40].

Differential scanning calorimetry (DSC) measurements were performed by using a Setaram micro DSC III instrument. Samples (20-30 mg) were sealed in aluminium-cells and heated to the initial temperature. As a reference, a sealed pan with the corresponding amount of water was used. To check water evaporation, the pans were weighed before and after the DSC measurements. The DSC thermograms were recorded in the temperature range from 5 to 80ºC. The heating rate was 1ºCmin^{-1}.

3 Results and discussion

PNIPAA mixtures

Figure 2 shows the dependence of complex viscosity, η$\Box$, on temperature, at different PNIPAA concentrations. The rheological behavior of PNIPAA solutions was studied in diluted and semidiluted concentration regimes, i.e. below and above the overlap concentration of the polymer. The overlap concentration (c*) is defined as the concentration where the monomer density inside the coil is equal to the overall monomer density in the solution. Empirically, c* is usually at a polymer concentration where its zero-shear viscosity (ηo) is about twice as high as that of the solvent [41].

In the dilute polymer samples, containing 0.1, 1 or 2wt% of polymer, the viscosity decreases by heating, disclosing a broad transition peak at c.a. 33-35ºC. For the concentrated sample, containing 5wt% of polymer, the picture is clearly different: instead of a peak, a jump in viscosity around the cloud point is seen. We will start the discussion focusing the dilute polymer situation.

Below 33ºC the solutions are transparent and the viscosity decreases on temperature. This can be explained by a concomitant effect of increased dynamics and also by the shrinkage of the polymer chains, which become less hydrophilic and self-associate into aggregates, as described above. This transformation gets increasingly relevance as the system is being heated up. Therefore, a consequence of the gradual weakness of the solvent quality is a progressively smaller polymer size due to better intra-association. Immediately above the cloud point the viscosity dependence on

temperature has a peak, explained to be due to strong association and network formation followed by contraction [10, 15]. The network collapses, seen by a decreased viscosity, may be explained by a lower number of inter-aggregate chains because of the shorter polymer globule size.
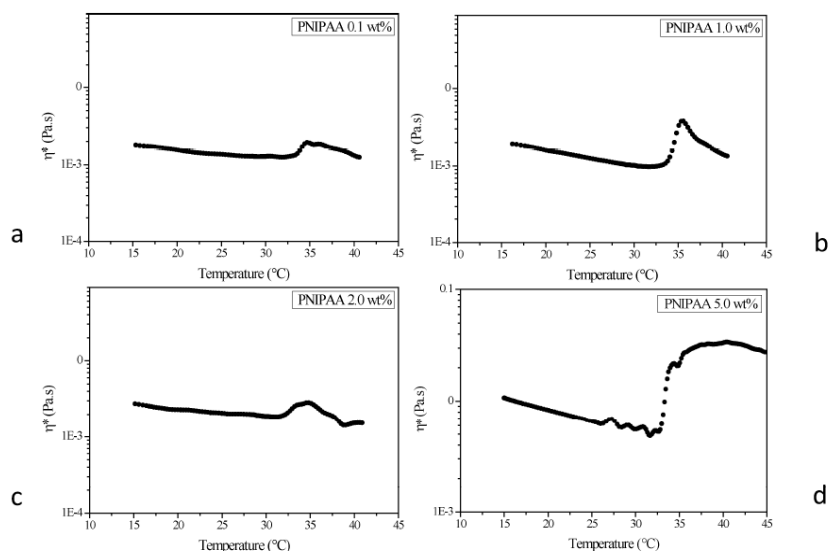

Figure 2 – Dependence of complex viscosity on temperature, for different PNIPAA concentrations (0.1-5wt%).

This profile is, however, not seen above the polymer overlap concentration, as can be seen in Figure 2d. Above the jump in viscosity at cloud point, no network collapse is detected. Instead, the viscosity jumps and keeps the high values at temperatures well above the cloud point. This phenomenon is better illustrated in Figure 3, where the temperature dependence of storage and loss moduli of PNIPAA, both below and above the overlap concentration, is displayed.

While at 2wt% of polymer G'' is always higher than G', i.e., the system is liquid-like within the entire temperature studied, at 5wt% of polymer, the system has solid properties above the 33ºC. This difference has to be addressed to the importance of polymer entanglements in the gel formation. Such issue was already pointed out as crucial in other clouding system [5].

Figure 4 reports the linear viscoelasticty for two mixtures (c=5 and 10 wt.% PNIPAA) at 35°C in the frequency range 0.1–15 Hz. Frequency spectra show a viscoelastic response, which is typical of a weak gel material [40]. The storage modulus, G', exceeds the loss modulus, G'' and they are slightly linear dependent on the frequency over the investigated frequency range. As observed by Winter42 this power law behavior indicates that the gel structure is self-similar over a wide range of length scale. It is worthy to note how both moduli are higher for the more concentrated sample due to network enhancement.
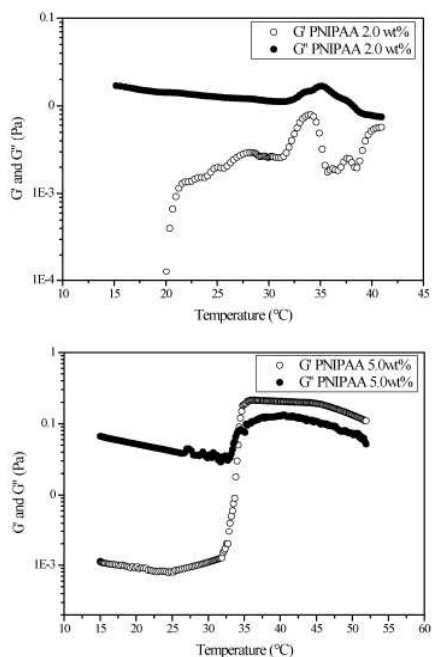
Figure 3 – Dependence of storage and loss moduli on temperature, at 2wt% and 5wt% PNIPAA.
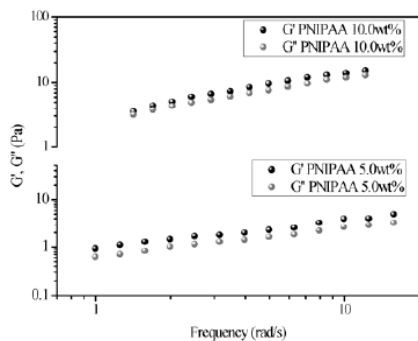

Figure 4 – Variation of dynamic moduli with oscillating frequency, of mixtures of 5 wt% and 10 wt% PNIPAA, at 35 °C.

A minimum concentration is required in order to ensure the presence of crosslinks between the aggregates well above the cloud point. Thus the rheological consequences and thermal gelation effects are dramatically different if one has a concentrated or dilute polymer solution. However, those differences only happen at rest: high shear rates inhibit thermal gelation. This can be seen in **Figure 5**, where shear viscosity at high shear rates (10 s-1) is plotted as a function of temperature.
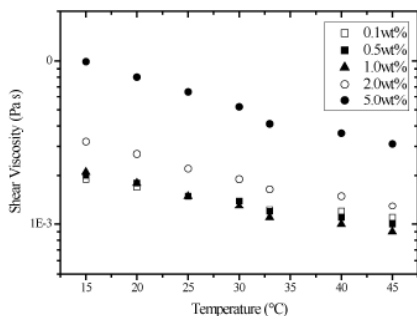
Fig.5 Shear viscosity dependence on temperature, at 10s-1.
PNIPAA concentration was varied from 0.1wt% to 5wt%.

At high shear rates, the viscosity decreases monotonically with temperature, even at high concentrations. This suggests that the growth of complexes, as well as the crosslinks between complexes, is suppressed under the influence of shear flow. Results in literature confirm this explanation [5, 10].

One of the highlights taken from the above discussion is that a liquid-gel phase transition occurs at high temperatures if the polymer concentration is high enough. The network formed by polymer aggregates can only be established if the inter-aggregate distance is not much longer than the permitted for polymer bridging. If such distance is too long, aggregates work only as individual obstacles to the deformation and the viscosity is low. However, if they are bridged by other polymers, the formed network gives rise to much higher viscosity. The polymer concentration has to be close to the overlap concentration of the polymer at high temperatures.

The question that arises here is how the thermal gelation would behave if one decreases the overlap concentration of the polymer? This could be achieved by increasing the molecular weight of the polymer and/or by converting PNIPAA into a polyelectrolyte, PNIPAAcoAAc. Charging the polymer leads to longer polymer gyration radius due to charge repulsion. Such coil-rod transformation decreases the overlap concentration of the polymer.

Comparison between PNIPAA and PNIPAAcoAAc solutions

PNIPAAcoAAc was synthesized with 1.4% of acrylic groups at pH 7.4 (1.4 negative charges per 100 monomer units). The overlap concentration (c*) of PNIPAAcoAAc was determined at around 0.5wt% by steady viscosity measurements. The clear PNIPAAcoAAc solution (single phase) at low temperatures also becomes a gel as the temperature reaches 30°C. At 43°C the gel starts to shrink by expelling water.

Rheological response upon heating of 5wt% of this polyelectrolyte is compared with the one from PNIPAA in Figure 6.
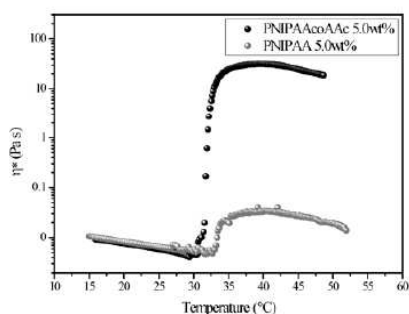

Figure 6 – Dependence of complex viscosity (at 1Hz) on temperature, for PNIPAA and PNIPAAcoAAc. The polymer concentration was kept constant at 5wt%. Heating rate was 1ºC/min.

The differences are clear: considering the polymer solution at 5 wt% the thermal gelation is much more pronounced in the charged polymer, with an increase on complex viscosity upon heating of c.a. 4 orders of magnitude. Much more than the 1 order of magnitude increase when dealing with PNIPAA aqueous systems. The viscosity does not fall above the maximum in viscosity, which indicates that the network is preserved, even when the polymer chains are even more compacted due to increased hydrophobicity. The inter-polymer distance is small enough for polymer bridging. These differences can be addressed to changes in the polymer size, induced both by Mw effect and by charge effect. PNIPAAcoAAc has c.a. 40 times higher Mw than PNIPAA. An increase of Mw can be associated to a decreased overlap concentration and to a facilitated bridging. By charging a PNIPAA coil, the polymer becomes more rod-like and with a longer gyration radius. This also affects the polymer overlap concentration and the polymer ability to form networks. When clusters are formed due to an increased hydrophobicity at higher temperatures, the clusters composed of PNIPAA are smaller due to shorter polymer chain and interact only weakly with other clusters. Thus, the polymer network is only weakly built or even absent, and the rheological response is of a weak gel or liquid-like. On the other hand, clusters built up by rodlike charged polymers with higher Mw are bigger and some of the polymers may bridge two or more clusters due to a small inter-cluster distance. Current work has been done in order to evaluate the contributions from Mw and charge separately. The Mw seems to be critical since very short chains of PNIPAAcoAAc do not exhibit gel phase [11].

The onset of the complex viscosity jump in PNIPAAcoAAc occurs approximately 3ºC below that of the uncharged polymer. This is probably due to the higher Mw of PNIPAAcoAAc and the consequent lower polymer entropy of mixing. Figure 7 shows DSC curves for the two polymer

132

systems. It is shown the presence of a shift on the endothermic peak to lower temperatures when the charged polymer is measured.
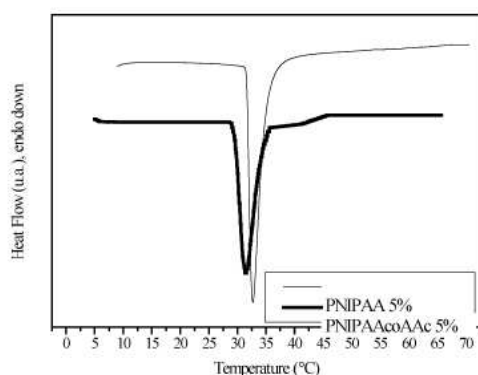

Figure 7 – DSC upscans of PNIPAA and PNIPAAcoAAc samples. Heating rate: 1.0ºC/min.

From this result it also comes out that the charge density of the polymer is not sufficiently high for the expected shift of the clouding to higher temperatures, due to the entropy of counterions.

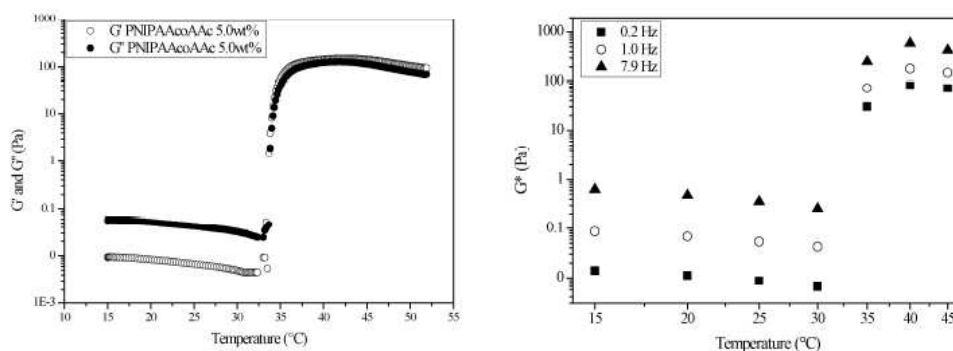A deeper rheological characterization of 5 and 10 wt% aqueous solution of PNIPAAcoAAc is shown in Figure 8.

Figure 8 – Dependence of storage modulus, loss modulus and complex modulus on temperature, for PNIPAAcoAAc samples.

Figure 8a illustrates the dependence of G' and G'' on temperature. While G'' is higher than G' within 15ºC and 33ºC, the situation becomes inverse above 33ºC, with a solid-like character permanent in the material response. Figure 8b shows the dependence of G* with temperature at different frequencies. When the gel is formed, the complex modulus jumps c.a. 3 orders of magnitude. Above 40ºC there is a sudden decrease in G*, this being associated to the gel-shrinking temperature. Once the gel is formed, it does not dissolve or change water content until the gel

shrinking temperature is reached. This process requires a high molecular weight, high concentration and/or high gyration radius of the polymer for the chain entanglement.

Weak gel model

The weak gel model provides a direct link between the microstructure of the material and its rheological properties. Introduced parameters are the "coordination number", z, and the interaction strength, A, defined above. Figure 9 shows A and z dependence on temperature, for 5 wt% PNIPAAcoAAc and PNIPAA solutions.
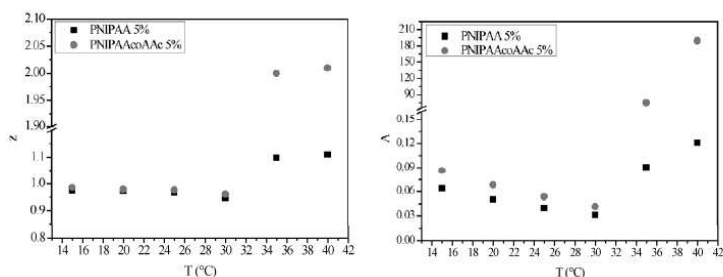

Figure 9 – A and z parameters versus temperature for 5 wt% solutions of PNIPAA and PNIPAAcoAAc.

Below the gel temperature, both solutions have a flow coordination number close to the unit and low values of "A". This can be ascribed to the absence of entanglements, evidencing that no interaction occurs among polymer coils. At 25ºC, in the PNIPAAcoAAc system, z and A are 0.96 and 0.045, respectively. At 40ºC, these values raise to 2.02 and 195. These data confirm the presence of the gel that gets more consistent with increasing the temperature.

4 Conclusions

A derivative of poly(N-isopropylacrylamide) was synthesized in order to investigate the effect of molecular weight and charge on the rheological behavior of poly(N-isopropylacrylamide). The differences between the rheological responses of the two systems are critical; the higher molecular weight and ionic system shows a much more evident thermal gelation above the cloud point. While the lower Mw and nonionic system shows, above the overlap concentration, a weak increase in complex viscosity, detected slightly above the cloud point, the higher Mw and charged polymer shows a markedly increase in complex viscosity. The latter keeps a gel-like structure well above the cloud point.

The difference is attributed to a decreased overlap concentration of the polyelectrolyte system and a consequent increase of inter cluster association. The thermal gelation is sensitive to the degree of connectivity between polymer clusters above the cloud point and can be achieved by different ways,

as by increasing the polymer concentration or Mw or by increasing the persistence length of the polymer by charging its chains. Thermal gelation in these systems only occurs when the polymer concentration is high enough and the intercluster distance is small enough to allow polymer bridging.

References

[1] Evans D, Wennerström H: The Colloidal Domain: Where Physics, Chemistry, and Biology Meet, Wiley, New York (1999).

[2] Holmberg K, Jönsson B, Kronberg B, Lindman B: Surfactants and polymers in aqueous solution, John Wiley & Sons, New York (2003).

[3] Almgren M, Bahadur P, Jansson M, Li P, Brown W, Bahadur A: Static and dynamic properties of a (PEO---PPO---PEO) block copolymer in aqueous solution, J. Coll Int Sci. 151 (1992) 157- 165.

[4] Haque A, Morris ER: Thermogelation of methylcellulose. Part 1 : molecular stuctures and processes, Carbohydr Polym. 22 (1993) 161–173.

[5] Silva Sérgio M C, Pinto F V, Antunes F E, Miguel M G, Sousa J J, Pais A C: Aggregation and gelation in hydroxypropylmethyl cellulose aqueous solutions, J Coll Int Sci. 327 (2008) 333-340.

[6] Xu X M, Song Y M, Ping Q N, Wang Y, Liu X Y: Effect of ionic strength on the temperature-dependent behavior of hydroxypropyl methylcellulose solution and matrix tablet, J. Appl. Polym. Sci. 102 (2006) 4066-4074.

[7] Sammon C, Bajwa G, Timmins P, Melia C D: The application of attenuated total reflectance Fourier transform infrared spectroscopy to monitor the concentration and state of water in solutions of a thermally responsive cellulose ether during gelation, Polymer 47 (2006) 577-584.

[8] Sarkar N: Thermal gelation properties of methyl and hydroxypropyl methylcellulose, J. Appl. Polym. Sci. 24 (1979) 1073-1087.

[9] Haque A, Richardson R K, Morris E R, Gidley M J, Caswell D C: Thermogelation of methylcellulose. Part II: effect of hydroxypropyl substituents, Carbohydr. Polym. 22 (1993) 175-186.

[10] Kjoniksen A L, Zhu K, Pamies R, Nystrom B: Temperature-Induced Formation and Contraction of Micelle-Like Aggregates in Aqueous Solutions of Thermoresponsive Short-Chain Copolymers, J Phys Chem B Letters 112 (2008) 3294-3299.

[11] Han C K, Bae Y H: Inverse thermally-reversible gelation of aqueous N-isopropylacrylamide copolymer solutions, Polymer 39 (1998) 2809-2814.

[12] Jeong B, Kim S, Bae Y H: Thermosensitive sol–gel reversible hydrogels, Adv Drug Deliv Rev 54 (2002) 37-51.

[13] Yoshida R, Uchida K, Kaneko Y, Sakai K, Kikuchi A, Sakurai Y, Okano T: Comb-type grafted hydrogels with rapid deswelling response to temperature changes, Nature 374 (1995) 240–242.

[14] Kaneko Y, Nakamura S, Sakai K, Aoyagi T, Kikuchi A, Sakurai Y, Okano T: Rapid Deswelling Response of Poly(N-isopropylacrylamide) Hydrogels by the Formation of Water Release Channels Using Poly(ethylene oxide) Graft Chains, Macromolecules 31 (1998) 6099-6105.

[15] Zhu K, Jin H, Kjoniksen A L, Nystrom B: Anomalous Transition in Aqueous Solutions of a Thermoresponsive Amphiphilic Diblock Copolymer, J Phys Chem B 111 (2007) 10862-10870.

[16] Durand A, Hourdet D: Thermoassociative graft copolymers based on poly(N-isopropylacrylamide): Relation between the chemical structure and the rheological properties, Macromol Chem Phys 201 (2000) 858-868.

[17] Lebon F, Caggioni M, Bignotti F, Abbate S, Gangemi F, Longhi G, Mantegazza F, Bellini T: Coil-to-Globule Transition of Poly(N-isopropylacrylamide) Doped with Chiral Amino Acidic Comonomers, J Phys Chem B 111 (2007) 2372-2376.

[18] Wanka G, Hoffman H, Ulbricht W: Phase Diagrams and Aggregation Behavior of Poly(oxyethylene)-Poly(oxypropylene)-Poly(oxyethylene) Triblock Copolymers in Aqueous Solutions, Macromolecules 27 (1994) 4145-4159.

[19] Alexandridis P, Hatton T A: Poly(ethylene oxide)---poly(propylene oxide)---poly(ethylene oxide) block copolymer surfactants in aqueous solutions and at interfaces: thermodynamics, structure, dynamics, and modeling, Coll Surf A 96 (1995) 1-46.

[20] Zhou Z, Chu C: Light-scattering study on the association behavior of triblock polymers of ethylene oxide and propylene oxide in aqueous solution, J Coll Int Sci 126 (1988) 171-180.

[21] Attwood D, Collett J H, Tait C J: The micellar properties of the poly(oxyethylene) - poly(oxypropylene) copolymer Pluronic F127 in water and electrolyte solution Int. J. Pharm. 26 (1985) 25-33.

[22] Alexandridis P: Amphiphilic Copolymers and their Applications, Curr Opin Colloid Interface Sci 1 (1996) 490-501.

[23] Yang Z, Zhang W, Zou J, Shi W: Synthesis and thermally responsive characteristics of dendritic poly(ether-amide) grafting with PNIPAAm and PEG, Polymer 48 (2007) 931-938.

[24] Schild H G: Poly(N-isopropylacrylamide): experiment, theory and application, Prog. Polym. Sci. 17 (1992) 163-249.

[25] Gariepy E, Leroux J: In situ-forming hydrogels—review of temperature-sensitive systems, Eur J Pharm Biopharm 58 (2004) 409-426.

[26] Chang C, Wei H, Quan C, Li Y, Liu J, Wang Z, Cheng S, Zhang X, Zhuo R: Fabrication of thermosensitive PCL-PNIPAAm-PCL triblock copolymeric micelles for drug delivery, J Polym Sci A 46 (2008) 3048-3057.

[27] Osada Y, Okuzaki H, Hori H: A polymer gel with electrically driven motility, Nature 355 (1992) 242-244.

[28] Xu X D, Wei H, Zhang X Z, Cheng S, Zhuo R: Fabrication and characterization of a novel composite PNIPAAm hydrogel for controlled drug releasev, J Biomed Mater Res A 81 (2007) 418-426.

[29] Chen G, Hoffman H: Graft copolymers that exhibit temperature-induced phase transitions over a wide range of pH, Nature 373 (1995) 49-52.

[30] Shibayama M, Fujikawa Y, Nomura S: Dynamic Light Scattering Study of Poly(N-isopropylacrylamide-co-acrylic acid) Gels, Macromolecules 29 (1996) 6535-6540.

[31] Chen H, Hsieh Y: Ultrafine hydrogel fibers with dual temperature- and pH-responsive swelling behaviors, J Polym Sci A 42 (2004) 6331-6339.

[32] Wang Z, Xu X D, Chen C, Wang G, Wang B, Zhang X, Zhuo R: Study on novel hydrogels based on thermosensitive PNIPAAm with pH sensitive PDMAEMA grafts, Coll Surf B 67 (2008) 245-252.

[33] Walker J A, Chester A V: Reappearing phases, Sci. Am. 253 (1987) 90-98.

[34] Tanford C: The Hydrophobic Effect: Formation of Micelles and Biological Membranes, Wiley, New York (1980).

[35] Heskins M, Guillet J E: Solution Properties of Poly(N-isopropylacrylamide), J Macromolec Sci A 2 (1969) 1441-1455.

[36] Williams C, Brochard F, Frisch H L: Polymer Collapse, Annu Rev Phys Chem 32 (1981) 433-451.

[37] Hiemenz P, Timothy L: Polymer Chemistry, Marcel Dekker Inc, New York (2007).

[38] Brandup J, Immergut E H: Polymer Handbook, John Wiley & Sons, New York (1993).

[39] Coppola L, Gianferri R, Oliviero C, Nicotera I, Ranieri G: Structural changes in CTAB/H2O mixtures using a rheological approach, Phys Chem Chem Physics 6 (2004) 2364-2372.

[40] Gabriele D, Cindio B, Antona P: A weak gel model for foods, Rheol Acta 40 (2001) 120-127.

[41] Boris D C, Colby R H: Rheology of Sulfonated Polystyrene Solutions, Macromolecules 31 (1998) 5746–5755.

[42] Mours M, Winter H: Mechanical spectroscopy. In Experimental methods in Polymer Science, Tanaka, T., Ed. Academic Press, San Diego (2000).

3.1.4 Synthesis and antioxidant activity evaluation of a novel cellulose hydrogel containing *trans*-ferulic acid

Sonia Trombino, Roberta Cassano, Ermelinda Bloise,

Rita Muzzalupo, Lorena Tavano and Nevio Picci

Department of Pharmaceutical Science, Calabria University, Edificio Polifunzionale,

87036 Arcavacata di Rende, Cosenza, ITALY.

Abstract

In the present work, we report the synthesis of cellulose hydrogel containing ferulic moieties and the evaluation of its antioxidant and scavenger activity. Acrylic groups were inserted onto cellulose backbone by a heterogeneous synthesis to produce two cellulose monomers with different degree of substitution (DS). The radical copolymerization of acrylcellulose (AcrC) with *N,N*-dimethylacrylamide (DMAA) was carried out in NH_3/Urea aqueous solution, in a range of composition between 24 and 60 wt% of AcrC. The obtained hydrogels were characterized by infrared spectroscopy (FT-IR). Their equilibrium swelling degree ($\alpha\%$) was evaluated. They showed good swelling behavior in simulating gastric, intracellular and intestinal fluids and no more different at various pH. The ferulic moieties were directly grafted on the free hydroxylic groups of cellulose hydrogel by acylation, using dicyclohexylcarbodiimide (DCC) and 4-hydroxybenzotriazole (HBT) as condensation agents. Finally, the antioxidant activity in inhibiting the lipid peroxidation, in rat-liver microsomal membranes, induced in vitro by two different sources of free radicals, 2,2′-azobis (2-amidinopropane) (AAPH) and *tert*-butyl hydroperoxide (*tert*-BOOH), was evaluated. The effects of scavenging DPPH (1,1-diphenyl-2-picrylhydrazyl) radicals were also investigated. Hydrogel was found to be very efficient scavengers of DPPH radicals. The results strongly suggested that the antioxidant hydrogel neutralize free radicals. This biomaterial could be successfully applied in pharmaceutical field both as prodrug of *trans*-ferulic acid than as carrier for photo and thermo-degradable drugs to improve their stability.

1. Introduction

Hydrogels are presently under investigation as matrices for the controlled release of bioactive molecules. They are based on crosslinked hydrophilic matrix insoluble in water which absorb and retain large amounts of water and biological fluids, releasing the drugs by slow diffusion. There are many studies on natural (e.g. alginate and chitosan) polysaccharide based hydrogels. These

materials are biocompatible, biodegradable, and non-toxic and used as drug delivery systems [1,2]. Recently, hydrogels based on commercial chemically crosslinked cellulose derivatives were studied for the production of dietary bulking agents [3]. In fact, cellulose is the most abundant polymer in nature and its derivatives are very popular due to their biocompatibility with tissues and blood, non-toxicity [4] and low price. They are already used in pharmaceutical formulations as inert matrix towards the incorporated drugs [5,6]. Over the past decade, a great deal of researches has focused on the application of antioxidants to medical treatments [7-10] to prevent free radicals formation. Antioxidant polymers have received ever-increasing attention, from both academic and cosmetic and pharmaceutical industries point of view. To confer antioxidant and free radical scavenger properties to hydrogels both acrylic or vinylic monomer bearing vitamin E as side groups than vinylic monomer binding eugenol were employed [11,12]. Moreover, in a previous paper, we reported the synthesis and characterization of cellulose, with antioxidant efficiency, bearing ferulic, lipoic and tocopherol moieties. This study showed that the designed systems, preserve the antioxidant activity of the free substrates and that the cellulose ferulate is the best antioxidant to protect against lipid peroxidation induced by two different sources of free radicals[13].

For such reason the idea to link ferulic moieties to cellulose hydrogels by covalent bond (Scheme 1) to produce a carrier that protects unstable drugs against oxidative stress and then could be useful in preparations for topical and oral administrations. Particularly, in this work we reported on the antioxidant compounds covalently linked to a hydrogel cellulose-based. The ferulic groups do not leach out of the polymer matrix. Furthermore, the immobilization of the antioxidant also improves its long-term stability. The synthesis disclosed in this paper proceeded under mild conditions and resulted in highly selective coupling of the antioxidant compounds to hydrogels, which ensured an effective dispersion of the antioxidant throughout the materials.

The present paper reports on (i) the synthesis of hydrogels cellulose-based, carried out by radical copolymerization of AcrC with DMAA; (ii) the swelling characteristics of the hydrogels by measurements of α at various pH values; (iii) the grafting reaction of *trans*-ferulic acid on cellulose hydrogel that showed the best α; (iv) the evaluation of its antioxidant activity in inhibiting the lipid peroxidation in rat-liver microsomal membranes [14], induced in vitro by 2,2′-azobis (2-amidinopropane) (AAPH), which exogenously produces peroxyl radicals by thermal decomposition, and *tert*-butyl hydroperoxide (*tert*-BOOH), which endogenously produces alkoxyl radicals by Fenton reactions; (v) the evaluation of its scavenging effects on DPPH radical by the decoloration method.
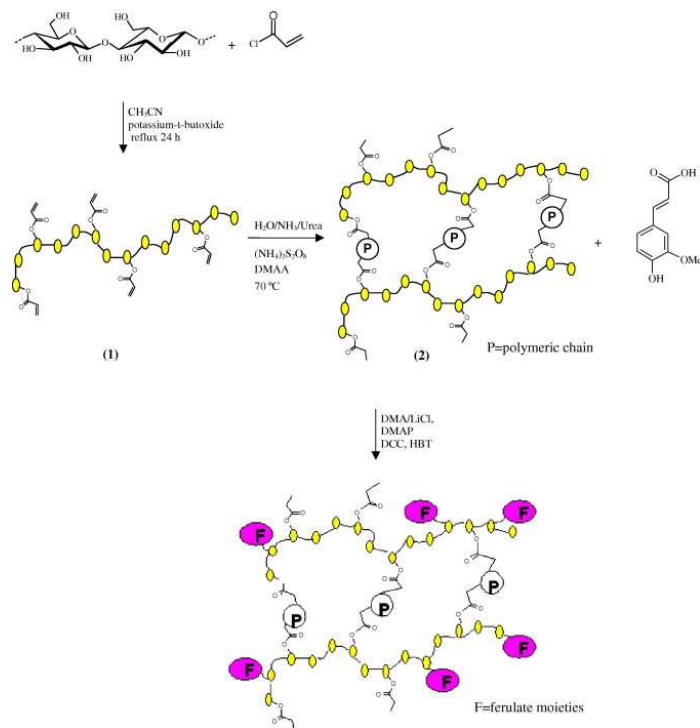
Scheme 1. Synthesis of ferulate hydrogel.

2. Cellulose acrylate (AcrC)

Cellulose monomer AcrC (1) was obtained by heterogeneous synthesis [15] with acryloyl chloride (Scheme 1). Briefly, microcrystalline cellulose was swollen in acetonitrile at room temperature for 1 h. The solution of potassium *tert*-butoxide in acetonitrile was added and the reaction mixture was allowed to react at room temperature for 4 h. An excess of acryloyl chloride in acetonitrile was added dropwise to the stirred reaction mixture at room temperature. Stirring was continued under reflux overnight. The product was filtered, washed thoroughly with water, ethanol, acetone, and diethyl ether and then dried in vacuum at 50 °C. FT-IR (KBr) spectra showed an absorption at 1721 cm^{-1} and the presence of pendant vinyl groups at 805 cm^{-1}. Varying molar ratio and reaction time (Table 1) were obtained two derivatives with different degree of substitution (DS) determined by volumetric analysis[7]. Briefly, a sample of 50 mg of ester derivative was dispersed in 5 ml of 0.25 M ethanolic sodium hydroxide solution under reflux for 17 h. The dosing, in return of the excess of soda, was realized by titration with 0.1 N HCl (first equivalent point). The moles of chloride acid used between the first and second equivalence correspond to the moles of free esters. The degree of substitution (DS) was determined by the Eq. (1):

$$DS = \frac{MM_{glu\cos e\ unit}}{(g_{sample} / n_{free\ ester}) - (MM_{free\ ester} - MM_{H_2O})}$$

140

In Eq. (1) $n_{\text{free ester}} = (V_{2\ \text{e.p.}} - V_{1\ \text{e.p.}}) \times [\text{HCl}]$; $\text{MM}_{\text{glucose unit}}$ is the molecular mass of a glucose unit; g_{sample} is the weight of the sample; $n_{\text{free ester}}$ is the number of moles of free ester; $\text{MM}_{\text{free ester}}$ is the molecular mass of free ester; and MM_{H2O} is the molecular mass of water.

Molar ratio cellulose/*tert*-butoxide/acryloyl chloride	Reaction time (h)	DS
1:3:3	8	0.28
1:3:10	20	0.68

Table 1. Reaction conditions and degree of substitution (DS) values

3. AcrC/DMAA hydrogel

Preparation of hydrogels (2) was carried out by radical polymerization of AcrC, the crosslinking agent, with DMAA (Scheme 1). Cellulose monomer (AcrC) was swollen under stirring for 10 min in 2.5 ml of NH_3 (30%)/Urea (12%) aqueous solvent, cooled at $-5\ °C$. Comonomer (DMAA) and ammonium persulfate, the polymerization initiator, were added. The mixture was heated to $70\ °C$ for few minutes, until the crosslinking took place and the mixture became like gel. The hydrogels were washed with several aliquots of hot water under stirring, filtered, deswollen with acetone, dried under vacuum at $50\ °C$ and then investigated by FT-IR spectroscopy that confirmed the copolymerization. Precisely, was observed a decrease of peak intensity in the double bonds region at $805\ \text{cm}^{-1}$ and the appearance of a new ester band at $1732\ \text{cm}^{-1}$ due to a formation of hydrogel between AcrC and DMAA. Carrying out the polymerization in *N,N*-dimethylacetamide and lithium chloride (DMA/LiCl) solvent system were obtained hydrogels with lower α.

4. Swelling studies

The swelling behavior of hydrogels was determined in order to check their hydrophilic affinity. Typically, aliquots (40–50 mg) of materials dried to constant weight were placed in a tared 5-ml sintered glass filter (Ø 10 mm; porosity G3), weighed, and left to swell by immersing the filter in a beaker containing the swelling media (acidic solution pH 1, simulated gastric fluid; phosphate buffer pH 6.8, simulated intercellular fluid; basic solution pH 8, simulated intestinal fluid). At predetermined times (1, 4 and 24 h), the excess of water was removed by percolation and then the filter was centrifuged at 3500 rpm for 15 min and weighed. The filter tare was determined after centrifugation with only water. The weights recorded at different times were averaged and used to give the equilibrium swelling degree (α%) by the Eq. (2). In Eq. (2) W_s and W_d are the weights of swollen and dried hydrogels, respectively. Each experiment was carried out in triplicate and the

results were in agreement within ±4% standard error. The amount of monomer and crosslinking agent used for hydrogels preparation and the relative α (%) values were reported in Table 2 and Table 3. All prepared hydrogels showed no more different swelling behaviors at various pH values. By changing the amount of comonomer hydrogels with different swelling behavior were obtained. Particularly, hydrogels synthesized by AcrC with higher DS showed lower α due to formation of a network with higher density. The larger amount of DMAA can increase the length of PDMAA segments which decreases the network density, respectively.

Molar ratio AcrC/DMAA	Equilibrium swelling degree % (α)		
	pH 1	pH 6.8	pH 8
1:3[a]	–	–	–
1:6	706	533	778
1:9	759	772	891

Table 2. Equilibrium swelling degree % of hydrogels prepared by AcrC with DS = 0.28

Molar ratio AcrC/DMAA	Swelling degree % (α)		
	pH 1	pH 6.8	pH 8
1:3	364	266	570
1:6	680	557	646
1:9	652	562	700

Table 3. Equilibrium swelling degree % of hydrogels prepared by AcrC with DS = 0.68

5. Cellulose hydrogel containing trans-*ferulic acid*

With the aim of taking advantage of the antioxidant properties of the *trans*-ferulic acid, an hydrogel containing this residue has been synthesized. The linking of antioxidant groups on the preformed hydrogel rather than on its precursor was effected to avoid the inhibitory action of *trans*-ferulic acid, a scavenger of radicals species, on the radical polymerization process. The grafting reaction of ferulic acid (FA) (Scheme 1) was carried out on hydrogel, synthesized by ArcC (DS 0.28)/DMAA with 1:9 molar ratio, that showed higher α value. The dry hydrogel (0.4 g corresponding to 3.3 mmol of free hydroxylic groups) was swollen in DMA/LiCl solvent system at 130 °C for 2 h. The mixture was cooled to room temperature then a catalytic amount of *N,N*-dimethylaminopyridine, an excess of FA and condensation agents (DCC, HBT) were added under stirring, heating to 100 °C for 4 h and to room temperature overnight. The solid was initially filtered and washed with water, methanol, tetrahydrofurane and acetone to remove the reaction

sub-products as dicyclohexylurea, and unreacted FA. After that, it was dried under vacuum at 50 °C and characterized by FT-IR that confirms the formation of a new ester bond (1698 cm^{-1}).

6. Determination of FA content in ferulate AcrC/DMAA hydrogel

DS value of ferulic portion was determined by the Folin-Ciocalteu (FC) method [16-18], a colorimetric assay that requires few reagents and relies on the use of the free ferulic acid as standard compound.
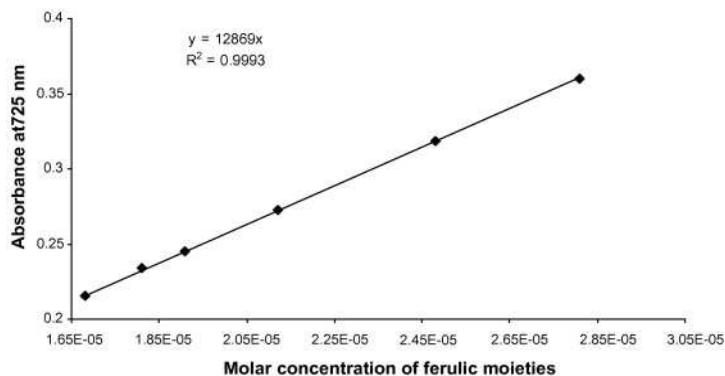

Fig. 1.Calibration curve obtained with six varying concentrations of *trans*-ferulic acid.

Fig. 1 shows the calibration curve used to obtain DS value of the ferulic moieties onto hydrogel. The calibration curve was obtained with *trans*-ferulic acid solutions ranging from 1.68×10^{-5} to 2.81×10^{-5} mol/L, and the results are given as moles of phenolic groups per grams of hydrogel. The results furnished a value of 2.36×10^{-5} mol of ferulic moieties.**7.**

Radicals scavenging activity of ferulate hydrogel

The ability of prepared hydrogel to act as radical scavengers was considered. The radical scavenging ability of ferulate hydrogel was assessed through their reaction with stable DPPH radicals, using the methodology of Wang [19]. DPPH typically extracts a proton to form DPPH during the reaction [20]. Briefly, in an ethanol solution of DPPH radical (final concentration 1.1×10^{-4} M), hydrogels was added, and their concentrations were 5, 10, 20, and 40 mg/ml. The reaction mixtures were soaken vigorously and then kept in the dark for 30 min. Their absorbances were then measured in 1cm cuvettes using a UV–Vis spectrophotometer (V-530 JASCO) at 516 nm against a blank, in which DPPH was absent. All tests were run in triplicate and averaged. Ferulate hydrogel was found to be very efficient scavengers of DPPH radicals as showed in the inhibition curve
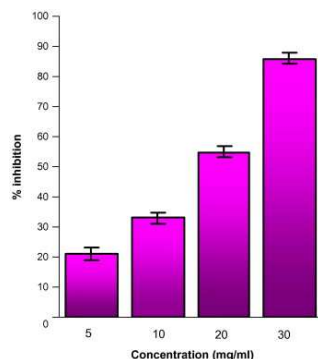
Fig. 2. Scavenging effects of ferulate hydrogel on the DPPH free radical. The results represent means ± SEM of three determinations.

8. Antioxidant properties of hydrogels

Finally, we evaluated the antioxidant activity of cellulose hydrogels in inhibiting the lipid peroxidation in rat-liver microsomal membranes [14], during 120 min of incubation, induced in vitro by two different sources of free radicals including AAPH and *tert*-BOOH. The same experiment was performed on a non-derivatized hydrogel and on a commercial *trans*-ferulic acid (data not shown). The results revealed that the hydrogel without ferulic groups has no antioxidant activity. The effects of cellulose derivatives on the lipid peroxidation were time-dependent and brought as nmol/mg proteins of MDA inhibition (Fig. 3). Ferulate hydrogel was a stronger antioxidant in protecting the membranes from *tert*-BOOH– than from AAPH-induced lipid peroxidation, showing in either case higher efficiency at 30 min of incubation (Fig. 4) and the preservation of antioxidant activity up to 2 h confirming results found previously [13].
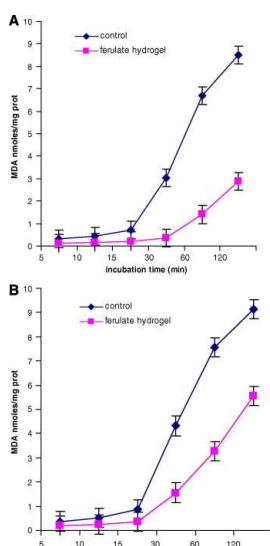

Fig. 3. Effects of ferulate hydrogel on MDA production induced by (A) *tert*-BOOH and (B) AAPH in rat-liver microsomal membranes. The microsomal membranes were incubated with 0.25×10^{-3} M *tert*-BOOH or 25×10^{-3} M AAPH at 37 °C under air in the dark. The results represent means ± SEM of six separate experiments.
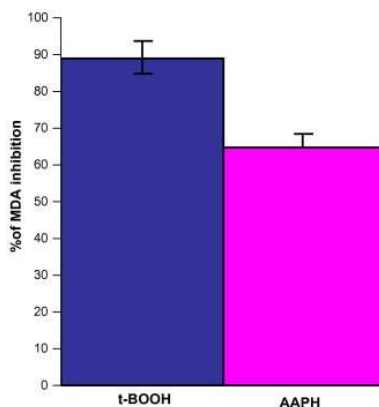
144

Fig. 4. **Percentage of inhibition of *tert*-BOOH– and AAPH-induced MDA formation in the presence of ferulate hydrogel in rat-liver microsomal membranes after 30 min of incubation. The microsomal membranes were incubated with 0.25×10^{-3} M *tert*-BOOH or 25×10^{-3} M AAPH at 37 °C under air in the dark. The results represent means ± SEM of six separate experiments.**

9. Conclusion

Antioxidant cellulose hydrogel was successfully prepared introducing FA moieties onto cellulose backbone. Two in vitro tests, the DPPH test, for direct free radical scavenging action, and the lipid peroxidation assay, for antioxidant activity, were used to assess its antioxidant properties. In fact, together both tests provide a better assessment of antioxidant properties.

The results suggested that ferulate material posses an excellent antioxidant and radical scavenger activity. For this reason, it could be well suited and sound approach to obtain carrier that could preserve drugs that tend to be unstable after prolonged exposure to air and light, during their vesiculation and release. On the other hand, our antioxidant hydrogel could also act as prodrug allowing a delivery of the *trans*-ferulic acid by means specific esterase. The so obtained antioxidant biopolymer could be used in cosmetic and pharmaceutical fields and would substantially reduce free radical damage and oxygen depletion.

References

[1] B.O. Jung, S.J. Chung and S.B. Lee, Preparation and characterization of eugenol-grafted chitosan hydrogels and their antioxidant activities, Journal of Applied Polymer Science 99 (2006), pp. 3500–3506.
[2] W. Wang, X. Liu, Y. Xie, H. Zhang, W. Yu and Y. Xiong et al., Microencapsulation using natural polysaccharides for drug delivery and cell implantation, Journal of Materials Chemistry 16 (2006), pp. 3252–3267.
[3] A. Sannino, M. Madaghiele, M.G. Lionetto, T. Schettino and A. Maffezzoli, A cellulose-based hydrogel as a potential bulking agent for hypocaloric diets: An in vitro biocompatibility study on rat intestine, Journal of Applied Polymer Science 102 (2006), pp. 1524–1530.
[4] D.A. Alderman, A review of cellulose ethers in hydrophilic matrices for oral controlled-release dosage forms, International Journal of Pharmaceutical Technology and Product Manufacture 5 (1984), pp. 1–9.

[5] K.P.R. Chowdary and Y. Srinivasa Rao, Design and in vitro and in vivo evaluation of mucoadhesive microcapsules of glipizide for oral controlled release: A technical note, AAPS PharmSciTech 4 (2003), p. 39.

[6] T. Yamada, H. Onishi and Y. Machida, In vitro and in vivo evaluation of sustained release chitosan-coated ketoprofen microparticles, Yakugaku Zasshi 121 (2001), pp. 239–245.

[7] B. Halliwell and J.M.C. Gutteridge, Role of free radicals and catalytic metal ions in human disease: An overview, Methods in Enzymology 186 (1990), pp. 1–85.

[8] McCall and B. Frei, Can antioxidant vitamins materially reduce oxidative damage in humans, Free Radical Biology & Medicine 26 (1999), pp. 1034–1053.

[9] I. Pinchuk and D. Lichtemberg, The mechanism of action of antioxidants against lipoprotein peroxidation, evaluation based on kinetic experiments, Progress in Lipid Research 41 (2002), pp. 279–319.

[10] U.P. Steinbrecher, Receptors for oxidized low density lipoprotein, Biochimica et Biophysica Acta 1436 (1999), pp. 279–298.

[11] C. Ortiz, B. Vàzquez and J. San Romàn, Synthesis, characterization and properties of polyacrylic systems derived from vitamin E, Polymer 39 (1998), pp. 4107–4114.

[12] M.A. Plasencia, C. Ortiz, B. Vàzquez, J. San Romàn, A. Lòpez-Bravo and A. Lòpez-Alonso, Resorbable polyacrylic hydrogels derived from vitamin E and their application in the healing of tendons, Journal of Materials Science Materials in Medicine 10 (1999), pp. 641–648.

[13] S. Trombino, R. Cassano, E. Bloise, R. Muzzalupo, S. Leta and F. Puoci et al., Design and synthesis of cellulose derivatives with antioxidant activity, Macromolecular Bioscience 8 (2008), pp. 86–95.

[14] S. Trombino, S. Serini, F. Di Nicuolo, L. Celleno, S. Andò and N. Picci et al., Antioxidant effect of ferulic acid in isolated membranes and intact cells: Synergistic interactions with alpha-tocopherol, beta-carotene, and ascorbic acid, Journal of Agricultural and Food Chemistry 52 (2004), pp. 2411–2420.

[15] V. Bojanic, S. Jovanovic, R. Tabakovic and I. Tabakovic, Synthesis and electrochemistry of grafted copolymers of cellulose with 4-vinylpyridine, 1-vinylimidazole, 1-vinyl-2-pyrrolidinone, and 9-vinylcarbazole, Journal of Applied Polymer Science 60 (1996), pp. 1719–1725.

[16] V.L. Singleton, R. Orthofer and R.M. Lamuela-Ravento´s, Analysis of total phenols and other oxidation substrates and antioxidants by means of Folin-Ciocalteu reagent, Methods in Enzymology 299 (1999), pp. 152–178.

[17] J.A. Vinson, Y. Hao, X. Su and L. Zubı´k, Phenol antioxidant quantity and quality in foods: Vegetables, Journal of Agricultural and Food Chemistry 46 (1998), pp. 3630–3634.

[18] H.L. Wildenradt and V.L. Singleton, The production of aldehydes as a result of oxidation of polyphenolic compounds and its relations to wine aging, American Journal of Enology and Viticulture 25 (1974), pp. 119–126.

[19] M. Wang, J. Li, M. Rangarajan, Y. Shao, E.J. La Voie and C.-T.H. Huang, Antioxidative phenolic compounds from sage (Salvia officinalis), Journal of Agricultural and Food Chemistry 46 (1998), pp. 4869–4873.

[20] W. Brand-Williams, M.E. Cuvelier and C. Berset, Use of a free radical method to evaluate antioxidant activity, Lebensmittel-Wissenschaft & Technologie 28 (1995), pp. 25–30.

3.1.5 A novel dextran hydrogel linking *trans*-ferulic acid for the stabilization and transdermal delivery of vitamin E

Roberta Cassano, Sonia Trombino, Rita Muzzalupo, Lorena Tavano and Nevio Picci

Department of Pharmaceutical Sciences, University of Calabria, Cosenza, Italy

Abstract

Long-term exposure of the skin to UV light causes degenerative effects, which can be minimized by using antioxidant formulations. The major challenge in this regard is that a significant amount of antioxidant should reach at the site for effective photoprotection. However, barrier properties of the skin limit their use. In the present study, vitamin E (α-tocopherol) was loaded into a dextran hydrogel containing ferulic moieties, covalently linked, to improve its topical delivery, and also to increase its relative poor stability, which is due to direct exposure to UV light. Methacrylic groups were first introduced onto the dextran polymer backbones, then the obtained methacrylated dextran was copolymerized with aminoethyl methacrylate, and subsequently esterified with *trans*-ferulic acid. The new biopolymer was characterized by Fourier transform infrared spectroscopy. The values of content of phenolic groups were determined. Its ability in inhibiting lipid peroxidation in rat liver microsomal membranes induced in vitro by a source of free radicals, that is *tert*-butyl hydroperoxide, was studied. Hydrogel was also characterized for swelling behaviour, vitamin E loading efficiency, release, and deposition on the rabbit skin. Additionally, vitamin E deposition was compared through hydrogels, respectively, containing and not containing *trans*-ferulic acid. The results showed that ferulate hydrogel was a more effective carrier in protecting vitamin E from photodegradation than hydrogel without antioxidant moieties. Then antioxidant hydrogel could be of potential use for cosmetic and pharmaceutical purposes as carrier of vitamin E that is an antioxidant that reduces erythema, photoaging, photocarcinogenesis, edema, and skin hypersensitivity associated with exposure to ultraviolet B (UVB) radiation, because of its protective effects.

1. Introduction

Dextran hydrogels have received an increased attention due to their variety of biotechnological and biomedical applications. Owing to their low tissue toxicity and high enzymatic degradability at desired sites, dextran hydrogels have been frequently considered as a potential matrix system for controlled release of bioactive agents. Several approaches to prepare dextran hydrogels have been

adopted. Hydrogels were obtained by crosslinking dextran with either 1,6-hexanediisocyanate or glutaraldehyde [1] and [2]; reaction of dextran with glycidyl acrylate followed by polymerization of acrylated dextran [3]; methacrylation of dextran by transesterification of glycidyl methacrylate, and radical polymerization of methacrylated dextran in aqueous solution, using ammonium peroxydisulfate and *N*,*N*,*N*′,*N*′-tetramethylethylenediamine (TMEDA) as initiator system [4,5]; methacrylation and acrylation of dextrans by reaction with methacrylic anhydride, and with bromoacetyl bromide and sodium acrylate, respectively [6,7]. Dextran hydrogels have been studied extensively in various areas, such as drug carriers. Due to their good tissue biocompatibility and the possibility of to transport specific drugs, they appear to be a viable alternative to the existing drug carriers [8-11]. Recently, researchers have realized and studied a variety of different dextran hydrogels as transdermal-delivery systems [12,13]. These hydrogels enhance the drug penetration improving the resulting pharmacological effects useful for the transdermal drug delivery that has always been challenged by the formidable barrier property of the intercellular lipid bilayer in the stratum corneum. For this reason, the idea is to use dextran hydrogel as a carrier of vitamin E, a topically administered antioxidant, that reduces erythema, photoaging, photocarcinogenesis, edema, and skin hypersensitivity associated with exposure to ultraviolet B (UVB) radiation [14,17]. It inhibits lipid peroxidation by preventing free radical generation, and/or reducing malondialdehyde [18]. Recently, the vitamin E is widely used in cosmetic products due to its obvious advantages for the skin [19]. However, its delivery through topical preparations such as creams, gels, lotions, and emulsion limits its effectiveness due to barrier properties of the skin, which hinder the drug deposition, and relative poor stability of vitamin due to direct exposure to UV light. Thus, the aim of this paper was to prepare and investigate a dextran hydrogel as a carrier to increase vitamin E deposition [20] and flux [21] on the skin. Moreover, to increase ulteriorly the stability of the vitamin E to the light, heat etc., we covalently linked *trans*-ferulic acid onto the dextran hydrogel, trapped vitamin E, and explored its topical delivery from the antioxidant carrier. The linking of antioxidant groups on the preformed hydrogel rather than on its precursor was effected to avoid the inhibitory action of *trans*-ferulic acid, a scavenger of radical species, on the radical polymerization process. We submitted both antioxidant hydrogel and non-antioxidant hydrogel to the insult with a radical source such as *tert*-butyl hydroperoxide, and verified the stability of vitamin E after this treatment. Finally, we compared the vitamin E deposition on the skin with that of analogous hydrogel not containing ferulic groups. In agreement with our expectations, the ferulate hydrogel was a more effective carrier in protecting vitamin E from photodegradation than hydrogel without antioxidant moieties.

2. Experimental

2.1. Materials

Dextran (Dex) (Fluka) (M_r = 15,000–25,000), vitamin E (α-Tocopherol (αT)) (Sigma), ferulic acid (FA) (Sigma), Folin-Ciocalteu reagent (FC reagent) (Fluka), and ammonium peroxydisulfate (APS) (Sigma) were used as received without further purification. *N,N*-dimethylformamide (DMF), pyridine (Py) aminoethyl methacrylate (AEMA), and methacryloyl chloride were supplied by Sigma, and were purified by the standard procedures. Lithium chloride (LiCl), dicyclohexylcarbodiimide (DCC), 4-hydroxybenzotriazole (HBT), *N,N*-dimethylaminopyridine (DMAP), potassium chloride (KCl), ethylenediaminetetraacetic acid (EDTA), sucrose, 4-2-hydroxyethyl-1-piperazineethanesulfonic acid (HEPES), trichloroacetic acid (TCA), hydrochloric acid, butylated hydroxytoluene (BHT), *tert*-butyl hydroperoxide (*tert*-BOOH), and 2-thiobarbituric acid (TBA) were supplied by Sigma (Sigma Chemical Co, St. Louis, MO), and were used as received. Methanol, ethanol, dihydrogen sodium phosphate, phosphoric acid, and acetonitrile were obtained from Fluka Chemika-Biochemika (Buchs, Switzerland) and Carlo Erba Reagents (Milan, Italy), and were used as received.

2.2. Measurements

^{1}H NMR and ^{13}C NMR spectra of dextran, dextran-methacrylate, FA, and AEMA were acquired on Bruker VM-300 ACP. Dextran, dextran methacrylate, and hydrogels, containing and not containing ferulic acid, were analyzed by FT-IR spectroscopy (Jasco 4200) using KBr disks. Estimation of vitamin E was carried out using Hewlett Packard GC-MSD 5972, UV–Vis spectrophotometer (V-530 JASCO), and HPLC (Jasco BIP-I pump and Jasco UVDEC-100-V detector). Digital Micrometer Carl Mahr D7300 Essilingen A.N. was used for measurement of the membranes thickness.

2.3. Synthesis of dextran-methacrylate (Dex-MA)

A fixed amount (0.5 g) of dextran (**1**) was added to a LiCl/DMF (4% w/v) solvent mixture inside a reaction flask maintained under a dry nitrogen environment. The temperature of the oil bath was raised from room temperature to 120 °C over a period of 2 h, and the resultant mixture became a homogeneous gold-colored solution. The solution was cooled to room temperature, and pyridine was added as an acid acceptor. After 15 min, a calculated amount of methacryloyl chloride in a DMF solution was added slowly into the flask with constant stirring. The reaction was conducted at room temperature until completion. The reaction mixture was precipitated in an excess amount of cold ethanol. The product was filtered, washed several times with cold ethanol, dried at 40 °C in

a vacuum oven for 2 days [22], and was characterized by FT-IR and ^{13}C NMR spectroscopy. Yield 0.64 g; substitution degree (DS) = 0.28. Varying the reaction conditions (time, temperature, and concentration), hydrogels with higher DS were obtained.

2.4. Preparation of the Dex-MA/AEMA hydrogel

The Dex-MA/AEMA hydrogel was obtained by free-radical polymerization of dextran-methacrylate (**2**) (0.500 g) and AEMA (0.209 g) using APS as an initiation system in an aqueous solution of NH_3/urea 2/12% w/w (2.5 g), a good solvent for poly-glucosidic systems, at 60 °C [23-25]. Briefly, dextran-methacrylate and AEMA were dissolved in an aqueous solution of NH_3/urea to obtain a final homogenous solution. Then, APS as an initiator was added to this solution, and mixed well for few minutes until a tacky hydrogel was obtained. The hydrogel was first washed with deionized water, and after with acetone to remove the unreacted dextran-methacrylate, AEMA, and solvents. Finally, the hydrogel was dried under vacuum at 50 °C for several days, and characterized by FT-IR spectroscopy. Yield 0.67 g.

2.5. Preparation of dextran hydrogels containing trans-ferulic acid

The dry hydrogel (0.5 g) was swollen in DMF/LiCl solvent system at 130 °C for 2 h. The mixture was cooled to room temperature, then a catalytic amount of *N*,*N*-dimethylaminopyridine, an excess of FA, and condensation agents (DCC, HBT) were added under stirring, heated to 100 °C for 4 h, and then to room temperature overnight. The solid was filtered and washed with hot methanol, then with tetrahydrofurane, and acetone to remove the reaction sub-products as dicyclohexylurea and unreacted FA. The removal of all impurities was confirmed by HPLC and GC/MS analysis of the washing solvents. The antioxidant hydrogel was dried under vacuum at 50 °C, and characterized by FT-IR spectroscopy. Yield: 1.32 g. Amount of ferulic groups: 2.28×10^{-5} moles/g polymer.

2.6. Vitamin E loading by soaking procedure

Dex-MA/AEMA (0.1 g) hydrogels, containing and not containing ferulic moieties, were soaked, for 3 days at room temperature, and under magnetic stirring, in a drug solution. Vitamin E was solubilized in ethanol/water (4/1). The amount of drug solubilized was chosen in order to have a drug loading of 20% (w/w). After filtration, the hydrogels were dried at 10.1 mmHg until a constant weight was reached.

2.7. In vitro skin permeation

Permeation study ($n = 3$) was performed on the excised skin of sacrificed rabbit (New Zealand rabbits of 2.9–3.1 kg), which was obtained from a local slaughter's house, using Franz Diffusion cells. Ear skin of rabbit was shaved, and the skin was carefully separated. Subcutaneous fat was cautiously removed using a bistoury, and the skin samples were washed with saline solution (NaCl 0.9%), and frozen at −20 °C. The skin thus obtained was allowed to equilibrate with dissolution medium (ethanol/distilled water 20/80 solution) for 12 h before using it for permeation studies, and was mounted on Franz Diffusion cells having a surface area of 0.4614 cm^2, and on receptor compartment having a capacity of 5.5 ml. Epidermal side of the skin was exposed to ambient condition while dermal side was kept facing the receptor solution. The receptor compartment was filled with double distilled water containing ethanol (ethanol/double distilled water 20/80 solution) as diffusion medium (37 ± 0.5 °C). Reservoir solution was stirred, and the diffusion cells were protected from light. Skin was saturated with dissolution medium for 1 h before the application of sample.

2.8. Swelling studies

Hydrogel without vitamin E was placed on the stratum corneum side of the skin. The donor compartment of the cell was covered with laboratory film (Parafilm®) to prevent dehydration of the gel. At predetermined times, the swelling degree (W_t) was obtained by withdrawing the hydrogel, lightly drying it with filter paper, and by weighing it quickly in a tared sample bottle by means of an electronic balance ($\pm 10^{-4}$ g), then the hydrogel was placed back in the receiver. W_t was calculated by using Eq. (1) [26,27], where Ws and Wd are the weights of the swollen, and initial dry hydrogels, respectively. The extent of equilibrium swelling of the hydrogel was reached when the weight of the swollen hydrogel was constant. The fluid volume of the receiver department was maintained constant by the addition of double distilled water/ethanol 80/20. Each experiment was carried out in triplicate ($n = 3$).

$$Wt(\%) = (\frac{W_s \quad W_d}{W_d}) \times 100$$

2.9. Permeability of vitamin E

Vitamin E (0.045 g, 1.04×10^{-4} mol) that was adequately dissolved in double distilled water/ethanol 80/20 solution was applied on the donor compartment, and was covered with laboratory film (Parafilm®). At specific intervals of time (0.5, 1.5, 2.5, 3.5, 4.5, 5.5, 6.5, and 24 h),

100 μl of receiver solution was withdrawn from the receiver compartment, and replaced with fresh distilled water/ethanol 80/20 solution in order to maintain the chemical gradient of the vitamin E between the two compartments, and to favour the spread (samples were kept in a freezer (−20 °C) until analyzed by UV–Vis spectrophotometer). Vitamin E amount released on the skin was assayed by UV–Vis spectrophotometry. Permeability measurements were performed in triplicate ($n = 3$).

2.10. Skin permeation of vitamin E from hydrogels

Vitamin E-loaded hydrogels, containing and not containing ferulic acid, were placed on the stratum corneum side of the skin, and the donor compartment was covered with laboratory film (Parafilm®). The surface area of hydrogel was the active diffusion area. At specific intervals (1, 2, 3, 4, 6, and 24 h), 100 μl of receiver solution was withdrawn from the receiver compartment, and replaced with fresh double distilled water/ethanol (80/20). After 24 h, the hydrogels were recovered, and the still present vitamin E that was still present extracted in ethanol under sonication, and its amount was estimated by UV–Vis spectrophotometer. The drug concentration in the receiver solution samples was assayed by UV–Vis spectrophotometry. The concentration of vitamin E in the receiver medium was always less than 15% of the maximum solubility of vitamin E in the solvent system (22 mg/ml in 20/80 ethanol/water), thus sink conditions were maintained. All experiments were performed in triplicate ($n = 3$).

2.11. Prooxidant test

Antioxidant and non-antioxidant vitamin E-loaded hydrogels (0.1 g) were soaked for 2 h at room temperature, and under magnetic stirring, in 5 ml of water containing 500 μl of *tert*-BOOH (0.25×10^{-3} M). After filtration, the excess of solvent was removed by evaporation under reduced pressure, and the hydrogels were dried at 10.1 mmHg until a constant weight was reached. After freezing and lyophilization, the effect of prooxidant was evaluated. Precisely, insulted vitamin E-loaded hydrogels, linking and not linking ferulic moieties, were divided into three equal portions and were placed in three round-bottomed flask, containing a solution of water/ethanol 80/20, under stirring for 30, 60, and 120 min, respectively. After the selected times, the solvent contained in the different flasks was recovered by filtration, and analyzed through mass spectrometry and HPLC that was effected using as stationary phase a C18 3 μ SUPELCOSIL™ column (150 mm × 4.6 mm), and as eluent 0.01 M dihydrogen sodium phosphate/0.01 M phosphoric acid with acetonitrile (88:12 v/v), pH 2.3. The flow rate was set at 0.5 ml/min, and the detector wavelength was 292 nm.

The vitamin E standards of 1–1000 μg/ml were run for the external standardisation, and linear curves, with a correlation coefficient of 0.999, were generated from the area under the peak measurements. The vitamin E retention time was 11.13 ± 0.2 min.

2.12. Determination of FA contents in ferulate Dex-MA/AEMA hydrogel

Folin-Ciocalteu (FC) method, based on the reduction of a phosphowolframate-phosphomolybdate complex by phenolics to blue reaction products, was used to determine phenolic compounds [28], [29] and [30]. The sample was allowed to react with Folin-Ciocalteu's reagent and sodium carbonate solution at room temperature for 48 h in the dark. Absorption at 725 nm was measured, and the total phenolic content calculated as ferulic acid equivalents. An absorbance was measured twice for our sample against blank using 2×10^{-2} mmol/L ferulic acid as the standard ($R^2 = 0.9916$)

2.13. MA contents in Dex-MA by volumetric analysis

A sample of 50 mg ester derivative was dispersed in 5 ml of 0.25 M ethanolic sodium hydroxide solution under reflux for 17 h. The dosing in return of the excess of soda was realized by titration with 0.1 N HCl (first equivalent point). The moles of chloride acid used between the first and second equivalence correspond to the moles of free esters. The degree of substitution (DS) was determined by Eq. (2) [31], where $n_{\text{free ester}}$ is $(V_{2° \text{ e.p.}} - V_{1° \text{ e.p.}})$ * [HCl]; $MM_{\text{glucose unit}}$ is the molecular mass of glucose unit; g_{sample} is the weight of sample; $n_{\text{free ester}}$ is the mol of free ester; $MM_{\text{free ester}}$ is the molecular mass of free ester, and MM_{H2O} is the molecular mass of water.

$$DS = \frac{MM_{glu\cos e\ unit}}{(g_{sample} / n_{free\ ester}) - (MM_{free\ ester} - MM_{H_2O})} \qquad (2)$$

2.14. Microsomal suspensions preparation

Liver microsomes were prepared from Wistar rats by tissue homogenization with 5 volumes of ice-cold 0.25 M sucrose containing 5 mM Hepes, 0.5 mM EDTA, pH 7.5 in a Potter–Elvehjem homogenizer [32]. Microsomal membranes were isolated by the removal of the nuclear fraction at 8000g for 10 min, and by the removal of the mitochondrial fraction at 18,000g for 10 min. The microsomal fraction was sedimented at 105,000g for 60 min, and the fraction was washed once in 0.15 M KCl, and was collected again at 105,000g for 30 min [33]. The membranes, suspended in 0.1 M potassium phosphate buffer, pH 7.5, were stored at $-80\,°C$. Microsomal proteins were determined by the Bio-Rad method [34].

153

2.15. Addition of Dex-MA/AEMA hydrogel to microsomes

Aliquots of hydrogel containing and not containing FA in the range of 0.5–6 mg/ml were added to the microsomes. The microsomes were gently suspended by a Dounce homogenizer, and then the suspensions were incubated at 37 °C in a shaking bath under air in the dark.

2.16. Malondialdehyde formation

Malondialdehyde (MDA) was extracted and analyzed as indicated [35]. Briefly, aliquots of 1 mL of microsomal suspension (0.5 mg proteins) were mixed with 3 mL of 0.5% TCA and 0.5 mL of TBA solution (two parts 0.4% TBA in 0.2 M HCl and one part distilled water), and 0.07 mL of 0.2% BHT in 95% ethanol. Samples were then incubated in a 90 °C bath for 45 min. After incubation, the TBA-MDA complex was extracted with 3 mL of isobutyl alcohol. The absorbances of the extracts were measured by the use of UV spectrophotometry at 535 nm, and the results were expressed as mmol per mg of protein, using an extinction coefficient of $1.56 \times 10^5 \, \mathrm{l \, mmol^{-1} \, cm^{-1}}$.

3. Results and discussion

3.1. Synthesis of dextran-methacrylate

With the aim of taking advantage of the antioxidant properties of the FA, a hydrogel containing this residue has been synthesized. The synthesis of hydrogel precursor was carried out with dextran and methacryloyl chloride in the presence of pyridine as catalyst (Fig. 1). The methacrylated dextran was isolated, purified, and characterized by FT-IR spectroscopy. Depending on the reaction conditions (time, temperature, and concentration), methacrylic derivatives with different DS were obtained (from 0.28 to 0.82) and evaluated by volumetric analysis, and the derivative with lower DS was used. In fact, the literature data show that the highly substituted hydrogels reach equilibrium swelling faster than the other hydrogels. Swelling ratios depend very much upon the DS of the dextran-methacrylate. As the DS of the dextran-methacrylate hydrogels increases, their swelling ratios decreased in all pH ranges [36].
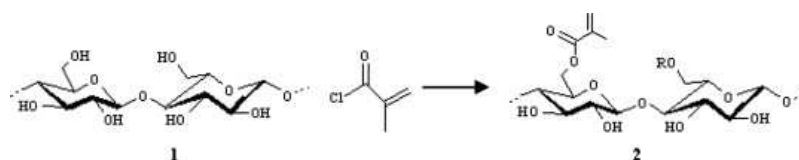

Fig. 1. Representative route to Dex-MA.

154

3.2. Preparation of ferulate hydrogel

NH$_3$/urea aqueous solution of dextran-methacrylate (Dex-MA) with DS of 0.28 has been crosslinked in the presence of aminoethyl methacrylate (AEMA) by free-radical polymerization using APS, to initiate the formation of radicals, as reported in Fig. 2. To make the obtained hydrogel antioxidant, characterized by FT-IR, FA was bonded. The synthesis was carried out from *trans*-ferulic acid and hydrogel, by condensation in the presence of *N,N*-dimethylaminopyridine as catalyst using DCC and HBT as condensing agents (Fig. 3). After purification, antioxidant hydrogel was characterized by FT-IR spectroscopy. A detailed study of its content of ferulic moieties was performed by the FC test, a colorimetric assay that requires few reagents and relies on the use of the free ferulic acid as the standard compound. Our results showed a value of $\sim$0.4% that corresponds to 2.36×10^{-5} mol of ferulic groups.
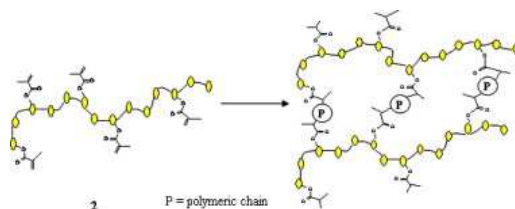

Fig. 2. Schematic representation of the polymerization of Dex-MA with AEMA.
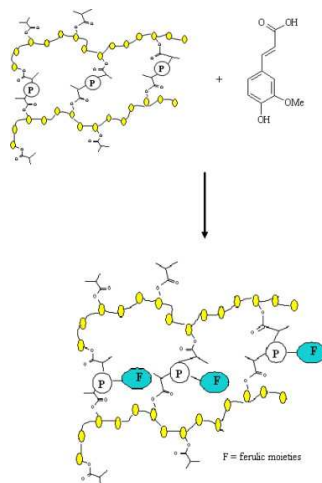

Fig. 3. Synthesis of ferulate hydrogel.

3.3. Characterization

The Dex, Dex-MA, Dex-MA/AEMA hydrogel, and hydrogel containing FA were analyzed by FT-IR spectroscopy. All samples were tested as compressed KBr pellets (polymer: KBr 51: 10 w/w). Dex-MA with DS of 0.28 showed an ester FT-IR band at 1735 cm^{-1}. Clearly, this ester band increased sharply with an increase in the degree of substitution of the methacrylate group to dextran. The presence of pendant vinyl groups in dextran-methacrylate was confirmed by the FT-

IR bands at 1636 cm^{-1} (C=C) and 803 cm^{-1} (C=C–H). The presence of pendant vinyl groups in dextran-methacrylate, was confirmed further by the ^{1}H NMR spectrum. There were two distinctive peaks in the double bond region (5.690 and 6.115 ppm) which correspond with the two hydrogens adjacent to double bond (C=CH$_2$). These two peaks were not present in the spectrum of the original dextran. The hydrogens of the methyl substitute (CH$_3$) in the methacrylate group also were observed as a single peak, at 1.903 ppm.

The polymerization of Dex-MA with AEMA was confirmed by FT-IR spectra that showed the consumption of double bonds as a result of crosslinking. Precisely, a decrease in peak intensity in the double bond region at 1636 and 803 cm^{-1} and the appearance of a new ester band at 1722 cm^{-1} due to a formation of hydrogel between Dex-MA and AEMA was observed.

The functionalization of amino groups of the hydrogel with FA gave a material that when analyzed by infrared spectroscopy showed an additional characteristic peak of carboxylic group of amide at 1650 cm^{-1}.

3.4. Swelling behaviour

Swelling behaviour of Dex-MA/AEMA hydrogel, through the ear skin of rabbits, was measured at a constant temperature of 37 °C. In this kind of experiment, Franz diffusion cells are mainly used, and the skin was mounted on the receptor compartment with the stratum corneum side facing upwards into the donor compartment containing water/ethanol solution 80/20.
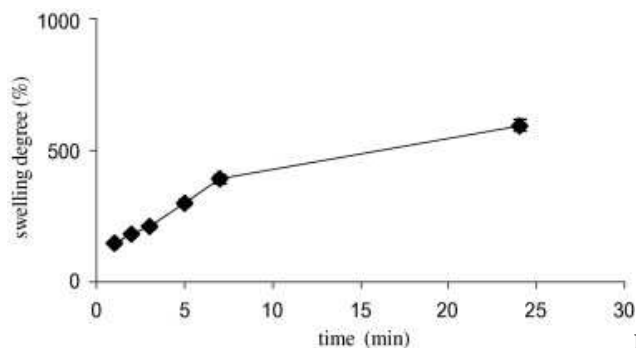

Fig. 4. Swelling degree of Dex-MA/AEMA hydrogel.

Fig. 4 shows the sorption of solution with the time of treatment. The curve plot clearly indicated that the swelling degree of the hydrogel slowly increased until 24 h.

3.5. Antioxidant properties of Hydrogels

The ability of ferulate hydrogel to protect against lipid peroxidation induced by the *tert*-BOOH, a source of free radicals, was examined in rat-liver microsomal membranes during an incubation

period of 120 min [37]. In order to evaluate the antioxidant properties of the non-derivatized polymeric structure, the same experiment was performed on hydrogel without ferulic moieties. The data revealed that this last material has no antioxidant activity. The effects of antioxidant hydrogel on the lipid peroxidation were time-dependent and effected as the MDA production (in nmol mg^{-1} protein) (Fig. 5). Our ferulate material was a strong antioxidant in protecting the membranes from tert-BOOH-induced lipid peroxidation showing a higher efficiency at 30 min of incubation, and the preservation of antioxidant activity up to 2 h.
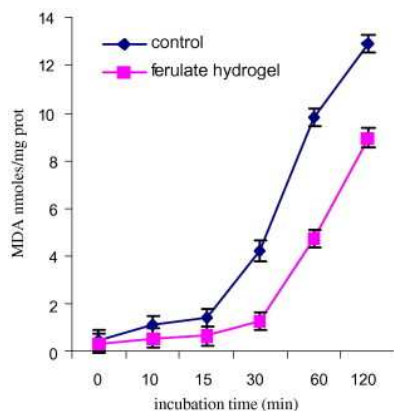

Fig. 5. Effects of ferulate hydrogel on malondialdehyde (MDA) production induced by tert-BOOH in rat liver microsomal membranes. The microsomal membranes were incubated with 0.25×10^{-3} M tert-BOOH at 37 °C under air in the dark. The results represent the mean ± SEM of six separate experiments.

3.6. Prooxidant test remarks

We exposed hydrogels bearing vitamin E and bonding and not bonding ferulic acids to *tert*-BOOH a free radical generator. The antioxidant activity of both ferulate and not hydrogels vitamin E-loaded was evaluated after their prooxidation with *tert*-BOOH and vitamin E release in water/ethanol 80/20. The results suggested that after the drug release (120 min), non-ferulate hydrogel possesses 2% antioxidant activity, perhaps due to the presence of small vitamin E traces. On the contrary, the ferulate hydrogel showed a higher antioxidant activity analogous to non-ferulate hydrogel but a minor activity than non-loaded antioxidant hydrogel (Fig. 6) confirming that the ferulic moieties protected the vitamin E during the prooxidation, and its release, as unequivocally confirmed by GC/MS analysis. In fact, as confirmed in the mass spectrum (not shown), vitamin E (retention time ~29.9) was almost integrally released already after 30 min from the hydrogel containing ferulic moieties. Analogous behaviour was observed at 60 and 120 min. On the contrary, the hydrogel without antioxidant groups released, in the same conditions, only a small amount of vitamin E and a great deal of unidentified products (Fig. 7b). The same results (not shown) were observed through HPLC.
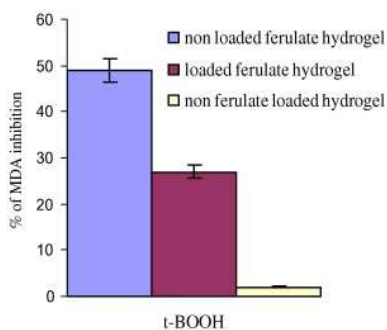
157

Fig. 6. Antioxidant activities of hydrogels after prooxidant test.

3.7. Drug release

Permeation of vitamin E from vitamin E-loaded hydrogels through the rabbit ear skin was studied for hydrogels containing and not containing ferulic loaded with 22 mg of the drug. In both cases, the vitamin E flux value is lower when the drug is included in the hydrogels than when it is dissolved in a ethanol/water (20/80) solution, since the drug must be first released from the gel and then permeate the skin. Particularly, the results indicated that when vitamin E was released from drug-loaded hydrogel without ferulic groups, only a small amount of vitamin E remained intact. In fact, UV–Vis analysis revealed that the most part of products in the receiver compartment was unidentified. On the other hand, permeation studies of antioxidant hydrogel showed that almost the total amount of vitamin E that permeated unchanged into and through the rabbit ear skin was of 65%, and it took place in 24 h. In particular, we observed that the vitamin E was released in decreasing way until 3 h. After that, the release increased with time. This behaviour was probably due to the initial release of the vitamin E-loaded hydrogel in proximity of the hydrogel surface, followed by the release of that one loaded in depth. The release of the inner-loaded portion of vitamin E is determined by the swelling rate of the hydrogel.

The amount of vitamin E from antioxidant hydrogel permeated per diffusion area as a function of time was determined by UV–Vis spectrophotometer is shown in Fig. 8.

This result has demonstrated that ferulic groups on the polymeric matrix prevent the effects of oxidative degradation preserving the drug.
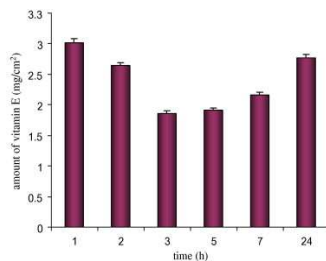
158

Fig. 8. Release of entrapped vitamin E from ferulate hydrogel through a rabbit ear skin.

4. Conclusions

Antioxidant dextran hydrogel was successfully prepared introducing FA moieties onto Dex-MA crosslinked with AEMA. Its antioxidant activity was evaluated through rat liver microsomal membranes. The results suggested that ferulate material possesses an excellent antioxidant activity. Moreover, preparation of ferulate hydrogel-based dextran was found to be well suited and a sound approach to obtain carrier that preserves vitamin E during its release. Linking FA in the hydrogel greatly influenced the drug deposition on the ear skin of rabbit. In fact, we observed increased drug deposition suggesting that the ferulic groups protect the drug during the deposition with respect to the analogous hydrogel without antioxidant moieties. Therefore, it can be said that our antioxidant hydrogel could be an adequate system for the controlled release of vitamin E in the human skin. Regarding that it is acknowledged that a photodamaged and/or age-damaged skin is characterized not only by the presence of radical oxygen species, but also by a lower quantity of lipids. For this reason, it could be advisable to use preparations that contribute to reestablishing the lipidic equilibrium of the stratum corneum as well as having some kind of molecules, such as vitamin E, with an antioxidant effect.

References

[1] L. Hovgaard and H. Brondsted, Dextran hydrogels for colon-specific drug delivery, J. Control Rel. 36 (1995), pp. 159–166.
[2] H. Brondsted, C. Anderson and L. Hovgaard, Crosslinked dextran – a new capsule material for colon targeting of drugs, J. Control Rel. 53 (1998), pp. 7–13.
[3] P. Edman, B. Ekman and I. Sjoholm, Immobilization of proteins in microspheres of biodegradable polyacyldextran, J. Pharm. Sci. 69 (1980), pp. 838–842.
[4] W.N.E. van Dijk-Wolthuis, O. Franssen, H. Talsma, M.J. van Steenbergen, J.J. Kettenes-van Den Bosch and W.E. Hennink, Synthesis, characterization and polymerization of glycidyl methacrylate derivatized dextran, Macromolecules 28 (1995), pp. 6317–6322.
[5] W.N.E. van Dijk-Wolthuis, J.J. Kettenes-van Den Bosch, A. van Der Kerk-van Hoof and W.E. Hennink, Reaction of dextran with glycidyl methacrylate: an unexpected transesterification, Macromolecules 30 (1997), pp. 3411–3413.
[6] S.H. Kim and C.C. Chu, Synthesis and characterization of dextran methacrylate hydrogels and structural study by SEM, J. Biomed. Mater. Res. 49 (2000), pp. 517–527.

[7] S.H. Kim, C.Y. Won and C.C. Chu, Synthesis and characterization of dextran-based hydrogels prepared by photocrosslinking, Carbohydr. Polym. 40 (1999), pp. 183–190.

[8] K.R. Kamath and K. Park, Biodegradable hydrogels in drug delivery, Adv. Drug Del. Rev. 11 (1993), pp. 59–84.

[9] P.J. Tarcha, Polymers for Controlled Drug Delivery, United States CRC: Boca Raton, FL. 1991.

[10] W.E. Hennink, H. Talsma, J.C.H. Borchert, S.C. De Smedt and J. Demeester, Controlled release of proteins from dextran hydrogels, J. Control. Rel. 39 (1996), pp. 47–55.

[11] W.N.E. van Dijk-Wolthuis, J.A.M. Hoogeboom, M.J. van Steenbergen, S.K.Y. Tsang and W.E. Hennink, Degradation and release behavior of dextran-based hydrogels, Macromolecules 30 (1997), pp. 4639–4645.

[12] E. Eljarrat-Binstock, F. Raiskup, J. Frucht-Pery and A.J. Domb, Hydrogel probe for iontophoresis drug delivery to the eye, J. Biomat. Sci.-Polym. Ed. 15 (2004), pp. 397–413.

[13] K. Moriyama, T. Ooya and N. Yui, Pulsatile peptide release from multi-layered hydrogel formulations consisting of poly(ethylene glycol)-grafted and ungrafted dextrans, J. Biomat. Sci.-Polym. Ed. 10 (1999), pp. 1251–1264.

[14] J.R. Trevithick, H. Xiong, S. Lee, D.T. Shum, S.E. Sanford, S.J. Karlik, C. Norley and G.R. Dilworth, Topical tocopherol acetate reduces post-UVB, sunburn-associated erythema, edema and skin sensitivity in hairless mice, Arch. Biochem. Biophys. 296 (1992), pp. 575–582.

[15] J.R. Trevithick, D.T. Shum, S. Redae, K.P. Mitton, C. Norley, S.J. Karlik, A.C. Croom and E.E. Schmidt, Reduction of sunburn damage to skin by topical application of vitamin E acetate following exposure to ultraviolet B radiation: effect of delaying application or of reducing concentration of vitamin E acetate applied, Scanning Microscopy 7 (1993), pp. 1269–1281.

[16] B. Idson, Vitamins and the skin, Cosm. Toilet. 108 (1993), pp. 79–94.

[17] M.P. Lupo, Antioxidants and vitamins in cosmetics, Clin. Dermatol. 19 (2001), pp. 157–161.

[18] M.G. Traber and J. Atkinson, Vitamin E, antioxidant and nothing more, Free Rad. Biol. Med. 43 (2007), pp. 4–15.

[19] Y. Yamamoto, Role of active oxygen species and antioxidants in photoaging, J. Dermatol. Sci. 27 (2001), pp. 1–4.

[20] D.D. Verma, S. Verma, S.G. Blume and A. Fahr, Particle size of liposomes influences dermal delivery of substances into skin, Int. J. Pharm. 258 (2003), pp. 141–151.

[21] F. Jia-You, L. Yann-Lii, C. Chia-Chun, L. Chia-Hsuan and T. Yi-Hung, Lipid nano/submicron emulsion as vehicle for topical flurbiprofen delivery, Drug Deliv. 11 (2004), pp. 97–105.

[22] Y. Zhang, C.-Y. Won and C.-C. Chu, Synthesis and characterization of biodegradable network hydrogels having both hydrophobic and hydrophilic components with controlled swelling behaviour, J. Polym. Sci. A: Polym. Chem. 37 (1999), pp. 4554–4569.

[23] J. Zhou and L. Zhang, Solubility of cellulose in NaOH/urea aqueous solution, Polym. J. 32 (2000), pp. 866–870.

[24] L. Zhang, J. Zhou, Patent CN 00114486.3 (2003).

[25] L. Zhang, J. Cai, J. Zhou, CN 03128386.1 (2005).

[26] T. Peng, K.D. Yao, C. Yuan and M.F.A. Goosen, Structural changes of pH-sensitive chitosan/polyether hydrogels in different pH solutions, J. Polym. Sci. A: Polym. Chem. 32 (1994), pp. 591–596.

[27] P.E.M. Allen, D.J. Bennet and D.R. Williams, Sorption and desorption properties of poly(2-hydroxyethyl methacrylateco-glycol dimethacrylate) networks, Eur. Polym. J. 28 (1992), pp. 347–352.

[28] J.A. Vinson, Y. Hao, Y.X. Su and L. Zubík, Phenol antioxidant quantity and quality in foods: vegetables, J. Agric. Food Chem. 46 (1998), pp. 3630–3634.

[29] H.L. Wildenradt and V.L. Singleton, The production of aldehydesas a result of oxidation of polyphenolic compounds and its relation to wine aging, Am. J. Enol. Vitic. 25 (1974), pp. 119–124.

[30] V.L. Singleton, R. Orthofer and R.M. Lamuela-Ravento´s, Analysis of total phenols and other oxidation substrates and antioxidants by means of Folin-Ciocalteu reagent, Methods Enzymol. 299 (1999), pp. 152–178.

[31] D. Klemm, B. Philipp, T. Heinze, U. Heinze, W. Wagenknecht, Comprehensive Cellulose Chemistry, Wiley-VCH Verlag GmbH, D-69469 Weinheim, 1998, vol. 1, pp. 139–140 and 227–251.

[32] V.L. Tatum, C. Changoit and C.K. Chow, Measurement of malondialdehyde by high performance liquid chromatography with fluorescence detection, Lipids 25 (1990), pp. 226–229.

[33] S. Trombino, S. Serini, F. Di Nicuolo, L. Celleno, S. Andò, N. Picci, G. Calviello and P. Palozza, Antioxidant effect of ferulic acid in isolated membranes and intact cells: synergistic interaction with alpha-tocopherol, beta-carotene, and ascorbic acid, J. Agric. Food Chem. 52 (2004), pp. 2411–2420.

[34] M.M. Bradford, A rapid and sensitive method for the quantitation of microgram quantities of protein utilizing the principle of protein-dye binding, Anal. Biochem. 72 (1976), pp. 248–254.

[35] A.E. Hagerman, K.M.J. Riedl, G. Alexader, K.N. Sovik, N.T. Ritchard, T.W. Hartzfeld and T.L. Riechel, High molecular weigh plant polyfenolics (tannins) as biological antioxidant, J. Agric. Food Chem. 46 (1998), pp. 1887–1892.

[36] K. Sin-Hee and C. Chin-Chang, Synthesis and characterization of dextran-methacrylate hydrogels and structural study by SEM, J. Biomed. Mater. Res. 49 (1999), pp. 517–527.

[37] S. Trombino, R. Cassano, E. Bloise, R. Muzzalupo, S. Leta, F. Puoci and N. Picci, Design and synthesis of cellulose derivatives with antioxidant activity, Macromol. Biosci. 8 (2008), pp. 86–95.

3.1.6 Synthesis and antibacterial activity evaluation of a novel cotton fiber (*Gossypium barbadense*) ampicillin derivative

Roberta Cassano, Sonia Trombino, Teresa Ferrarelli,

Rita Muzzalupo, Lorena Tavano and Nevio Picci

Department of Pharmaceutical Sciences, University of Calabria, Arcavacata di Rende, 87036 Cosenza, Italy

We prepared cellulose cotton fibers containing ampicillin moieties and evaluated their antibacterial activity. In spite of recent progress in experimental and clinical medicine, the problem of chronic wounds treatment remains to be solved. In fact conventional methods are based on solutions of antibiotics and antiseptics and ointment bandages but the efficacy of this method is low and so the idea to use modified cotton gauzes would have to prevent infections insorgence during wounds healing. Ampicillin, a large spectrum antibiotic, was covalently coupled to cellulose backbone of hydrophilic cotton fibers by a heterogeneous synthesis to produce a functionalized biopolymer with a satisfactory degree of substitution (DS) and antibacterial activity. The obtained biopolymer was characterized by infrared spectroscopy (FT-IR). Finally, the antibacterial activity in inhibiting microorganism growth in Petri dishes, was evaluated. The results suggested that these biomaterials posses an excellent "in vitro" antibacterial activity and so they can be efficiently employed in biomedical fields for chronic wounds management to ensure a valid protection against infections and contaminations. Biopolymers so functionalized were found to be very efficient to contrast sensible bacteria growth.

1. Introduction

Wound dressing before the 1960s were considered to be only the so-called passive products having a minimal role in the healing process. The pioneering researches in the last decade introduced the concept of an active involvement of a wound dressing in establishing and maintaining an optimal environment for wound repair [1]. The new advances in wound healing resulted in the development of dressing from traditional passive materials to functional active dressing which, through the interaction with the wounds they cover, create and maintain a moist and healing environment [2]. An ideal wound dressing should protect the wound from bacterial infection, provide a moist and healing environment, and be biocompatible [3]. Recently blends made by natural polymers such as starch, cellulose, chitin, chitosan, cotton, gelatin, alginate and dextran have been reported for the development of wounds dressings [4-8]. New fibrous and wound dressing media have been

developed to encourage wound occlusion, exudate transport and drug dispensation on demand with much reduced distress to the patient [9]. However, natural fibers are presently under investigation as materials for the controlled release of bioactive molecules to contrast the progression of infection in chronic wounds management. On the other hand, literature reports on biomaterials in which the antibacterial molecules were simply absorbed on the polymer surface by the adsorption methodology [10]and not covalently grafted. In this way only medicated soaked gauzes have been prepared [11,12].

Cellulose is the most important constituent of natural fibers and it can be functionalized with bioactive molecules using its primary hydroxylic groups; natural fibers are biocompatible, biodegradable and non-toxic so they can be used to cover infected wounds. In the present work, ampicillin moieties have been covalently linked to cotton fibers to produce a functionalized biomaterial that is able to protect wounds from infections thanks to the presence of the active molecules. This study showed that the designed systems preserve the antibiotic activity of ampicillin moieties also compared with the non-functionalized cotton dishes. The synthesis of this biomaterial has been conducted under mild conditions using thionyl chloride in dry THF. The evaluation of antibacterial activity has been demonstrated by "in vitro" tests using Petri dishes of the type "Mueller–Hinton Agar". Furthermore Infrared Spectroscopy showed the presence of the covalent bond with ampicillin and the degree of substitution was determined by saponification and then volumetric analysis.

2. Cellulose functionalization

Functionalized biopolymer was obtained by heterogeneous synthesis [13] (Scheme 1) of ampicillin acylic chloride with primary hydroxylic groups of glucose units to form an ester bond. Briefly, ampicillin (0.00827 mmol, 2.89 g) was dissolved in dry THF and then was added thionyl chloride (0.009 mmol, 0.6 mL) in little excess and the reaction mixture was allowed to react for two hours at 50–60 °C with magnetic stirring and under N_2 reflux. After that, a sample of cellulosic cotton fiber (0.14 g) was added and the reaction was conducted for three hours in the same conditions. After five hours, reaction was left overnight at room temperature under magnetic stirring. The so obtained product was, finally, washed with a sodium bicarbonate saturated aqueous solution until neutrality and with acetonitrile. Finally functionalized cotton was dried under vacuum [14]. Cotton fiber ampicillin derivative yield = 0.2361 g.
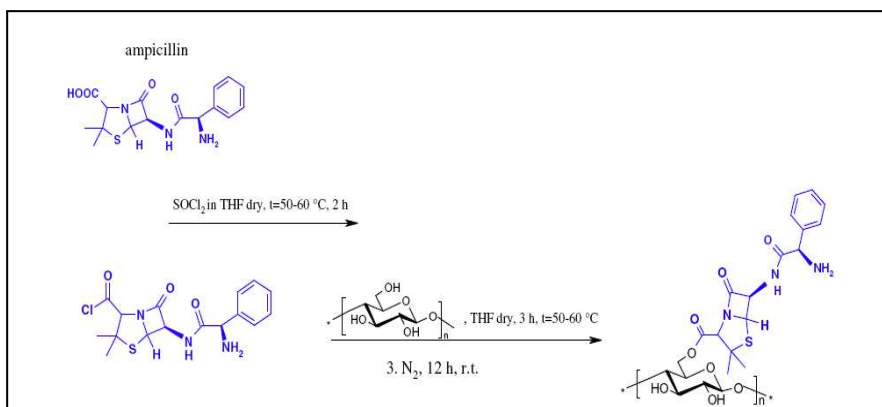
Scheme 1. Synthetic route to the cotton fiber ampicillin derivative.

3. Characterization

FT-IR spectra, realized by Jasco 4200 using KBr disks, made by compressing the powder obtained by grinding the fibers with KBr, confirmed ampicillin linkage to the fibers. In fact, we observed a detectable modification of hydrophilic cotton spectrum especially in the wavenumber range between 1600 and 2000 cm^{-1} (Fig. 1a and c). There is a new band at 1740 cm^{-1} which confirms ester linkage formation (Fig. 1c). Anyway experimental evidences suggested that functionalized cotton fibers, after alkaline hydrolysis, give back hydrophilic cotton and ampicillin sodium salt as showed in Figs. 1a, b, 2a and b. In particular, Fig. 2a displays some strong bands, around 1650, 1500 and 850 cm^{-1}, with an higher intensity than analogous bands in ampicillin sodium salt spectrum, attributable to NaOH, used for previous alkaline hydrolysis.
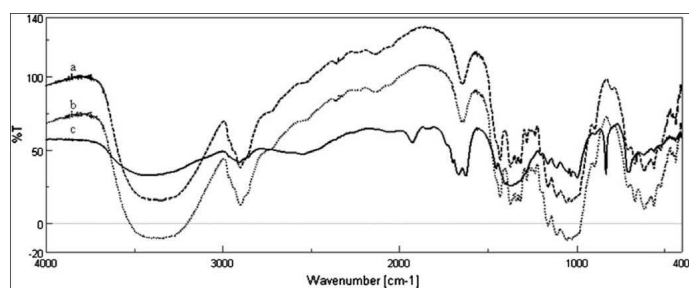

Fig. 1. IR analysis of (a) hydrophilic cotton, (b) cotton after alkaline hydrolysis, (c) ampicillin derivatized cotton.
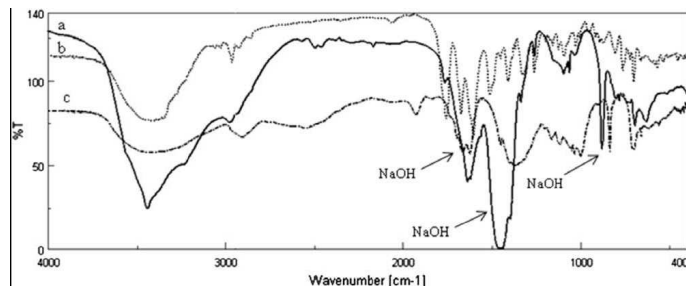
Fig. 2. IR analysis of (a) ampicillin sodium salt, (b) ampicillin sodium salt after alkaline hydrolysis, (c) ampicillin derivatized cotton.

4. Determination of the degree of substitution of functionalized cotton fibers

The substitution degree was determined by volumetric analysis dispersing a sample of 50 mg of ester derivative in 5 mL of 0.25 M ethanolic sodium hydroxide solution under reflux for 17 h. The dosing, in return of the excess of soda, was realized by titration with 0.1 N HCl (first equivalent point) [15]. The moles of chloride acid used between the first and second equivalence correspond to the moles of free esters. The degree of substitution (DS) was determined by the Eq. (1). In this equation $MM_{glucose\ unit}$ is the molecular mass of a glucose unit; g_{sample} is the weight of the sample; $n_{free\ ester}$ is the number of moles of free ester; $MM_{free\ ester}$ is the molecular mass of free ester; and MM_{H2O} is the molecular mass of water. DS for functionalized cotton is 0.63, a very interesting value considering the difficulties due to the proper nature of cotton fiber and to the heterogeneous strategy of synthesis.

$$DS = \frac{MM_{glu\cos e\ unit}}{(g_{sample} / n_{free\ ester}) - (MM_{free\ ester} - MM_{H_2O})} \tag{1}$$

5. Antimicrobial testing

The antimicrobial testing was done in accord with accepted biological practices to test antibacterial efficacy. A pressed functionalized cotton disk, suitably sterilized at high temperatures, similarly to the disks used for a normal antibiogram [16] has been used. On Petri dishes was inoculated a sensible bacterium, Streptococcus faecalis, at a concentration of 0.51 McFarland. After 18–24 incubation hours in a thermostat at 37 °C to encourage the growth of bacterial lawn, microrganisms form a primary inhibition zone in which death is total (100%) and a secondary zone in which bacterial hemolysis is less pronounced. This shows that ampicillin, although covalently attached to the glucose units of cellulose in cotton fiber, preserves its antibacterial activity against a sensible microorganism. For this test has been used a solid culture soil of the type Mueller–Hinton agar containing agar, casein idrolisate, soluble stark.

6. Conclusion

Antibacterial cotton fibers were successfully prepared introducing ampicillin moieties onto cellulose backbone. An "in vitro" test was used to assess their antibacterial activity. In fact this test shows a positive behavior of ampicillin in inhibition of bacteria proliferation. The results suggested that these biomaterials posses an excellent antibacterial activity and so this synthetic strategy can be used to obtain versatile biopolymers that could be efficiently employed in biomedical fields for chronic wounds management to ensure a valid protection against infections and contaminations.

References

[1] Z. Değim, Use of microparticulate systems to accelerate skin wound healing, Journal of Drug Targeting 16 (2008), pp. 437–448.

[2] M.H. Huang and M.C. Yang, Evaluation of glucan/poly(vinyl alcohol) blend wound dressing using rat models, International Journal of Pharmaceutics 346 (2008), pp. 38–46.

[3] C.W. Lou, Process technology and properties evaluation of a chitosan-coated tencel/cotton nonwoven fabric as a wound dressing, Fibers and Polymers 9 (2008), pp. 286–292.

[4] Edwards et al., 2004 J.V. Edwards, P. Howley and I.K. Cohen, In vitro inhibition of human neutrophil elastase by oleic acid albumin formulations from derivatized cotton wound dressings, International Journal of Pharmaceutics 284 (2004), pp. 1–12.

[5] Kim et al., 2007 I.Y. Kim, M.K. Yoo, J.H. Seo, S.S. Park, H.S. Na and H.C. Lee et al., Evaluation of semi-interpenetrating polymer networks composed of chitosan and poloxamer for wound dressing application, International Journal of Pharmaceutics 341 (2007), pp. 35–43.

[6] F.H. Lin, J.C. Tsai, T.M. Chen, K.S. Chen, J.M. Yang and P.L. Kang et al., Fabrication and evaluation of auto-stripped tri-layer wound dressing for extensive burn injury, Materials Chemistry and Physics 102 (2007), pp. 152–158.

[7] Mi et al., 2001 F.L. Mi, S.S. Shyu, Y.B. Wu, S.T. Lee, J.Y. Shyong and R.N. Huang, Fabrication and characterization of a sponge-like asymmetric chitosan membrane as a wound dressing, Biomaterials 22 (2001), pp. 165–173.

[8] R.A.A. Muzzarelli, M. Guerrieri, G. Goteri, C. Muzzarelli, T. Armeni and R. Ghiselli et al., The biocompatibility of dibutyryl chitin in the context of wound dressings, Biomaterials 26 (2005), pp. 5844–5854.

[9] Miraftaba et al., 2003 M. Miraftaba, Q. Qiaoa, J.F. Kennedyb, S.C. Ananda and M.R. Groocockc, Fibres for wound dressings based on mixed carbohydrate polymer fibres, Carbohydrate Polymers 53 (2003), pp. 225–231.

[10] L. Adamopoulos, J. Montegna, G. Hampikian, D.S. Argyropoulos, J. Heitmann and L.A. Lucia, A simple method to tune the gross antibacterial activity of cellulosic biomaterials, Carbohydrate Polymers 69 (2007), pp. 805–810.

[11] E.B. Denkbas, E. Öztürk, N. Özdemir, K. Kekeci and C. Agalar, Norfloxacin-loaded chitosan sponges as wound dressing material, Journal of Applied Biomaterials 18 (2004), pp. 291–303.

[12] M. Zilberman and J.J. Elsner, Antibiotic-eluting medical devices for various applications, Journal of Controlled Release 130 (2008), pp. 202–215.

[13] D. Klemm, B. Philipp, T. Heinze, U. Heinze and W. Wagenknecht, Systematics of cellulose functionalization: Comprehensive cellulose chemistry (p. 197), Wiley-WCH, Weinheim (1998).

[14] R. Cassano, S. Trombino, E. Bloise, R. Muzzalupo, F. Iemma and G. Chidichimo et al., New broom fiber (Spartium junceum L.) derivatives: Preparation and characterization, Journal of Agricultural and Food Chemistry 55 (948) (2007), pp. 9–9495.

[15] Trombino et al., 2008 S. Trombino, R. Cassano, E. Bloise, R. Muzzalupo, S. Leta and F. Puoci et al., Design and synthesis of cellulose derivatives with antioxidant activity, Macromolecular Bioscience 8 (2008), pp. 86–95.

[16] Jawetz et al., 2008 E. Jawetz, J.L. Melnick and E. Adelberg's In: G.F. Brooks, K.C. Karroll, J.S. Butel and S.A. Morse, Editors, Medical microbiology (24th ed.), McGraw Hill, New York (2008).

4

Lyotropic Liquid Crystals

This section reviews the Lyotropic Liquid Crystals generated during my PhD research, with the emphasis on the peculiar properties showed by my novel devices. In particular I reported our review on the Lyotropic Liquid Crystal for topical delivery system, that is used as introduction of this section, and a research paper produced in this field.

4.1 Lyotropic liquid crystals for topical delivery systems. (Review)

Rita Muzzalupo, Lorena Tavano, Sonia Trombino, Roberta Cassano and Nevio Picci

Department of Pharmaceutical Sciences, University of Calabria, 87036

Arcavacata di Rende, Cosenza, Italy

Abstract

The design of new forms that increase the effectiveness of existing drugs is one of new trends observed in pharmaceutical technology in recent years. Surfactants have been extensively used for drug delivery in various forms such as liposomes, semisolid and solid-matrices. The focus of this review is the evaluation of liquid crystalline phases, spontaneously formed when amphiphilic molecules are placed in aqueous environment. The possibility of availability of liquid crystal formulations with optical transparency and gelled appearance is highly appreciated in several fields of application such as cosmetics and pharmaceuticals. In this context, liquid crystals (LC) have aroused great interest as novel dosage forms, due to their considerable solubilizing capability for both oil and water soluble compounds. The total therapeutic effect of percutaneous preparations depends not only on the action of the drug itself, but also on other factors related to the structure of the vehicle. The lamellar liquid crystal phases, very similar to those present in living organisms are especially interesting as delivery systems when hydrophilic or lipophilic actives are incorporated in the corresponding domains.

1. Introduction

The liquid crystalline state, obtained from certain surfactants in water or organic solvent, at given temperature and concentration, combines properties of both liquid and solid states. The liquid state is associated with the ability to flow whereas solids have an ordered, crystalline structure [1]. Liquid crystals have at least orientational long-range order and may show short-range order whereas the positional long-range order as characteristic in real crystals has disappeared [2]. More than one form of liquid crystals could exist and the three well known are: lamellar, hexagonal and cubic phases [3-5].

These structures were obtained by solvation of surfactant molecules that results in different geometries, i.e. cone or cylinder [6].

Cylinder arrangement results in a lamellar phase with alternating polar and non-polar layers. In addition to the increased layer thickness of the lamellar phase, lateral inclusion between molecules is also possible with an increase in the solvent concentration, which

transforms the rod shape of the solvated molecules to a cone shape. This leads to a phase

change and depending on the polarity of the solvating agent and the surfactant itself, the

transition results in a hexagonal or inverse hexagonal phase. The hexagonal phase is named after the hexagonally packed rod micelles of solvated molecules, whereby their polar functional groups either point to the outside or inside of the structure. As the molecular geometry changes further during solvation, a cubic or inverse cubic form develops, consisting of spherical or ellipsoidal and/or inverse micelles.

During the past decade, there has been great interest in lyotropic liquid crystalline (LLC), as delivery systems in the cosmetic and chemical industries and also in the field of pharmacy [2,4, 7-9]. The reasons for this interest include the extensive similarity of these LLC systems to those in living organisms [10,11] as skin, biological membranes and certain chromosomes.

The skin is a very heterogeneous membrane, but the layer that controls absorption is the outermost layer, the stratum corneum (SC), a multilayered wall-like structure in which corneocytes embed in a matrix of lipids, that provides a very effective barrier towards the penetration of drugs both to and through the skin. Its barrier properties are essential to the protective role of SC but hinder transdermal drug delivery. Transdermal drug delivery is a viable administration route for potent, low-molecular weight therapeutic agents which cannot withstand the hostile environment of the gastrointestinal tract and/or are subject to considerable first-pass metabolism by the liver.

The LLC systems exhibit good penetration, due to the very low interfacial surface tension arising at the oil/water interface [12, 13], and they may facilitate the progressive diffusion of biologically active substances into the skin and also systemic circulation [14-16]. They can bring about a considerable increase in the solubility of drugs by means of solubilization, which are either insoluble or slightly soluble in water [17-20].

2. Lyotropic liquid crystal

Liquid crystals, also named "mesophase", are organic substances that pure, or in aqueous solutions, are capable to reach a special state of aggregation, intermediary between liquid and solid state. They preserve both the flow properties of a liquid and the ordering of a crystal and present multiple anisotropies. In particular, some organic substances, in aqueous solutions, reach the mesomorphic domain by varying temperature and concentration and have been named Lyotropic Liquid Crystals (LLC).

Lyotropic liquid crystals are examples par excellence of self-assembling nanomaterials. The molecular systems which adopt liquid crystalline phases are quite diverse: their organization is normally not based on mesogenic properties of a certain molecule but rather on the interaction between two, or even more, molecular units in solution. Therefore, their sequence of phases rather depends on the concentration of the different components added to the mixture than on temperature and the mesophases usually observed are classified as lamellar, cubic, hexagonal (Fig. 1)[3].
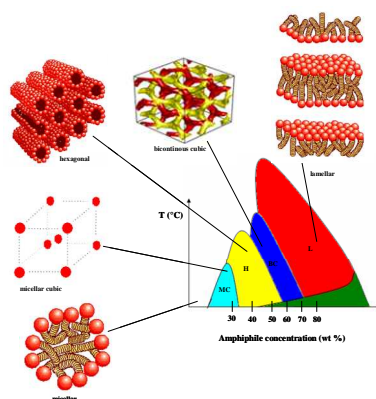

Fig.1 Schematic showing the aggregation of surfactants into micelles and then into lyotropic liquid crystalline phases as a function of their concentration and of temperature.

Using these LLC phases as topical drug delivery systems is favourable because of their high solubilization capacity, thermodynamical stability or broad range of rheological properties. Moreover, LLC incorporated in a special dermatological formulations exhibit hydrating properties and they have been used as excipients to protect sensitive substances (vitamins, antioxidants, oils).

Molecules that make up lyotropic liquid crystals are surfactants consisting of two distinct parts: a polar, often ionic, head and a nonpolar, often hydrocarbon tail.

Surfactants have been extensively used in simulating biomembrane [21–25], biomembranes for drug delivery and in solubilizing poorly water soluble drugs in pharmaceutical formulations [26, 27].

3. Cubic phase

When the concentration of micelles dispersed in a solvent (usually water) is sufficiently high a micellar cubic phase is formed. This, denoted by the symbol I1, is the first lyotropic liquid crystalline phases but not the only existing. In fact, the quite interesting for drug delivery is the bicontinuous cubic phase (V1), usually located between the hexagonal and lamellar ones. From an optical point of view, cubic phases present no texture, because they are isotropic and can be distinguished from the isotropic micellar solutions only by their high viscosity [28].

Cubic liquid crystal phase are interesting for drug delivery for a number of reasons:

• The cubic phases are generally characterized by a high stiffness. This offers opportunities for fixation of the formulation at desired site after administration and in situ formation.

• The bicontinuous cubic phase can solubilize large amount of both hydrophilic and hydrophobic drugs.

• Through controlling the microstructure, the drug release rate can be controlled over a wide range.

• Through control of the microstructure, protein drugs can be immobilized, thereby allowing them to function at the same time as they are not exposed to proteolytic enzymes, antibodies, etc.

A wide variety of drugs with different physico-chemical properties have been incorporated in Glyceryl monooleate (GMO) based cubic phases [29]. GMO is a metabolite formed during the lipid digestion of oleic triglycerides [30]. Its water solubility is low, about 10-26 mol/ l, but it swells in water and the resulting phase is a cubic liquid crystal one. This cubic phase has other interesting properties, all relevant for a partition experiment: it forms spontaneously and can coexist with excess water, and its internal structure is that of a congruent monoolein bilayer extending in threedimensions, with a high specific bilayer /water interfacial area (500–600 m^2/g lipid).

The pharmaceutical interest in monoolein as a drug delivery system is based on the amphiphilic nature of the gel formed in an aqueous environment, facilitating the incorporation both hydrophilic and hydrophobic molecules. Monoolein is non-toxic, biodegradable and biocompatible and has become a potential candidate as drug delivery system useful for various routes of administration. The cubic liquid–crystalline phase, a well-known microheterogeneous system spontaneously formed when an amphiphilic lipid such as monoolein (glyceryl monooleate, GMO) is placed in an aqueous environment, has become an excellent candidate as a drug delivery matrix [31-33].

A short list of applications includes the delivery of actives for periodontal disease [34] and implants [35] via *in vivo* [36] and topical delivery [37], and as bioadhesives [38]. Two recent reviews by C.J. Drummond and C. Fong [39] and J.C. Shah et al.[40] provides an extensive listing of drug-related applications in the cubic phases but the topical applications are very limited.

R.F. Turchiello et al.[41] investigated the cubic phase obtained by monoolein/water for topical delivery of pro-drug and photosensitizers used in photodynamic therapy (PDT) and of cutaneous diseases. Pro-drug 5-aminolevulinic acid (5-ALA, a PpIX precursor), its ester derivatives (hexylester, octylester and decylester), and a classical second generation photosensitizer such as the chlorine derivative *meso*tetra(hydroxyphenyl)chlorine (*m*-THPC or Foscan®) were incorporated into the gel cubic phase and their physico-chemical properties such as stability, maximum absorption wavelength, and fluorescence emission were investigated by spectroscopic techniques at 37 °C. This study represents the first report of the use of the cubic phase as a delivery system of pro-drugs and photo-sensitizers for topical use in PDT. It opens the possibility to explore other

172

photosensitizers that remain stable in the gel cubic phase and can be used for topical treatment of dermatological diseases. These results confirm that the gel formulation monoolein/ water, associated with its enhanced skin permeation properties [42], could be used to reduce the amount of drug applied to the lesion, with the same or higher PpIX production effect, so the monoolein gel is a potential delivery matrix and can be used for topical delivery of pro-drugs and photosensitizers in PDT treatment of cutaneous diseases.

Another study used the bicontinuous Monoolein phase to release of 5-ALA and its methyl ester (m-ALA). The iontophoretic and passive delivery of ALA and m-ALA from this formulation through porcine skin *in vitro* were measured and compared to formulations used in clinical practice [43]. The cubic phase, in this work, is formed in a ternary mixture of Monoolein, water and relatively high amounts, 30%, of propylene glycol. Overall, the results indicated that the cubic phase have a potential as drug delivery vehicle for the passive and iontophoretic delivery of drugs such as m-ALA across the skin.

In addition, some of these scientists compared the 5-ALA and m-ALA release of the cubic phases formed of monoolein or phytantriol in water [44]. These systems had similar phase behavior, but there are some differences that may be important as delivery water soluble drugs. One is that the maximum degree of water swelling differs. A lower water content in the cubic phase implies more narrow water channels in the tortuous structure. Since both ALA and m-ALA will reside in the water channels, the release of water soluble drugs from this kind of cubic phase decreases with decreasing water pore diameter. Monoolein systems have a superior ability to transport the drug into and through the tissue, in such a way that it rapidly reaches the circulation of the mice. In addition, the phytantriol systems showed only a small systemic effect with ALA.

Other investigation about the cubic phase was realized by M.G. Carr et al. [45], using Myverol as drug vehicle. The commercial material Myverol was used in place of pure GMO as it has been shown that the phase behaviour of pure GMO and Myverol are very similar [46], and both materials form cubic phase in excess water at physiological temperatures. In their matrices the scientists incorporated nicotine and salbutamol sulphate as drugs and they evaluated the ability to include solutes into these structures, the modification of phase properties of the system and consequently the drug release characteristics. Apparent diffusion coefficients for both drugs were determined, in each gel matrices, by performing *in vitro* experiments using Visking membranes as barriers to the receptor solutions; the work was extended to transport to across human stratum corneum. The rates of drug delivery into the receptor compartment were determined by plotting the quantities of drug released across Visking from Myverol gels versus time. These plots were found to be non-linear for

both nicotine and salbutamol. The fig.2 show the linear relationship observed when the quantities of drugs released were plotted against the square root of time.
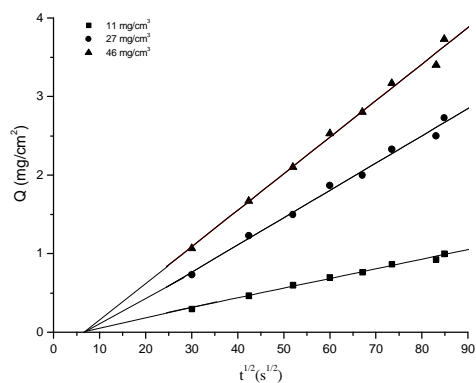

Fig.2 The quantity of salbutamol sulphate Q transported per unit area versus the square root of time (adapted with modifications from ref.45).

M.G. Carr et al. observed that increasing the water content in the range 0-40% greatly increased the apparent diffusion coefficient of nicotine, whereas there was a decrease in the apparent diffusion coefficient of salbutamol sulphate. Partitioning of the drug between Myverol base and the aqueous layers is thought to be responsible for this behaviour. The release profiles for passive transport across human stratum corneum, as shown in Fig. 3, were linear and the rates of delivery were typically 2-3 times those reported from 4% agar gel vehicles, used as control, containing comparable concentrations of the drug.
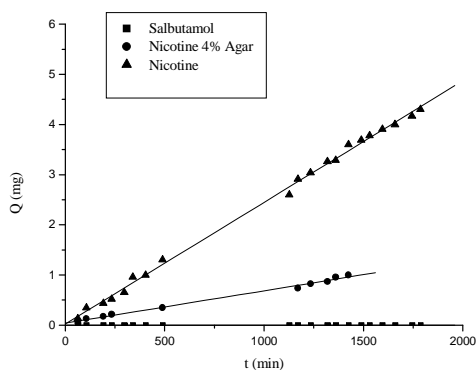

Fig.3 Release profiles for passive transport across human stratum corneum (adapted with modifications from ref.45).

174

`The scientists suggested that the Myverol acts as possible penetration enhancer thanks to some of its constituents. In addition this paper showed that a significant increase in the transport of both drugs were obtained by the passage of a direct current through the vehicle and the rates of the assisted transport were found to be depend on the magnitude of this current.

L.S. Helledi and L. Schubert [47] incorporated in GMO cubic phase acyclovir, a drug widely used as agent in the treatment of herpes virus infections of the skin. In this study, acyclovir was suspended in a cubic phase of glycerol monooleate (GMO) and water 65:35% w/w, and the phase behavior and release kinetics demonstrated that the cubic phase containing 1-10% (w/w) acyclovir retains its phase condition in the temperature range 20-70°C. The drug was readily released from the system, and its release increased with the initial drug load concentration; about 25-50% of drug was released after 24 h. In addition in this study, the release was dependent on the square root of time, and the kinetics can be described by the Higuchi theory. The rate-limiting step in the release process was most likely diffusion. Comparison of the release rates of acyclovir delivered from a cubic phase and from the commercial product, Zovir®cream, showed the rate to be six times faster from the cubic phase. The cubic phase is a promising percutaneous drug delivery system for Acyclovir.

Other studies on the GMO cubic phase were realized by D. Fitzpatrick and J. Corish. They have reported on the passive release profiles and those resulting from the incorporation of a chemical enhancer in the vehicle and the behaviour of the system under iontophoretic conditions and also under those of combined physical and chemical enhancement [48-50]. In particular they investigated for a range of anionic drug molecules with particular emphasis on sodium diclofenac, the suitability of an isotropic liquid crystalline gel. Parameters, which have been investigated, include the mode of vehicle preparation, the effect of the concentration of the drug and how buffering the gel and/or the receptor medium affect the release profiles. Such profiles have been measured for the sodium salts of benzoate, salicylate and indomethacin.. The percentages released of the sodium salts of benzoate, salicylate and indomethacin, after 24 h, were determined to be 25, 26 and 19%, respectively, and these are significantly greater than the release of sodium diclofenac. This suggests that diclofenac undergoes ion-pairing or complexation within the gel, which inhibits its diffusion from the vehicle.

It has been demonstrated that the incorporation of the cationic surfactants into the liquid crystalline gel, in the presence of an anionic drug, greatly reduces the quantity of drug which is available to diffuse from the vehicle across a non-rate-limiting membrane. This is due to the formation of ion-pairs between the drug and model enhancer within the vehicle. Moreover the authors established a linear relationship between the percentage release of the drug and the concentration of model enhancer incorporated into the vehicle Cubic phases of monoolein and water have shown to

improve the topical/ transdermal delivery of relatively small molecules such as nicotine, salbutamol, acyclovir, diclofenac and aminolevulinic acid esters [41-50], but it remains to be determined whether this phase is capable of promoting the topical delivery of larger molecules, such as several peptides and proteins.

For this reason a recent study reported the investigation about the reverse cubic phase of Monolein (Myverol) loaded with cyclosporin A(CysA)[51]. Cyclosporin A (CysA) is a cyclic and highly lipophilic peptide that presents extremely poor skin penetration, unless a chemical or physical strategy is used [52–57], moreover, this peptide is an immune-suppressant agent and has therapeutic potential in the treatment of skin inflammatory disorders [53,56].

In their investigations L.B. Lopes et al. showed that cubic phases are formed in the presence of CysA, and *in vitro* skin penetration of this model peptide was significantly increased when it was incorporated in such systems. In particular, the cubic phase gel increased the penetration of CysA in the stratum corneum (SC) and epidermis plus dermis [E+D], but did not influence the percutaneous delivery of the peptide compared with the control formulation. *In vivo* experiment (Fig. 4) revealed that incorporation of CysA in the cubic phase also results in an increase in the skin penetration of the peptide at 6 h post-application.

Penetration enhancing effects are often caused by structural alteration of the stratum corneum [58]. Several effective permeation enhancers have been shown to induce some inflammatory effects on the skin in a concentration-dependent manner. In this system, the authors observed some alterations, though not severe, in the skin sections of animals treated with cubic phases, which suggest the occurrence of mild skin irritation in hairless mice after a 3-day exposure.
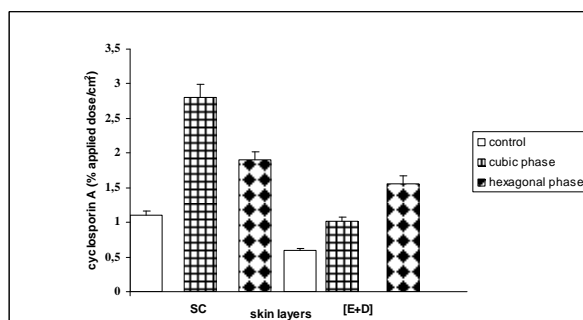

Fig.4 *In vivo* **penetration of CysA incorporated in different formulation, SC: stratum corneum, [E+D]: epidermis without stratum corneum+ dermis (adapted with modifications from ref.52).**

An increase of the loading of water-soluble actives in bicontinuous cubic phase liquid crystals was obtained by including ionic surfactants, to prevent the preference of the water-soluble actives to associate with water rather than with the liquid crystals.

In this context M.L. Lynch et al. [59] demonstrated the enhanced loading of negatively charged, water-soluble active ketoprofen by the inclusion of positively charged surfactants into the liquid crystal. Loading differences resulting from the inclusion of dioctadecyl dimethyl ammonium chloride (DODMAC) and dioctadecyl ammonium chloride (DOAC) into the liquid crystal showed that the magnitude of the enhancement is dependent on the surfactant concentration and the steric nature of its head group.

The introduction of a third component in the system GMO-water was utilized to increase the solubility of water insoluble ion pairs, as recently reported by R. Efrat et al. In this investigation the scientists detected a new small isotropic region within the phase diagram of glycerol monooleate (GMO) and water in the presence of ethanol (EtOH) characterized by a nonviscous stable fluid as micellar phase of cubic symmetry [60, 61]. This phase can solubilize very significant loads of water-insoluble anti-inflammatory sodium diclofenac (Na-DFC). Close examination of the internal structures of the lyotropic liquid phase upon increasing the solubilization loads reveals the existence of three structural transitions controlled by the Na-DFC levels. In particular, at increase of the Na-DFC the micellar phase of cubic symmetry become a bicontinuous cubic phase, a lamellar phase and a disorder lamellar phase.

4. Hexagonal phase

An hexagonal phase of lyotropic liquid crystal is formed by some amphiphilic molecules when they are mixed with water or another polar solvent. In this phase the amphiphile molecules are aggregated into cylindrical structures of indefinite length and these cylindrical aggregates are disposed on a hexagonal lattice, giving the phase longrange orientational order. If increasing solvent concentration in the cubic phase, the hexagonal phase occurs and forms *normal* structures HI in which the hydrocarbon chains are contained within the cylindrical aggregates such that the polar-apolar interface has a positive mean curvature, or *reversed* structures HII in which water within the cylindrical aggregates and the hydrocarbon chains fill the voids between the hexagonally packed cylinders. When viewed under a polarising microscope thin films of both normal and inverse topology hexagonal phases exhibit birefringence, giving rise to characteristic optical textures. The phases are highly viscous and small air bubbles trapped within the preparation have highly distorted shapes.

The physical properties of reverse hexagonal liquid crystals (HII) are less studied compared with those of cubic and lamellar phases [62, 63] and very few are the pharmaceutical and, in particular, percutaneous applications. The reverse hexagonal mesophase is characterized by dense packing of infinitely long water-filled rods, each surrounded by a lipid layer and exhibiting two dimensional

ordering. E. Farkas et al. investigated the influence of two types of chlorhexidine species, chlorhexidine base and its salts [64], on the physicochemical features of liquid crystalline systems and on drug transport through lipophilic membranes and they illustrated the applicability of liquid crystalline systems of sensitively changing structures to provide sustained release of drugs using their base and salt forms.

A non-ionic surfactant, Synperonic A7 (PEG7-C13-15) was selected for the preparation of the liquid crystalline systems. Mixtures of different ratios of Synperonic A7 and water were prepared and only that at 40% in surfactant formed a hexagonal liquid phase. The addition of chlorhexidine species to the systems modified the structure of the liquid crystalline phases and this results in a change of the drug release. The combination of the base and salt forms of the drug in one dosage form could eliminate the drug release changes from liquid crystalline

systems of dynamically changeable structures. In fact, the studies indicates that below 50% (w/w) Synperonic concentration, the isotropic and less ordered structure allowed more chlorhexidine base to be released from the liquid crystals compared to the more viscous system containing ordered hexagonal structural elements, which hindered the release of chlorhexidine digluconate. As the water solubility of the latter is somewhat 10,000 times higher than one of the free base, these results suggest that drug release is governed mainly by the structure of the liquid crystal.

L.B. Lopes et al. [52] demonstrated that, *in vivo*, the HII phase of GMO/water/oleic acid increased the skin penetration of CysA as well as the cubic phase, before reported. The reverse hexagonal phase increased CysA penetration in [E + D] at 6 h and percutaneous delivery at 7.5 h post-application. The use of the hexagonal but not the cubic phase, also enhanced the percutaneous delivery of CysA. Incorporation of CysA in the hexagonal phase resulted in a increase in peptide concentration in the SC and a increase in the concentration in the [E+D]. Incorporation of CysA in both formulations enhanced the *in vitro* penetration of the peptide across the skin and it was probably due to the action of monoolein (in combination with oleic acid in the case of hexagonal phase) as penetration enhancer. Indeed, monoolein has been demonstrated to be released from liquid crystalline phases and to influence the skin permeation of the incorporated compounds [45].

Another hexagonal liquid crystal system, composed of monoolein, tricaprylin, and water .was used to enhancer the CysA penetration across the skin by D. Libster et al.[65]. In particular, this study show how solubilization CysA and the penetration enhancers Labrasol and ethanol modified the physical properties of bulk HII mesophases of GMO/tricaprylin/water stabilized by phosphatidylcholine. Due to the large quantities of solubilized CysA and three dermal penetration enhancers (phosphatidylcholine, ethanol, or Labrasol) the HII mesophases are promising candidates for topical release. I. Amar-Yuli et al investigated the solubilization of four bioactive molecules

178

with different polarities, in three reverse hexagonal (HII) systems [66]. The three HII systems were typical reverse hexagonal composed of glycerol monooleate (GMO)/tricaprylin/ water and two fluid hexagonal systems containing either 2.75 wt % Transcutol or ethanol, as a fourth component. The phase behaviour of the liquid crystalline systems in the presence of ascorbic acid, ascorbyl palmitate, D-α-tocopherol and D-α-tocopherol acetate were evaluated. The results of this work suggest that these systems have a potential in dermatological field and in particular in cosmetic applications.

5. Lamellar phase

The structural units for the lamellar phase are the simple and double layers. It has to be mentioned that the bilayer, as a repetitive unit, forms the main matrix of the biological membranes that contain phospholipids as lyotropic compounds and not soaps. The ordered bilayer structure is formed by amphiphilic molecules disposed in bidimensional infinite layers, delimited by water compartements, having a parallel disposition. The polar heads of the molecules are contacting the aqueous medium, while the hydrocarbon chains are interdigitating in order to avoid water. The bilayers are disposed one under another through the third dimension, periodically alternating with water layers [67]. Because the bilayer ordering is not disturbed by the gravitational effect, the repetitive vertical distance between layers is constant. This phase is not a viscous one and the bilayers can slip easily one on the other. The specific optical characteristics of its textures make easier the identification of this phase. The optical axis is parallel to the long axis of the molecules of the layers; the phase can be optically uniaxial, positive or negative, depending on the temperature values.

New possibilities for the development of controlled drug delivery systems are inherent in the lamellar liquid crystal systems due to their stability and special skin similarly structure, in fact these systems have been proposed as semisolid vehicles for topical administration of drugs [68].

The work realized by D.I. Nesseem is a trial to apply theory and practice of liquid crystals

in pharmaceutical topical delivery systems [69]. The scientist formulated and evaluated an antifungal agent with topical therapeutic activity in pharmaceutically acceptable nonionic surfactant system to enhance its cutaneous penetration. A model drug, itraconazole was chosen as antifungal agent while the lamellar phase was obtained by the ternary system polyoxyethylene stearyl ether/silicon oil and water. N.H. Gabboun et al. investigated the release of salicylic acid, diclofenac acid, diclofenac diethylamine and diclofenac sodium, from lamellar and hexagonal liquid crystalline phases, across mid-dorsal hairless rat skin into aqueous buffer [70]. The mesomorphic vehicles were composed by the nonionic surfactant polyoxyethylene (20) isohexadecyl ether in water or hydrochloric acid buffer and the drug. By changing the anisotropic donor medium from lamellar to

hexagonal phase, drug flux decreased in case of salicylic acid and diclofenac sodium. In the mean time, flux increased in case of the diethylamine salt and appeared nearly similar in case of diclofenac acid. Rates of drug transfer across the skin from the anisotropic donors seemed to be largely controlled by

the entropy contribution to the transport process. The type and extent of drug-liquid crystal interactions probably influenced the latter. The results of this investigation indicate that, transport of diclofenac acid (DA) and its salts (diclofenac sodium (DS), diclofenac diethylamine (DDEA)) across the rat skin were more than thirty times slower than salicylic acid (SA). This was attributed to structural differences between the diclofenac compounds and SA in so far molecular weight, shape and size, as well as polarity, polarizability and configuration of the molecules. It is also concluded that solute–solvent interactions in the anisotropic environment, in contrast to such interactions in the isotropic medium, caused the release of DA and its salts to proceed at different rates.

S. Mackeben et al. investigated the effects of timolol maleate (TM) as a model drug on the physicochemical properties of a lamellar mesophases arise at higher water contents and of a reverse micellar solution (RMS) consisting of lecithin in isopropyl myristate [71]. They studied, in particular, the interactions between the TM drug and the surfactant and the structural modifications introduced by the drug. An indication of the interactions between TM and lecithin was confirmed by the formation of a lamellar mesophase with defects when the water content is high enough.

I. Csóka et al. evaluated the influence of vehicle compositions (hydrogel, lamellar liquid crystal and o/w cream) on topical drug availability. *In vitro* drug release and *in vivo* experiments were performed in the case of the hydrophilic ketamine hydrochloride and the lipophilic piroxicam [72]. In the case of piroxicam (Fig.5), the liquid crystal system and the hydrogel showed to be efficient, while o/w cream exerts only a moderate oedema inhibition.
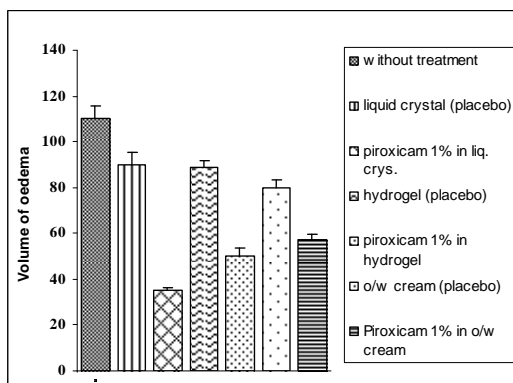

Fig. 5. Antiinflammatory effect of different preparations on carrageenan-induced oedema in rat.

A preliminary study for skin application was developed by M. Makai et al. They utilized a nonionic surfactant, the Brij 96V, a short-chain alcohol as co-surfactant, and, to increase the dissolving capacity of systems for lipophylic drugs liquid paraffin was added [73]. The lamellar phase observed in these preparations was stable, in particular, the four component lamellar liquid-crystalline systems, with relatively low surfactant concentrations, are suitable for development of dermal dosage forms. This system was used by M. Makai et al. to evaluate the connection between the structure of the samples and drug release of the incorporated model drug, ephedrine hydrochloride, with good water-solubility and tenoxicam, with practically water insolubility [74]. Samples containing ephedrine hydrochloride and tenoxicam in a concentration of 1% (w/w) also retained their organized lamellar structure.The drug release of ephedrine hydrochloride showed a first-order kinetic (Fig.6). A fast drug release was observed followed by a slow release in case of samples containing glycerol 15–20% (w/w). Zero-order release kinetic was measured in case of sample with higher glycerol content. The release of tenoxicam corresponded to zero-order release kinetic (Fig.7).
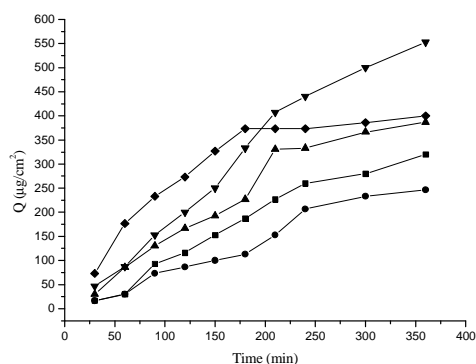

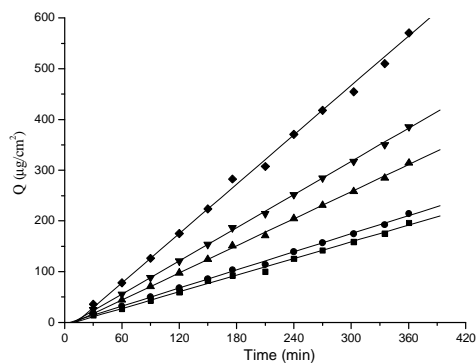**Fig.6 Ephedrine hydrochloride release from 5 samples (adapted with modifications from ref.74)**

Fig.7 Tenoxicam release from 5 samples (adapted with modifications from ref.74)

The highest amount of released tenoxicam was measured from sample with the highest diffusion coefficient. Other glycerol-containing samples showed slower drug release. This phenomenon was explained by the authors as follows: the water amount present in the lamellar liquid crystal systems was sufficient for dissolving the very soluble ephedrine hydrocloride. Tenoxicam as a practically insoluble drug, was completely solubilized in the selected systems. An increase in the interlamellar distance was detected in the case of both incorporated model drugs, meaning that the drugs were partly built between the lamellar space, and partly located at the given polarity part of the amphiphilic surfactant molecules. The experiments reported in this study ensured that the developed lamellar liquid crystalline systems were proper not only for incorporating of a poorly water soluble drug, but were adequate for achieving a prolonged drug release in case of very water-soluble drug.

An emerging class of natural surfactants, named alkylpolyglucosides, were studied in two works of S. D. Savic et al. [75, 76]. Vehicles based on cetearyl glucoside and cetearyl alcohol, contained oils of different polarity, showed a complex colloidal polarity. The oils utilized in these studies were Miglyol® 812, a medium chain triglycerides, isopropyl myristate and light liquid paraffin. Three formulations were studied *in vitro* and *in vivo* bioavailability of hydrocortisone (HC), in comparison with a standard pharmacopoeial vehicle. *In vivo* results suggested that the vehicle with Miglyol® 812 retarded the hydrocortisone permeation, whereas less polar, isopropyl myristate and non-polar paraffin enhanced it. It is suggested that the enhancement is achieved either by a direct interaction with lipid lamellae of the SC or indirectly by improving skin hydration. There were no adverse effects during *in vivo* study, which indicates a good safety profile of these alkylpolyglucoside surfactants. These findings imply an enhanced delivery of hydrocortisone from this vehicle and its putative penetration enhancing effect, probably dependent on specific distribution of the vehicle's inherent water.

Nonionic surfactant, Synperonic A7 (PEG7–C13–15) was selected for the preparation of the examined liquid crystalline systems. Mixtures of different ratio of Synperonic A7 and water were produced by E. Farkas et al. that examined different liquid crystalline preparations containing chlorhexidine diacetate and established connection between their structure and the kinetic of drug release [77]. By increasing the water content of the systems, lamellar and hexagonal liquid crystal structures were observed. The chlorhexidine diacetate release from hexagonal liquid crystalline preparations was characterised by zero-order kinetics, while the drug released from lamellar liquid crystalline systems was described by anomalous (non- Fickian) transport. The chlorhexidine diacetate release from the lamellar liquid crystalline systems was more than three times less compared to the hexagonal mesophases. The results indicated that the drug release kinetic is strongly dependent on the liquid crystalline structure and it has a decisive impact bioavailability of the chlorhexidine diacetate.

In a successive work E. Farkas et al. investigated the influence of three chlorhexidine species, chlorhexidine base and its salts (diacetate and digluconate), on the physicochemical

features of liquid crystalline systems and on drug transport through lipophilic membranes [78]. Mixtures of different ratios of Synperonic A7 and water were prepared. As a result of liquid crystal–drug interaction, the solubility of chlorhexidine base and its diffusion through lipophilic membranes increased in comparison with those of the chlorhexidine salts. The results obtained in this study indicated that the location of the chlorhexidine base is between the Synperonic A7 molecules, and that diffusion mainly takes place within the constraints of the hydrophobic parts of the lamellar structure.

The drug–vehicle interaction modified the liquid crystalline structure, thus solubilizing the active substance and consequently increasing the extent of diffusion through a lipophilic membrane. A novel gel was developed for the enhanced transdermal delivery of propranolol

hydrochloride (PH) by A. Namdeo et al. [79], which synthesized the prodrugs, propranolol palmitate hydrochloride (PPH) and propranolol stearate hydrochloride (PSH) selfassembled to form gel simply upon mixing alcoholic solution of prodrug with an aqueous solution in a specified ratio. The gel phase exhibited birefringence under planepolarized light corroborating the presence of lamellar liquid crystals. These prodrugs might intercalate and fluidize the intercellular lipids and increase its own permeation through this layer of skin. Prodrugs bearing hydrophilic and lipophilic portion acquires amphiphilic character, therefore is supposed to permeate better through both the lipophilic and hydrophilic layers of the skin. The palmitate and stearate prodrugs of propranolol might also be hydrolyzed by non-specific esterases present in the skin and producing fatty acids, which are known to act as penetration enhancers. The gel formulations also caused less irritation

than control, while mixed gel showed least irritation. This novel self-assembled pharmacogel providing high transdermal permeation with many variables to regulate the delivery is therefore having a great potential in percutaneous delivery.

An interesting study by L. Brinon et al. investigated the effects of two non-ionic surfactants, C12EO4 and C12EO23, with liquid crystalline structures on the cutaneous availability of two sunscreens [80]. Three liquid crystalline structures, obtained by ternary system water- C12EO23-C12EO4, were evaluated: lamellar, hexagonal and cubic. The diffusion of sunscreens within the liquid crystals was determined by measuring transport kinetics into an unloaded surfactant medium from a similar system loaded with the sunscreens. The diffusion coefficients were higher in the cubic systems for benzophenone-4 (a hydrosoluble sunscreen) and in lamellar systems for octylmethoxycinnamate (a liposoluble sunscreen). So the diffusion in this surfactant system was strongly dependent on the structure of the liquid crystal and on the physicochemical properties of the solute. The liquid crystalline vehicles modified the transcutaneous fluxes of benzophenone-4 but did not change those of octyl methoxycinnamate. The solute diffusion within the vehicle was not the rate-determining step for transcutaneous permeation for either sunscreen. The diffusion of benzophenone-4 across the stratum corneum and that of octyl methoxycinnamate across the dermis could be the rate determining steps for their transcutaneous permeation. These two steps could be affected

differently by nonionic surfactant vehicles.

References

[1] H. Kelker, R. Hatz, Handbook of Liquid Crystals, Verlag Chemie,Weinheim, Germany, 1980.
[2] C.C. Müller-Goymann, Flüssigkristalline Systeme in der Pharmazeutischen Technologie, PZ Prisma 5 (1998).
[3] G.H. Brown, Am. Scientist 60 (1972) 64.
[4] D. Attwood, A.T. Florence, Surfactant Systems, their Chemistry, Pharmacy and Biology. Biological Implication of Surfactant Presence in Formulations. Chapman & Hall, London, 1982, pp 389–418.
[5] A.T. Florence, D. Attwood, Physicochemical Principles of Pharmacy, second ed., Macmillan, New York, 1988, Chapter 6, pp 209, 246-247.
[6] B. Silver (Eds.), The Physical Chemistry of Membranes, Solomon Press, Winchester, VA, 1985.
[7] S. Wahlgren, A.L.Lindstrom, S.E. Friberg. J. Pharm. Sci. 73 (1984) 1484.
[8] A.Y. Özer, A. Hincal, J.A. Bouwstra. Eur. J. Pharm. Biopharm. 37 (1991) 75.
[9] S.P. Vyas, V. Jaitely, P. Kanaujia, Pharmazie 52 (1997) 259.
[10] L. Bata, Folyadékkristályok. Liquid crystals. Mszaki Könyvkiadó, Budapest, 1986, pp 122-145.
[11] D. Chapman, Lyotropic mesophase in biological systems. In: Bahadur, B. (Ed.), Liquid Crystals Applications and Uses. World Scientific, Singapur, 1991 pp 186–214.
[12] W. Benton J. Disper. Sci. Technol. 3 (1982) 1.
[13] T. Suzuki, H. Takei, S. Yamazaki. J. Colloid Interface Sci. 129 (1989) 491.
[14] J. Ziegenmeyer,. The influence of the vehicle on the absorption and permeation of drugs. in: Brandau, R., Lippold, B.H. (Eds.), Dermal and Transdermal Absorption. Wissenschaftliche Verlagsgesellschaft mbH, Stuttgart, 1982 pp. 73–89.

[15] H.E. Boddé, T. De Vringer, H.E. Junginger. Prog. Colloid. Polym. Sci. 72 (1986) 37.

[16] E. Cooper, B. Berner, Penetration enhancers. In: Kydonieus, A.F., Berner, B. (Ed.), Transdermal Delivery of Drugs, vol.3. CRC Press, Boca Raton, 1987 pp 57–61.

[17] K.L. Mittal, Micellization, solubilization and microemulsions. In: Prince, L.M. (Ed.), Micellization, Solubilization and Microemulsions, vol. 1. Plenum Press, New York, 1976 pp. 45-54.

[18] P.H. Elworthy, A.T. Florence, C.B. Macfarlane, Solubilization by Surface Active Agents. Chapman & Hall, London, 1986 pp. 63–225.

[19]. K. Kriwet, C.C. Müller-Goymann. Eur. J. Pharm. Biopharm. 39(1993) 234.

[20] S. Engström. Eur. J. Pharm. Sci. 8 (1999) 243.

[21] N. Taulier, C. Nicot, M. Waks, R.S. Hodges, R. Ober, W. Urba. Biophys J. 78 (2000) 857.

[22] Y. Chaudier, F. Zito, P. Barthelemy, D. Stroebel, B. Ameduri, J.L. Popot and B. Pucci, Bioorg Med Chem. Lett. 12 (2002)1587.

[23] C. Prata, F.Giusti, Y. Gohon, B. Pucci, J.L. Popot, C. Tribet Biopolymers 56 (2001) 77.

[24] F.R. Poulain, S. Nir, S. Hawgood Biochim Biophys Acta 169(1996) 1278.

[25] Y.Q. Guo, S.W. Hui. Biochim Biophys Acta 185 (1997) 1323.

[26] D.Attwood A.T, Florence. Pharmaceutical Aspects of Solubilized Systems. In: Surfactant Systems; London: Chapman and Hall, 1983 pp 293-387.

[27] M.J. Lawrence. Chem. Soc. Rev.23 (1994) 417.

[28] M. Malmsten, Surfactant and polymers in drug delivery. Series: Drug and pharmaceutical sciences vol.122, Marcel Dekker, New York 2002 pp 51-86.

[29] S.T. Hyde, S. Andersson, B. Ericsson, K. Larsson. Z. Kristallogr. 168 (1984) 213.

[30] J.S Patton, M.C.Carey.Watching fat digestion. Science 204 (1979) 145.

[31] S. Engström, Polym. Prep (Am. Chem. Soc. Div. Polym. Chem.) 31 (2) (1990) 157.

[32] D.M. Wyatt, D. Dorschel, Pharm. Technol. 16 (10) (1992) 116.

[33] S. Engstrom, T.P. Norden, H. Nyquist, Eur. J. Pharm. Sci. 8 (1999) 243.

[34] R.F. Czarnecki, D.L.Williams, U.S. Patent 5,230,895, 1993.

[35] S. Engström, K. Alfons, M. Rasmusson, H. Ljusberg-Wahren, Prog. Colloid Polym. Sci. 108 (1998) 93.

[36] T. Landh, K. Larsson, U.S. Patent 5,531,925, 1993.

[37] a) S. Andersson, S. Jonn, T. Landh, W.O. Patent 991517, 1999; b) S.M. Niemiec, J.C.T. Wang, S.J. Wisniewski, K.S. Stenn, G.W. Lu,U.S. Patent App. W.O. 99US17387, 2000.

[38] a) L.S. Nielsen, W.O. 9847487, 1998; b) J. Hansen, L.S. Nielsen, T. Norling, U.S. Patent 5,955,502, 1999.

[39] C.J. Drummond, C. Fong, Curr. Opin. Colloid Interface Sci. 4 (2000) 449.

[40] J. C. Shah, Y. Sadhale, D. M. Chilukuri Adv. Drug Del. Reviews 47 (2001) 229.

[41] R.F. Turchiello, F.C.B. Vena, Ph. Maillard, C.S. Souza, M.V.B.L. Bentley, A.C. Tedesco, Journal of Photochemistry and Photobiology B: Biology 70 (2003) 1.

[42] T. Ogiso, M. Iwaki, T. Paku, J. Pharm. Sci. 84 (4) (1995) 482.

[43] N. Merclin, J. Bender, E. Sparr, R.H. Guy, H. Ehrsson, S.Engström. J. Control. Release 100 (2004) 191.

[44] J. Bender, M.B. Ericson, N. Merclin, V. Iani, A. Rosen, S. Engstrom, J. Moan. J. Control. Release106 (2005) 350.

[45] M. G. Carr, J. Corish, O. I. Corrigan. Int. J. Pharm. 157 (1997) 35.

[46] J. Clogston, J. Rathman, D. Tomasko, H. Walker, M. Caffrey. Chem. Phys. Lipids 107 (2000) 191.

[47] L.S. Helledi, L. Schubert. Drug Dev. Ind. Pharm. 27 (2001) 1073.

[48] D. Fitzpatrick , J. Corish. Int. J. Pharm. 301 (2005) 226.

[49] D. Fitzpatrick , J. Corish. Int. J. Pharm. 311 (2006) 139.

[50] D. Fitzpatrick , J. Corish. Int. J. Pharm. 325 (2006) 90.

[51] L. B. Lopes, J. L.C. Lopes, D.C.R. Oliveira, J. A. Thomazini ,M. T. J. Garcia, M. C.A. Fantini, J. H. Collett, M. V.L.B. Bentley. 6 Eur. J. Pharm. Biopharm. 3 (2006) 146.

[52] L.B. Lopes, J.H. Collet, M.V.L.B. Bentley. Eur. J. Pharm. Biopharm. 60 (2005) 25.

[53] J.I. Duncan, S.N. Payne, A.J. Winfield, A.D. Ormerod, A.W. Thomson. Br. J. Dermatol. 123 (1990) 631.

[54] D.P. Wang, C.Y. Lin, D.L. Chu, L.C. Chang. Drug Dev. Ind. Pharm. 23 (1997) 99.

[55] J. Guo, Q. Ping, G. Sun, C. Jiao. Int. J.Pharm.194 (2000) 201.

[56] J.B. Rothbard, S. Garlington, Q. Lin, T. Kirschberg, E. Kreider, P.L. Mcgrane, P.A. Wender, P.A. Khavari. Nat. Med. 6 (2000) 1253.

[57] H.K. Choi, G.L. Flynn, G.L. J. Pharm. Sci. 84 (1995) 581.

[58] J.Y. Fang, T.L. Hwang, C.L. Fang, H.C. Chiu. Int. J. Pharm. 255 (2003) 153.

[59] L. M. Lynch, A. Ofori-Boateng, A. Hippe, K. Kochvar Patrick T. Spicer. J. Colloid Interface Sci. 260 (2003) 404.

[60] R. Efrat, A. Aserin, E. Kesselman, D. Danino, E.J.Wachtel, N. Garti, Aust. J. Chem. 58 (2005) 762.

[61] R. Efrat, A. Aserin, E. Kesselman, D. Danino, E.J.Wachtel, N. Garti, Colloids Surf. A Physicochem. Eng. Aspects 299 (2007) 133.

[62] G. Montalvo, M. Valiente, E. Rodenas, Langmuir 12 (1996) 5202.

[63] R. Mezzenga, C. Meyer, C. Servais, A.I. Romoscanu, L. Sagalowicz, R.C. Hayward, Langmuir 21 (2005) 3322.

[64] E. Farkas, D. Kiss, R. Zelkó, Int. J.Pharm. 340 (2007) 71.

[65] D. Libster, A. Aserin, E. Wachtel, G. Shoham, N. Garti, J. Colloid Interface Sci. 308 (2007) 514.

[66] I. Amar-Yuli, A. Aserin, N.Garti J. Phys. Chem. B, 112 (2008)1017.

[67] Muscutariu, Cristale lichide si aplicatii, Ed. Tehnica, Bucarest, (1981).

[68] S. Walgren, A. Lindstrom, S. Friberg. J. Pharm. Sci. 73 (1984) 1484.

[69] D. I. Nesseem, J. of Pharm and Biomed Anal 26 (2001) 387.

[70] N. H. Gabboun, N. M. Najib, H. G. Ibrahim , S. Assaf. Int. J.Pharm. 212 (2001) 73-80.

[71] S. Mackeben, M. Műller, C. C. Műller-Goymann, Coll. Surf. A: Physicochem. Eng. Aspects 183–185 (2001) 699.

[72] I. Csóka, E. Csányi, G. Zapantis, E. Nagy, A. Fehér-Kiss, G. Horváth, G. Blazsó, I. Erős, Int. J. Pharm. 291 (2005) 11.

[73] M. Makai, E. Csányi, I. Dékány, Z. Németh, I. Erős, Colloid Polym Sci 281(2003) 839.

[74] M. Makai, E. Csányi, Zs. Németh, J. Pálinkás, I. Erős, Int. J. Pharm. 256 (2003) 95.

[75] S. D. Savić, M. M. Savić, S. A. Vesić, G. M. Vuleta, C.C. Műller-Goymann,. Int. J. Pharm. 320, (2006) 86.

[76] S. D. Savić, M. M. Savić, S. Tamburić, G. M. Vuleta, S. A. Vesić, C.C. Műller-Goymann, Eur. J. Pharm. Biopharm.30 (2007) 441.

[77] E. Farkas, R. Zelkó, Zs. Németh, J. Pálinkás, S. Marton, I. Rácz. Int. J. Pharm. 193 (2000) 239.

[78] E. Farkas, R. Zelkó, Gy. Török, I. Rácz, S. Marton. Int. J. Pharm. 213 (2001) 1.

[79] A. Namdeo, N.K. Jain, Journal of Controlled Release 82 (2002) 223.

[80] L. Brinon, S. Geiger, V. Alard, J. Doucet, J. F. Tranchant , G. Couarraze Journal of Controlled Release 60 (1999) 67.

Research Project

on Lyotropic Liquid Crystal
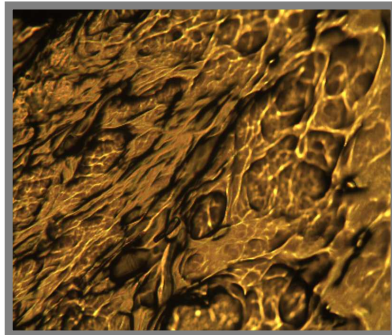
4.2.1 Liquid crystalline Pluronic 105 pharmacogels as drug delivery systems: preparation, characterization and in vitro transdermal release

Rita Muzzalupo, Lorena Tavano, Fiore Pasquale Nicoletta,

Sonia Trombino, Roberta Cassano, Nevio Picci

Department of Pharmaceutical Sciences, Calabria University,

Ed. Polifunzionale, 87030 Rende, Italy

Abstract

In this study we report the results of our investigations on the percutaneous permeation profiles of Diclofenac sodium, Paracetamol, Propanolol hydrochloride and α-Tocopherol from the different lyotropic liquid crystalline phases obtained by Pluronic P105/water mixtures, in order to understand if the particular assembly shown in the formulations could influence the delivery across the skin.

Recent studies have focused on the Pluronic liquid crystalline phases to evaluate the potential use of these phases in drug delivery, but no comparative investigation has been yet performed on the drug permeation from the different liquid crystalline phases obtained by the same Pluronic surfactant.

The cubic, hexagonal and lamellar mesophases (loading the above mentioned drug), were characterized by Deuterium Nuclear Magnetic Resonance spectroscopy and Polarized Optical Microscopy observations. Results revealed that the liquid crystalline gel ~~gel~~ microscopic structure obtained in the different formulations drastically affects the drug percutaneous availability. As a consequence these systems could to be proposed as novel transdermal drug delivery systems.

1. Introduction

Transdermal drug delivery is a viable administration route for potent, low-molecular weight, therapeutic agents which cannot withstand the hostile gastrointestinal tract environment and/or are subject to considerable first-pass metabolism by the liver. Topical drug delivery, for either dermatological or transdermal therapy, strongly depends on the skin nature. The skin is a very heterogeneous membrane, but the layer that controls absorption is the outermost layer, the stratum corneum (SC). SC is a multilayered wall-like structure in which corneocytes are embedded in a matrix of lipids, and provides a very effective barrier towards the drug penetration. These barrier properties hinder the transdermal drug delivery.

However, the success of a transdermal drug delivery system depends on the drug ability to permeate the skin in a sufficient amount to maintain its therapeutic levels. An ideal drug candidate would

have sufficient lipophilicity to partition into the SC, but also sufficient hydrophilicity to enable the second partitioning step into the viable epidermis and, eventually, the systemic circulation.

In altering the lipid structural organization, one could increase the stratum corneum permeability and aid the drug transdermal delivery avoiding side-effects and allowing a better control than other conventional delivery methods, such as oral, intravenous or intramuscular administration [1].

Several physical and chemical methods have been reported in the literature to temporary enhance the membrane permeability, such as incorporation of penetration enhancers (e. g. fatty acids), temperature increase, ionophoresis, vesicle incorporation, prodrug formation, etc. [2, 3]. It is not clear how a penetration enhancer acts to increase SC permeability; some scientists have invoked either a phase separation [4, 5] or an increase of the disordering in the stacking of lipid lamellae [6, 7].

LLC are excellent examples of self-assembling nanomaterials. These lyotropic mesophases are usually formed from water and one or more surfactants at very definite proportions. Their phase sequence (cubic, hexagonal, lamellar) depends on both the different components concentration and the temperature. In the most well known cubic phases the arrangement of molecular aggregates is similar to that shown by micelles. The cubic phases are extremely viscous, optically isotropic, and consequently they are often called viscous isotropic phase. In the hexagonal phase the surfactant molecules are aggregated in cylindrical structures of indefinite length disposed on a hexagonal lattice, giving rise to a long-range orientational order. Hexagonal phases are birefringent when viewed between crossed polarized and show characteristic optical textures at the polarizing optical microscope. Due to their high viscosity the small air bubbles trapped within the hexagonal preparations show highly distorted shapes. The structural unit for the lamellar phase are the simple and double layers. The bilayer structure is formed by surfactant molecules disposed in bidimensional stacking of infinite layers, delimited by water. The polar heads of the molecules are in contact with the aqueous medium, while the hydrocarbon chains are interdigitating in order to avoid water. The bilayers are disposed one under another through the third dimension, periodically alternating with water layers [8].

This phase is rather fluid and the bilayers can slip easily one on the other. The presence of specific optical textures make easy the identification of the lamellar phase.

The lyotropic liquid crystals (LLC) exhibit good penetration, due to the very low interfacial surface tension arising at the oil/water interface [9], and they may facilitate the progressive diffusion of biologically active substances into the skin and the systemic circulation [10,11]. They can increase the drugs solubility of drugs, which are either insoluble or slightly soluble in water [12].

During the past decade, there has been great interest in these LLC as delivery systems in ~~the~~ cosmetic and chemical industries and in the field of pharmacy [13, 14]. The reasons for this interest include the extensive similarity of these colloid systems to those occurring in living organisms [15] and their advantageous properties over those of traditional semisolid dermal dosage forms [16]. In addition, their production results therefore relatively simple and energy-saving [17].

Poloxamer block copolymers are amphiphilic triblock copolymers consisting of a relatively long hydrophobic poly(propylene oxide) (PPO) middle block and two hydrophilic poly(ethylene oxide) (PEO) end blocks, and are commercially available as Poloxamers or Pluronics. In the presence of a either solvent selective for the hydrophilic PEO blocks, such as water, or a solvent selective for the hydrophobic PPO block, such as xylene ("oil"), PEO-PPO-PEO block copolymers self-organize into a variety of LLC "gel" phases with lamellar, hexagonal, or cubic structure. A notable feature that distinguishes the self-assembling behaviour of the PEO-PPO-PEO block copolymers from that of the low-molecular-weight surfactants is their ability to form a great variety of both normal and reverse liquid crystalline microstructures, as demonstrated in recent reports [18, 19]. Several works evaluated the Pluronic lyotropic phases influence on percutaneous absorption, but no comparative investigation has been yet performed, to our knowledge, on the drug permeation from the different liquid crystalline phases obtained by the same Pluronic surfactant.

The aim of this paper is to evaluate the percutaneous permeation profile of various drugs from the different liquid crystalline phases of Pluronic P105/water mixtures, in order to understand if the particular assembly shown in the formulations could give rise to a different, or even enhanced, transdermal delivery of drugs. In particular, the loaded drugs were Diclofenac sodium, Paracetamol, Propanolol hydrochloride and α-Tocopherol, which were chosen for their anionic, non-ionic, cationic and lipophilic chemical structures, respectively. The obtained cubic, hexagonal and lamellar mesophases, loading the above mentioned drugs, were characterized by Deuterium Nuclear Magnetic Resonance spectroscopy (^{2}H-NMR) and Polarized Optical Microscopy observations (POM) to evaluate the occurred structural modifications.

2. Materials and methods

2.1 Materials

Pluronic P105, poly(ethylene oxide)-block-poly(propylene oxide)-block-poly(ethylene oxide) copolymer, was provide from BASF (Mount Olive, NJ, USA). Deionized water with 5 wt %. deuterium oxide (Aldrich, Milan) was used in order to perform ^{2}H-NMR measurements. Diclofenac sodium, Paracetamol, Propanolol hydrochloride, and α-Tocopherol were supplied by Sigma. The drug content in the permeation studies was analyzed by UV-VIS JASCO V-530 spectrometer using

1 cm quartz cells at the wavelength of 264, 288, 262 and 292 nm for Paracetamol, Propanolol hydrochloride, Diclofenac sodium and α-Tocopherol, respectively.

2.2. Preparation of Pluronic LLC gels

LLC gel samples were prepared using a fixed drug percentage and varying the ratio between Pluronic and water, in order to obtain the different P105 liquid crystalline phases. Briefly, the preparation is as follows: 0.4 g of hydrophilic drug was dissolved in the appropriate amount of water and mixed with the block copolymer until a homogeneous mixture was obtained. The α-Tocopherol samples were prepared by direct mixing of all components. Before use, samples were centrifuged several times and, stored at room temperature, or at 4°C, to favour their homogenization since some of these samples exhibit negative thermorheological behaviour, (a i.e. they are liquid at low T values, but LLC at body temperature) [20]. The samples were analyzed only after one week. Details on the samples preparation are reported in Table 1.

Phases	P105 wt %	H₂O wt %	Drug wt %
Cubic phase	35	61	4
Hexagonal phase	55	41	4
Lamellar phase	80	16	4

Table 1. Liquid crystalline phases composition (wt%)

2.3 Methods

2.3.1 ^{2}H-NMR theory and experiments

Phases and phase transitions in lyotropic liquid crystals can be identified by ^{2}H-NMR and POM. In the case of aggregates dispersed in deuterium oxide, ^{2}H-NMR spectroscopy can be used to investigate both the local order of molecules and the structure of the aggregates. ^{2}H-NMR spectra are dominated by the quadrupole interaction, which gives the following spectral frequencies:

$$v_\pm = \pm\frac{3}{8}v_Q\left(3\cos^2 \partial - 1 + \eta\sin^2 \partial\cos 2\varphi\right)$$ Eq.1

where n_Q is the partially averaged quadrupole coupling constant, q and f are the polar and azimuthal angles defining the direction of the external magnetic field in the aggregate frame and h is the asymmetry parameter. Figure 1 shows some characteristic ^{2}H-NMR lineshapes. In a powder-like spectrum of the lamellar phase (h = 0) the lineshapes are characterized by two shoulders and two edge singularities separated by $\frac{3}{2}v_Q$ and $\frac{3}{4}v_Q$, respectively. The singularities correspond to the

contribution from the nuclei with the principal axis frame oriented at an angle q = 90°, while the orientations with q = 0° contribute to the intensity at the shoulders (Figure 1a). Hexagonal phases present similar lineshapes but with narrower (about one half) separation between shoulders and edges (Figure 1b). When an isotropic sample, as a cubic phase, is investigated, a singlet is observed (Figure 1c). If a system forms a mixture of phases with an exchange time slow on the NMR timescale between the different phases, a superimposition of the signals originating from these phases will appear in NMR spectrum. In the case of fast exchange NMR lineshapes will be affected by additional motional averaging.
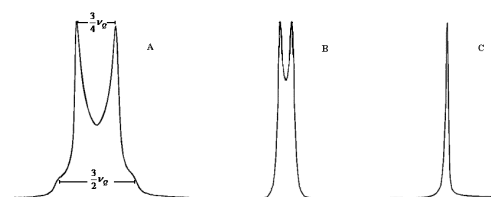

Fig.1 ^{2}H-NMR spectra of cubic, hexagonal and lamellar mesophases.

In our study ^{2}H-NMR experiments were performed at a resonance frequency of 46.53 MHz on a Bruker AVANCE 300 pulsed superconducting spectrometer working in Fourier Transform mode. The sample temperature was controlled during NMR measurements by passing air at the desired temperature ($35 \pm 1°$ C) through the sample holder.

A quadrupole echo sequence with a p/2 pulse width of 3.5 ms was used for acquiring ^{2}H-NMR spectra. The delay between the two p/2 pulses was 40 ms and repetition was 1 s. To allow samples to reach thermal equilibrium, spectra were recorded 30 min after each temperature setting.

2.3.2 Optical microscopy observations

Phase characterization of the samples was also performed with a Leica 12 Pol optical polarizing microscope. In fact, POM is suitable for the identification of lyotropic liquid crystals (except cubic phases) by comparing the typical textures of each liquid crystalline mesophase with those reported in liquid crystal texture handbook [21].

2.3.3 Percutaneous permeation studies

In vitro percutaneous permeation studies were performed using vertical diffusion Franz cells with an effective diffusion area of 0.416 cm^2. The experiments were carried out using rabbit ear skin, obtained from a local slaughterhouse. The skin from the outer surface of a freshly excised rabbit ears (6 months old) was carefully dissected (making sure that the subcutaneous fat was maximally

removed), stored a -18° C, and pre-equilibrated in physiological solution at room temperature for 2 h before the experiments.A circular piece of this skin was securely sandwiched between the receptor and donor compartments: epidermal side of the skin was exposed to ambient conditions while dermal side was kept facing to receptor solution. The donor compartment was charged with 0.6 g of drug-loaded LLC gel and covered with Parafilm^{TM} to prevent water loss. The receptor compartment was filled with 5.5 mL of distilled water which was maintained at $37 \pm 0.5°C$ and stirred by a magnetic bar. The permeation experiments of α-Tocopherol, used as lipophilic drug, were performed by inserting in the acceptor compartment a water-ethanol solution (80:20), to promote the drug solubility. At regular intervals and up to 48 h aliquots of 2.0 mL of receptor solution were withdrawn and the receptor compartment was refilled with the receptor solution to keep constant the receptor compartment volume during the experiment. The content of drug in the samples was analyzed by UV-Vis spectrometry. The permeation of the free drugs solutions were also investigated in the same way. The experimental procedure was repeated three times.

2.3.4. Statistical analysis of data

Data analysis was carried out with the software package Microsoft Excel version 2007. Results were expressed as a mean ± standard deviation.

3. Results and discussion

Block copolymers as poly(oxyethylene)-poly(oxypropylene)-poly(oxyethylene), $[(EO)_x(PO)_y(EO)_z]$ (Pluronics or Poloxamers), are found to form lyotropic liquid crystalline phases (cubic, hexagonal and lamellar) at high concentrations [22, 23]. The structural polymorphism afforded by the PEO-PPO-PEO polymers has only recently been recognized depending on the polymer chemical composition: cubic, hexagonal, and/or lamellar LLC phases can be formed with increasing polymer content in a mixture with water (or oil) [24].

P105, i.e. $(EO)_{37}(PO)_{58}(EO)_{37}$, as reported by reference [25], is capable of self-assembling in water with increasing polymer concentration into micellar, cubic, hexagonal, and lamellar LLC phases. A stable cubic, hexagonal and lamellar mesophases are generally obtained at 20°C when the polymer concentration ranges around 26-44 wt%, 47-66 wt% and 73-87 wt %, respectively.

The influence of cosolutes as well as cosolvents on the self-assembly of amphiphilic block copolymers has been studied for some PEO-PPO-PEO block copolymers and a pronounced structural modifications were found [26, 27]. In particular, it has been demonstrated that the incorporation of a drugs as a third component could induce a structural modifications and enhance

the *in vitro* penetration of the therapeutic agents in the skin, probably due to the action of liquid crystalline phases as penetration enhancers [28, 29].

In the present study, drugs with anionic, non-ionic, cationic and lipophilic chemical structures and different properties such as Diclofenac sodium, Paracetamol, Propanolol hydrochloride, and α-Tocopherol, respectively, were incorporated into P105 liquid crystalline phases and the percutaneous permeation profiles across the skin were performed.

Diclofenac sodium percutaneous permeation profile

Diclofenac sodium is an anionic, non-steroidal, anti-inflammatory drug. Its daily oral administration is accompanied, however, by its known adverse effects that include gastrointestinal toxicity, gastric ulcers, and anaphylaxis [30]. For the sake of clarity, charged drug molecules are, in general, unsuitable for transdermal drug delivery. However, a lot of effort is devoted to find new methods to promote the transdermal delivery of anionic species [31-33].

The ^{2}H-NMR spectra and POM textures analysis shows that Diclofenac incorporation partially changes the P105 lamellar and hexagonal mesophases, but not the cubic one (Figure 2A). In fact, at 55 wt% of Pluronic, ^{2}H-NMR spectra indicate the presence of an isotropic component and a hexagonal phase lineshape (Figure 2B); a similar behaviour is observed at 80 wt % of polymer. In both cases the original microstructure (hexagonal and lamellar) shows an additional isotropic peak due, probably to the a coexistence of a cubic phase, (Figure 2C).
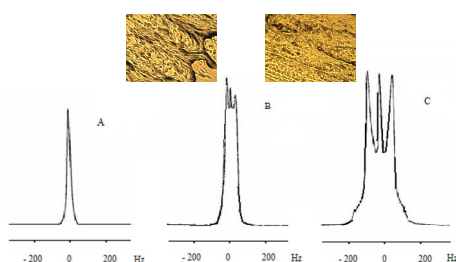

Fig.2 ^{2}H-NMR spectra and POM images of mesophases containing Diclofenac sodium with different P105 concentrations: A, 35 wt %, B, 55 wt %, C, wt %.

The Diclofenac sodium permeation profile is reported in Figure 3 and the amount of drug present in the donor compartment was 56 mg/cm^2. The cumulative permeated drug amount within 48 h is 20% for cubic, 35% for hexagonal/cubic and 26% for lamellar/cubic phase, respectively. Results suggest that the hexagonal/cubic phase is the optimal for the Diclofenac permeation. Probably, the presence of hexagonal phase allows weaker interactions between Diclofenac and the Pluronic chains, increasing the drug diffusion rate and, consequently, the permeation.
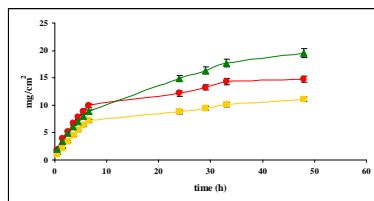
Fig.3 Permeated Diclofenac sodium cumulative amount from P105 liquid crystalline phases as a function of time: (●) 80 wt %, (▲) 55 wt % and (■) 35 wt % of P105, respectively.

Figure 3 shows that the mesophases diffences become relevant after 8 hours and the P105 acts as a percutaneous permeation enhancer in all formulations. In fact, all cumulative permeated drug amounts were always higher than that from the free drug solution (data not shown).

Paracetamol percutaneous permeation profile

Paracetamol is analgesic and antipyretic agent widely used as medications for infants and children. The currently available formulations have been designed for oral and rectal administration [34], following which absorption is fast, predominantly from the small intestine. These formulations are not practical in young patients with vomiting and diarrhoea, or in those who refuse to take the full dose and alternative administration route would be a significant contribution to the paediatric therapy.

After 48 hours, the Paracetamol permeated amount from the different LLC gels was found to be 24%, 37% and 22% of the initial loaded drug from cubic, hexagonal and lamellar phases, respectively (Figure 4).
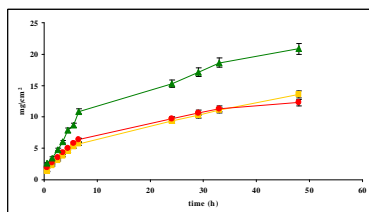

Fig.4 Permeated Paracetamol cumulative amount from P105 liquid crystalline phases as a function of time: (●) 80 wt %, (▲) 55 wt % and (■) 35 wt % of P105, respectively.

The recorded ^{2}H-NMR spectra show significant structural modifications in the mesophases, as above reported for Diclofenac sodium. In particular, except for the sample with lower wt% of P105 content which remains in the cubic phase, both 55% wt and to 80% wt samples give rise to a mesophases coexistence: hexagonal/cubic and lamellar/cubic, as confirmed by the presence of anisotropic and isotropic regions detected using crossed polarizers. The hexagonal/cubic mesophase

shows a greater capacity to enhance the drug permeation and skin permeation profiles were significantly higher in all formulations than in the free drug solution.

Propanolol percutaneous permeation profile

Propanolol is one of the most widely prescribed beta-blockers in the long-term treatment of hypertension and is usually taken by os. Available sustained release dosages of oral Propanolol ~~is~~ are not as effective as the equivalent amounts of single dosages because slower oral absorption leads to greater hepatic metabolism. The transdermal drug administration effectively bypasses the first pass metabolism and, provides a sustained delivery [35].

The Propanolol, used as a model cationic drug, shows a different permeation profile~~s~~ respect to Diclofenac or Paracetamol loaded carriers (Figure 5).
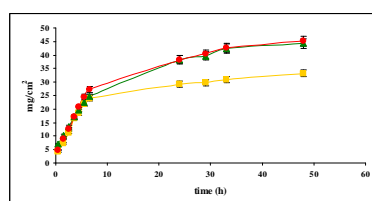

Fig.5 Permeated Propanolol hydrochloride cumulative amount of from P105 liquid crystalline phases as a function of time: (●) 80 wt %, (▲) 55 wt % and (■) 35 wt % of P105, respectively.

As previously reported the total loaded drug amount was 56 mg/cm^2 and the Propanolol permeation was very pronounced, especially for the hexagonal/cubic and lamellar/cubic phases, that show a similar permeation trends with a cumulative drug permeation of 78% and 80% respectively. The cubic phase permeated 59% of Propanolol within 48 hours. This is probably due to the synergistic action between Pluronic surfactant liquid crystalline phases, used as vehicle, and the positive charge of the drug that interacts with the cell membrane negative potential of the stratum corneum. The ^{2}H-NMR spectra analysis (Figure 6) and POM observations suggest that the lamellar phase, in this case, is less *contaminated* by the cubic one. In other words, the cubic phase amount found in Propanolol lamellar/cubic sample is less than that found in Diclofenac and Paracetamol LLC gels. The permeation data show that in the case of Propanolol, a more pure lamellar phase increases the drug absorbtion.
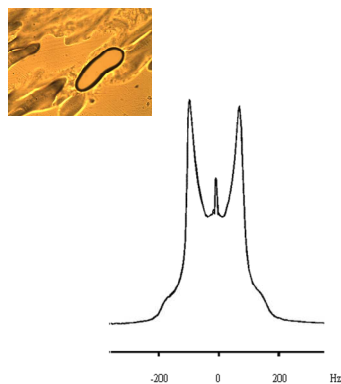
196

Fig.6 ^{2}H-NMR spectra of mesophases containing Propanolol hydrochloride at 80 wt% of P105.

α-Tocopherol percutaneous permeation profile

α -Tocopherol is the most important lipid-soluble antioxidant and it protects cell membranes from oxidation by reacting with lipid radicals produced in the lipid peroxidation chain reaction. It is claimed to reduce erythema, photoaging, photocarcinogenesis, edema, and skin hypersensitivity associated with exposure to UV-B radiation [36].

Unlike other systems, the introduction of a lipophilic drug changes the phase diagram of the P105/water binary system in the cubic range concentration, as evidenced by POM observations and ^{2}H-NMR spectra. In particular, when the P105 concentration is about 35 wt%, the cubic phase disappears (Figure 7A), the system becomes anisotropic and ^{2}H-NMR spectra indicate the presence of a hexagonal phase similar to that of the sample with 55 wt% P105 (Figure 7B). The sample with higher content of polymer (80%) gives a pure lamellar mesophase (Figure 7C).
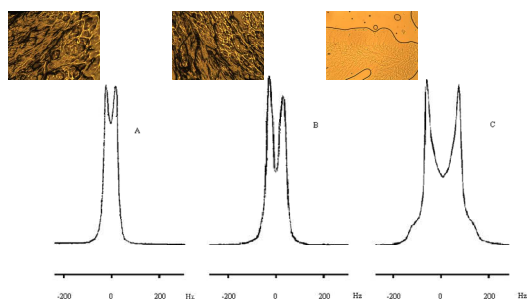

Fig.7 ^{2}H-NMR spectra and POM imagesof mesophases containing α-Tocopherol with different P105 concentrations: A, 35 wt %, B, 55 wt %, C, 80 wt %.

As reported in Figure 8 the permeated drug amount increases as a function of Pluronic content. In fact, the highest *α*-Tocopherol permeated amount was found for the lamellar mesophase, due

197

probably to the structural analogy between lamellar phase, stratum corneum and lipophilic drug. The 55 wt% P105 LLC gel permeated the 42% of loaded drug within 48 h, while 35 wt% of P105 (hexagonal phase) permeated only 32%, even it the permeation profile was similar. In this case aqueous solution of α-Tocopherol could not be used as control, due to its poor water-solubility.
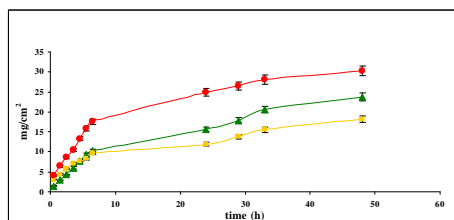

Fig.8 Permeated α-Tocopherol cumulative amounts of from P105 liquid crystalline phases as a function of time: (●) 80 wt %, (▲) 55 wt % and (■) 35 wt % of P105, respectively.

4. Conclusions

The percutaneous permeation of Diclofenac sodium, Paracetamol, Propanolol hydrochloride and α-Tocopherol, used as model drugs, was modulated by the liquid crystalline phases obtained from Pluronic P105. In the formulations containing hydrophilic drugs (Diclofenac sodium, Paracetamol, Propanolol hydrochloride) there was a remarkable enhancement of permeation: pure cubic mesophase showed the lowest permeation than biphasic systems, such as cubic/lamellar and cubic/hexagonal. The introduction of α-Tocopherol, as lipophilic drug, in the lyotropic system P105/water changed the phase diagram: the disappearance of cubic phase occurred and a pure hexagonal phase was observed. Moreover the lamellar phase showed the highest percutaneous permeation capacity. This behaviour can be attributed to the drug different physico-chemical properties; moreover it is possible that liquid crystalline phases modify the drug partition in the carrier–stratum corneum and/or the stratum corneum properties.

As a consequence, all formulations can be considered optimal percutaneous permeation enhancers. In addition, the use of cationic drugs further enhance the permeation due, probably, to the onset of most favourable interactions between cationic molecules and stratum corneous. In particular experiments show that the Propanolol hydrochloride introduction in the P105/water systems gives the most favourable results, with a 70 % and 80% of permeated drug from the hexagonal/cubic and lamellar/cubic phases, respectively.

References
[1] E.W. Smith, H.I. Maibach, Percutaneous Penetration Enhancers, New York:CRS Press, 1995.

[2] H. Takeuchi, H. Yamamoto, T. Niwa, T. Hino, Y. Kawashima, Enteral absorption of insulin in rats from mucoadhesive chitosan coated liposomes, Pharm. Res. 13 (1996) 896.

[3] B. Barry, A. Williams, Penetration enhancers, Adv. Drug Deliv. Rev. 56 (2003) 603.

[4] A. Ortiz, J.C. Gomez-Fernandez, A differential scanning calorimetry study of the interaction of free fatty acids with phospholipid membranes, Chem. Phys. Lipids 45 (1987) 75.

[5] R.D. Klausner, A.M. Kleinfeld, R.L. Hoover, M.J. Karnovsky, Lipid domains in membranes. Evidence derived from structural perturbations induced by free fatty acids and lifetime heterogeneity analysis, J. Biol. Chem. 255 (1980) 1286.

[6] G.S. Gooris, J.A. Bouwstra, Infrared spectroscopic study of stratum corneum model membranes prepared from human ceramides, cholesterol, and fatty acids, Bioph. J. 92 (2007) 2785.

[7] A.C. Rowat, N. Kitson, J.L. Thewalt, Interactions of oleic acid and model stratum corneum membranes as seen by ^{2}H NMR, Int. J. Pharm. 307 (2006) 225.

[8] R. Muzzalupo, L. Tavano, S. Trombino, R. Cassano, N. Picci, "Lyotropic liquid crystals for topical delivery system". In Current focus on colloids and surfaces, editor Li S., Kerala, India: Transworld Research Network, 2009, 295-312.

[9] T. Suzuki, H. Takei, S. Yamazaki, Formation of fine three-phase emulsions by the liquid crystal emulsification method with arginine-branched monoalkyl phosphate, J. Colloid Interface Sci. 129 (1989) 491.

[10] E. Cooper, B. Berner, Penetration enhancers. In: Kydonieus, A.F., Berner, B. (Eds.), Transdermal Delivery of Drugs, vol.3. CRC Press, Boca Raton, 1987, p. 57.

[11] J. Ziegenmeyer, The influence of the vehicle on the absorption and permeation of drugs. In: Brandau, R., Lippold, B.H. (Eds.), Dermal and Transdermal Absorption. Wissenschaftliche Verlagsgesellschaft mbH, Stuttgart, 1982, p. 73.

[12] G.A. Kossena, W.N. Charman, B.J. Boyd, C.J.H. Porter, A novel cubic phase of medium chain lipid origin for the delivery of poorly water soluble drugs, J. Contr. Rel., 99 (2004) 217.

[13] D. Attwood, A.T. Florence, Surfactant systems, their chemistry, pharmacy and biology. biological implication of surfactant presence in formulations. Chapman & Hall, London, 1982.

[14] S.P. Vyas, V. Jaitely, P. Kanaujia, Self-assembling supramolecular biovectors a newer dimension in novel drug delivery system, Pharmazie 52 (1997) 259.

[15] D. Chapman, Lyotropic mesophase in biological systems. In: Bahadur, B. (Ed.), Liquid crystals applications and uses. World Scientific, Singapur, 1991, p. 186.

[16] P.B. Geraghty, D. Attwood, J.H. Collet, Y. Dandiker, The in vitro topic release of some antimuscarinic drugs from monoolein/water lyotropic liquid crystalline gels, Pharm. Res. 13 (1996) 1265.

[17] R.F. Turchiello, F.C.B. Vena, P. Maillard, C.S. Souza, M.V.L.B. Bentley, A.C. Tedesco, Cubic phase gel as a drug delivery system for topical application of 5-ALA, its ester derivatives and m-THPC in photodynamic therapy (PDT), J. Photochem. Photobiol. B 70 (2003) 1.

[18] B. Svensson, P. Alexandridis, U. Olsson, Self-Assembly of a poly(ethylene oxide)-poly(propylene oxide) block copolymer (Pluronic P104, $(EO)_{27}(PO)_{61}(EO)_{27}$) in the presence of water and xylene, J. Phys. Chem. B, 102 (1998) 7541.

[19] M. Svensson, P. Alexandridis, P. Linse, Modelling of the phase behaviour in ternary triblock copolymer-water-oil systems, Macromolecules 32 (1999) 5435.

[20] J. Juhasz, V. Lenaests, P. Raymond, H. Ong, Diffusion of rat atrial natriuretic factor in thermoreversible poloxamer gels, Biomaterials, 10 (1989) 265.

[21] D. Demus; L. Richther; Textures of Liquid Crystals; VEB Duutscher Verlag fűr Grundstoffindustrie, Leipzig, 1978

[22] P. Spicer, In: H. Nalwa, Editor, Encyclopedia of Nanoscience and Nanotechnology, Marcel Dekker, USA (2004) p. 881.

[23] B. Yang, B. Armitage, S. Marder, Cubic liquid-crystalline nanoparticles, Angew. Chem. Int. Ed. 43 (2004) 4402.

[24] P. Alexandridis, U. Olsson, B. Lindman, Self-Assembly of Amphiphilic block Copolymers: the $(EO)_{13}(PO)_{30}(EO)_{13}$-Water-p-Xylene System, Macromolecules 28 (1995) 7700.

[25] P. Alexandridis, D. Zhou, A. Khan, Lyotropic liquid crystallinity in amphiphilic block copolymers: temperature effects on phase behavior and structure for poly(ethylene oxide)-b-poly(propylene oxide)-*b*-poly(ethylene oxide) copolymers of different composition, Langmuir, 12 (1996) 2690.

[26] P. Alexandridis, J.F. Holzwarth, Differential scanning calorimetry investigation of the effect of salts on aqueous solution properties of an amphiphilic block copolymer (Poloxamer), Langmuir, 13 (1997) 6074.

[27] R. Ivanova, B. Lindman, P. Alexandridis, Effect of glycols on the self-assembly of amphiphilic block copolymers in water. I. Phase diagrams and structure identification, Langmuir 16 (2000) 3660.

[28] J. Bender, M.B. Ericson, N. Merclin, V. Iani, A. Rosen, S. Engstrom, J. Moan, Lipid cubic phases for improved topical drug delivery in photodynamic therapy, J. Control. Rel. 106 (2005) 350.

[29] N. Merclin, J. Bender, E. Sparr, R.H. Guy, H. Ehrsson, S. Engström, Transdermal delivery from a lipid sponge phase-iontophoretic and passive transport in vitro of 5-aminolevulinic acid and its methyl ester, J. Control. Rel. 100 (2004) 191.

[30] G. Cevc, G. Blume, New, highly efficient formulation of diclofenac for the topical, transdermal administration in ultradeformable drug carriers, Transferosomes, Biochim. Biophys. Acta 1514 (2001) 191.

[31] R. Valjakka-Koskela, M. Kirjavainen, J. Mönkkönen, A. Urtti and J. Kiesvaara, Enhancement of percutaneous absorption of naproxen by phospholipids, Int. J. Pharm. 175 (1998) 225

[32] N. Dayan and E. Touitou, Carriers for skin delivery of trihexyphenidyl HCl: ethosomes vs. liposomes, Biomaterials 21 (2000) 1879

[33] K. Kigasawa, K. Kajimoto, M. Watanabe, K. Kanamura, A. Saito, K. Kogure, In vivo transdermal delivery of Diclofenac by ion-exchange iontophoresis with Geraniol, Biol. Pharm. Bull. 32 (2009) 684

[34] S. Miyazaki, W. Kubo, K. Itoh, Y. Konno, M. Fujiwara, M. Dairaku, M. Togashi, R. Mikami, D. Attwood, The effect of taste masking agents on in situ gelling pectin formulations for oral sustained delivery of paracetamol and ambroxol, Int. J. Pharm. 297 (2005) 38.

[35] P.R. Rao, M.N. Reddy, S. Ramakrishna, P.V. Diwan, Comparative in vivo evaluation of propanolol hydrochloride after oral and transdermal administration in rabbits, Eur. J. Pharm. Biopharm., 56 (2003) 81.

[36] M.P. Lupo, Antioxidants and vitamins in cosmetics, Clin. Dermatol., 19 (2001) 157.

5

Scientific collaboration with EUROCHEMICALS s.p.a.

This section reviews my research project performed during my PhD course in collaboration with a chemical company (EUROCHEMICALS S.p.A.) on the development of niosomal formulations carrying bioactive molecules for cosmetic formulations.

Since the new formulations could be patented and marketed, it is not possible to reveal the composition of the new vesicular systems or the encapsulated bioactive substances, or the composition of the emulsion used as a vehicle.

The optimal properties of niosomes can be utilized also in the delivery of bioactive molecules in cosmetics, since they present a convenient method for solubilizing active substances in the hydrocarbon core of the bilayer. They will always form lamellar liquid crystalline structures on the skin and, therefore, they do not disrupt the structure of the stratum corneum, (unless the surfactant molecules used for making the vesicles are themselves skin irritants.)

Niosomes as a carrier itself offers advantages because amphiphilic molecules are well hydrated and can reduce the dryness of the skin which is a primary cause for its ageing. Also, niosomes can act as a supply which acts to replenish lipids and, importantly, linolenic acid.

In general the rules for topical drug applications and delivery of other compounds are less stringent than the ones for parenteral administration and several hundred cosmetic products are commercially available since Niosomes (L'Oreal) were introduced in 1987.

These niosomes can be more stable than their natural analogues (liposomes), can be easily produced in large quantities and are very inexpensive and these can be great advantages for the industrial production.

In this light we design in collaboration with the chemical company new niosomal vesicles for topical cosmetic applications.

My research project was divided in two parts:

- During the first 18 months I evaluate the possibility to use new commercial surfactants (named X and Y) to produce niosomes, without any membrane additives, such as cholesterol, by using different bilayer composition.

  As above mentioned for the preparation of drug-loaded niosomes, the obtained vesicles were characterized in terms on dimensional and morphological properties, with particular attention to the relationship between bilayer composition and physical-chemical properties. These properties were optimized and the optimal composition was identified.

Bioactive molecules with hydrophilic, amphiphilic and lipophilic characteristic were encapsulated in all formulation and the entrapment efficiency was evaluated for each sample.

The stability of the systems and the degradation of the active molecules loaded in the niosomes were monitored for 6 months.

The possibility to use these new carrier for the requested topical applications was evaluated by performing percutaneous permeation studies. These studies were carried out by using the static Franz cells equipped with rabbit ear skin.

● During the last 18 months I focused my attention on the preparation of a new emulsion O/A as cosmetic vehicle for the above obtained niosomes. The composition of the emulsion was studied by varying the amount of surfactant, water and oil content. In addition the optimal antioxidant, antibatteric and parfum content was evaluated. The properties of the new emulsion were optimized.

After mixing the appropriate volume of loaded niosomal suspension in the vehicle, the percutaneous permeation studies of active molecules formulated in the new emulsion O/A were estimated.

In conclusion stability test of niosomes and niosomes/emulsion at 25°C and 40°C and active molecules degradation test were performed.

The results of this study showed that both the new commercial surfactants were able to form niosomes also in absence of membrane additives. These vesicles could be successfully used

1. to entrap both lipophilic and hydrophilic drug,
2. to protect the bioactive molecules from degradation,
3. to promote the percutaneous permeation across the skin both as solution and in formulation (emulsion).

For these reasons the new obtained carriers have a potential in cosmetic fields as requested.